B CELLS IN ACUTE AND CHRONIC LUNG DISEASE

A thesis submitted to the University of Manchester for the degree of Doctor of Philosophy in the Faculty of Biology, Medicine and Health

2022

Halima A Shuwa

School of Biological Sciences

Division of Infection, Immunity and Respiratory Medicine

List of Content

Word count: 42,343

List of Figures

List of Tables

List of Supplementary Figures

List of Supplementary Tables

List of Abbreviations

5′-AMP	Adenosine 5′-monophosphate
Abs	Antibodies
ACE2	Angiotensin-Converting Enzyme 2
ADO	Adenosine
AhR	Aryl Hydrocarbon Receptor
ANOVA	Analysis of variance
APC	Antigen Presenting Cells
ARDS	Acute Respiratory Distress
ARDS	Acute Respiratory Distress Syndrome
ASC	Antigen Secreting Cell
AT1a	Angiotensin II Receptor Type 1
BAFF	B cell-Activating Factor of TNF Family
BAFF-R	BAFF-Receptor
BCL-6	B Cell Lymphoma 6
BCR	B Cell Receptor
Beffs	Effector B cells
BFA	Brefeldin A
Blimp-1	B lymphocyte-induced maturation protein-1
Blys	B lymphocyte stimulator
BM	Bone Marrow
Br1	Regulatory B1
Bregs	Regulatory B cells
BRM	Resident Memory B cells

12

BSA	Bovine serum albumin
CCL19	C-C Motif Ligand 19
CCL21	C-C Motif Ligand 21
CCR10	C-C Motif Chemokine Receptor 10
CCR7	C-C Motif Chemokine Receptor 7
CD	Cluster of Differentiation
cDNA	Complementary DNA
CIRCO	Coronavirus Immune Response and Clinical Outcomes
COPD	Chronic Obstructive Pulmonary Disease
COVID-19	Coronavirus Disease 2019
CpG-B	5'—C—phosphate—G—3' Class B
CPM	Counts-per-million
CS	Cigarette Smoke
CSB	Cell-staining buffer
CTLA-4	Cytotoxic T-lymphocyte-Associated Protein 4
CXCL12	C-X-C Motif Chemokine Ligand 12
CXCL13	C-X-C Motif Chemokine Ligand 13
CXCR3	C-X-C Chemokine Receptor 3
CXCR4	C-X-C Chemokine Receptor 4
CXCR5	C-X-C Chemokine Receptor 5
CyTOF	Cytometry time of flight
DC	Dendritic Cell
DE	Differential expression
DEGs	Differentially expressed genes

dH$_2$O	Distilled Water
DMSO	Dimethyl Sulfoxide
DN	Double-Negative
DNA	Deoxyribonucleic acid
ECM	Extracellular matrix
EDTA	Ethylenediaminetetraacetic Acid
ELT	Ectopic Lymphoid Tissue
FACS	Fluorescence-activated cell sorting
FcR	Fc Receptors
FCRL4	Fc Receptor-Like Protein 4
FCRL5	Fc Receptor-Like Protein 5
FCS	Foetal Calf Serum
FcγR	Fc-gamma Receptors
FDC	Follicular Dendritic Cell
FDR	False discovery rate
FEV1	Forced Expiratory Volume in One Second
FFPE	Formalin-Fixed Paraffin-Embedded
FMO	Fluorescence Minus One
FO	Follicular
FoxP3	Forkhead box P3
FVC	Forced Vital Capacity
GC	Germinal Centre
GEMs	Gel Beads-in-emulsion
GOLD	Global Initiative on Obstructive Lung Disease

GTCF	Genome Technology Core Facility
GzmB	GranzymeB
H&E	Haematoxylin and Eosin
H. *polygyrus*	Heligmosomoides polygyrus
hCoVs	Human Coronaviruses
HEPES	Hydroxyethyl Piperazineethanesulfonic Acid
HEV	High Endothelial Venules
HIF-1α	Hypoxia-Inducible Factor 1α
HIV	Human Immunodeficiency Virus
HSC	Hematopoietic Stem Cell
HVGs	Highly variable genes
iBALT	Inducible Bronchus-Associated Lymphoid Tissue
iBregs	Induced Bregs
ICAM-1	Intercellular Adhesion Molecule-1
IDO	Indoleamine 2,3 Dioxygenase
IFN	Interferon
IFN-I	Type-I Interferons
IgA	Immunoglobulin-A
IgD	Immunoglobulin-D
IgE	Immunoglobulin-E
IgG	Immunoglobulin-G
IgM	Immunoglobulin-M
IL	Interleukin
ILC	Innate Lymphoid Cell

ILD	Interstitial Lung Disease
IMC	Imaging mass cytometry
iNKT	inducible Natural Killer T cell
IPA	Ingenuity Pathway Analysis
IPF	Idiopathic Pulmonary Fibrosis
IRF4	Interferon Regulatory Factor 4
iTCR	Invariant T cell Receptor
KLF4	Krüppel-like Factor 4
KLF9	Krüppel-like Factor 9
LF	Lymphoid Follicles
LFA-1	Lymphocyte Function-Associated Antigen-1
LN	Lymph Node
LPS	Lipopolysaccharide
LTα1β2	Lymphotoxin-α-β Heterotrimer
LT-β	Lymphotoxin-β
MAD	Median absolute deviation
MALT	Mucosal Associated Lymphoid Tissues
ManARTS	Manchester Allergy, Respiratory and Thoracic Surgery
MBC	Memory B cells
MCD	MathCad
MDSCs	Myeloid-Derived Suppressor Cells
MERS-CoV	Middle East Respiratory Syndrome Coronavirus
MHC	Major Histocompatibility Complex
MMP	Matrix Metalloproteinases

MNN	Mutual nearest neighbours
mRNA	Messenger RNA
MZ	Marginal Zone
Nab	Natural Antibodies
NALR	Nasal-Associated Lymphoid Tissues
nBregs	Neonatal Bregs
NF-κB	Nuclear factor kappa-light-chain-enhancer of activated B cells
NK	Natural Killer cells
PB	Plasmablasts
PBMCs	Peripheral Blood Mononuclear Cell
PBS	Phosphate Buffered Saline
PC	Plasma Cell
PCP	Pneumocystis pneumonia
PCR	Polymerase Chain Reaction
PD	Programmed cell Death
pDCs	Plasmacytoid Dendritic Cells
PD-L1	Programmed cell Death-Ligand 1
PHOSP-COVID	Post-hospitalisation COVID-19 study
PLZF	promyelocytic leukaemia zinc finger
RA	Rheumatoid Arthritis
RBD	Receptor-Binding Domain
RNA	Ribonucleic Acid
ROIs	Regions of interests
RSV	Respiratory Syncytial Virus

RT	Reverse transcription
S. *mansoni*	Schistosoma mansoni
SARS-CoV	Severe Acute Respiratory Syndrome Coronavirus-2
SCF	Stem Cell Factor
scRNA-seq	Single-cell RNA-sequencing
SHM	Somatic Hypermutation
SLAM	Self-ligand receptor of the signalling lymphocytic activation molecule
SLE	Systemic Lupus Erythematosus
SLO	Secondary Lymphoid Organ
SSc	Systemic Sclerosis
STAT3	Signal Transducer and Activator of Transcription 3
T2-MZP	Transitional 2-Marginal Zone Precursor
TAMs	Tumour-Associated Macrophages
TB	Tuberculosis
T-bet	T-box Expressed in T cells
TCR	T Cell Receptor
TD	T-Dependent
TFH	Follicular helper T cell
TGF-β	Tumour Growth Factor-β
Th	T-helper
Tim-1	T cell Immunoglobulin and Mucin-domain-containing protein
TNF	Tumour Necrosis Factor
TNFSF13	TNF Superfamily Member 13
Tregs	Regulatory T cells

TRL	Toll-like Receptor
TSLP	Thymic Stromal Lymphopoietin
t-SNE	t-stochastic neighbour embedding
UMAP	Uniform manifold approximation and projection
UMI	Unique molecular identifier
VCAM-1	Vascular Cell Adhesion Molecule-1
VEGF	Vascular Endothelial Growth Factor
VLA-4	Very Late Antigen-4
XBP1	X-Box Binding Protein 1

Thesis Abstract

B cells do not just produce antibodies, they are critical antigen-presenting cells and produce a battery of cytokines. Their role in disease pathogenesis, however, is relatively less studied. A pathogenic outcome can arise from individual or overlapping mechanisms. In the case of B cells, this could arise through uncontrolled production of inflammatory cytokines (like IL-6 and TNFα), prolonged antigen presentation leading to excessive T cell responses, production of autoantibodies and disruption of tissue architecture, function, and physical properties. In this thesis, I examine B cells in chronic obstructive pulmonary disease (COPD) in the presence or absence of cigarette smoking and also B cell subsets in COVID-19 (introduced to allow continued laboratory work through the pandemic shutdown).

The research described in this thesis takes our knowledge of B cell subsets in the lung and blood to an unprecedented depth. Previously unidentified discoveries included the new identification of Tim1+ B cells in COPD, enhanced double-negative memory B cells in COPD and infection that likely explain increased susceptibility to autoimmunity, the influence of smoking on B cell subsets and a predominance of IL-10-producing B cells in convalescent COVID – amongst others. Using Hyperion imaging, we also describe ectopic B cell follicles adjacent to bronchioles that may perturb lung function. Overall, the data in this thesis indicates that B cells are likely to be involved in disease pathogenesis, and therapeutic manipulation should be considered as a treatment option.

Declaration

No portion of the work referred to in the thesis has been submitted in support of an application for another degree or qualification of this or any other university or other institute of learning.

Copyright Statement

i. The author of this thesis (including any appendices and/or schedules to this thesis) owns certain copyright or related rights in it (the "Copyright") and s/he has given The University of Manchester certain rights to use such Copyright, including for administrative purposes.

ii. Copies of this thesis, either in full or in extracts and whether in hard or electronic copy, may be made only in accordance with the Copyright, Designs and Patents Act 1988 (as amended) and regulations issued under it or, where appropriate, in accordance with licensing agreements which the University has from time to time. This page must form part of any such copies made.

iii. The ownership of certain Copyright, patents, designs, trademarks and other intellectual property (the "Intellectual Property") and any reproductions of copyright works in the thesis, for example graphs and tables ("Reproductions"), which may be described in this thesis, may not be owned by the author and may be owned by third parties. Such Intellectual Property and Reproductions cannot and must not be made available for use without the prior written permission of the owner(s) of the relevant Intellectual Property and/or Reproductions.

iv. Further information on the conditions under which disclosure, publication and commercialisation of this thesis, the Copyright and any Intellectual Property and/or Reproductions described in it may take place is available in the University IP Policy (see http://documents.manchester.ac.uk/display.aspx?DocID=24420), in any relevant Thesis restriction declarations deposited in the University Library, The University Library's regulations (see http://www.library.manchester.ac.uk/about/regulations/) and in The University's policy on Presentation of Theses.

Acknowledgements

Overall Thesis Structure

The overall aim of this project was to investigate the characteristics of B cell phenotype and function in the lungs of patients with Chronic Obstructive Pulmonary Disease (COPD). This aim was completed but interrupted by the COVID-19 pandemic. Over one year of laboratory, time was lost on the original project due to the pandemic.

This thesis was written in journal format because 1) the introduction was partially published as a review article in Immunology Reviews in January 2022. The first results Chapter is currently being written for publication (Chapter 3), and the second results chapter (Chapter 4) details longitudinal alterations in B and T cell functions in acute and convalescent COVID-19 patients and is published in Med (N Y) 2021.

Chapter 5 finishes with an overall discussion linking our findings from COPD and COVID-19 studies.

Due to the interruption caused by the pandemic, writing the work in a traditional format was not appropriate.

Chapter 1:

General Introduction

1.0 Statement

Part of this introduction has been published as a review in Immunological Reviews. Halima Ali Shuwa and Madhvi M wrote this review, analyzed previous literature, and prepared the figures and tables with critical and intellectual input from Tracy H. This manuscript occupies pages 56 – 73 of this thesis ([10.1111/imr.12941](10.1111/imr.12941))

1.1 Introduction

This thesis explores the different B cell subsets in the lungs of patients with acute and chronic lung inflammation, specifically in chronic obstructive pulmonary disease (COPD) and SARS-CoV-2 infection. B cells are an abundant cell type in chronic inflammatory lung disease, yet their role in disease pathogenesis is controversial. As an integral part of the adaptive humoral immune system, B cells produce antibodies that protect the body from a wide range of microbial (antigenic) agents. Abnormalities in B cell development and function lead to autoimmunity, tumours, immune deficiencies, and allergic reactions. B cells can exist as one of several subsets, but this detail in lung disease is not precisely known. Furthermore, B cells may adapt to different tissue microenvironments like that described for macrophages.

1.2 B cell development

B cells originate from the hematopoietic stem cells (HSC) in the bone marrow (BM) [1]. The initial signal for B cell development in the BM starts when VCAM-1 (Vascular Cell Adhesion Molecule-1) on the stromal cells binds to VLA-4 (Very Late Antigen-4) on HSCs, this initiates heavy chain gene rearrangement in early pro-B cells [2]. The second signal is from stem cell factor (SCF) expressed on stromal cells, that binds and activates the receptor tyrosine kinase, c-kit, on the surface of early pro-B cells; this causes the expression of interleukin-7 (IL-7) by stromal cells leading to heavy chain V(D)J gene recombination [3–5,6(p7)]. IL-7 binds to its receptor on pro-B cells, driving their further maturation [4]. At this stage, the genes for the heavy-chain immunoglobulin are transcribed and translated. There is downregulation of VLA-4 and c-kit, causing the release of

pro-B cells from the stromal cell in the late pro-B cell stage [7,8]. The translated heavy chains organise and are expressed on the surface of the B cell along with a protein complex called the surrogate light chain; this is known as the pre-B cell receptor (pre-BCR). At this point, light chain VJ gene rearrangement occurs [7,8]. Light and heavy chains are expressed on the B cell surface as immunoglobulin-M (IgM), which also serves as the B cell receptor (BCR). The cell is referred to as an immature B cell [9]. Immature B cells migrate to secondary lymphoid organs (SLO), upregulating IgD and IgM and is referred to as a naïve B cell. The naïve B cell remains in this state until it meets its antigen and becomes a mature B cell. **Figure 1.1** summarises the stages of B cell development.

B CELL MATURATION
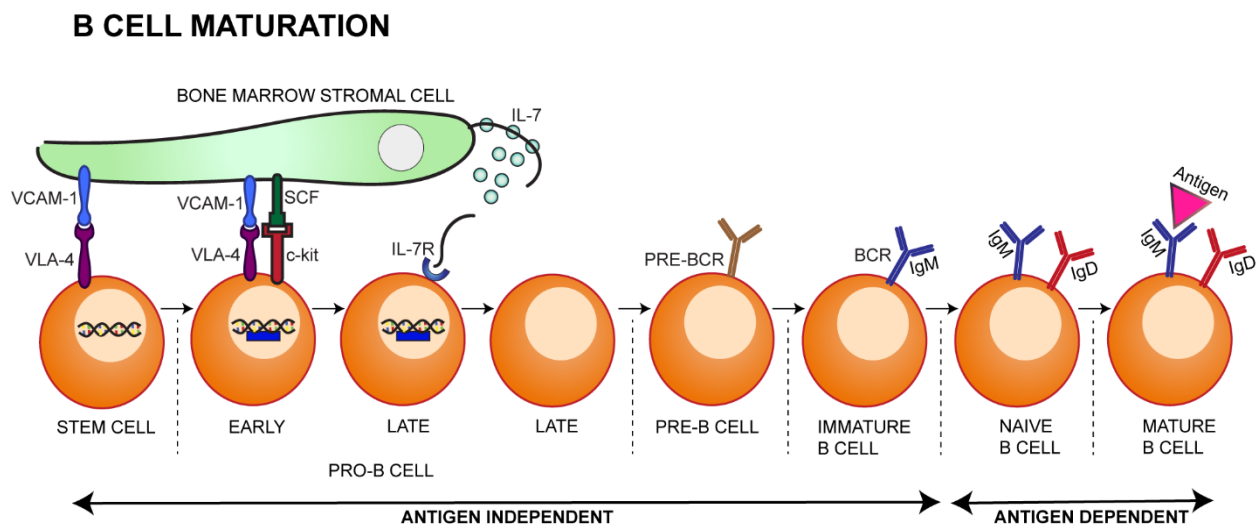
Figure 1.1: Schematic outline of B cell development

1.2.1 B cell activation

Immature B cells exit the BM and travel to the SLO via the circulation. The SLO is the primary site of B cell activation and has specific anatomical locations for B and T cells. B cells reside in germinal centres (GC) within follicles, whereas T cells are predominantly present in the para-cortex [10]. B cell signaling requires clustering or cross-linking of BCR upon antigen recognition. This clustering of the BCR is required to activate accessory proteins like Igα and Igβ. The antigen-binding signal is then conveyed to the nucleus. This clustering of BCR depends on the type of antigen a B cell encounters. An antigen with multiple repeating epitopes (like polysaccharides, glycolipids, nucleic acids) can directly cross-link the BCR and activate B cells to produce antibodies without T cell help. Such antigens are called T-independent antigens, and B cell

activation without T cell help is called T-independent B cell activation [11–15]. However, the largest groups of antigens are protein in nature and do not contain multiple repeating epitopes, making the cross-linking of the BCR difficult. So, when a B cell encounters protein antigens, T cell help is required to trigger B cell activation. Antigens that trigger B cell activation with the help of T helper cells are known as T-dependent antigens, and B cell activation, which requires T cell help, is known as T-dependent B cell activation [11].

1.2.1.1 T cell Independent Activation

T-independent antigens are multivalent and have multiple, repetitive, and identical epitopes [15]. B cells recognize and bind to this antigen via BCR clustering, which is the first signal required for the T-independent activation of B cells. The second signal can be derived from other molecules present on the antigen. For example, B cells also have toll-like receptors (TLR) that recognize various microbial surface molecules. The recognition and binding of antigens by TLRs generate a second signal for T-independent B cell activation (**Figure 1.2**). B cells activated via this route mainly differentiate into plasma cells that secrete IgM antibodies and not memory B cells because memory cell production requires T cell help [11–13,15,16].

T-INDEPENDENT B CELL ACTIVATION
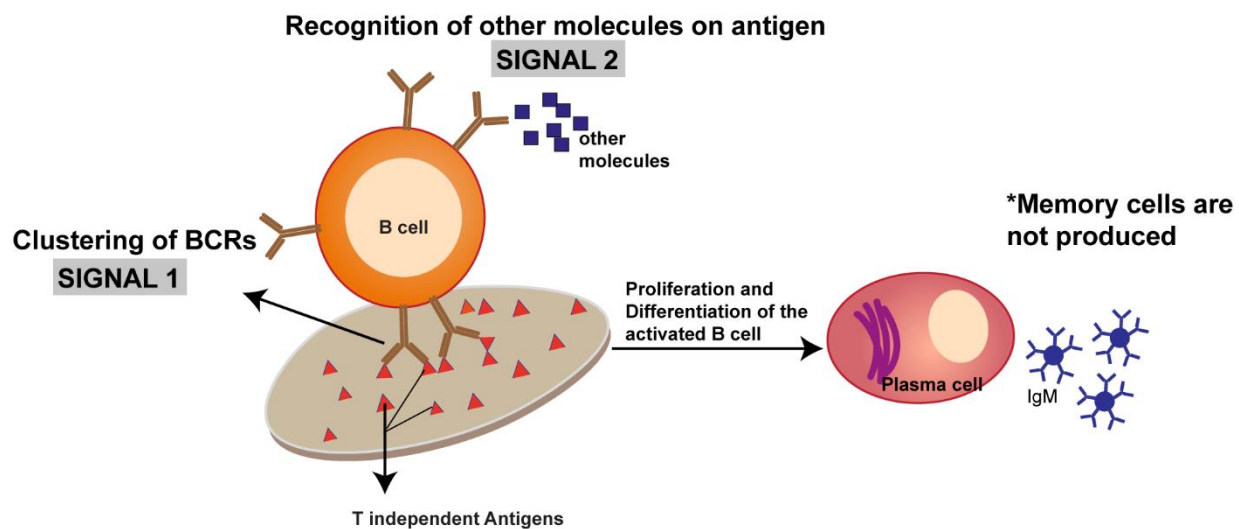
Figure 1.2: T-independent activation of B cell

1.2.1.2 T cell Dependent Activation

As discussed earlier, protein antigens cannot crosslink multiple BCRs, because these antigens lack repetitive and identical epitopes. Thus, when B cells encounter protein antigens, they require T cell help to get activated [11]. T-dependent B cell activation is a three-signal process; the first signal is generated by antigen recognition and binding by the B cell. Besides antigen recognition, B cells can also function as antigen-presenting cells; they internalize antigens, process them into peptides and present them on their surface via major histocompatibility complex class II (MHC II) peptide complexes. T cells recognizing the same antigen can also be activated by dendritic cells and macrophages that have ingested the antigen and presented it in the same way [17].

Activated B cells express a variety of cytokines and co-stimulatory receptors, of which CD40 is essential [18–21]. When B cells and T helper cells come in proximity, T helper cells recognize and bind to peptide antigens presented on MHC-II complexes on the surface of B cells. CD40 on B cells interacts with CD40-ligand (CD40L) on T helper cells, providing a critical second signal for B cell activation [18,19(p40),20(p40)].

Cytokine released by T helper cells provides the third signal for T-dependent B cell activation. The interaction of B and T cells induces the expression of new cytokine receptors on the surface of the B cell. T cells release cytokines such as IL-4 that bind the cytokine receptors present on B cells. As a result, B cells start to proliferate and differentiate into antibody-secreting plasma cells and memory B cells (**Figure 1.3**) [22,23].

T-DEPENDENT B CELL ACTIVATION

SIGNAL 1
Antigen Recognition and
Binding by B cell

SIGNAL 2
B and T cell interaction
(CD40-CD40L binding)

SIGNAL 3
Cytokine Help by
T Helper cells
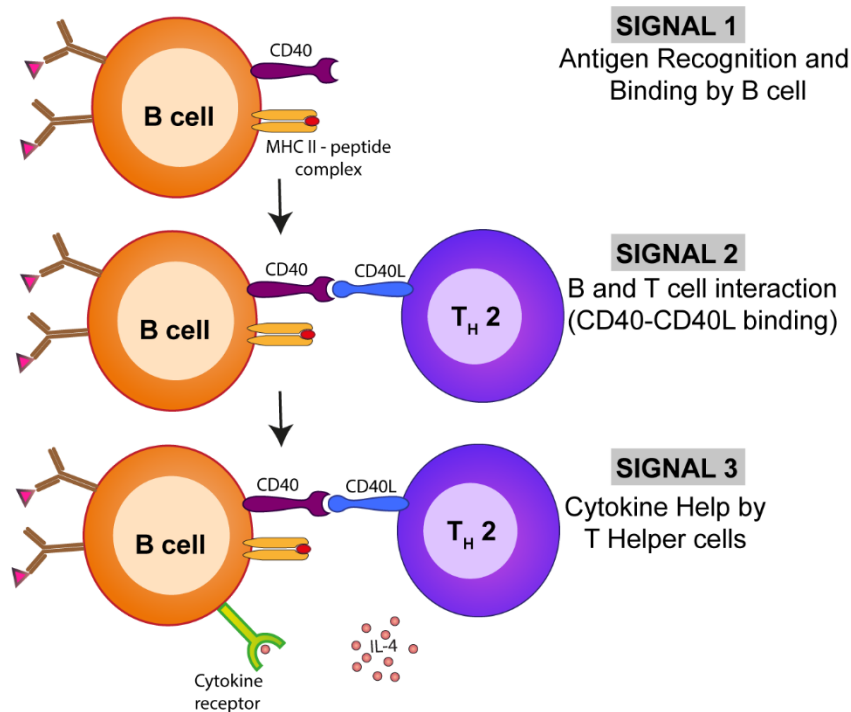
Figure 1. 3: T-dependent activation of B cell

1.3 B cell subsets

Much of the knowledge on B cell subsets have arisen from mouse models [24–26]. However, with the study of tonsils, peripheral blood, non-malignant lymph nodes, and spleen cells, our understanding of human B cell subsets has increased in recent years [27–44]. In mice, three subgroups of B cells arise during fetal life: B-1, B-2 and marginal zone (MZ) B cells (some reports combine B2 with MZ B cells). B-1 cells differ considerably from B-2 and are formed during early development in the fetus. They have peculiar tissue distribution and phenotypic and functional characteristics [45]. B-1 cells are divided into two subpopulations, B-1a and B-1b that differ in their development, phenotype and function. B-2 cells, on the other hand, are produced during late fetal development and in adults [45–47] and act mainly in adaptive immune responses [48]. MZ B cells are those found predominantly in the marginal zones of B cell follicles in the white pulp of the spleen and share some features with both B-1 and B-2 cells [49–53].

1.3.1 B-1 cells

B-1 cells are predominantly located in the pleural and peritoneal cavities [54,55]. A small percentage of B-1 cells are found in the spleen but rarely in the circulation, bone marrow (BM) and lymph nodes (LNs) [54,56]. B-1 cells are typically not found in the germinal centre (GC) of B cell follicles [48], but they can move from pleural and peritoneal spaces into the secondary lymphoid organs (SLOs) upon infection with influenza virus or after intravenous injection of lipopolysaccharide (LPS) where they differentiate into plasma cells (PCs) [57]. B-1 cells produce the majority of Igs found at mucosal sites of both respiratory and gastrointestinal tracts [48,58]; they predominantly secrete IgM and preferentially class switch to IgA upon stimulation [59,60].

In contrast to other B cell subsets, which are produced throughout life in the bone marrow, the generation of B-1 cells occurs early in life from progenitors present in the fetal bone marrow [61]. In humans, B-1 cells are the main producers of natural antibodies (Nabs), a type of antibodies that are produced naturally and have been demonstrated to be important in early protection against infectious substances [62].

1.3.1.1 B-1 cells in mice

Initially, B-1 cells in mice were recognised by the production of self-reactive IgM molecules and the expression of CD5 marker on their surface [46,62–64]. Later, sub-populations of B-1 cells that do not express CD5, but with similar phenotypic characteristics were isolated [65], hence, B-1a and B-1b cells. Different markers are now used to differentiate between B-1 subsets, these include: $CD5^+CD11b^+(Mac-1)CD45RA^{low}(B220)IgM^{hi}IgD^{low}CD23^-CD43^+$ for B-1a cells; $CD5^-CD45RA^{low}IgM^{hi}IgD^{low}CD23^-CD43^+$ for B-1b cells; and $CD5^-CD11b^-CD45RA^{hi}IgM^{low}IgD^{hi}CD23^+CD43^-$ for B-2 cells [66–68]. So B-1a cells are the major $CD5^+$ expressing B cells in mice [68].

1.3.1.2 B-1 cells in humans

B-1 cells in humans, like their murine counterparts, also express CD5 molecules [69]. However, unlike in mice, CD5 expression is inducible by stimulating the B cell receptor (BCR) and CD40 [70]. Aside from B-1 cells, other cells in humans are also $CD5^+$; these include the pre-naïve, naïve transitional, immature and memory B cells [71–73]. Human B-1 cells are found in abundance in early ontogeny [71,74]; they produce a large number of NAbs that are reactive to various antigens, including self-antigens [75,76]. In humans, CD5 expression is assumed to occur naturally in B-1 cells but can be induced in B-2 cells [77,78].

1.3.2 B-2 cells

B-2 cells complete their development in the spleen to become MZ or follicular (FO) B cells. The spleen is the largest SLO in the body; it is divided into the erythrocyte-rich zone (red pulp) and the lymphocyte-rich zone (white pulp). The white pulp comprises B cell, FO and T cell zones and is the home for the FO B cells[79]. This lymphocyte-rich area of the white pulp scans the filtered blood from the red pulp for antigens [80]. FO B cells form the GCs of the spleen; their activation depends on T cells (TD), and they act as professional antigen-presenting cells (APCs) to T helper cells present in the follicles [81]. The MZ is a special area of the spleen that allows the passing of filtered blood from the red to the white pulp; it scans the filtered blood for the presence of antigens and is the home of MZ B cells. MZ B cells react with antigens directly from filtered blood that passes through the MZ, and their activation is usually independent of T cells [82].

1.3.2.1 Follicular B Cells

B cells leave the BM as immature B cells, undergo transitional stages before reaching maturity and becoming FO or MZ B cells in the spleen [83–85,86]. Transitional B cells have a short lifespan of about 1-5 days. In the T1 stage, B cell receptors (BCR) with a strong reaction to self-antigens are deleted by apoptosis [87]. In contrast, in the T2 stage, BCRs with an intermediate/low response to self-antigens are positively selected for survival [88,89].

FO B cells reside in the splenic follicles, LNs, and ectopic and tertiary lymphoid follicles (LFs). FO B cells are activated by T-dependent activation and develop into either PCs or memory B cells [90]. FO B cells that can actively react to antigens develop into PCs with a short lifespan. In contrast, FO B cells with a weak response to antigens mature into GC B cells that live longer and undergo somatic hypermutation (SHM) and affinity maturation [90,91]. These choices are controlled by the transcription repressor protein BCL-6 [92].

GCs are biological sites within SLOs predominantly made up of FO B cells, follicular dendritic cells (FDCs), follicular helper T cells (TFH), and others. FDCs continuously present antigens to the FO B cells and maintain them in an activated state; this enhances their affinity to the presented antigens (a process called affinity maturation). TFH acts as a co-stimulatory cell that activates FO B cells via the CD40-CD40 ligand (CD40L) interaction and the release of interleukin-21 [93,94]. Mutations of single nucleotides within the gene sequence of the antigen-binding site of Igs also occur in the GC, this mutation is called somatic hypermutation (SHM). It allows Igs to become extremely specific to the encountered antigen [90,91].

1.3.2.2 Marginal Zone (MZ) B Cells

Immature B cells enter the spleen during development and transition to MZ or FO B cells. The MZ of the spleen is the site of blood filtration, so cells within it are continuously exposed to blood-borne antigens. The MZ primarily comprises the MZ B cells, DCs, macrophages, and reticular fibroblasts. MZ B cells are activated in a TI manner through stimulation of toll-like receptor (TLR) molecules and help from the B cell-activating factor of TNF family (BAFF) and Notch 2/δ1 signalling [95]. MZ B cells, like B-1 cells, produce poly-reactive antibodies that are usually IgM and react to a variety of antigens, including a few self-antigens, and can also present antigens on CD1d molecules [96,97].

Aside from MZ and FO areas of the spleen, B cells are found in the sinuses of lymph nodes (LNs), the epithelial dome of Payers patches, and the epithelium of the tonsils. Like the spleen, these sites also have unlimited access to antigens and contain macrophages and DCs [98–101]. In humans, MZ B cells are identified by $IgM^{hi}IgD^{low}CD1c^+CD21^{hi}CD23^-$ $CD27^+$ markers [98,102–105]. **Figure 1.4** highlight the main features and surface phenotypes of B cell subsets in human.
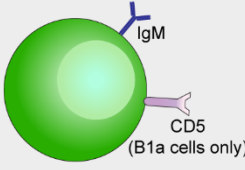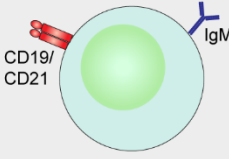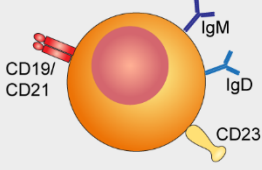
Cell Surface Phenotype	CD5$^+$, CD19^{hi}, CD1d^{mid} CD43$^+$, CD23$^-$, IgM^{hi} IgD^{low}	CD5$^-$, CD19^{mid}, CD1d^{hi}, CD1c$^+$, CD21^{hi}, CD43$^-$, CD23$^-$, CD27$^{+'}$ IgM^{hi} IgD^{low}	CD5$^-$, CD19^{mid}, CD1d^{hi} CD43$^-$, CD23$^+$, IgM^{low} IgD^{hi}
Features	Located in pleural and peritoneal cavities.	Located in outer zone of white pulp of the spleen (marginal zone)	Located in secondary lymphoid organs
	Originate from self renewing (division of existing B1 cells)	Derived from T2 transitional population	Derived from precursors in bone marrow
		Specialised for recognizing blood-borne antigens	Highly diverse V-region
			Somatically hypermutated
	Respond to carbohydrate antigens	Respond to both protein and carbohydrate antugens	Respond to protein antigens
	Produce high levels of IgM	Produce broad cross-reactive IgM antibodies	Produced high levels of IgG
	Very little or no memory	Long lived (memory)	Long lived (memory)

| B1 B cells | Marginal zone | Follicular |

Figure 1.4: Different B cell subsets and their primary features

1.4 B cell compartmentalisation, growth, and survival

Many cellular and molecular mechanisms are involved in B cell movement and homing to the SLOs. These mechanisms usually consist of chemo-attractants that attract B cells to migrate into the SLOs, and proteins (like *pyk*-2) that nourish and sustain the cells within the lymphoid organs [106,107,108]. Adhesion molecules like lymphocyte function-associated antigen-1 (LFA-1) and α4β1 integrins are expressed on B cell surfaces and bind to the intercellular adhesion molecule-1 (ICAM-1) and vascular cell adhesion molecule-1 (VCAM-1), respectively. ICAM-1 and VCAM-1 ligands are expressed on the surfaces of endothelial and hematopoietic cells within the MZ and assist in guiding B cells into the MZ [109]. On the other hand, FO B cells express the chemokines CXCL13 and CCR7 that bind with their cognate ligands, CXCR5 and CCL19/21, respectively. The FO stromal cells and FDCs express CXCR5, while CCL19/21 is expressed within the T cell zone.

These chemokines ensure the migration and retention of FO B cells in the FO and GCs of lymphoid organs [110]. Proteins like BAFF (also known as Blys or TNFSF13) are expressed on surfaces of macrophages, stromal and dendritic cells and bind with BAFF-receptors (BAFF-R) expressed on the surface of B cells. The interaction between BAFF and BAFF-R helps B cell survival in the spleen [111,112].

1.5 Classification of B cells in humans

Upon antigen encounter, B cells proliferate and differentiate into PCs or memory B cells depending on the amount and type of antigens they encounter, their interaction with T cells, and their BCR signalling strength. T cell-independent responses produce PCs that secrete short-lived IgM with weak antigen binding. While B cells that are activated through T cell-dependent stimulation differentiate into either memory B cells, B cells that enter GC reaction or become long-lived PCs that secrete antibodies with strong antigen-binding ability [12,113–115]. In the GCs, B cells undergo a GC reaction where FDCs, with the help of T helper cells, continuously present antigens to the B cells, a process called affinity maturation. Here, the antigen binding ability of the surface Igs is sharpened and becomes exceptionally specific to a particular antigen. In addition to affinity maturation, genes of the antigen-binding region of Igs are constantly mutated through SHM to improve the framework of the antigen-binding site [113–115]. Some B cells in the GC experience class switch recombination, where the initial Cμ and Cδ genes (IgM and IgD genes, respectively) of the Ig constant region are replaced with either Cγ1-4, Cα or Cε (IgG1-4, IgA or IgE, respectively) [113]. **Table 1.1** summarises the major B cell subsets, the markers used to identify them, and their main properties.

Table 1.1: Summary of different B cell subsets, their phenotypic markers and property

B cell population		Primary markers	Additional markers	Properties
Transitional	T1/T2	CD19+ IgD+ CD24hi CD27- CD38hi	IgM++ CD10hi/+	Development precursor
	T3	CD19+ IgD+ CD24hi CD27- CD38+ CD21+	IgM+ CD10+/-	Activated naïve

Naive	Resting	CD19+ IgD+ CD24+ CD27- CD38+ CD21+	IgM+	Mature antigen inexperienced B cells
	Activated	CD19+ IgD+ CD24- CD27- CD38- CD21-	IgM+ CD23-	Precursor of short-lived plasmablasts
Memory	Unswitched	CD19+ IgD+ CD24+ CD27+ CD38+/low CD21+	IgM++ CD1c+	Natural memory
	Switched	CD19+ IgD- CD24- CD27+ CD38- CD21-	IgG/IgA+	Effector memory, plasmablasts/plasma cell precursor
Double negative (DN)	DN1	CD19+ IgD- CD24+ CD27- CD38+ CD21+	IgM/IgG/IgA+ CXCR5+ FcRL4- FcRL5-	Memory precursor
	DN2	CD19+ IgD- CD24- CD27- CD38- CD21-	IgM/IgG/IgA+ CXCR5- FcRL4+ FcRL5+ CD11c+ Tbet+	Extrafollicular antibody-secreting cell precursor
Antibody secreting cells	Plasmablasts	CD19+/- IgD- CD24- CD27hi CD38hi	CD20- CD138- Ki67+	Antibody secretion
	Plasma cells	CD19+/- IgD- CD24- CD27hi CD38hi	CD20- CD138+ BLIMP-1+	Antibody secretion

1.5.1 Transitional B cells

Following exit from bone marrow, new Immature B cells differentiate through several transitional maturation stages before becoming functional naïve FO B cells [116]. These B cells are termed transitional B cells. Similar to their mouse counterparts, three major transitional B cells have been identified in human circulation; T1, T2 and T3 [33,43,117]. Transitional B cells are usually characterised by their varying levels of expression of IgM, CD24, CD9, CD38, and CD10 [33,43]. They are the primary link between immature B cells in the BM and the peripheral mature B cells. Transitional B cells, specifically those CD24hiCD38hi, are phenotypically and functionally related to regulatory B cells (Bregs) [118]. They can produce IL-10 and regulate the proliferation and differentiation of CD4+ T cells to T helper (Th) effector cells [119].

1.5.2 Naïve B cells

Naïve B cells in humans are characterised by their high IgD expression and positive staining of IgM. Naïve B cells can be separated from transitional B cells by their down-regulation of CD24 and CD38 and lack of CD27 expression [116]. Other markers used to characterise naïve B cells include the expression of CD21 and CD23 and the absence of activations markers, CD25, CD80, CD86, and CD95 [116,120].

1.5.3 Memory B cells

Memory B cells are formed when a naïve immature B cell encounters an antigen in the spleen or other lymphoid organs. Upon antigen encounter, the naïve B cell differentiates into either a PC (that starts releasing a large number of antibodies immediately) or a memory B cell (that circulates in the body and becomes reactivated in a second encounter with the same antigen). The molecular mechanisms surrounding the development of memory B cells are not well understood. Some proteins, like interleukin-24 (IL-24) and NF- κB (a transcription protein that induces the activation of CD40 and BCR), encourage the formation of B cells in SLOs [121]. In humans, almost all memory B cells are generated after the GC reaction; they have mutated Ig (as a result of SHM), are usually class-switched, and are defined by CD19$^+$CD27$^+$CD38$^{-/low}$ expression [122,123].

1.5.3.1 Functional and phenotypic features of Memory B cells

Memory B cells (MBCs) are antigen-experienced cells that are primed to generate fast and effective antibody responses upon secondary exposure [124–126]. In humans, circulating MBCs are

mainly classified based on the surface expression of CD38, CD21, IgD and CD27 but not exclusively. Most MBCs express a BCR with a relatively high antigenic affinity [100]. They secrete mutated and class-switched Igs depending on the type and quantity of the antigen that activates them [127,128] and can survive for months, decades or even a lifetime [101]. MBCs spend most of their lives in a lag phase until a secondary antigen encounter, where they immediately become reactivated and differentiate into PCs (and begin to release antibodies) or re-enter the germinal centre (to undergo another round of affinity maturation to further adapt to the invading antigens) [129,130][131]. MBCs usually occupy high-density antigen areas like the MZ and Peyers patches, they undergo frequent clonal expansion, with high expression of co-stimulatory molecules (like SLAM, TNF, TLR7/9, CD27, CD80, CD86, and IL-21 receptor), a higher expression of anti-apoptotic molecules (like BCL-2) and signal transducers, but they have reduced or low expression of transcription factors (like KLF4, KLF9, and PLZF) [132–134].

1.5.3.2 Memory B-cell Subsets in human

Human MBC subsets were initially thought to be predominantly composed of IgG$^+$ class-switched MBCs, ~ 25% of peripheral blood (PB) B cells[135]. However, the discovery of IgM+ B cells that are somatically mutated pointed to the existence of non–class-switched or unswitched MBCs [38,136–138]. MBC subsets are commonly identified based on the expression of IgD and CD27 [138,139]. IgD$^+$ subsets of MBCs include the IgM$^+$ (CD27$^+$IgD^{low}IgM^{++}) and IgM$^-$ (IgD-only) MBCs [138]. While CD27$^+$IgD$^-$ MBCs, include both IgM-only (pre-switched) and IgG, IgA, or IgE-expressing (switched) MBCs [137–141]. Since CD27 is expressed on class-switched MBCs, it is generally used as MBC marker [135]. However, recent studies identified other MBC populations with low to negative expression of CD27 and switched Ig heavy chain, leading to the discovery of the CD27-IgD-atypical double-negative (DN) MBC populations [142].

1.5.3.2.1 IgD-only memory B cells

These rare MBCs are seen in less than 10 % of individuals and account for about 0.1-0.5 % of total B cells in the body [135]. IgD-only B cells are hypothesised to be generated in response to super-antigens and in some upper respiratory tract infections (like Moraxella *catarrhalis*) [143]. Among the MBC subsets, IgD$^+$IgM$^-$ MBCs have the highest Ig gene mutation [144,145].

1.5.3.2.2 IgM-only and IgM⁺IgD⁺ memory B cells

Two subsets of IgM MBCs are present in humans: IgM⁺IgD[low/ −] and IgM⁺IgD⁺ MBCs. Both have mutated Ig genes, both are CD27⁺ cells, and account for approximately 5 % and 15 % of total B cells (respectively) in both SLOs and the circulation [127,128,146]. IgM⁺IgD⁺CD27⁺ MBCs are developed in a pre-GC reaction due to mutation through BCR diversification. In contrast, IgM⁺IgD⁻CD27⁺ MBCs are developed during a GC reaction after SHM [147,148]. IgM antibodies have a low affinity to antigens because they are produced before SMH; they, however, form pentameric IgM molecules with ten antigen binding sites to compensate for the low affinity of the IgM monomers [149]. This pentameric IgM molecule can simultaneously bind multivalent antigens like the bacterial capsular polysaccharides [149–152].

1.5.3.2.3 IgG memory B cells

About 15-20 % of circulating B cells in adults are IgG⁺ MBCs, mostly of IgG1, IgG2, or IgG3 and rarely IgG4 subtype [153]. Most IgG⁺ MBCs are CD27⁺, have undergone SHM and have mutated Ig gene [153,154]. However, about 20-25 % of Ig⁺ MBCs do not express CD27 (IgG⁺CD27⁻), have no or few mutated Igs, and are primarily of the IgG3⁺ subtype. These IgG⁺CD27⁻ subpopulations are mostly seen in the elderly and less frequently in young adults [155,156]. Most IgG MBCs differentiate into PCs on a secondary antigenic challenge; only a few re-enter a GC reaction [90,157,158]. The primary function of IgG MBCs is prompt differentiation into IgG-secreting PCs. The secreted IgG antibodies can be found in the blood and extracellular fluid with higher affinity, where they neutralise viruses, bacteria and toxins, and opsonise them for phagocytosis, and subsequently activate the complement system [159–161].

1.5.3.2.4 IgA memory B cells

Most IgA MBCs are found in the intestinal and other mucosal-associated lymphoid tissues (MALT), where they function as the first line of defence, with only about 10 % in circulation [135,162]. Most IgA produced at mucosal sites is secreted into the lumen in a dimeric form joined together by a secretory component [163]. Dimeric IgA agglutinates antigens in a process known as immune exclusion [163]. IgA MBCs are usually CD27⁺ cells with somatically mutated Ig genes, although a few of these cells are IgA⁺CD27⁻. These IgA⁺CD27⁻ memory cells have reduced Ig gene mutation and secrete poly-reactive Ig that reacts with numerous bacterial antigens [164]. Secreted IgA antibodies are either monomeric or dimeric [165]. The monomeric IgA antibodies enter the blood or

extracellular fluid, while the dimeric IgA antibodies enter the lamina propria of various epithelia at mucosal sites to establish healthy microbiota and protect against infection [166].

1.5.3.2.5 IgE memory B cells

Despite their role in asthma and allergic reactions, IgE MBC subsets are understudied in humans, and IgE subsets have not been identified to date. Some studies in mice have shown a few IgE MBCs that descend from class switching of IgG1^{+} GC B cells. However, these IgE^{+} B cells are promptly transformed into PCs upon switching to IgE+ memory B cells [167]. IgE MBCs play a vital role in IgE-mediated allergic reactions because of their ability to promptly differentiate into IgE-secreting plasma cells that secrete allergen-specific IgE antibodies, which sensitize mast cells and basophil to release pro-inflammatory mediators resulting in type 1 hypersensitivity reaction [168]. IgE MBCs are also involved in protection against parasitic helminth infections and toxins [169].

1.5.3.2.6 Atypical Memory B cells (Double Negative, DN)

Aside from the commonly known subsets of MBCs discussed above, several other subsets are reported. These unusual B cells are usually tissue-resident and are commonly observed in response to chronic infections like Human Immunodeficiency Virus (HIV) [170], Hepatitis C virus [171], malaria [172], influenza [173,174], tetanus vaccination [175] and autoimmune diseases [32,176]. They are termed double-negative (DN) memory B cells because they lack the expression of both the conventional naïve (IgD) and memory (CD27) B cell markers. The tissue-resident CD21^{low}CD27^{−} MBCs are generated by T-dependent responses, are class-switched, have mutated Ig genes, and express the Fc receptor-like protein 4 (FCRL4; a type of inhibitory receptor) molecule on their surface [177]. These cells are generated upon stimulation by T cell cytokines (T dependent). Conversely, peripheral blood CD21^{low}CD27^{−} memory B cells are usually seen in response to autoimmunity, ageing, and some unusual infectious conditions, and they are FCRL5^{+} [178,179].

DN B cell phenotypes differ depending on local factors but generally are CD19^{hi}; CD38^{+/-}; CD11c^{++}; T-bet^{++}; CD11c^{+}T-bet^{+}; FcRL4^{+}; FcRL5^{+}; CD24^{+/-}; CD23^{-}. DN cells are predominantly IgG^{+} or IgA^{+}, with a small fraction of IgM^{+} cells [29,116,142]. Two types of DN cells were identified in Systemic Lupus Erythematosus (SLE); DN1 cells comprise the majority of the DN populations in health and are CD21^{+}CXCR5^{+}CD11c^{-}, and DN2 are predominantly observed in SLE and are CD21^{-}CXCR5^{+}CD11c^{++} [180].

The main functions of DN cells are still unclear. However, DN MBCs were initially considered part of exhausted or anergic B cells that arise from chronic antigenic stimulation because of their

association with chronic infection. However, recent studies of patients with systemic lupus erythematosus suggested DN cells as short-lived activated cells that subsequently differentiate into plasma cells [180]. DN cells are also thought to be responsible for secreting auto-antibodies that target membrane proteins on uninfected erythrocytes leading to anaemia [181].

1.5.4 Human Antibody Secreting Cells (ASCs)

1.5.4.1 Plasmablasts

In humans, plasmablasts are proliferative blood short-lived antigen-secreting cells (ASCs) generated in response to acute infection or vaccination that transiently produce serum antibodies [182]. IgG-secreting plasmablasts can also be generated from MBCs in response to a secondary systemic immune response [183]. Human plasmablasts are characterised as $CD19^{low/+}$, $CD27^{hi}$, $CD38^{hi}$, $CD24^-$, $CD20^{-/low}$, and $CD138^-$ [116,184–187]. The origin of human plasmablasts is unclear, with many suggesting that they are precursors of long-lived plasma cells. However, studies show that most ASCs undergo apoptosis once the infection is cleared. Only a small proportion differentiate into long-lived plasma cells [188]. Plasmablasts are also attracted by CXCL12 and express CCR10 and β7 integrin (an adhesion molecule), suggesting that they come from mucosal immune responses and can return to the mucosal tissue [189].

1.5.4.2 Plasma Cells

Plasma cells are terminally differentiated B cells that actively secrete the antibodies needed for humoral immunity. These cells occupy the red pulp of the spleen and the medullary cords of the LNs that are rich in blood supply and are said to be found around the sinusoidal endothelial cells of the BM; they travel in the blood circulation to the BM in the form of plasmablasts. PCs have the distinct characteristic of a small and condensed nucleus with extensive cytoplasm that contains an enlarged Golgi body and numerous rough endoplasmic reticulum [190]. PCs generated outside GCs are short-lived and secrete high amounts of unmutated Igs (usually IgM and IgG) [191]. They occupy the border between the B and T cell zones in the spleen's red pulp and medullary cords and LNs, respectively [191]. PCs formed in GC reactions are long-lived, secrete Igs with high antigen affinity and are found predominantly in the GCs or BM [191]. Antibody-secreting PCs are characterised by high levels of CD38 and CD27 with downregulation of CD19 and CD20 expression [116,192]. PCs are more mature cells that are usually distinguished from plasmablasts by CD138 expression. They also express transcriptional factors, including Blimp-1, IRF4, and XBP1, that are important for ASC differentiation [192,193,194(p4),195,196,197(p1),198].

PCs' primary function is producing antibodies following vaccination or infections, thus fostering immune development. So PCs are solely responsible for maintaining the immunity in both animals and humans through antibody secretion. Aside from antibody secretion, PCs also affect other pathologic and non-pathologic processes; they function as critical regulators of immune responses via cytokine secretion like IL-21 [193,199,200].

Initial studies of B cells focused on their role in antibody secretion. However, they are known to play other critical roles in many processes (reviewed in **Figure 1.5**).
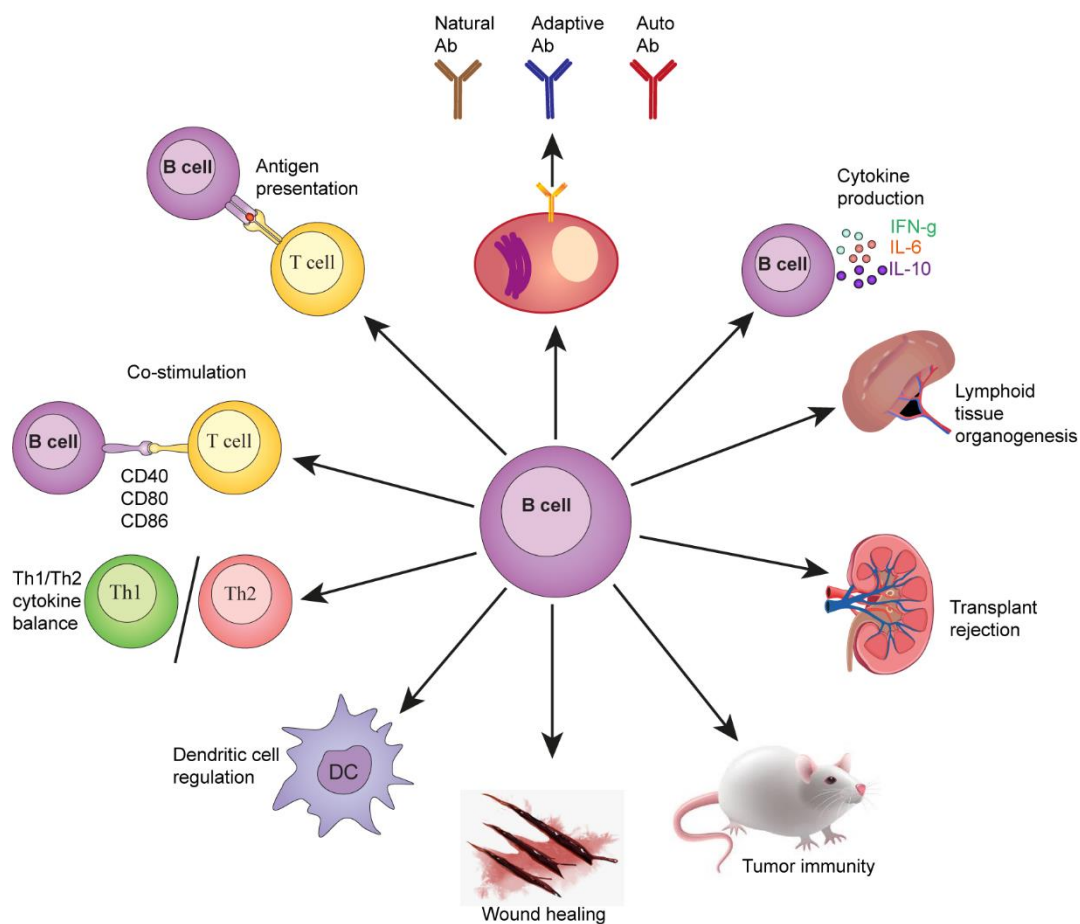
Figure 1.5: **Examples of multifunctional characteristics of how B cells regulate immune homeostasis aside from antibody production.**

1.5.5 Regulatory B cells

Traditionally, B cells are known to participate in adaptive immunity via humoral immunity (by active and continuous antibody secretion), antigen processing and presentation, and secretion of cytokines.[201–203] Recently, however, some populations of B cells were revealed to have regulatory features; these cells are regulatory B cells or Bregs in short. In animal models, Bregs reduce inflammation [201–203], promote tolerance in transplantation [204–206] and improve experimental autoimmune diseases [207–211]. Several subsets of Bregs were reported, and most of them act by secreting IL-10. Regulatory B cells are discussed in detail below as part of an article published on regulatory B cells in respiratory health and diseases.

1.6 Human respiratory system

This thesis is predominantly focused on inflammatory conditions of the lung. The respiratory system's primary function is facilitating gaseous exchange from the environment into the bloodstream [212]. The human respiratory system is functionally divided into two regions; a conducting, or the upper respiratory tract, comprising the external thoracic organs (nose, pharynx and larynx). And the respiratory, or the lower respiratory tract, that include all the organs within the thorax – trachea, bronchi, bronchioles, and alveoli (**Figure 1.6**) [213].
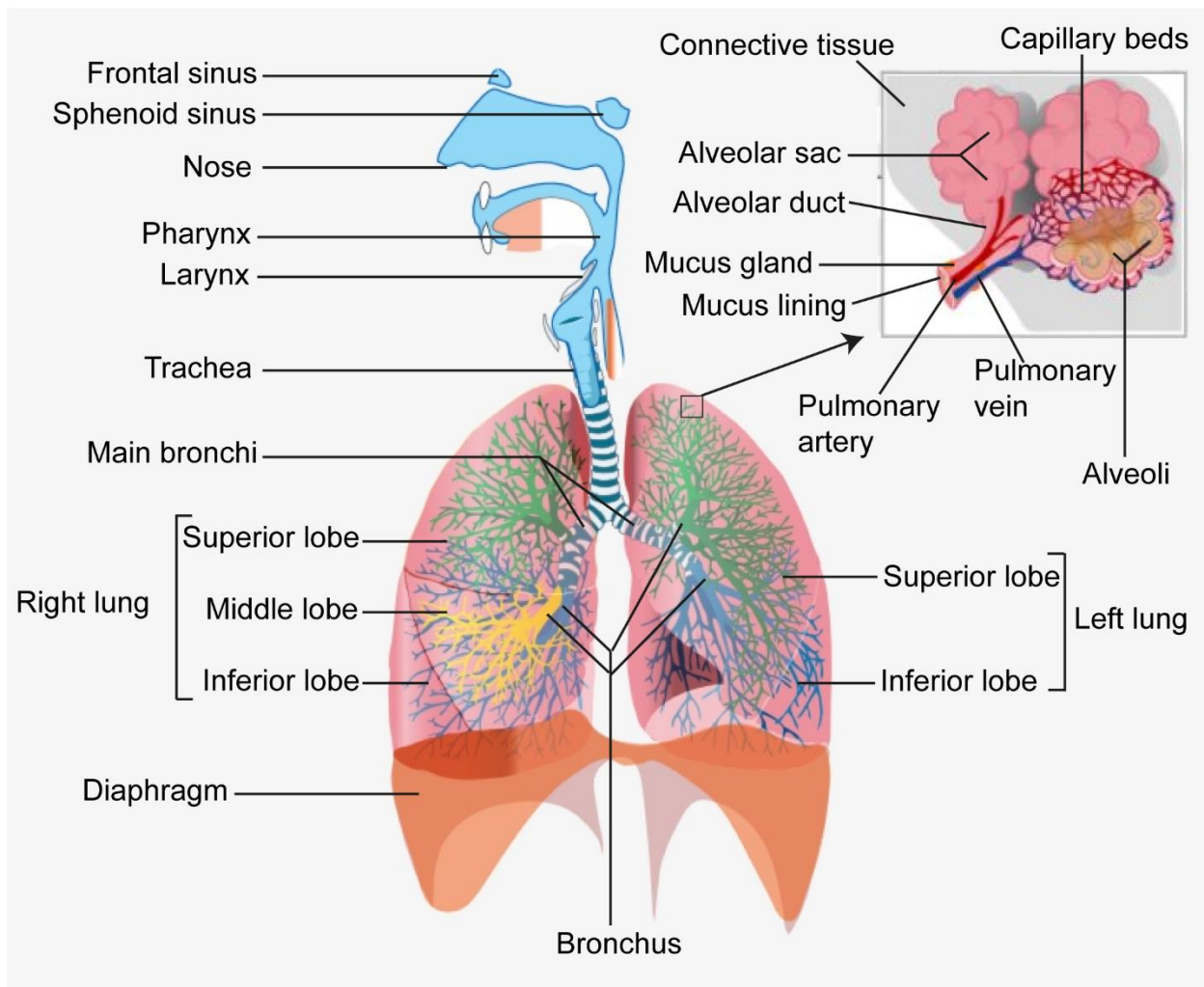
Figure 1. 6: Human respiratory system

During inhalation, the diaphragm contracts to pull downward and the chest muscles contract to pull open the chest, which helps suck in air. Then, during an exhale - the muscles relax, allowing the lungs to spring back to their normal size, pushing that air out. During breathing, air flows through the nostrils and enters the nasal cavity, which is lined by cells that release mucus; the mucus contains enzymes and peptides that help trap and kill bacteria. The air goes from the nasal cavity into the pharynx or throat. The region connecting the two is called the nasopharynx, and the part connecting the pharynx to the oral cavity is called the oropharynx. Then there is the laryngopharynx, the part of the pharynx that extends into the larynx or voice box [212,214].

The air continues down through the larynx into the trachea or the windpipe, which splits into two mainstem bronchi that enter the lungs. The trachea and the bronchi are wide and primarily composed of cartilages and smooth muscles. The bronchi or large airway is divided into smaller

bronchi or bronchioles, lined mainly by ciliated columnar cells and goblet cells that secrete mucus [215–217]. The secreted mucus and the ciliated cells help trap particles and bacteria from the air and propel them towards the pharynx, a process called the mucus escalator, providing mechanical protection. The bronchioles conduct air through smaller bronchioles called conducting bronchioles. These bronchioles are also lined by ciliated columnar epithelial cells and mucus-secreting goblet cells, as well as club cells that secrete glycosaminoglycans (a critical material that protects the bronchiolar epithelium) and are capable of transforming into ciliated columnar cells (club cells) that helps to regenerate and replace damaged ciliated columnar epithelial cells when needed [215–218].

The last part of the conducting bronchioles is the terminal bronchioles. After that, the air reaches the respiratory bronchioles, which have tiny outpouchings called alveoli. There are about 500 million alveoli within the lungs [219,220]. The respiratory bronchioles end at alveoli. At this point, the airway is called an alveolar duct rather than the respiratory bronchioles. This is the final destination of the inhaled air.

The alveolar wall has an entirely different structure from the bronchioles. There are no cilia or smooth muscle; instead, the wall is lined by thin epithelial cells called pneumocytes [216,217,221]. Most of the regular pneumocytes are called type I pneumocytes, but some are called type II pneumocytes [221,222]. The pneumocytes secrete a substance called surfactant, which helps decrease the surface tension within the alveoli and keeps them open [221–223]. Like the club cells, the type II pneumocytes can also transform into type I pneumocytes to regenerate and replace damaged cells [224,225]. Finally, alveolar macrophages help clear any tiny particle that makes it deep into the lung by physically moving them up to the conducting bronchioles, where they can be exported out to the pharynx via the mucus escalator [222].

The air, now in the alveolus, is surrounded mainly by a single layer of type I pneumocytes. Endothelial cells are in close proximity to the pneumocytes and in many areas, the basement membrane of pneumocytes and endothelial cells are fused to facilitate gaseous exchange. At this point, carbon dioxide diffuses from the deoxygenated blood and into the alveoli, which gets breathed out [216,226]. With each breath, oxygen enters the alveoli and freely diffuses into the blood.

1.6.1 Immune responses in the Lung

The air we breathe is accompanied by potentially harmful microbes and particles that can damage delicate lung tissue. In health, the lungs are enriched with immune cells that repulse these foreign substances and repair injury. Prolonged or inappropriate immune responses in the lung may result in diseases such as asthma and COPD.

Innate immune cells are few in number in health but some are present as sentinels to survey lung health. Dendritic cells (DCs) are typically embedded throughout the bronchial wall to sample antigens in the airway lumen [227]. Also present are sporadic mast cells packed with granules rich in histamine and other mediators [228]. Various subtypes of innate lymphoid cells (ILCs) are also evident, mostly associated with the epithelial barrier [227–229]. The dominant macrophage population in health are alveolar macrophages that are tuned by the local microenvironment (particularly the epithelium) to be more resistant to activation [228,229]. When inhaled antigens contact the epithelium, they trigger the release of two cytokines, IL-25 and thymic stromal lymphopoietin (TSLP), which stimulate nearby DCs and ILCs. The DCs leave the epithelium for the lymph nodes, where they activate T cells and initiate an adaptive immune response [230,231]. Antigens can also pass through the epithelium, especially in conjunction with damaging particles such as those found in tobacco smoke or diesel fumes. Some of these antigens can reach the mast cells (in the case of asthmatic individuals) housed in the smooth muscle tissue. The activated T cells in the lymph nodes enter the interstitial spaces of the lung, where they secrete chemical signals that recruit other immune cells [232,233]. Cells like eosinophils (in the case of allergic reaction) squeeze through the epithelium into the lumen and release IL-5, IL-13 and platelet-activating factors [234,235]. These act on goblet cells causing them to secrete more mucus in a process known as goblet hyperplasia. Prolonged exposure over time may lead to fibrosis and permanent lung injury [168,231,234,235].

1.6.2 B cells and the respiratory system

Immunologic reactions were initially thought to occur in SLOs only. However, recent evidence suggests that immune reactions can occur outside these organs in lymphoid-like tissues called ectopic or tertiary lymphoid structures. Ectopic lymphoid tissues (ELTs) are loosely organized, poorly defined aggregations of lymphoid cells that develop in response to chronic infection, chronic inflammation, or autoimmunity [236,237]. Morphologically, ELTs are similar to SLOs, with separated B and T cell zones and specialized immune DCs, TFH cells, high endothelial venules (HEVs) and stromal cells that develop at the site of local pathology. Like the SLOs, ELT requires the expression of CXCL12 and CXCL13 and signalling from lymphotoxin for its development [237]. ELTs develop in a variety of tissue that includes the gut, lungs, and upper respiratory tract [237].
B cells are not ordinarily resident in the lung. However, the small fraction of B cells in healthy airways secrete antibodies that act locally and at mucosal surfaces. These antibodies are predominantly IgA and IgM and are polymeric. Polymeric antibody is transported across the epithelium via the poly IG receptor to facilitate antigen expulsion from the lung and to agglutinate antigens in the lumen [238–241]. Like the gut, B cells activated in airway lymphoid tissues (like nasal-

associated lymphoid tissue; NALT) differentiate into IgA-secreting PCs that predominantly act in the airway lumen [242]. Due to the lack of data on airway B cells, mechanisms guiding B cell homing and class switching in the airway in poorly understood. Some studies suggest CCR10-CCL28 and α4β7-VCAM-1 interaction play an integral role in B cell homing in the airway [242].

1.7 COPD

COPD is an inflammatory lung disease estimated to be the third leading cause of morbidity and mortality worldwide [243]. COPD is ranked the fourth cause of disability, affecting about 10 % of persons older than 45 years [244]. COPD is a chronic lung inflammatory disease characterized by persistent and progressive airflow limitation that is poorly reversible. The limitation of airflow is due to uncontrolled inflammatory responses to toxic gases or particles in the airways and lung that leads to emphysematous destruction of the lungs [243]. Cigarette smoke (CS) is the primary cause of COPD in developed countries, followed by genetic factors and other environmental factors like burning biomass fuels (usually in developing countries) (**Figure 1.7**) [243,245]. Despite several studies on the pathophysiology of COPD, it is still not understood why only a small percentage of long-term smokers develop COPD while others do not, and why the disease still persists even after smoking cessation [246]. COPD pathogenesis is hypothesized to be a cascade of innate immune responses together with epithelial cells, neutrophils and macrophages, and adaptive immune responses [246,247]. B cells, CD8, and CD4 T cells have been demonstrated in the small airways and lung tissue of patients with more severe disease. Their structural configuration as tertiary lymphoid tissue indicates that antigen-specific stimuli elicit an immune reaction, potentially enhancing the ongoing inflammation.
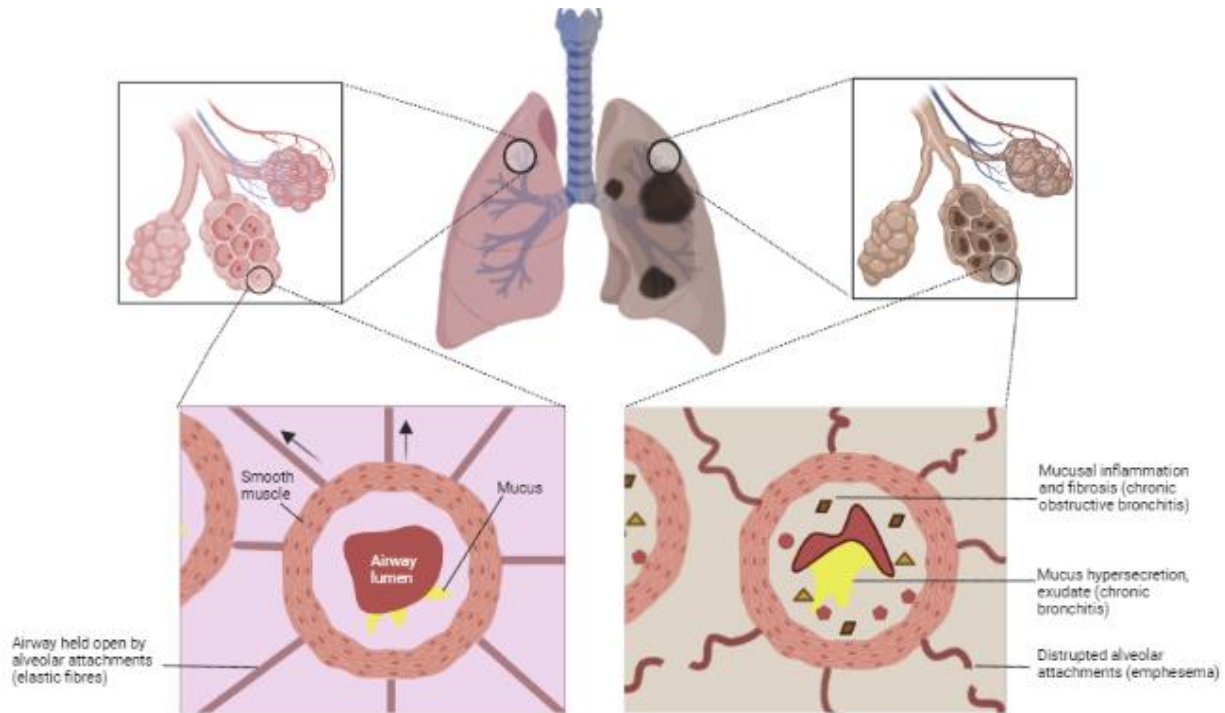
Figure 1.7: Small airway in healthy versus COPD lung

Alveolar wall attachments contain elastic fibres that open the bronchioles (small airways) in the healthy lung. However, in COPD, chronic inflammation and fibrosis causes thickening of the peripheral wall of the bronchioles. This leads to disruption of alveolar attachment and narrowing of small airways as a result of emphysema and occlusion of lumina by mucus and inflammatory exudate.

1.7.1 Emphysema in COPD

Emphysema means "inflate or swell", and in patients with lung emphysema, the alveoli sacs are damaged or destroyed, leading to permanent alveoli enlargement and loss of elasticity resulting in difficulty in exhaling air from the lungs [248]. With COPD, the airways become obstructed, and the lungs do not empty properly, leaving trapped air inside the lungs. For this reason, the maximum amount of air people with COPD can breathe out in a single breath, known as FVC, or forced vital capacity, is lower. This reduction is particularly noticeable in the first second of air breathed out, called FEV1 (forced expiratory volume in one second), which typically is reduced even more than the FVC. A useful metric, therefore, is the FEV1 to FVC ratio, which, since the FEV1 goes down even more than FVC, causes the FEV1 to FVC ratio to go down as well. So emphysema is a form

of COPD based on the structural changes in the lungs, specifically, the destruction of the alveoli [248–251]. Inflammatory reactions attract various immune cells, which release inflammatory mediators like leukotriene B4, IL-8, and TNF-α, as well as proteases like elastases and collagenases. These proteases break down critical structural proteins in the connective tissue layer like collagen and elastin (a protein that gives the tissue elasticity), leading to the problem seen in emphysema [247,252,253].

1.7.2 COPD pathophysiology

Various pathologic processes occur during COPD formation; this includes chronic bronchitis (over-secretion of mucus), emphysematous destruction of the small airways, reduced airway recoil, and air trapping in the lung that leads to lung hyperinflation [254]. Aside from lung inflammation, two other processes are involved in COPD pathogenesis; oxidative stress (imbalance between oxidants and antioxidants) and protease and antiprotease imbalance [255–258].

The GOLD (Global Initiative on Obstructive Lung Disease) definition is usually used to define the chronic airflow blockage in different stages of COPD [243]. The GOLD definition uses a threshold of 0.1 for the post-bronchodilator ratio of forced expiratory volume in 1 second (FEV1) to forced vital capacity (also known as the Tiffeneau index) [243], this ratio decreases with age [259]. Four stages of COPD exist depending on the severity of the airflow obstruction: stage 1 (mild, FEV1 ≥ 80 % of lung function predicted), stage 2 (moderate, FEV1 50 – 80 % of predicted), stage 3 (severe, FEV1 30 – 50 % of predicted), and stage 4 (very severe, FEV1 < 30 % of predicted) [243].

1.7.3 Exacerbations

COPD exacerbations result from inflammatory events commonly triggered by bacterial pneumonia, respiratory viruses, air pollution and non-adherence to medication [260]. Exacerbation in COPD is characterized by short periods (typically less than 48 h) of increased cough, dyspnea, and sputum production that become purulent and aggravate COPD leading to transient symptoms that significantly increase morbidity and mortality [260–262]. Exacerbations range from mild to severe; the mild and moderate forms can be treated with medications, while the severe forms usually require hospitalization for treatment [263,264].

1.7.4 Inflammatory responses in the lower airway of COPD patients

COPD lung is associated with the heightened presence of immune cells, where products of immune responses cause deterioration of the cells in the lower airway [265–268]. Many studies have shown presence of infiltrating immune cells in COPD compared to control lung. However, levels and functions of the infiltrating immune cells vary with disease type and severity, where neutrophils and B cells are seen to be the predominant cells in the most severe form of the disease (usually in stages 3 and 4) [266–269]. In CS-induced COPD, immune cells frequently accumulate in the lung submucosa in response to irritants from CS [270,271]. Ectopic lymphoid tissues are then formed by the infiltrating cells. This supports uncontrolled inflammatory reactions in the small airways that subsequently destroy cells of the small airways and causes smooth muscle hypertrophy and fibrosis [269,272].

As previously discussed, COPD is associated with a constant influx of inflammatory cells into the pulmonary tissue due to the persistent inflammatory response. Innate immunity in the lung is often suppressed following chronic exposure to cigarette smoke and other harmful environmental factors, this occurs in addition to endogenous processes like ageing and other pathological changes in COPD. Suppressed innate immunity increases the chances of respiratory infections that cause secondary inflammation and consequently promote the destruction of lung tissue and subsequent decline in lung function. The COPD current smoker's airway is associated with an imbalance between CD4+ and CD8+ T cells, where CD8+ T cells are the predominant T cells [246,273]. The increase in CD8+ T cells is observed throughout the tracheobronchial tree, suggesting persistent inflammation in smokers with COPD [246,273]. In the COPD lung, CD8+ T cells target cells with MHC-I leading to their cytolysis (by proteolytic enzymes released by the CD8+ T cells) and apoptotic destruction [274]. Cytokines like IL-17, that are secreted by CD8+ and CD4+ T cells, play a major role in cigarette-smoke-induced emphysema development in COPD [275,276]. IL-17 induces IL-8 (neutrophil chemoattractant) that attracts neutrophils and, subsequently, macrophages. The activated neutrophils and macrophages then release proteolytic enzymes like neutrophil elastase and matrix metalloproteinases (MMPs), for example, MMP8, MMP9, and MMP12 [274]. **Figure 1.8** highlights the key innate and adaptive immune responses in COPD pathogenesis.
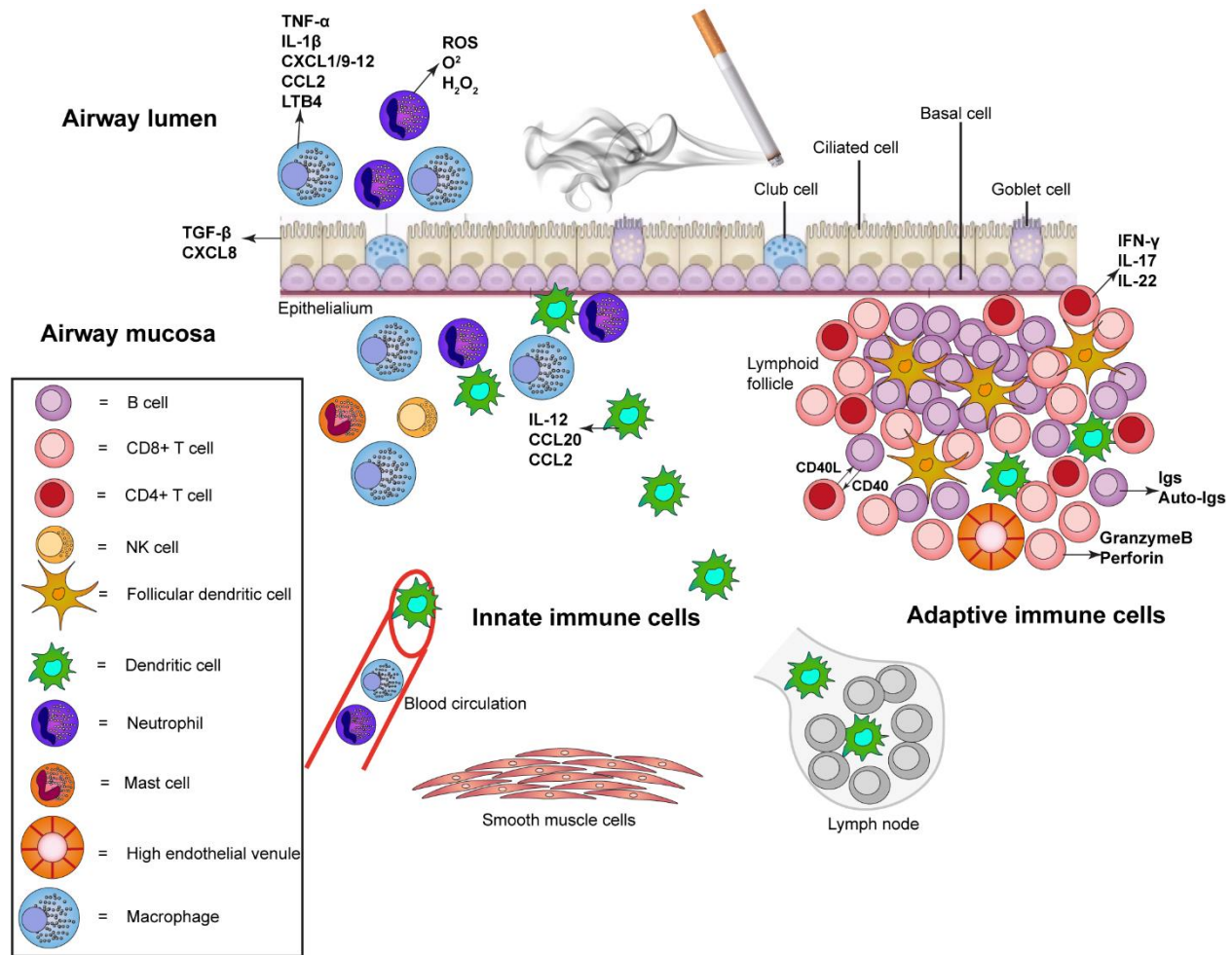
Figure 1.8: Mechanisms of Innate and adaptive immune cell response in COPD

Toxins in Cigarette smoke activate neutrophils, macrophages, NK cells and epithelial cells in the innate immune response. Dendritic cells at the site of the inflammation initiate the adaptive immune response by activating B cells, T helper cells and cytotoxic T cells, leading to chronic inflammation and lymphoid follicle development with the help of follicular dendritic cells and high endothelial venules.

1.7.5 B cell in COPD immunopathology

The role of B cells in COPD pathogenesis is not well known. Studies of the small airways of COPD patients show an increase in B cell concentration and ELTs in the adventitia of the small airways compared with controls. The number of ELTs and B cells increases with COPD severity but are absent in the small airways of non-smokers [269,272]. The ELT usually consists of an aggregate of B

cells (IgM$^+$IgD$^-$CD27$^+$ cells) [277], FDCs, helper T cells, and cytotoxic T cells [269,272,278]. The concentration of B cell-activating factor, BAFF, also increases in advanced forms of COPD and in patients with emphysema [279]. Several emphysema phenotypes have been linked with B cell-rich lymphoid follicles that contribute to clonal proliferation in the emphysematous lung [278,280]. Also, studies in transcriptomics show upregulated B cell signaling in patients with severe emphysema[281].

1.7.5.1 Recruitment and activation of B cells in COPD lungs

Several factors are involved in the recruitment and activation of B cells during the chronic inflammatory reaction in COPD lungs. For instance, lymphotoxin-α-β heterotrimer (LTα1β2) that is expressed on activated B cells interacts with lymphotoxin-β (LT-β) on the lung stromal cells.[282] This interaction induces the expression of lymphocytes and DCs chemo-attractants (CCL19 and CCL21; CXCL12 and CXCL13 and adhesion molecules) by the stromal cells and subsequent recruitment of the immune cells into the lungs.[283]

1.7.6 Autoimmunity in COPD

Considerable evidence suggests possible autoimmune activities in COPD patients. This evidence includes; genetic and environmental predisposition [284,285], presence of autoantibodies[286], persistent inflammatory reactions even after smoke cessation, and continuous recruitment of activated APCs into COPD lungs that secrete pro-inflammatory cytokines [287]. Production of autoantibodies in COPD is associated with an increase in lung levels of self-antigens that are generated in response to an increase in oxidative stress levels. There is a strong link between COPD severity and levels of these autoantibodies [288]. The development of emphysema in COPD is associated with proteolytic destruction of extracellular proteins, which also leads to the production of fragments of extracellular matrix (matrikines) that recruit inflammatory cells [289,290]. Destruction of cellular components of COPD lungs increases emphysema development and generates neoepitopes that can be targeted as self-antigens by autoantibodies [283]. Different factors of COPD development (e.g., environment and genetic factors, infectious agents), coupled with genetic differences and different pathologies occurring in COPD lungs and other organs, make it challenging to understand the autoimmune contribution of B cells to COPD development [291]. Similarly, the number and functions of different B cells and their different subsets (e.g., Bregs) in the COPD lung are yet to be assessed, which prompted this research.

1.8 SARS-CoV-2 virus

The emergence of the COVID-19 pandemic meant that this thesis was adjusted to allow laboratory access. Despite this divergence, many parallels, as well as many differences, emerged when comparing COPD and COVID-19.

First reported in Wuhan, China, in December 2019, the coronavirus disease 2019 (COVID-19) pandemic has affected more than half a billion people globally and caused more than six million fatalities. Severe acute respiratory syndrome coronavirus 2 (SARS-CoV-2) is the etiological agent of COVID-19, where the virus binds the cells expressing angiotensin-converting enzyme 2 (ACE2), which is abundant on surfaces of pulmonary type II alveolar cells [292–294]. There were a total of six human coronaviruses (hCoVs) before the novel SARS-CoV-2; this includes the four seasonal strains that mainly caused upper respiratory illnesses or common cold (hCoV-NL63, -OC43, -229E, and HKU1), and the more current MERS-CoV5 and SARS-CoV4 that are transfected from animals (zoonosis) that emerged in 2003, and 2012 respectively [295].

SARS-CoV-2 belongs to the coronaviridae family and contains a variety of viral species that infect humans and animals [296–298]. Coronavirus infections cause about 20-30 % of the common cold in humans, and is usually a mild respiratory infection that does not require hospital assistance [299]. However, MERS-CoV and SARS-CoV have higher fatality despite having low transmissibility, with SARS-CoV-2 having the highest transmissibility [300].

Coronaviruses are single-stranded RNA viruses, about 30 Kbp long with a diameter of 80-120 nm and spheroidal shape. Their envelope contains the membrane-M-, envelope-E-, and spike-S-proteins, and the RNA is covered with a virion that contains the nucleocapsid-N [301]. The S protein contains the receptor-binding domain (RBD) housing the antigenic epitope that induces immune responses and binds its ligand (ACE2) on the host cell membrane, making it the most widely studied protein of the coronavirus [302].

The pathology of COVID-19 involves numerous clinical features varying from asymptomatic infections to mild, moderate, and severe infections that usually requires hospitalization and mechanical ventilation and possible death. However, most mild and asymptomatic cases of COVID-19 (approximately 80%) are not documented [303]. There are several risk factors associated with severe COVID-19 disease and death; these include age, gender, cardiovascular diseases, diabetes, and treatments or diseases that affect the immune system [304–308]. Pathology in acute respiratory infections can be mediated either by SARS-CoV-2 directly, by cytokine storm from overaggressive immune response, or both [309–311]. Although the role and characteristics of immune

reactions in COVID-19 are known, how that affects the clinical outcome of patients is still not clearly understood.

The primary contact route of SARS-CoV-2 is via inhaling exhaled microdroplets from infected individuals or by direct contact with viral particles in contaminated objects. The virus then targets the bronchial epithelial cells and pneumocytes of the alveolar epithelium that have an abundant expression of ACE2. Infection with SARS-CoV inhibits ACE2 expression and causes basal membrane detachment and autophagy, resulting in the binding of angiotensin II to the angiotensin II receptor type 1 (AT1a) receptor that subsequently results in acute lung damage [312,313,314(p9),315,316].

1.8.1 Role of B and T cells in COVID-19

Outcomes of SARS-CoV-2 infection are diverse and range from asymptomatic infections to severe pneumonia, acute respiratory distress (ARDS), multiple organ failure and death. The immunity to SARS-CoV-2 depends on disease severity and virus inoculum. B cells play a crucial part in the humoral immunity against COVID-19 infection, although their contribution is not fully understood. Early immune response by B cells is seen during the first few days of SARS-CoV infection, where antibodies against both S and N proteins can be detected [317,318]. The N protein is highly immunogenic, lacks glycosylation sites, and is smaller than the S protein, resulting in early production of N-specific antibodies within a few days post-infections [319]. IgM, IgG, and IgA antibodies against SARS-CoV have been detected at both onsets of acute infection and at different time points of the disease. Levels of IgM antibodies usually drop three months post-infection, whereas IgG antibodies were detected after an extended period.[320,321].

B and T cells are essential in the clearance of viral infection, and their induction against SARS-CoV-2 is vital for long-term protection (**Figure 1.9**). Viral infection elicits virus-specific B and T cell responses, and cytokines and chemokines released by APCs determine the effector function of T cell subsets. Concurrently, the production of neutralizing antibodies by plasma cells determines the protective function of the humoral immunity against infection [322]. In SARS-CoV-2 infection, IgM first appears three days post-infection, followed by high-affinity IgG, then long-term memory against the virus [323]. However, PCs continue to release antibodies that have serological memory. The generated memory B cells will then rapidly differentiate into PCs and produce high-affinity antibodies in response to secondary infection, ensuring long-term immunity [324]. Long-term immunity against viral infection is ensured by viral-specific memory B and T cells [325]. SARS-CoV-2-specific memory B cells are seen within a month of infection, with levels of switched MBCs

associated with reduced duration of symptoms in patients with COVID-19 [326]. This shows the presence of memory response even prior to the MBC formation in some COVID-19 patients, probably as a result of previous coronavirus infection, since coronaviruses are likely to generate cross-reactive B and T cell immunity [327].

Viral-specific CD4+ T cells are required to elicit potent B cell responses against the spike protein of SARS-CoV-2 virus [328–330]. They are essential in the formation and sustenance of GCs that lead to B cell differentiation, isotype class switch and immunoglobulin maturation via T-dependent activation. Depletion of CD4+ T cells is associated with defective GC formation in COVID-19 patients [331], leading to poor viral immunity and longer persistent infection in patients [332]. Furthermore, the hallmark of severe COVID-19 is typically associated with reduced CD4+ and CD8+ T cells or lymphopenia, T cell exhaustion with reduced proliferative ability, and increased pro-inflammatory cytokines [333].
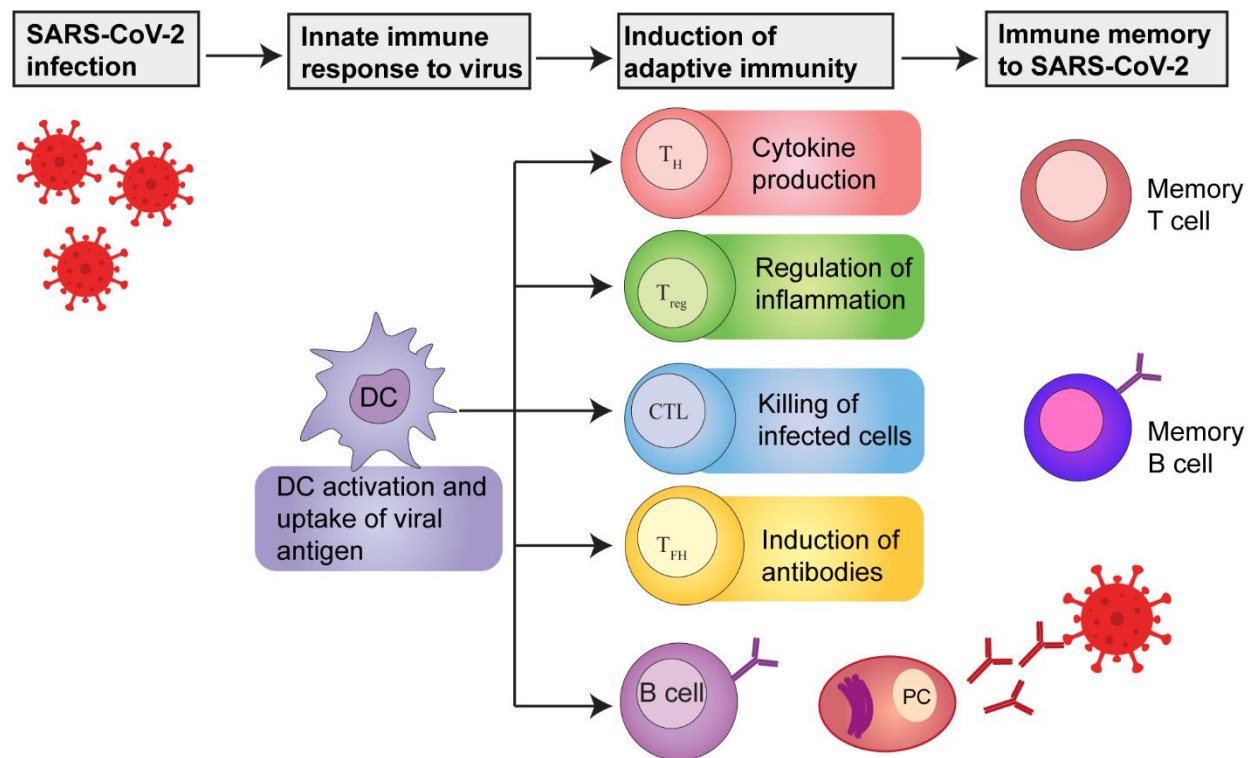
Figure 1.9: Immune response in SARS-CoV-2 infection

Infection with SARS-CoV-2 activates innate immunity and dendritic cells, causing the activation of viral-specific B and T cell responses.

In recognition of the discoveries made in this thesis, we wrote a review article on regulatory B cells, which is included here.

1.9 Regulatory B cells in respiratory health and diseases

M. Menon[1*], T. Hussell[1], H. A. Shuwa[1]

[1]Lydia Becker Institute of Immunology and Inflammation, Division of Infection, Immunity & Respiratory Medicine, School of Biological Sciences, Faculty of Biology, Medicine and Health, University of Manchester, Manchester Academic Health Science Centre, Room 2.16, Core Technology Facility, 46 Grafton Street, Manchester, M13 9PL, U.K.

* Correspondence: madhvi.menon@manchester.ac.uk

Running title: Regulatory B cells in respiratory health and diseases

1.9.0 Summary

B cells are critical mediators of humoral immune responses in the airways through antibody production, antigen presentation and cytokine secretion. In addition, a subset of B cells, known as regulatory B cells (Bregs), exhibit immunosuppressive functions via diverse regulatory mechanisms. Bregs modulate immune responses via the secretion of IL-10, IL-35 and tumour growth factor-β (TGF-β), and by direct cell contact. The balance between effector and regulatory B cell functions is critical in the maintenance of immune homeostasis. The importance of Bregs in airway immune responses is emphasized by the different respiratory disorders associated with abnormalities in Breg numbers and function. In this review, we summarize the role of immunosuppressive Bregs in airway inflammatory diseases and highlight the importance of this subset in the maintenance of respiratory health. We propose that improved understanding of signals in the lung microenvironment that drive Breg differentiation can provide novel therapeutic avenues for improved management of respiratory diseases.

Keywords: B cells, lung, IL-10, infection, airway inflammation, immune regulation

1.9.1 Introduction

B cells are an essential part of humoral immune responses in the airways through antibody production, antigen presentation, and cytokine secretion [334]. Although these functions are pivotal in the clearance of invading pathogens and the development of long-term immunity, unrestrained inflammation can cause irreversible damage to tissues [334]. To prevent this, we require mechanisms of suppression that prevent exaggerated immune responses and maintain tissue homeostasis.

In addition to well-established effector functions, a subset of immunosuppressive B cells, known as regulatory B cells or Bregs, contribute to preventing uncontrolled inflammation [335]. Bregs, as negative regulators of the immune system, suppress inflammatory responses via the production of IL-10 and other anti-inflammatory mediators, as well as via direct cell contact. Depending on the disease context, Bregs can be either pathogenic or beneficial; whereas an expansion of Bregs is advantageous in autoimmunity and other chronic inflammatory conditions, increased Breg frequencies can cause detrimental immune suppression in infectious diseases and cancers [336].

The signals required for the induction of Bregs include a combination of toll-like receptor (TLRs) ligands, CD40-ligand (CD40-L), antigens activating the B cell receptor (BCR), co-stimulatory molecules (CD80, CD86) and inflammatory cytokines [335,337]. Majority of these stimuli are found in the lung microenvironment [334,338], supporting an expansion of Bregs in the airways. Moreover, numerical and functional abnormalities in Bregs have been associated with various immune-related lung pathologies [339–342], highlighting the importance of this B cell subset in mounting an appropriate immune response in the airways. For these reasons, there is an increased interest in understanding the role of Bregs in respiratory health and disease settings. This review summarizes the role of immunosuppressive Bregs in airway inflammatory diseases, including lung cancer, respiratory infections, allergy, pulmonary fibrosis, and autoimmune pulmonary manifestations, thus emphasizing the importance of this subset in the maintenance of respiratory health.

1.9.2 Overview of Breg induction, phenotype, and function

Over the past decade, studies in experimental animal models and patients with autoimmune diseases have identified multiple Breg subsets exhibiting diverse mechanisms of immune suppression [336]. Evidence suggests that the environmental milieu play a pivotal role in the induction of Bregs. In addition to TLR, BCR and CD40 signalling, as well as CD80 and CD86

activation, inflammatory cytokines have been shown to play an important role in expanding immunosuppressive Bregs [337]. For example, exposure to inflammatory cytokines IL-1β and IL-6 have been shown to induce Breg differentiation in a mouse model of arthritis [343]. Moreover, mice with B cell-specific deletion of IL-1R1 or IL-6R displayed reduced Bregs and exacerbated arthritis. Interestingly, the production of IL-10 and IL-6 are modulated by gut bacteria, highlighting an indirect role for microbiota in Breg induction [343]. Other inflammatory cytokines, such as type-I interferons (IFN-I), IL-21 and B cell-activating factor (BAFF) have also been shown to play a role in Breg differentiation [344–347]. Although anti-inflammatory cytokine IL-35 has been shown to expand IL-10- and IL-35-producing Bregs [348], evidence suggests that IL-35 is itself induced in response to inflammatory stimuli [349]. Of note, activation of STAT3 is important for induction of IL-10 expression by B cells, as inhibition of STAT3 has been shown to abrogate IL-10$^+$ B cells [350]. Taken together, the expansion of suppressive Bregs in response to inflammatory signals appears to be a mechanism that has evolved to prevent excessive inflammation and tissue damage.

In addition to inflammatory stimuli, recent studies have identified aryl hydrocarbon receptor (AhR) as an important transcription factor involved in Breg differentiation [351,352]. Ahr has been shown to regulate the transcription of IL-10 by B cells while actively repressing the transcription of pro-inflammatory mediators [351]. In a mouse model of arthritis, the lack of Ahr expression on B cells has been demonstrated to increase Th1/Th17 responses, decrease regulatory T cells (Tregs) and lead to exacerbated arthritis as a result of impaired IL-10-producing Breg differentiation [351]. Interestingly, Blimp1, a transcription factor critical for plasma cell differentiation [193], has also been shown to play a role in IL-10$^+$ Breg function; as Bregs lacking Blimp-1 expression fail to efficiently suppress naïve CD4$^+$ T cell proliferation [353]. Furthermore, recent evidence suggests that Bregs have the ability to differentiate into IL-10-producing plasmablasts and plasma cells *in vitro* and *in vivo* [354,355]. Although antibody-producing plasmablasts/ plasma cells are largely associated with pro-inflammatory responses [356], a subset of IL-10$^+$ regulatory plasmablasts have been shown to suppress immune responses while producing antibody [357,358]. These findings suggest that B cells at any stage of development can exhibit a regulatory phenotype.

Several Breg subsets with overlapping markers and functions have been identified in mice and humans [336]. In animal models, Bregs suppress allergic airway inflammation [359], promote tolerance in transplantation [360,361], and improve experimental autoimmune diseases [362,363,354]. Among the different subsets, IL-10-producing B cell subpopulations that constitute ~10% of circulating human B cells are the most studied in different disease settings [336,364]. These subsets include CD1d^{hi}CD5$^+$ B10 Bregs [365], CD5$^+$CD21$^+$CD23$^-$ marginal zone (MZ) Bregs [16,366], CD1d^{hi}CD21^{hi}CD23^{hi}CD24^{hi}

T2-MZP Bregs [362,367] and CD138$^+$CD44^{hi} plasmablasts [354]. In addition, T cell immunoglobulin and mucin-domain-containing protein (Tim-1) has been identified as a marker for IL-10-producing B cells in mice and is expressed by multiple Breg subsets [368,369]. Importantly, B cell-specific Tim-1 deletion results in spontaneous multi-organ tissue inflammation, supporting a role for this Breg subset in maintaining self-tolerance and restraining tissue inflammation [352,369]. Other Breg populations include MZ-like and MZ-progenitor B cells that express programmed cell death-ligand 1 (PD-L1) molecule in mice [370]. Immune suppression by PD-L1^{hi} Bregs is independent of IL-10 and mediated by the PD-1/PD-L1 pathway that can regulate follicular T helper (Tfh) cell responses [370].

Due to the limited access to human lymphoid tissues, majority of human Bregs identified thus far are in the peripheral blood. The characterized human Breg subsets include CD24^{hi}CD38^{hi} transitional B cells [364], CD24^{hi}CD27$^+$ human B10 cells [371], CD25^{hi}CD71^{hi}CD73^{lo} regulatory B1 (Br1) cells [372], CD27^{int}CD38^{hi} plasmablasts [354], CD38$^+$CD1d$^+$IgM$^+$CD147$^+$granzymeB (GzmB)$^+$ B cells [373] and CD39$^+$CD73$^+$B cells [374,375]. Similar to mouse models, Tim-1$^+$ B cells that co-express IL-10 have also been reported in humans [376]. The different Breg subsets, their mechanisms of suppression and role in different disease settings have been described in detail elsewhere [336,337,377], and summarized here in **Table 2**.

Table 1.2: Phenotype and function of Breg subsets

Subset	Phenotypic markers	Mechanism of action	Functions	Reference
B10 cells	CD1d^{hi}CD5$^+$ (mouse) CD1d$^+$CD24^{hi}CD27$^+$ (human)	IL-10	Inhibits Th17 cells, effector CD4$^+$ T cells, macrophages and DCs, expands Tregs and Tr1 cells	[351,371,378–380]
Tim-1 B cells	Tim-1$^+$ (mouse and human)	IL-10, TGF-β	Expands Tregs and reduces Th1 cells, increases allograft tolerance	[352,368,369,376]
T2-MZP B cells	CD1d^{hi}CD21^{hi}CD23^{hi}CD24^{hi} (mouse)	IL-10	Promotes Treg differentiation, inhibits Th1/ Th2 cells,	[362,367,380]

Cell type	Markers	Secretes	Function	Ref
			suppresses effector CD4$^+$ and CD8$^+$ T cells	
MZ B cells	CD5$^+$CD21$^+$CD23$^-$ CD1d$^+$CD24^{hi}IgM^{hi}IgD^{lo} (mouse)	IL-10	Suppresses effector CD4$^+$ and CD8$^+$ T cells, promotes Treg differentiation	[16,367]
Plasma cells	CD138^{hi}CD1d$^+$ IgM$^+$B220$^+$TACI$^+$ CXCR4$^+$ Tim1$^{+/-}$ (mouse)	IL-10, IL-35	Inhibits NK cells, Th cells, macrophages, and neutrophils, promotes antigen presentation	[348,355]
Plasmablasts	CD138$^+$CD44^{hi} (mouse) CD27^{hi}CD38^{hi} (human)	IL-10	Suppresses DCs ability to expand effector T cells	[354,357,358]
Br1 cells	CD25^{hi}CD71^{hi}CD73^{lo} (Human)	IL-10, IgG4, PD-L1	Secretes anti-inflammatory IgG4, reduces differentiation of Th cells	[372]
Transitional/ Immature B cells	CD24^{hi}CD38^{hi} (human)	IL-10, PD-L1, CD86	Suppresses Th1/ Th17, TNFα$^+$ monocytes, virus specific CD8$^+$ T cells, expands Tregs and iNKT cells.	[364,380,385]
GzmB$^+$ B cells	CD5$^+$CD27$^+$CD138$^+$ (human)	Granzyme-B	Induces CD4$^+$ T cell apoptosis, inhibit proliferation of CD4$^+$ T cell	[373]
iBregs	-	TGF-β, IDO	Differentiates T cells into IL-10- and TGF-β-producing Tregs	[386]

| PD-L1^{high} B cells | PD-L1^{hi}Blimp1^{lo} CD138^{lo}B220^{hi} (mouse) | PD-L1 | Inhibits Tfh expansion, suppress T cell differentiation | 370 |
| CD39^{+}CD73^{+} B cells | CD39^{+}CD73[hi/lo] (mouse and human) | 5′-AMP, ADO | Inhibits proliferation of CD4^{+} and CD8^{+} T cells | 374,375 |

MZ, marginal zone; T2-MZP, transitional-2 marginal zone precursor; PD-L1, programmed cell death-ligand 1; DC, dendritic cell; Br1, B regulatory 1 (Br1) cells; NK, natural killer cell; GzmB, Granzyme B; iNKT, inducible natural killer T cell; Tim-1, T cell immunoglobulin and mucin-domain containing protein 1; Tregs, regulatory T cells; 5′-AMP, adenosine 5′-monophasphate; ADO, adenosine; IDO, indoleamine 2,3 dioxygenase.

Inhibitory mechanisms of Bregs are best described by their secretion of the anti-inflammatory cytokine, IL-10 [335]. Breg-derived IL-10 can convert CD4^{+}T cells into Tregs and type-I regulatory T (Tr1) cells [379], inhibit Th1/ Th17 differentiation [364,380], suppress TNF-α production by monocytes [371] and maintain the number and function of immunosuppressive invariant natural killer (iNKT) cells [385,387]. IL-10-producing Bregs also suppress the production of IFN-α, an anti-viral cytokine that is secreted by plasmacytoid dendritic cells (pDCs) [344], thereby implicating a role for Bregs in preventing hyperinflammation and tissue damage caused by unresolved infections. Bregs also act through the secretion of other anti-inflammatory cytokines like tumour growth factor-β (TGF-β) and IL-35. Breg-derived IL-35 induces Treg expansion and inhibits Th1 and Th17 differentiation [348,355], whereas TGF-β induces CD8^{+}T cell anergy and apoptosis of effector CD4^{+} T cells [388,389]. Furthermore, a subset of induced Bregs (iBregs, induced by CTLA-4^{+}T cells) expand Tregs in a TGF-β and indoleamine 2,3 dioxygenase (IDO)-dependent manner [386]). Another subset of Bregs, known as Br1 cells, secrete IL-10 and allergen-specific IgG4 antibodies that regulate tolerance to allergic reactions and suppress allergen-specific T cell proliferation [372]. Additionally, a population of CD39^{+}CD73^{+} B cells suppress inflammatory reactions by inhibiting the proliferation of CD4^{+} and CD8^{+} T cells, via the production of adenosine 5′-monophosphate (5′-AMP) [374,375]. Other mechanisms of Breg immune suppression include co-stimulatory interaction with T cells, iNKT cells and DCs that involve CD80, CD86, CD1d CTLA-4, PD-L1 and MHC class II [337]. PD-L1[hi] Bregs inhibit the expansion of Tfh cells in spleen/ lymph nodes and suppress effector T cell differentiation by modulating downstream signaling pathways [370]. **Figure 1.10** summarizes the mechanisms of suppression by Bregs.
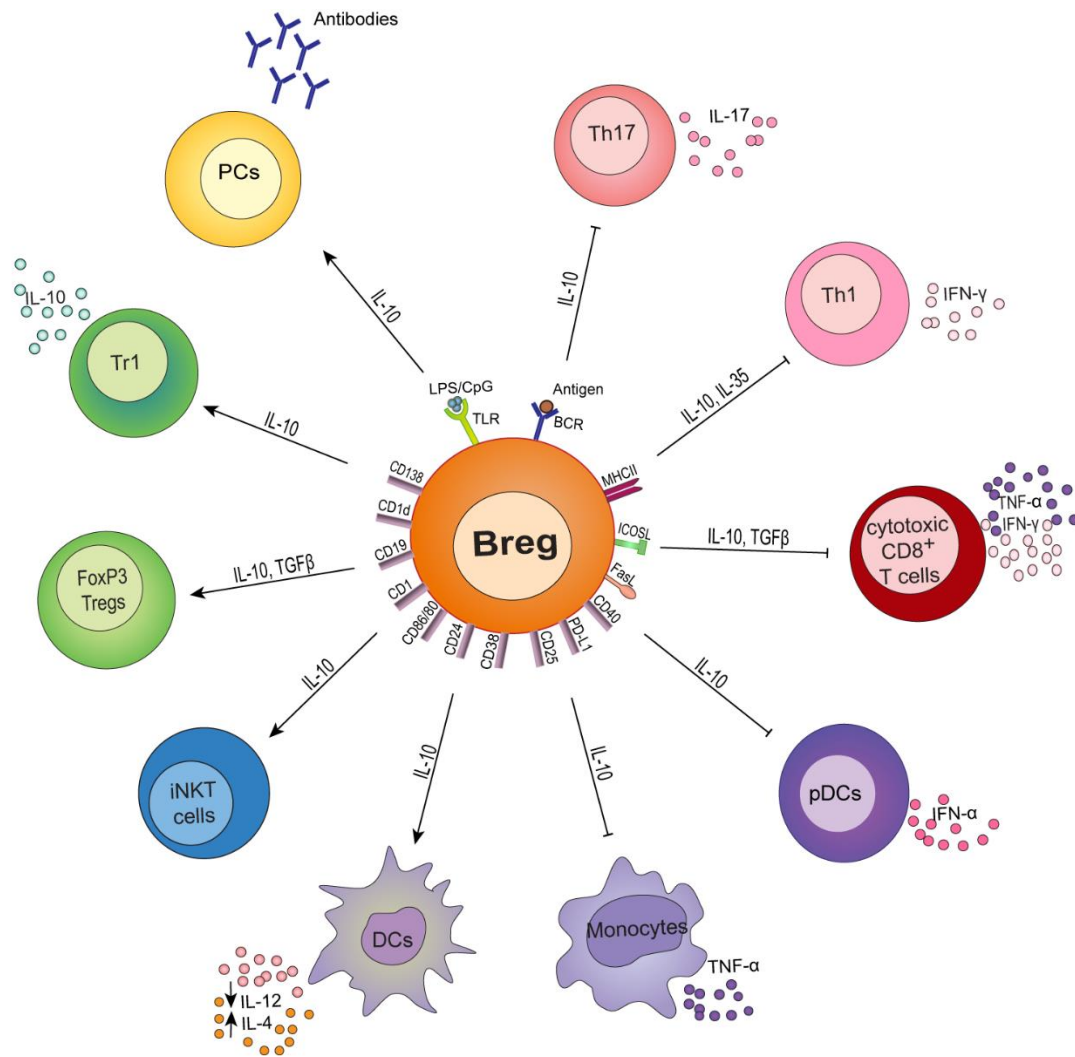
Figure 1.10: Spectrum of mechanisms of immune suppression by Bregs

Human Bregs suppress Th1 and Th17 responses and inhibit cytotoxic activity by CD8$^+$ T cells. They also induce the differentiation of CD4$^+$T cells into FoxP3$^+$ Tregs and IL-10$^+$ T regulatory-1 (Tr1) cells. In addition to modulating T cell responses, they suppress TNFα production by monocytes, IFN-γ production by plasmacytoid dendritic cells (pDCs) and IL-12-producing DCs. Breg-mediated suppression of the immune response is achieved predominantly via the production of IL-10, and to an extent by TGF-β and IL-35 production. Further, immune suppression by Bregs can be mediated via co-stimulatory interactions with T cells, invariant natural killer T (iNKT) cells and DCs. Bregs support iNKT cell homeostasis by presenting lipid antigens via CD1d to the invariant T cell receptor (iTCR).

1.9.3 B cells in the respiratory system

The respiratory tract is structurally designed with immune structures to protect the body against a wide range of potentially harmful external air-borne antigens [334,390]. B cells are normally not found in the lungs of healthy humans; their presence in the lung is almost exclusively associated with lung injury, usually infection or chronic inflammation [334]. B cells are typically located within tertiary or ectopic lymphoid tissues (ELTs) in the lung, like the inducible bronchus-associated lymphoid tissue (iBALT) [334,338]. Unlike well-organized secondary lymphoid organs, ELTs are loosely organized, poorly defined aggregates of lymphoid cells that develop rapidly in response to infection, chronic inflammation, or autoimmunity [391]. ELTs have separate B and T cell-rich zones, Tfh cells, a network of follicular dendritic cells (FDCs), stromal mesenchymal cells, and high endothelial venules, and can vary depending on the type of pathogen or inflammatory condition that triggered their formation [338,391,392]. Importantly, they display localized expression of CXCL12 and CXCL13 (a strong homing signal for CXCR5$^+$ B cells [393]), that promote naïve B cell recruitment to the ELTs [394]; recruited B cells then produce lymphotoxin-β that further sustain the ELT [395,396]. Tfh cells also express CXCR5, that responds strongly to CXCL13 and allows them to stay in close contact with B cells within the ELT [397–399]. Thus, ELTs contain functional germinal centers (GCs) for local B cell differentiation, expansion, somatic hypermutation and antibody production [391,400]. It is noteworthy that resident memory B cells (BRM) are a common feature of antigen-experienced lungs, and have been shown to play an important role in acquired anti-viral and anti-bacterial lung immunity [401,402]. Like the gut, B cells in the airways secrete antibodies that act both locally and at mucosal surfaces [334,338]. These antibodies are predominantly IgA and IgM that bind to glandular epithelial and mucosal surfaces and help in expelling antigens out of the body [334,403–405]. Similar to B cells activated in Peyer's patches, B cells that are activated in airway lymphoid tissues also differentiate into IgA-secreting PCs that predominantly act in the airway [406,407]. Current understanding of B cell homing and class-switching in the airway remains limited, with CCR10-CCL28 and α4β7-VCAM-1 interactions suggested to play an integral role in B cell homing in the airway [408–411], and CXCR3 found to uniquely identify BRMs [412].

Studies of airway inflammatory diseases have recently demonstrated the involvement of B cells in disease pathology [334]. B cells act as both pro- and anti-inflammatory agents via secretion of antibodies and cytokines, as well as by antigen presentation to Th cells. Airway inflammatory diseases such as hypersensitivity, chronic obstructive pulmonary disease (COPD), asthma, sarcoidosis, idiopathic fibrosing alveolitis, lung transplant rejection, and autoimmune diseases have been strongly linked with dysfunctional B cells and their products [334,338]. For instance, B cells

promote overall inflammation, Th2 responses and eosinophilia in allergic diseases typically via the production of IgE [413]. Increased progenitor B cell subsets (pre- and pro-B cells) in the lung are capable of proliferating, resisting apoptosis and expressing chemotaxis markers (CCR10 and CXCR4) in allergic airways reactions [414]. In asthmatic lungs, an increased accumulation of tissue resident memory B cells, IgG1-secreting cells and BAFF levels have been associated with severe disease [415,416]. Furthermore, COPD patients display elevated levels of autoantibodies (predominantly IgG1) as well as increased numbers of B cells and ELTs in the adventitia of small airways of patients compared to controls, that associate with disease severity [417,418]. Concentration of BAFF is also observed to increase in the advanced forms COPD and patients with emphysema [419]. Several phenotypes of emphysema have been linked with B cell-rich lymphoid follicles that contribute to clonal proliferation in the emphysematous lung [420,421] and associate with increased B cell signaling [419]. Similarly, lymphoid tissues with increased B cell aggregates are commonly seen in lung biopsies of patients with idiopathic pulmonary fibrosis (IPF), however, the precise role of B cells in this disease is not well demonstrated [422,423].

Abnormalities in both circulating and tissue resident B cell subsets have been implicated in the pathophysiology of autoimmune diseases that include systemic lupus erythematosus (SLE), rheumatoid arthritis (RA), systemic sclerosis (SSc), and Sjögren's syndrome. These abnormalities include defects in B cell activation, cytokine production, induction of other immune cells, increased autoantibody production, and lymphoid organogenesis [424–427]. ELTs are thought to be the site for generating autoreactive B cells and are frequently found in the airways of patients with RA and Sjögren's syndrome [334]. Furthermore, interstitial lung disease (ILD) is a common feature of RA, SSc and Sjögren syndrome, where lung biopsies from patients show increased B cell infiltration, B cell hyperactivation and formation of B cell-rich BALT with elevated CXCL13 and CCL21 expression (not observed in healthy individuals) [428–430]. Activated B cells produce IL-6 and TGFβ that can further contribute to lung fibrosis in SSc patients [431]. In other diseases such as chronic lung transplant rejection, B cells have been shown to be key drivers of rejection via antibody production [432,433], where secreted IgGs activate macrophages and NKT cells through the FcγR [432]. Although not conclusively established in sarcoidosis, altered antibody responses are suspected to be one of the major drivers of disease pathogenesis, as observed by the increased IgG and IgA-secreting B cells in lung biopsies from patients compared to controls [434,435].

Importantly, abnormalities in immunosuppressive Breg numbers and function have also been linked to various lung pathologies, highlighting the importance of Bregs in modulating airway inflammation and maintaining tissue homeostasis [339–341,436]. While Bregs are well recognized as

important modulators of the airway inflammatory responses, specific signals in the lung microenvironment that induce Bregs currently remain unknown. Inflammatory signals that play an important role in Breg induction are upregulated in the lung microenvironment in infections and chronic inflammatory conditions, suggesting their potential involvement in Breg induction [437–441].

1.9.4 Role in disease

1.9.4.1 Lung cancer

Lung cancer is currently the leading cause of cancer deaths worldwide, with a complex pathophysiology that is not well understood [442]. Bregs play an important role in suppressing anti-tumour responses and driving tumour progression by attenuating cytotoxic CD8$^+$ T cells and NK cells while promoting functions of Tregs, myeloid-derived suppressor cells (MDSCs) and tumour-associated macrophages (TAMs) [441]. Tumor-infiltrating Bregs have been shown to mediate immunosuppression by secreting anti-inflammatory cytokines IL-10 and TGF-β, and by upregulating expression of regulatory ligands CTLA4 and PD-L1 [443–445]. Several phenotypically distinct Breg subsets have been identified in tumour settings, including CD24^{hi}CD27$^+$ memory, CD24^{hi}CD38^{hi} transitional, and CD138$^+$IgA$^+$ or CD147$^+$IgM$^+$ plasma cell phenotypes [446]. A growing body of evidence suggests that tumour-infiltrating B cells are not intrinsically suppressive and that the induction of Bregs is likely upon exposure to the lung microenvironment. The expansion of IL-10$^+$ tumor-evoked Bregs has been associated with inflammatory signals derived either directly from the tumour or indirectly from tumour-infiltrating cells in the surrounding microenvironmental milieu [446].

Studies from mouse models have provided substantial evidence supporting a role for Bregs in tumour immunity. Tumour-evoked Bregs have been shown to expand FoxP3$^+$ Tregs, induce the regulatory activity of myeloid-derived dendritic cells (MDSCs), and inhibit the tumoricidal activity of NK cells and effector T cells in a TGF-β-dependent manner [446–449]. These Bregs were found to express high levels of CD40, CD80 and CD86, suggesting the involvement of additional mechanisms of cell-contact-mediated suppression. More recently, tumor-infiltrating PD-L1^{hi}CD80^{hi}CD86^{hi}CD69^{hi} B cells have been shown to suppress Th17 cell differentiation via the PD-1/PD-L1 pathway, in a model of lung cancer [445]. Interestingly, in mouse models of lung metastasis, STAT3-expressing Bregs have also been reported to promote tumour-angiogenesis via the induction of vascular endothelial growth factor (VEGF); a feature strongly associated with B cells in human tumours [450].

Albeit limited, a new wave of evidence has also implicated a role for human Bregs in lung cancer progression. Increased frequencies of peripheral IL-10-producing $CD27^+CD24^{hi}$ Bregs and tumour-infiltrating $IL-10^+CD19$ B cells have been reported in patients with lung cancers, compared to healthy controls [339]. Together with data from murine models, these data implicate a role for Bregs in the suppression of anti-tumour immune responses. However, it is still unclear whether Bregs directly or indirectly influence the progression of lung cancer. Improved understanding of Breg induction and function in lung tumours could lead to the development of Breg-targeted therapies to enhance anti-tumour immunity.

1.9.4.3 Allergic airway inflammation

Asthma is chronic inflammation of the airway characterized by heightened reactivity and sensitivity of the airway to a variety of inhaled stimuli [465]. Bregs play a protective role against hyperresponsive airway inflammation, where IL-10-producing B cells significantly suppress inflammatory reactions [466]. Functional impairments in Bregs have been associated with enhanced asthma-like inflammation and airway hyperresponsiveness. In mouse models of disease, adoptive transfer of $CD9^+$ Bregs suppress all asthma-related features by inhibiting effector T cells in an IL-10-dependent manner [467]. In addition, IL-10-producing $CD5^+CD21^{hi}CD1d^{hi}$ Bregs can reverse allergic airway inflammation by actively recruiting immunosuppressive Tregs to the lungs [468]. Interestingly, infection with *Schistosoma mansoni* worms has been shown to protect against ovalbumin-induced allergic airway inflammation by inducing IL-10-producing T2-MZP Bregs [469]. In contrast to hypersensitivity, pathology in chronic obstructive pulmonary disorder (COPD) is a result of proteolytic destruction of the extracellular lung matrix by the immune response [470]. The main symptoms of COPD include chronic coughing, sputum production, and breathing difficulties. COPD patients have elevated frequencies of B cells and ELTs in their lungs [338], however, the role of Bregs in disease pathogenesis remains unknown. Unpublished studies from our lab identify an expansion of $Tim-1^+$ and $IL-10^+$ Bregs in the lung of COPD patients, supporting a plausible for Bregs in modulating inflammation in disease.

Idiopathic pulmonary fibrosis (IPF) is a rare form of chronic and progressive fibrosing lung disease that is characterized by an increase in collagen deposition in the lung parenchyma; it is a type of interstitial lung disease (ILD) [471]. In IPF, inhaled environmental pollutants (organic and inorganic dust) and toxins from cigarette smoke (CS) are implicative factors in the disease aetiology, since byproducts of these factors are frequently identified in the lungs of patients with this disease [471]. Lymphoid structures are commonly seen in lung biopsies of patients with IPF; however, the role

of B cells in disease pathogenesis remains ill-defined [422]. Recent evidence suggests there is a significant decrease in CD24^{hi}CD27^{+}Bregs in IPF patients, mirrored by an increase in Tfh cells and levels of BAFF in the lungs and in circulation [472]. This suggests that a lack of Breg-mediated immunosuppression and expansion of effector B cells (Beffs) likely contribute to disease pathogenesis.

1.9.4.4 Autoimmunity

Autoimmune diseases, including SLE, RA, SSc, and Sjogren's syndrome can often result in pulmonary manifestations [473]. Multiple studies have identified increased infiltration of B cells in lung tissues of patients, indicating a plausible role for B cells in disease pathogenesis [334]. Although the involvement of Bregs in lung pathology remains largely uninvestigated, numerical and functional defects in circulating Bregs have been reported in patients with SLE, SSc, RA and Sjogren's syndrome, and found to associated with disease severity [342,364,380,474]. Whether the defects in Bregs are a cause or consequence of chronic inflammation remains to be addressed.

In systemic autoimmune diseases, such as SLE and SSc, reduced frequencies of circulating CD24^{hi}CD27^{+} and CD24^{hi}CD38^{hi} Bregs have been reported in patients compared to controls [342,364]. Numerical defects are accompanied by compromised Breg functions with a significant decrease in IL-10 expression. Importantly, B cells infiltrates have been identified in the lung of SSc patients with ILD and in mouse models of pulmonary lupus [429,475]. Increased infiltration of CD20^{+} B cells and plasma cells have also been reported in lung biopsies of RA patients with interstitial pneumonia, compared to normal lungs [476]. While the phenotype of lung-infiltrating B cells remains unknown, reduced frequencies of circulating IL-10^{+} Breg subsets have been reported in RA patients compared to controls and found to correlate with disease severity [380,477]. These defects are associated with an expansion of pro-inflammatory effector B and T cells leading to exacerbated disease symptoms.

Due to the multiple abnormalities in the B cell compartment, patients with SLE, SSc and RA with pulmonary manifestations are often treated with rituximab (anti-CD20) or B cell depletion therapy. Rituximab has shown success in the treatment of early and refractory pulmonary haemorrhage in patients with SLE [478,479], as well as in improving lung function in patients with RA and SSc with ILD [480,481]. Long-term remission after B cell repopulation in rituximab-treated patients has been associated with a higher immature-to-memory B cell ratio, suggesting that repopulation of immunosuppressive CD24^{hi}CD38^{hi} Bregs might be associated with improved clinical outcomes [33,482]. This is further supported by studies reporting an expansion of CD24^{hi}CD38^{hi} Bregs with

restored STAT3 activation and IL-10 production in patients responding to rituximab therapy [344]. Further, the expansion of repopulated Bregs corresponded with normalization of pDC activation and iNKT cell function [344,387]. However, it is important to note that not all patients respond to rituximab [483], and to date, there is no strategy to predict which patients will respond to rituximab. One possible explanation is that an incomplete depletion of 'pathogenic' B cells infiltrating the lung or/ and other tissue sites contributes to the lack of clinical response. A second possibility is that repopulating B cells in non-responding patients are being skewed towards pro-inflammatory Beffs and not suppressive Bregs by environmental milieu. Another scenario is that rituximab depletes beneficial tissue-resident Bregs that suppress inflammation, and therefore exacerbates disease. Overall, the underlying mechanisms that determine clinical response to rituximab remain to be ascertained.

1.9.5 Challenges and outstanding questions

The role of Bregs as negative regulators of the immune response is now well established. More recently, it has become evident that Bregs play a role in the pathophysiology of respiratory diseases such as lung cancer, asthma, autoimmunity and IPF. While alterations in Breg numbers and function have been identified as contributors to disease pathology, the precise role of Bregs in disease pathogenesis remains to be ascertained. There are several aspects of Breg phenotype and function that must be addressed in order to exploit their therapeutic potential.

1.9.5.1 Signals inducing Breg differentiation in the lung

The environmental milieu is known to play an important role in the induction of Bregs, however specific signals in the lung microenvironment that induce Bregs remain ill-defined. In addition to TLR, BCR and CD40 signalling, exposure to inflammatory cytokines IFN-α, IFN-β, IL-1β, IL-6, IL-21 and BAFF has been shown to enhance Breg differentiation [335,337]. These signals are upregulated in the lung microenvironment in infections and chronic inflammatory conditions [438,484], suggesting their involvement in Breg induction in the airways. For instance, studies from mouse models of lung cancer suggest that Breg differentiation occurs in response to the lung tumour microenvironment [446].

The lung can experience hypoxia in pathological but sometimes also physiological situations, with associated alveolar hypoxia [485]. Moreover, cigarette smoke (CS) and CS extract activate hypoxia-inducible factor 1 (HIF-1α) in lung-epithelial cells under non-hypoxic conditions [486]. In addition to activating innate immune responses in the lung [487], systemic hypoxia and HIF-1α could play a role

in the expansion of Bregs in the lungs. Hypoxia is considered a critical factor for the induction of IL-10 by B cells and the expansion of CD1d^{hi}CD5$^+$ Bregs [488]. Importantly, mice with B cell-specific deletion of HIF-1α display reduced IL-10-producing B cells, and as a consequence exacerbated collagen-induced arthritis and experimental autoimmune encephalomyelitis. Thus, HIF-1α expression by B cells could play a protective role in tissue injury, and further studies are needed to determine whether or not the net effects of HIF-1 α in the context of inflammatory disease is beneficial.

As detailed above, AhR is a key transcription factor involved in Breg differentiation [351,352]. AhR and its ligands exhibit important immunomodulatory properties and can modulate the respiratory immune response [489]. On the one hand, AhR ligands have been shown to suppress allergic airway inflammation and prove beneficial in models of asthma [490]. On the other hand, the pathogenesis of COPD has been attributed to various cell populations expressing AhR. AhR has been shown to be a master regulator of inflammatory responses in innate immune cells and T cells, critical in driving COPD pathology [491]. The precise role of AhR in modulating respiratory disease appears to be disease and context-dependent. Further research is required to understand the multifaceted role of AhR in inflammatory lung diseases. Other signals that modulate Breg differentiation include commensal bacteria [343]. The importance of microbiota in the expansion of Bregs was confirmed by the treatment of mice with antibiotics; antibiotic-treated mice displayed reduced Bregs in comparison to untreated mice. Improved understanding of signals driving Breg differentiation in the lung could provide new therapeutic strategies.

1.9.4.2 Infections

In addition to their effector functions, B cells also produce IL-10 that limits excessive inflammation and suppresses potential pro-inflammatory cytokine over-production, known as a "cytokine storm". B cell-derived IL-10 acts as an immunoregulator, inhibiting pro-inflammatory responses and preventing tissue damage resulting from exacerbated innate and adaptive immune responses [451]. Here, we focus on the role of Bregs in the immune response during respiratory infections. The role of Bregs in other infection settings have been described in detail elsewhere [451].

Respiratory viruses, such as H1N1 influenza and SARS-CoV-2 coronavirus, are a common cause of severe pneumonia and acute respiratory distress syndrome (ARDS) [452,453]. The virus-triggered immune response is capable of resolving an infection in a majority of individuals; however, a subset of patients generate a dysfunctional immune response resulting in severe immune-mediated lung pathology and systemic hyper-inflammation. Recent evidence suggests that the

uncontrolled inflammation is partly due to abnormalities in immunosuppressive Bregs. Critically ill COVID-19 patients display a significant decrease in peripheral CD24^{hi}CD38^{hi} transitional B cells (precursors to human Bregs [364]) mirrored by an expansion of extrafollicular B cells, compared to patients with mild disease [454]. Further, B cells from acute COVID-19 patients display a reduction in IL-10 production mirrored by an expansion of IL-6, in response to TLR activation, in comparison to healthy B cells [455]. This suggests an imbalance in circulating B cells from COVID-19 patients towards a more pro-inflammatory phenotype. The reduced IL-10$^+$ Bregs are likely a result of impaired type-I interferon (IFN-I) responses previously reported in critically unwell COVID-19 patients [456]; anti-viral IFN-I is a key signal for IL-10$^+$ Breg differentiation [344]. Remarkably, IL-10$^+$ Breg frequencies are normalised in COVID-19 patients upon recovery [455]. In contrast, respiratory syncytial virus (RSV) causing lower respiratory tract infections in infants is associated with an increased infiltration of pulmonary neonatal Bregs (nBregs) that secrete IL-10 in response to RSV and dampen Th1 function. The frequencies of RSV-infected nBregs have been shown to correlate with increased viral load and predict severity of acute bronchiolitis disease, suggesting that nBregs are detrimental to host response in early-life . While the expansion of Bregs in neonates inhibits generation of an effective immune response to the virus, the lack of Bregs and resulting exacerbated inflammation appears to contribute to severe disease and ARDS in older adults. This is supported by multiple studies reporting an age-related numerical and functional decline in transitional Bregs that might contribute towards 'inflammaging' or the chronic inflammation observed with ageing [367,458]. Reduced frequency of transitional B cells as well as impaired STAT3 phosphorylation and IL-10 production in response to TLR/ CD40 activation has been reported in healthy older donors (>60 years old) compared to healthy younger donors (20-40 years old). Of note, no age-associated changes in CD80 and CD86 were observed, suggesting that contact-dependent suppressive capacity of Bregs might remain intact with age [458].

Parasitic infections of the lung may affect the respiratory system by causing pulmonary alveolar haemorrhage, bronchiolitis, and pneumonitis [459]. Bregs suppress damaging inflammation in parasitic airway infection via the production of IL-10 and TGF-β, thus playing an essential immunosuppressive role in various helminth infections, including *Ascaris, Toxocara, Onchocerca and Trichuris* [460]. In addition, IL-10-producing CD1d^{hi} Bregs were shown to induce immunomodulation by influencing FoxP3$^+$ Tregs in S. *mansoni* and H. *polygyrus* infections [461,462]. In contrast, studies in other infection settings have implicated a role for Breg expansion in hindering pathogen clearance. For instance, in bacterial infections such as tuberculosis (TB), caused by *Mycobacterium tuberculosis*, CD19$^+$CD1d$^+$CD5$^+$ Bregs suppress IL-22 secretion (vital in combating TB infection) and selectively inhibit Th17 responses [340,383]. Furthermore, response

69

to TB treatment has been associated with a decrease in CD19^{+}CD1d^{+}CD5^{+} Bregs and an increase in IL-22 production, thereby emphasizing the detrimental effects of Bregs in this infection [383]. Another unique subset of lung-resident IL-10-producing CD19^{+}B220^{-} B cells has been shown to exacerbate *Streptococcus pneumoniae* infection [463]. Similarly, in fungal infections such as pneumocystis pneumonia (PCP), an increase in IL-10-producing Bregs has been associated with the inhibition of Th1/ Th17 responses and effective pathogen clearance [464]. Overall, it appears that immunosuppressive functions of Bregs can be either detrimental or beneficial depending on the disease context.

1.9.5.2 Plasticity and stability of Bregs in the lung

Another critical question is whether Bregs remain stable over time. Although abnormalities in Breg numbers and function have been associated with various respiratory diseases, the stability of lung infiltrating Bregs remains unknown. Bregs have been identified at various stages of B cell development, and thus far, no lineage-specific transcription factor has been identified [336]. It remains unknown whether Bregs can differentiate into Beffs upon exposure to chronic inflammatory conditions. Although pro-inflammatory cytokines induce Breg differentiation, the level of exposure is crucial in determining B cell fate. Whereas low-moderate concentrations of IFN-α simultaneously induce Breg and plasmablast differentiation, high concentrations have been shown to preferentially skew B cell differentiation towards Beffs and fail to expand Bregs [344]. In patients with SLE, increased IFNα signalling is associated with an expansion of autoantibody-secreting plasmablasts and a loss of Bregs, linked to alterations in STAT1/ STAT3 phosphorylation downstream of the IFN-α/β receptor. As a result, chronic exposure of B cells to increased levels of pro-inflammatory signals, such as in autoimmune diseases, could impair Breg function and enhance Beff differentiation. Although IL-10-secreting plasmablasts exhibiting immunosuppression have been identified in models of autoimmune diseases [354], an independent study has shown that Bregs transiently secrete IL-10 and terminally differentiate into antibody-secreting cells [492]. This is further supported by studies reporting a role for plasma cell-specific transcription factor Blimp1 in the generation and function of IL-10-producing Bregs [353]. Further investigations on Breg plasticity and stability are necessary to understand the possibility of generating a prolonged Breg phenotype.

1.9.6 Therapies targeting Bregs

Current therapies for various respiratory diseases focus on disease management rather than offer a cure and become toxic and ineffective over a period of time. Highly targeted immunotherapies offer several advantages over conventional steroid and immunosuppressants and have proven highly effective in the treatment of pulmonary diseases [493,494]. The use of rituximab for the treatment of pulmonary manifestations in autoimmune diseases has shown some success [478–481]. While targeting aberrant B cells is beneficial, the lack of clinical response in some patients could be associated with the depletion of immunosuppressive Bregs. Therapies targeting specific subsets of Bregs could be advantageous in different disease settings. For instance, increased infiltration of PD-L1[hi]Bregs in lung tumours has provided the rationale for PD-L1 and PD-1 blockade [495]. Remarkably, studies show that targeting the PD-1/PD-L1 pathway can improve the survival of patients with advanced lung cancer [496]. Several strategies to isolate, expand or deplete Bregs to treat various immune-related pathologies have been discussed elsewhere [337]. Taken together, these reports suggest that a better understanding of lung infiltrating Bregs could provide novel therapeutic targets for improved management of various respiratory diseases.

1.9.7 Conclusions

A balance in effector and regulatory responses is necessary to maintain proper immune surveillance in the lungs, while at the same time preventing chronic inflammation, fibrosis, and autoimmunity. The various airway inflammatory diseases resulting from abnormalities in Breg function emphasize the importance of immunosuppressive Bregs in maintaining immune homeostasis. Notably, the identification of multiple phenotypically distinct Breg subsets at different stages of B cell development suggest that any B cell can become regulatory upon exposure to specific environmental stimuli and exhibit suppressive capacity. Further research into the biology of lung infiltrating Bregs and the signals that drive Breg differentiation could provide novel therapeutic avenues for improved management of respiratory diseases.

1.9.8 Acknowledgements

1.10 Aims:

The aim of this thesis is to:

1. Characterise the B cell phenotypes in the blood and lung of COPD patients.
2. Demonstrate B cell function in COPD patients.
3. Characterise spatial B cell distribution in COPD lung.
4. Investigate the differential gene expression in B cells from COPD lungs.
5. Investigate the longitudinal effects of B and T cells in acute and convalescent COVID-19 patients.

Chapter 2.

Materials and Methods

2.1 Samples

2.1.1 Lung samples

Healthy margins of lung tissue (> 6 cm from cancer) were identified by a histopathologist and dissected under the ethical approval of the Manchester Allergy, Respiratory and Thoracic Surgery (ManARTS) Biobank at the University Hospital of South Manchester. This was collected, together with matched peripheral blood samples. National Research Ethics Service Committee granted ethical approval; Northwest – Haydock (ref; 15/NW/0409). Written consent was obtained from all the patients that participated in this study.

2.1.1.2 Sample selection.

All participants were lung cancer patients undergoing cardiothoracic surgery for lung resections. Participants with a forced expiratory volume in 1 second/forced vital capacity (FEV1/FVC) of ≥ 0.80 with no other underlying respiratory disease were categorized as 'healthy'. Participants with COPD were defined by physician diagnosis and exhibited an FEV1/FVC < 0.80 At the time of collection, the patients' clinical details provided included age, sex, smoking history, COPD status, FEV1, FEV1% predicted, FVC, and FEV1/FVC ratio, with occasional medication history and co-morbidities. We, however, don't have the information about the type of cancer and location of the resected tumor. Details of patients' demography are outlined in **Table 2.1**.

Table 2.1: COPD and non-COPD Patients' demographics

Demography	COPD	Control
Age		
51 - 60	0	4
61 - 70	5	2
71 - 80	3	10
81 - 90	4	3
Smoking history		
Current smokers	6	6
Ex-smokers	5	6
Never-smokers	1	7
FEV1 (% predicted)		
≥ 80	5	13

50 – 79	6	6
30 – 49	1	0
< 30	0	0
Gender		
Male	8	8
Female	4	11
Total	**12**	**19**

2.1.2 Cell isolation

2.1.2.1 Lung single-cell suspension

Dissected lung tissue was finely chopped and digested with Hanks buffer (Sigma – H9269) supplemented with 150 µg/ml Liberase TL (Sigma 05401020001) and 50 µg/ml DNAse (Sigma D5025) at 37°C for 40 minutes on a shaker. The reaction was stopped with RPMI 1640 containing 10% fetal calf serum (FCS), L-Glutamine, non-essential amino acids, HEPES,100 U/ml of penicillin, 100 µg/ml streptomycin, and 0.5 mM EDTA (complete media). This is followed by straining with a 70 µm cell strainer (BD labware, New Jersey, USA). The resulting single-cell suspension was centrifuged for 5 minutes at 500 g, then washed in complete media. The cells were resuspended complete media, layered over Ficoll (Sigma GE17-1440-03) and centrifuged at 500 g for 30 minutes with zero breaks. Mononuclear cells were collected at the interface, washed, resuspended in complete media, and counted. Isolated cells were resuspended in 10 % Dimethyl sulfoxide (DMSO) 90 % FCS (freezing media), transferred into cryovials (≤ 10^7 cells/vial) and stored overnight at - 80°C then at -150°C for longer period. A piece of the tissue is fixed for histology analysis prior to digestion. All samples were processed not more than 24 hrs from lung resection

2.1.2.2 Peripheral Blood Mononuclear Cell (PBMC) Isolation

EDTA peripheral blood sample was diluted 1:1 in PBS and carefully layered on Ficoll, and centrifuged at 500 g for 30 minutes with zero breaks. PBMCs were collected from the interface, washed and resuspended in PBS, and then counted using trypan blue and a haemocytometer. The isolated cells were then stored at -150°C as described above.

2.2 Cell suspension analysis

2.2.1 Cell thawing

Frozen cells were thawed (one vial at a time) by warming the vial in a 37°C water bath for 30 seconds. 200 µl of pre-warmed complete media was added slowly to the cryovial and was gently mixed; the cryovial content was then transferred into a pre-warmed media drop by drop with an intermittent shake. The thawed cells were centrifuged at 500 g for 5 minutes, washed twice in complete media, and counted.

2.2.2 Cell culture

Thawed mononuclear cells from blood and lung tissue were washed and resuspended in complete media. 5×10^5 cells were stimulated with either; (i) 1 µM CpG-B DNA (Cambridge Bioscience: Hycult HC4039) alone, (ii) 1 µg/ml CD40L (R&D Systems: 6245-CL-050) alone, (iii) combination of i and ii for 48 hours followed by 2µL/ml of stimulation cocktail (eBioScience: 00-4970-93) in the presence of 10 µg/ml Brefeldin A (BFA) in the last four hours (B cells). For unstimulated controls, cells were incubated with culture buffer alone for 48 hours, followed by incubation with the stimulation cocktail and BFA in the last four hours. Following stimulation, cells were washed and stained for flow cytometric analysis.

2.2.3 Flow Cytometry

Cells (freshly thawed or cultured) were stained with live/dead stain (Zombie UV™ Fixable Kit: Biolegend) for 10 minutes at 4°C in the dark. Cells were washed once in FACS buffer (2% FCS in 1x PBS) and incubated in FcR block (Miltenyl Biotech) for 10 mins, followed by centrifugation at 500 g for 5 mins. Cells were stained in primary antibody cocktails (**Table 2.2**) at 4°C for 20 minutes in the dark. Cells were washed twice in FACS buffer, followed by fixing in fixation and permeabilisation buffer (concentrate: diluent, 1:3) (eBioscience™) for 20 mins at 4°C, followed by a wash in FACS buffer.

For intracellular staining, cells were washed once in permeabilisation buffer (concentrate:dH_2O, 1:9) (Invitrogen™) then stained in secondary antibody cocktail (**Table 2.2**) in permeabilisation buffer for 30 at mins 4°C in the dark. The cells were washed in perm buffer, then in FACS buffer and finally resuspended in FACS buffer. The cells were acquired on a BD FACS Symphony™ flow cytometer (BD Bioscience). The data were analysed using FlowJo version 10.9 (Treestar,

Oregon). Appropriate isotypes were used for all markers as controls, and gating was established using Floresecnce minus one (FMO) control.

Table 2.2: Outline of antibodies used for flow cytometry analysis

Antibody Target	Fluorochrome	Concentration	Clone	Company
Extracellular Abs				
Live/Dead	Zombie UV	1:500		BioLegend
CD45	BUV395	1:50	HI30	BD Bioscience
CD3	BV605	1:50	SK7	BioLegend
CD19	BUV737	1:50	HIB19	BD Bioscience
CD24	APC-e-Floor	1:50	eBioSN3	eBioscience
CD38	PerCP-Cy5.5	1:50	HIT2	BioLegend
CD27	BV711	1:50	M-T271	BioLegend
IgD	BV785	1:50	IA6-2	BioLegend
IgM	FITC	1:50	MHM-88	BioLegend
IgA	APC	1:50	REA1014	Miltenyi Biotec
Tim1	PE	1:50	1D12	BioLegend
CXCR3	BV510	1:50	G025H7	BioLegend
Hif-α	PE	1:50	546-16	BioLegend
Pax5	BV421	1:50	1H9	BD Bioscience
CD86	APC	1:50	BU63	BioLegend
CD11c	BB515	1:50	B-ly6	BD Bioscience
Intracellular Abs				
IL-10	APC	1:25	JES3-19F1	BD Bioscience
Bcl-6	APC	1:50	7D1	BioLegend
Tbet	BV421	1:50	4B10	BioLegend
Ki67	PE	1:50	ki-67	BioLegend
Blimp1	AF 488	1:25	646702	R&D Systems
IgG	BV421	1:50	M1310G05	BioLegend

TNF-α	PE-Cy7	1:50	MAb11	BD Bioscience
IL-6	PE	1:100	MQ2-13A5	BioLegend

2.2.4 B cell sorting

Thawed cells were incubated in FcR block in FACS buffer for 10 mins at 4°C in the dark, followed by centrifugation at 500 g for 5 mins. Cells were stained with CD19, CD3, and CD45 antibodies (Table 2.2) for 20 mins at 4°C in the dark then washed in FACS buffer. B cells were sorted as live CD45+CD-CD19low/+ at 4°C on BD Influx cell sorter (BD Bioscience). The sorted cells were washed in FACS buffer and submitted to genomic technology core facilities (University of Manchester) for sing-cell RNA sequencing analysis.

2.2.5 Mass Cytometry (CyTOF Helios)

Antibodies pre-conjugated to metal tags from Fluidigm or purchased protein-free elsewhere and conjugated in-house using the Fluidigm MaxPar labelling kits following the manufacturer's instructions. Cells were washed in MaxPar PBS and incubated in 200 µm Rhodium intercalator (1:500 dilution) (Fluidigm) for 15 min at room temperature for cellular viability. Cells were washed in MaxPar PBS, then in Cell-staining buffer (CSB, Fluidigm), followed by incubation in FcR block (Miltenyi) diluted 1:100 in MaxPar PBS for 15 minutes at room temperature. Cells were stained in primary antibody cocktail (**Table 2.3**) in CSB for 30 min at room temperature, then washed twice in CSB. Cells were fixed for 15 minutes in 1X Fix I buffer (Fluidgm) at room temperature.

For intracellular staining, cells were permeabilised by washing in Perm-S-buffer (Fluidigm), followed by staining in intracellular Abs in Perm-S-buffer for 30 min at room temperature, then 2x washing in Perm-S-buffer. Cells were then resuspended overnight in cell-ID Iridium intercalator (Fluidigm) diluted 1:2000 in fixation and permeabilisation buffer (Fluidigm), followed by washing in MaxPar PBS. Data were acquired on the CyTOF Helios mass cytometer, and files were exported in flow cytometry files (FCS) format for analysis. Data normalisation was done in CyTOF software (Fluidigm), and data analysis was done with R scripts and FlowJo software.

Table 2.3: List of antibodies and their metal conjugates for CyTOF analysis

Antibody Target	Metal Tag	Concentration	Clone	Company

Extracellular Abs				
CD45	89Y	1:100	HI30	Fluidigm
CD19	113In	1:20	HIB19	BioLegend
CD3	115In	1:50	UCHT1	BioLegend
CD10	141Pr	1:33	HI10a	BioLegend
CD5	143Nd	1:100	UCHT2	Fluidigm
CD20	147Sm	1:100	2H7	Fluidigm
CD21	196Pt	1:30	#544408	R&D Systems
CD24	142Nd	1:50	ML5	BioLegend
CD27	195Pt	1:50	323	BioLegend
CD22	159Tb	1:100	HIB22	Fluidigm
CD33	169Tm	1:100	WM53	Fluidigm
CD36	152Sm	1:100	5271	Fluidigm
CD38	194Pt	1:100	HIT2	BioLegend
CD40	151Eu	1:40	5C3	BioLegend
CD43	155Gd	1:33	#290111	R&D Systems
CD44	166Er	1:100	BJ18	Fluidigm
CD62L	153Eu	1:100	DREG56	Fluidigm
CD69	162Dy	1:100	FN50	Fluidigm
CD80 (B7-1)	161Dy	1:100	2D10.4	Fluidigm
CD86	164Dy	1:40	IT2.2	BioLegend
CD138	170Er	1:40	DL-101	BioLegend
CD11c	174Yb	1:50	3.9	BioLegend
CD1c	172Yb	1:20	REA694	Miltenyi Biotec
CD1d	176Yb	1:40	51.1	BioLegend
B220	144Nd	1:50	RA36B2	BioLegend
HLA-DR	198Pt	1:50	L243	BioLegend
IgD	146Nd	1:100	IA62	Fluidigm
IgM	149Sm	1:40	MHM-88	BioLegend
IgG	145Nd	1:30	#97924	R&D Systems
IgA	148Nd	1:100	Polyclonal	Fluidigm
NOTCH-1	165Ho	1:33	#527425	R&D Systems
Tim-1	167Er	1:33	#219211	R&D Systems

TLR-4/CD284	173Yb	1:40	#610015	R&D Systems
CXCR4	156Gd	1:100	12G5	Fluidigm
CXCR5	171Yb	1:100	RF8B2	Fluidigm
CXCR6	160Gd	1:100	K041E5	Fluidigm
CCR4/CD194	175Lu	1:100	L291H4	Fluidigm
BAFF-R (CD268)	158Gd	1:33	#2403C	R&D Systems
CXCR3	154Sm	1:40	#49801	R&D Systems
Intracellular Abs				
IL-10	150Nd	1:50	JES3-9D7	BioLegend
Bcl-2	168Er	1:40	E17	Abcam
Bcl-6	163Dy	1:100	K11291	Fluidigm

2.3 Histology

2.3.1 Tissue processing

All tissue processing was done in the histology facility (University of Manchester). Lung tissue was placed in 10% formaldehyde overnight then stored in 70% ethanol. Tissue was removed from 70% ethanol, placed in a histology cassette, and then placed in a Shandon Citadel 2000 automated tissue processor (Thermo Scientific). The automated process consisted of passing samples through different stages, including dehydration in ascending ethanol concentrations, clearing in Xylene, and embedding in molten paraffin wax.

Processed tissue was then manually embedded in paraffin wax blocks using a Shandon Histocentre2 (Thermo Scientific). The tissue blocks were sectioned with Microm HM 330 (Thermo Scientific) microtome at 5 µm thickness and placed on superfrost™ adhesion slides.

2.3.2 Haematoxylin and Eosin (H&E) staining

Paraffin sections were dewaxed in xylene solutions, rehydrated in descending ethanol concentrations (100%, 95%, 80%, and 75%), then washed with distilled water. Sections were subsequently H&E stained using the Shandon Linistain GLX (Thermo Scientific).

2.3.2.1 H and E image analysis

Stained H&E slides were imaged using the Pannoramic 250 Flash III (3DHistech) in the Bioimaging facility (University of Manchester). Images were further analysed using CaseViewer (3DHistech) to identify the region of interest for Hyperion analysis.

2.3.3 Imaging Mass Cytometry (CyTOF Hyperion)

Freshly cut sections were deparaffinised in Xylene and rehydrated in descending ethanol concentrations (100%, 95%, 80%, 70%) and finally washed in Milli-Q water. The tissue slides were then incubated in 1X pre-heated antigen retrieval buffer (Abcam, 100X Tris Buffer, pH = 10.0) for 30 min at boiling temperature. Then left in the antigen retrieval solution for another 30 min at room temperature to cool down. The slides were dried, and a hydrophobic barrier was drawn around the tissue on the slide with a PAP pen. The tissue was then blocked with 3% bovine serum albumin (BSA) in MaxPar PBS for 45 min at room temperature, followed by three washes in MaxPar PBS and staining with metal-conjugated antibody cocktail (**Table 2.4**) in MaxPar PBS overnight at 4°C. The slides were then washed in 0.2% Triton^{TM} X-100 (Thermo Scientific) in MaxPar PBS at room temperature for 8 min, followed by 3X washing with MaxPar PBS and staining with cell ID intercalator Iridium (concentration: MaxPar PBS, 1:400), (Fluidigm) for 30min at room temperature. The slides were finally washed with Milli-Q water and air-dried overnight. Data were acquired on a Hyperion imaging system coupled to a Helios mass cytometer (Fluidigm).

2.3.3.1 Hyperion Imaging analysis

Regions of interests (ROIs) were imaged using the H&E-referenced image of the same section. Images created by the Hyperion system were exported as MathCad (MCD) files. These were initially analysed in MCD viewer software (v1.0.560.6) and exported as OME-TIFF 16-bit file format. Cellular segmentation masks were generated using CellProfiler (4.2.1) data analysis pipeline as recommended by Fluidigm. The extracted OME-TIFF ROIs data from MCD and the generated segmented masks were imported into HistoCAT and finally exported as CSV files for statistical analysis in GraphPad Prism version 9.

Table 2.4: List of antibodies and their metal conjugates for Imaging Mass Cytometry analysis

Antibody Target	Metal Tag	Concentration	Clone	Company
aSMA (1A4)	141Pr	1:300	1A4	Fluidigm
Vimentin	143Nd	1:200	D21H3	Fluidigm
E-Cadherin	158Gd	1:200	24E10	Fluidigm
Collagen I	169Tm	1:400	Polyclonal	Fluidigm
Histone H3	171Yb	1:200	D1H2	Fluidigm
Pan-Keratin	148Nd	1:150	C11	Fluidigm
FoxP3	155Gd	1:100	236A/E7	Fluidigm
CD4	156Gd	1:150	EPR6855	Fluidigm
CD68	159Tb	1:100	KP1	Fluidigm
CD20	161Dy	1:100	H1	Fluidigm
CD8a	162Dy	1:100	C8/144B	Fluidigm
CD3	170Er	1:100	Polyclonal, C-Terminal	Fluidigm
CD45RO	173Yb	1:200	UCHL1	Fluidigm
CD14	144Nd	1:100	EPR3653	Fluidigm
CD11b	149Sm	1:100	EPR1344	Fluidigm
CD31	151Eu	1:100	EPR3094	Fluidigm
CD11c	154Sm	1:100	Polyclonal	Fluidigm
CD21	153Eu	1:50	# 544408	R&D Systems
FoxJ1	176Yb	1:50	# 407003	R&D Systems
IgD	150Nd	1:50	IgD26	Miltenyi Biotec
IgA	164Dy	1:50	EPR5367-76	Abcam
IgM	165Ho	1:50	MHM-88	BioLegend
Cytokeratin-5	175Lu	1:100	EP1601Y	Abcam
Cell ID Intercalatorr	Ir	1:400		Fluidigm

2.5 single-cell RNA-sequencing

The genome technology core facility (GTCF: University of Manchester) did all sample analyses, and the Bioinformatics core facility (University of Manchester) performed all the data analysis.

2.5.1 Single-cell isolation and library construction

Gene expression libraries were prepared from single cells using the Chromium Controller and Single Cell 3' Reagent Kits v3.1 (10x Genomics, Inc. Pleasanton, USA) according to the manufacturer's protocol (CG000315 Rev B). Briefly, nanoliter-scale Gel Beads-in-emulsion (GEMs) were generated by combining barcoded Gel Beads, a master mix containing cells, and partitioning oil onto a Chromium chip. Cells were delivered at a limiting dilution, such that the majority (90-99%) of generated GEMs contain no cell, while the remainder largely contain a single cell. The Gel Beads were then dissolved, primers released, and any co-partitioned cells lysed.

Primers containing an Illumina TruSeq Read 1 sequencing primer, a 16-nucleotide 10x Barcode, a 10-nucleotide unique molecular identifier (UMI) and a 30-nucleotide poly(dT) sequence were then mixed with the cell lysate and a master mix containing reverse transcription (RT) reagents. Incubation of the GEMs then yielded barcoded cDNA from poly-adenylated mRNA.

Following incubation, GEMs were broken and pooled fractions recovered. First-strand cDNA was then purified from the post GEM-RT reaction mixture using silane magnetic beads and amplified via PCR to generate sufficient mass for library construction.

Enzymatic fragmentation and size selection were then used to optimise the cDNA amplicon

size. Illumina P5 & P7 sequences, a sample index, and TruSeq Read 2 sequence were added via end repair, A-tailing, adaptor ligation, and PCR to yield final Illumina-compatible sequencing libraries.

2.5.2 Sequencing

The resulting sequencing libraries comprised standard Illumina paired-end constructs flanked with P5 and P7 sequences. The 16 bp 10x Barcode and 10 bp UMI were encoded in Read 1, while Read 2 was used to sequence the cDNA fragment. Sample index sequences were incorporated as the i7 index read. Paired-end sequencing (26:98) was performed on the Illumina NextSeq500 platform using NextSeq 500/550 High Output v2.5 (150 Cycles) reagents. The .bcl sequence data were processed for QC purposes using bcl2fastq software (v. 2.20.0.422) and the resulting .fastq

files assessed using FastQC (v. 0.11.3), FastqScreen (v. 0.9.2) and FastqStrand (v. 0.0.5) prior to pre-processing with the CellRanger pipeline.

2.5.3 Raw data processing

Raw sequencing data were processed using the 10x Genomics Cell Ranger pipeline (v6.0.0). The Illumina Binary Base Call (BCL) files were demultiplexed using the command `cellranger mkfastq` to produce FASTQ files. The FASTQ files were then processed using the command `cellranger count` with a pre-built Cell Ranger human reference package (GRCh38-2020-A) to generate the gene-cell barcode matrix. The key metrics generated by the Cell Ranger pipeline about the barcoding and sequencing process are provided in **Table 2.5**.

Table 2.5: Gene expression metrics for 10x Genomics scRNA-seq of the six lung tissue samples

A detailed description of the metrics can be found on the 10x Genomics website at: https://support.10xgenomics.com/single-cell-gene-expression/software/pipelines/latest/output/gex-metrics

Metric	6209HN	6270CE	6435HE	6435HN	6756CC	6808CC
Disease category	Control	COPD	Control	Control	COPD	COPD
Estimated Number of Cells	4,810	6,069	6,391	3,437	4,043	5,384
Fraction Reads in Cells	78.60%	94.50%	96.00%	83.70%	74.30%	89.50%
Mean Reads per Cell	20,293	32,471	33,691	31,283	25,497	19,608
Median Genes per Cell	1,100	2,238	2,979	1,386	1,236	1,179
Total Genes Detected	22,982	23,293	23,307	22,868	22,034	23,568
Median UMI Counts per Cell	2,836	8,577	12,988	3,708	3,269	3,334
Number of Reads	97,610,684	197,066,854	215,320,178	107,518,846	103,083,854	105,570,365

Number of Short Reads Skipped	0	4,765,998	5,034,128	0	0	0
Valid Barcodes	97.40%	98.00%	98.20%	97.60%	97.40%	97.90%
Valid UMIs	99.90%	99.90%	99.90%	99.90%	99.90%	99.90%
Sequencing Saturation	37.40%	51.00%	42.30%	52.20%	43.40%	36.40%
Q30 Bases in Barcode	97.80%	97.80%	97.80%	97.80%	97.80%	97.80%
Q30 Bases in RNA Read	92.80%	93.20%	92.90%	93.00%	93.00%	92.50%
Q30 Bases in UMI	97.10%	97.20%	97.20%	97.10%	97.10%	97.10%
Reads Mapped to Genome	96.90%	97.50%	97.50%	96.90%	96.90%	95.40%
Reads Mapped Confidently to Genome	93.20%	94.20%	95.50%	93.30%	93.10%	92.20%
Reads Mapped Confidently to Intergenic Regions	5.60%	3.90%	3.10%	5.50%	4.80%	5.50%
Reads Mapped Confidently to Intronic Regions	35.80%	21.10%	18.50%	33.30%	34.20%	28.00%
Reads Mapped Confidently to Exonic Regions	51.80%	69.30%	73.90%	54.50%	54.10%	58.80%
Reads Mapped Confidently to Transcriptome	48.90%	67.30%	72.00%	51.80%	51.30%	56.50%
Reads Mapped Antisense to Gene	1.50%	0.70%	0.60%	1.40%	1.40%	1.00%

2.5.4 Cell filtering and cell type annotation

Expression matrices were processed in R environment (v4.1) using various R packages. Briefly, the matrix data (HDF5) of each sample was imported as *SingleCellExperiment* object using the `read10xCounts` function in the DropletUtils R package (v1.12.1). The `addPerCellQC` and `addPerFeatureQC` functions from the scuttle R package (v1.2.0) were used to compute and add per-cell and per-gene quality control metrics to the *SingleCellExperiment* object. We used a combination of median absolute deviation (MAD), as implemented by the `isOutlier` function in the scuttle R package and exact thresholds to evaluate the per-cell QC metrics, including UMI count, the UMI count, number of detected genes, proportion of mitochondrial reads and complexity of RNA species, to identify and subsequently remove poor quality cells before further processing.

To compute deconvolution size factors, we first used the `quickCluster` function to group cells into clusters of similar expression, then used the `computeSumFactors` function to normalise cell-specific biases to compute size factors for each cell. Both functions are available from the scran R package (v1.20.1). The `calculateCPM` function from the scuttle R package was used to calculate counts-per-million (CPM) values from the count data, which make use of the size factors calculated previously. The log2-transformed normalised values were stored in the *logcounts* slot of the *SingleCellExperiment* object.

The SingleR R package (v1.6.1) was used to annotate cells against curated reference expression datasets (namely *DatabaseImmuneCellExpressionData*, *MonacoImmuneData*, and *NovershternHematopoieticData*) from the celldex R package (v1.2.0).

2.5.5 Data integration

The log-normalised expression values of the six samples were re-calculated using the `multiBatchNorm` function from the batchelor R package (v1.8.0) to adjust for the systematic differences in coverage between them. Per-gene variance of the log-expression profiles was modelled using the `modelGeneVarByPoisson` function and top 5000 highly variable genes (HVGs) were identified using the `getTopHVGs` function, both from the scran R package. The mutual nearest neighbors (MNN) approach implemented by the `fastMNN` function from the batchelor R package was used to integrate the scRNA-seq data. At the same time, multi-sample principal components analysis was performed internally. The proportion of variance lost with each batch at each merge step was examined to detect if the correct process is removing genuine biological heterogeneity.

2.5.6 Data visualisation and cell clustering

The first 50 dimensions from the MNN corrected low-dimensional coordinates for each cell were used as input to produce the t-stochastic neighbour embedding (t-SNE) projection and uniform manifold approximation and projection (UMAP) using the `runTSNE` and `runUMAP` functions from the scater R package (v1.20.0) respectively.

Next, we performed graph-based clustering of cells using the Walktrap algorithm from the igraph R package (v1.2.6) to identify "communities" of cells. Specifically, we used the `clusterRows` function from the bluster R package (v1.2.1) to streamline the clustering procedure and obtained 19 clusters.

From the larger dataset, clusters containing B cells (clusters 2 and 5) were subsetted from the main *SingleCellExperiment* object, projected into t-SNE and UMAP and re-clustered into six clusters.

2.5.7 Marker and differential expression analysis

Cluster-specific markers were identified using the `FindMarkers` function from the scran R package, which performs pairwise t-tests between clusters. To perform differential expression (DE) analysis, we created "pseudo-bulk" expression profiles from scRNA-seq data by summing raw counts from cells with the same combination of cluster label, sex, and disease state, resulting in 23 profiles in total. Pseudo-bulk profiles with less than 10 cells were removed from the DE analysis. Pseudo-bulk profiles were analysed for differential gene expression using the quasi-likelihood pipeline from edgeR (v3.34.0). Genes with a false discovery rate (FDR) below 10% were considered differentially expressed.

Results returned by edgeR, including Gene ID, log2 fold change, P-value, and FDR, were imported into the Ingenuity Pathway Analysis (IPA) software (QIAGEN Inc.). Pathway and network analysis was conducted with the IPA Winter Release 2021.

2.6 Statistical analysis

GraphPad Prism (version 9) was used for all statistical analyses. Normality tests were performed on all datasets. COPD and control groups were compared using an unpaired Mann-Whitney test. One-way ANOVA with Holm-Sidak post hoc testing (normal distribution) or Kruskal-Wallis's test with Dunn's post hoc testing (failing normality testing) was for multiple comparisons. Data are

presented as the mean ± SED. P-values < 0.05 were considered significant (*P < 0.05, **P < 0.01, ***P < 0.001).

Chapter 3.

B cell alterations in Chronic Obstructive Pulmonary Disease

Halima A. Shuwa[1], Sylvia Lui[1], Christopher Jagger[1], David. J. Morgan[1], Oliver Brand[1], I-Hsuan Lin[2], Tracy Hussell[1]*, Madhvi Menon[1]*.

[1]Lydia Becker Institute of Immunology and Inflammation, Division of Infection, Immunity & Respiratory Medicine, School of Biological Sciences, Faculty of Biology, Medicine and Health, University of Manchester, Manchester Academic Health Science Centre, Room 2.16, Core Technology Facility, 46 Grafton Street, Manchester, M13 9PL, UK.

[2]Bioinformatics Core Facility, Faculty of Biology, Medicine and Health, University of Manchester, Michael Smith Building, Dover Street, Manchester, M13 9PT, UK

Correspondence: tracy.hussell@manchester.ac.uk; madhvi.menon@manchester.ac.uk

3.0 Statement

Halima AS, Madhvi M and Tracy H conceived the overall design of the project. Halima AS implemented the experiments, analysed the data and wrote the manuscript under the supervision of Madhvi M and Tracy H. SL, CJ, DJM and OB assisted with experiments, and IL analysed the single cell-RNA-seq data. The manuscript was written according to the guidelines for publication in Nature Medicine and occupies pages 89 – 128 of this thesis.

3.1 Abstract

Background: Chronic obstructive pulmonary disease (COPD) is an inflammatory lung disease characterised by uncontrolled inflammatory responses that lead to emphysematous destruction of the lungs, which ultimately results in airflow limitation and decline in pulmonary function with limited reversibility. Recent studies show increased numbers of B cells in the COPD lung that are associated with disease severity. B cells are critical mediators of humoral immune responses in the airways through antibody production, antigen presentation and cytokine secretion. Despite their increased accumulation and persistence in the COPD lung, their role in disease pathogenesis remains understudied. In these studies, we characterize B cell subsets and their spatial distribution in the lung of COPD patients and non-COPD controls.

Results: Here, we identify dramatic alterations in B cell profiles in the lung, but not blood, of COPD patients, compared to controls. We report increased frequencies of airway-associated B cells in the COPD lung, found to be in close proximity to bronchioles and blood vessels, as well as other immune cells such as T cells and macrophages. In addition to increased frequencies of plasma cells and plasmablasts, we observe an expansion of double negative and class-switched memory B cells. Importantly, we also report a significant increase in B cells expressing Tim1 and IL-10, associated with a regulatory phenotype, in the COPD lung. Further, B cell abnormalities in the COPD lung were identified to be associated with RELA and p38 MAPK pathways involved in the activation of the signal transductions that regulate B cell activation maturation and survival, as well as the HIF-1α pathway that affects IL-10 signalling in plasma cells.

Conclusion: The data presented here suggest an increased density of organised B cell follicles and an expansion of IL-10-producing regulatory B cells in the COPD lung. Whether B cells are directly or indirectly involved in disease pathogenesis remains unclear. However, excess B cells would likely affect gaseous exchange and lung elasticity. Therefore future investigations will be required to determine the therapeutic potential of targeting B cell subsets in COPD.

Keywords
B cells, Breg, COPD, Lung, cigarette smoke

3.2 Introduction

B cells are critical mediators of humoral immune responses in the airways through antibody production, antigen presentation and cytokine secretion [334]. In addition to effector responses, a subset of B cells, known as regulatory B cells (Bregs), exhibit immunosuppressive functions and prevent uncontrolled inflammation [335]. The balance between effector and regulatory B cell functions is critical in maintaining immune homeostasis. Bregs modulate immune responses primarily, although not exclusively, via the production of IL-10 [497]. Tim-1 is a phosphatidylserine receptor on B cells that is required for appropriate IL-10 production by binding to apoptotic cells [337]. Tim1^{+} B cells are enriched for IL-10 and found to exhibit immune suppression in mice and humans [337]. Dysregulated IL-10^{+}Tim1^{+} B cells have been associated with several inflammatory disorders in humans [498].

COPD is an inflammatory lung disease caused predominantly by cigarette smoke, with a poorly reversible disease progression even after smoking cessation [271]. COPD is characterized by emphysema (alveoli destruction) and chronic bronchitis (airway inflammation and mucus hypersecretion) [268]. B cells are sparse in healthy lungs and exist as individual scattered cells or within single B cell follicles present at the major bifurcations of the conducting airways [499,500]. Depending on the inflammatory stimulus, however, B cells can form loose B cell clusters near the airways or organise into inducible bronchus-associated lymphoid tissue (iBALT). Cigarette smoke drives B cell recruitment and lymphoid neogenesis, particularly in severe stages of COPD [418] via IL-17-induced RANK-ligand [501] and the chemokines CXCL12 and CXCL13 [502,503]. Prolonged retention of B cells is likely to depend on several factors, including the production of the B cell activating factor (BAFF) that promotes survival [504] and, in mice, the production of oxysterols [505]. Compared to other immune components within the inflammatory context of COPD, the role of B cells in disease pathogenesis has received relatively less attention. Increased autoantibodies are observed in the lung and blood of COPD patients [506,507]. IgG is the most abundant form of Ig, and its levels were also dysregulated in COPD [508]. While IgA is the principal Ig found in the airway and accounts for 80% of mucosal plasma cells in healthy subjects [508,509]. The primary function of IgA is the removal of antigens at mucosal sites and requires transport across the respiratory epithelium by the poly Ig receptor, and such transport is defective in COPD [510–512].

An in-depth study of human lung B cells is complicated by the difficulty in sampling relevant tissue compartments. Biopsies recover a small representation of the lung and do not reach the terminal branches, which means the small airways are under-represented in experiments. The use of

marginal tissue from lung resections for cancer creates a mixed opinion of their relevance to the healthy lung. However, with sufficient histopathology expertise to choose regions distant from the cancer mass and the use of multi-omic RNA and protein analyses, the appropriateness of lung resections to unravel B cell biology is increasing [513]. Furthermore, patients undergoing lung resection for cancer have a range of underlying pathologies, including COPD or asthma [514], enabling dissection of B cell phenotype in a different setting. The importance of studying B cells in COPD pathogenesis is underscored by the discovery of a disease endotype with emphysema, but not decreased airflow that is dominated by B cells [419,515]. This study investigated B cell phenotype and function in COPD patients.

3.3 Results

B cells in the lung show a distinct profile from circulating B cells

Most human studies in COPD have focussed on peripheral B cell responses [338] due to limited access to human tissue samples. Here, we initially evaluated how peripheral B cell responses differ from lung B cell responses. For an in-depth comparison of B cells in lung and blood, we ran deep phenotypic profiling using CyTOF mass cytometry of cell suspensions from matched PBMCs and pulmonary mononuclear cells (PMCs) from 3 COPD patients and 4 non-COPD controls. The panel included markers of B cell lineage, chemotaxis, and function (**Table S3.2**). Following normalisation, debarcoding, quality control and gating on $CD45^+CD3^+CD19^+$ B cells (**Figure S3.1**), multidimensionality reduction of samples identified 12 unique B cell subsets in the blood and lung (**Figure 3.1a**). Next, we performed a separate hierarchical clustering on all the B cell subsets from lung and blood based on 37 measured parameters (excluding CD3, CD45 and CD19). We observed that B cell subsets from the lung clustered separately from their blood counterparts (**Figure 3.1a**). B cells from the lung displayed reduced expression of CD20 and increased expression of CD27, CD38, CD11c, Tim-1, IL-10, IgA and CD10, indicating an increase in antigen-experienced PC, switched-memory and atypical B cell populations. In contrast, circulating B cells expressed more CD20, IgD, CD62L and CD5, indicating the presence of more naïve B cells with increased tissue trafficking (**Figure 3.1b** and **S3.2**). These data demonstrate distinct B cell responses in the lung and blood, thus highlighting the importance of studying lung-resident B cells in chronic respiratory diseases.

Figure 2

Figure 3.1: B cells from matched lung and blood samples show distinct profiles

a) Mass cytometry data showing (left) tSNE plots of B cells from lung and matched blood overlaid with Phenograph subclusters and (right) heatmap showing all expressed markers, dendrogram constructed by hierarchical clustering and clusters identified using K-means. b) tSNE plots from mass cytometry data showing the expressions of selected B cell markers from the lung and matched blood overlaid with Phenograph subclusters. PC: Plasma cells, B1 PCs: B1 plasma cells, SM: Switched memory, USM: Unswitched memory, T: Transitional, N: Naïve, DN: Double negative, MZB: Marginal zone B cells.

Lung-infiltrating B cells in COPD patients show an expansion of Tim1$^+$IL-10$^+$B cells and double negative memory B cells compared to controls

Given the differences in B cells in the lung and blood, we next investigated their phenotypic differences in COPD patients and controls by multidimensionality reduction. B cell subsets from COPD lung were clustered separately from those in control (**Figure 3.2a**). We observed an increase in the percentage of B cells in COPD compared to control. The majority of the B cell subsets are plasma cells with notably reduced expression of CD20 and increased expressions of CD27, CD38, CD11c, IgG, IgA, Tim1, and IL-10 (**Figure 3.2b, c** and **S3.4**). In contrast, we observed modest differences between circulating B cells from COPD patients and controls, with mostly a uniform distribution of all measured parameters (**Figure S3.3**).

Figure 3
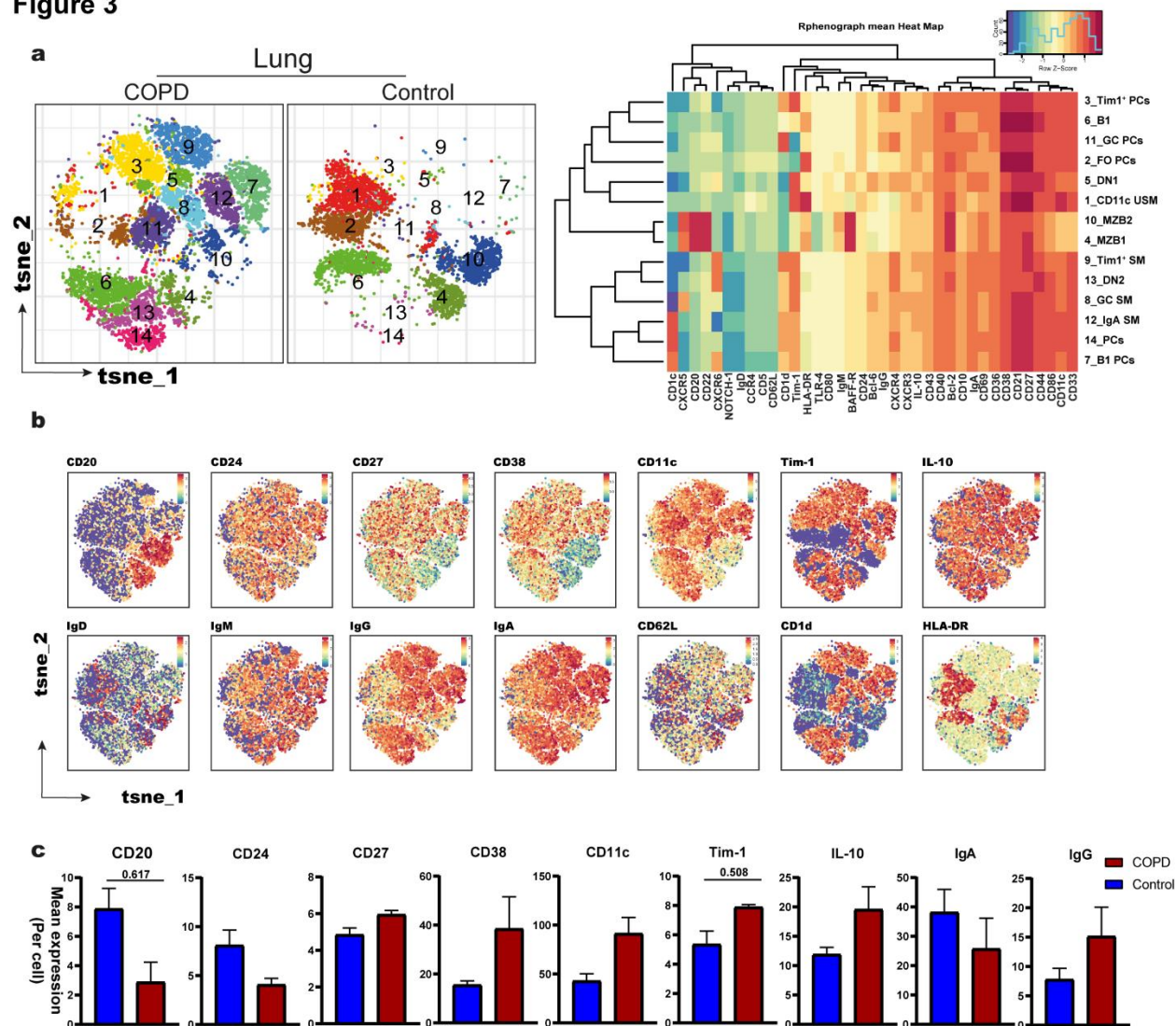
Figure 3.2: Lung resident B cells subsets from COPD and controls clusters separately and have distinct marker expression

a) Mass cytometry data showing (left) tSNE plots of B cells from COPD and control lung, overlaid with Phenograph subcluster and (right) heatmap showing all expressed markers with dendrogram constructed by hierarchical clustering and clusters identified using K-means. b) Expressions of selected markers on tSNE of B cell plots from COPD lung and control lungs, overlaid with Phenograph subclusters. c) Histogram plots showing statistics of CD20, CD24, CD27, CD38, CD11c, Tim-1, IL-10, IgA and IgG percentages in COPD versus control. PC: Plasma cells, B1 PCs: B1 plasma cells, SM: Switched memory, USM: Unswitched memory, N: Naïve, DN: Double negative, MZB: Marginal zone B cells, GC: Germinal center.

We further phenotyped B cells from PMCs and matched PBMCs by flow cytometry analysis to quantify B cells in COPD and control. In agreement with previous studies, we also observed increased percentages of CD45$^+$CD3$^-$CD19$^+$ B cells and CD38^{hi}Blimp1$^+$ plasma cells in both COPD lung and blood compared to controls, with current smokers displaying the highest increase (**Figure 3.3a** and **S3.5**). Although there was a significant increase in IgG+B cells, no differences in IgA$^+$ and IgM$^+$ B cells were observed in COPD versus control's lung and blood (**Figure 3.3a**). When characterising B cells based on the expression of IgD and CD27, we noted a significant expansion of CD27$^-$IgD$^-$ double-negative (DN) memory B cells and CD27$^+$IgD$^-$ switched memory B cells in COPD lung compared to controls mirrored by a decrease in CD27$^-$IgD$^+$ naïve B cells in the blood (**Figure 3.3b**). No differences in un-switched memory were observed. Importantly, we observed increased Tim1$^+$ (indicative of regulatory B cells [368]), Ki67+ (indicative of proliferation [516]), CXCR3+ (chemokine receptor [517(p3)]), CD86$^+$ (activation [518]) B cells expression, and CD11c+Tbet+ double-positive B cells (indicative of ongoing inflammation [142]) in the COPD lung compared to the control lung (**Figure 3.3c**).

Next, we stimulated matched PBMCs and PMCs from COPD and control patients with either CpG-B (a TLR9 agonist [519]), CD40L or the combination of both for 48 hours and measured cytokine expression by flow cytometry. We observed a significant expansion of IL-10$^+$ B cells from the lungs but not the blood of COPD current smokers in all stimulating conditions (**Figure 3.3d** and **S3.5**). However, no significant differences in the frequencies of TNF-α^+ and IL-6$^+$ B cells were observed in the lung and blood from COPD patients and controls (**Figure 3.3d** and **S3.5**). Interestingly, albeit with limited numbers, we observed a significant increase in percentages of total B cells, plasma cells, IgG+, Cd11c+, Tim-1+ and IL-10+ B cells in severe (FEV1 < 50 % of lung function predicted) compared to mild (FEV ≥ 50 % predicted) COPD (**Figure 3.3e**).
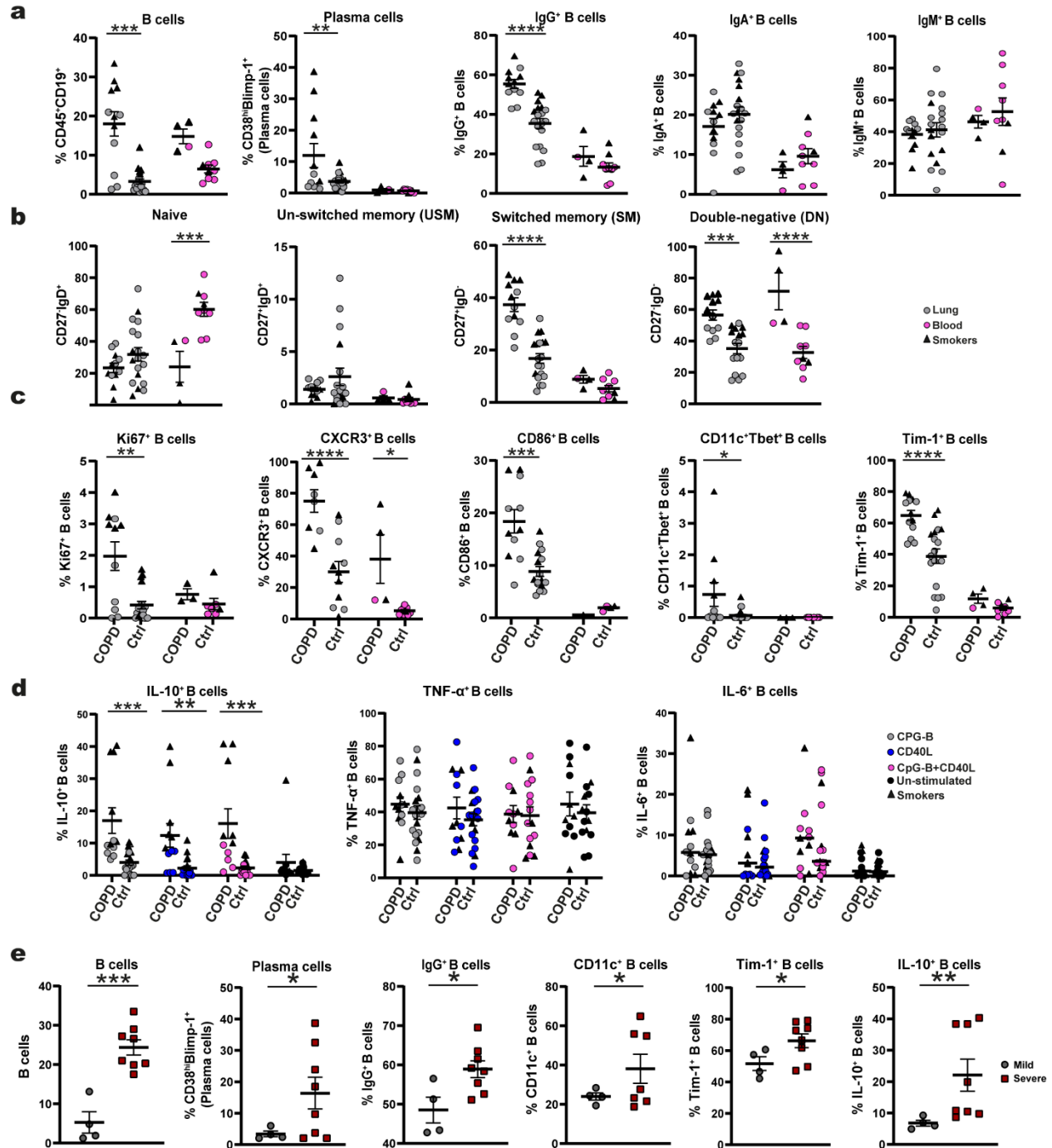
Figure 3. 3: B cell subsets in COPD and controls. Flow cytometry data showing

a) Percentages of CD45+CD3-CD19+ B cells, CD38++Blimp1+ B cells (plasma cells), IgG+, IgA+, and IgM+ B cells. b) Percentages of CD27-IgD+ as Naïve, CD27+IgD+ as un-switched memory (USM), CD27+IgD- as switched memory (SM), and CD27-IgD- as double-negative (DN) B cells in COPD (n = 12) versus control (n = 19) lung, and matched COPD (n = 4) versus control (n = 6)

blood. c) Percentages of Ki67^{+}, CXCR3^{+}, CD86^{+}, CD11c^{+}Tbet^{+} and Tim-1^{+}B cells. d) Percentages of IL-10^{+}, TNF-α^{+}, and IL-6^{+} B cells. e) Percentages of B cells, plasma cells, IgG^{+}, CD11c^{+}, Tim-1^{+} and IL-10^{+} B cells in mild versus severe COPD lungs.

Single-cell RNA sequencing of B cells from COPD lung identifies novel pathways of B cell abnormality

To identify differentially expressed genes by B cells in COPD compared to controls, we used 10x Genomics Chromium droplet single-cell RNA sequencing (scRNA-seq) of sorted B cells from three COPD and two control lung samples. Of note, all samples included were from ex-smokers to exclude the direct impact of CS exposure on B cells. Following quality control (Methods), we profiled gene expression data from 2808 B cells for clustering analysis. Our analysis revealed six B cell populations that were visualised as uniform manifold approximation and projection (UMAP) embeddings (**Figure 3.4a**). Population nomenclature was designed by specific gene expression, identifying plasma cells, plasmablasts, memory, double-negative, naive, and activated B cell populations (**Figure 3.4a, c**); COPD donors have more double-negative and memory B cells and less naïve B cells than control (**Figure 3.4b** and **S3.6a, b**).

Furthermore, within these subpopulations, we identified differentially expressed genes (DEGs) in total B cells (**Figure 3.4d, e**) and in the individual B cell populations from COPD and control lungs (**Figure 3.5 a,c,d,f and Figure S3.7 a-d**). As expected, we saw increased IL-10 gene expression in B cells from COPD patients compared to controls. (**Figure 3.4d, e**). When we compared the DE genes from COPD and controls of individual B cell subsets, we observed that the increase in IL-10 gene expression seen in B cells from COPD lungs is restricted to only the PCs and activated B cell populations (**S3.6c).** Additionally, we also found several other genes differentially expressed by B cells in COPD patients compared to controls. Upregulated genes include MMP19 (a member of matrix metalloproteases), APOE (Apolipoprotein gene), and SCGB1A1 (Secretoglobin family 1a member 1). MMPs are key mediators of lung fibrosis by regulating the extracellular matrix (ECM) and are, therefore, crucial in the development of COPD. MMP19 has a strong regulatory effect on the synthesis of extracellular matrix (ECM) components and plays a critical protective role in the progression of fibrotic lung diseases [520,521]. Thus, upregulated MMP19 expression by B cells in COPD might be critical in regulating lung inflammation. APOE is an essential component in the pathogenesis of lung disease because of their ability to promote adaptive immunity and host defense by enhancing antigen presentation [522], and to suppress inflammation, tissue remodeling and oxidative stress [523–525]. As a result, increased APOE expression by B cells

suggests increased lipid antigen presentation and iNKT cell modulation. SCGB1A1 is a pulmonary surfactant protein with anti-inflammatory and immunoregulatory effects in lung diseases [526]. SCGB1A1 expression by B cells suggests increased anti-inflammatory effects in COPD lungs. Downregulated genes include ICOSLG (ICOS ligand) [527], CCL4 and CCL 22, among others. ICOS- ICOSL binding is crucial for T cell response, and CLL4 and 22 are essential chemokines for follicular helper T cell recruitment [528,529]. Hence, their reduced expression might suggest impaired T-cell response in COPD patients.

To better understand the relationship between the DE genes, we performed an Ingenuity Pathway Analysis (IPA) of genes from total B cells that were differentially expressed between COPD and control, and observed the regulatory effects of the upstream regulators. We found RELA and p38 MAPK as the two main pathways predicted to be upregulated in B cells from COPD patients compared to controls. RELA (p65) is one of the downstream transcriptional activators of the classical NF-κB pathway that is critical for developing and surviving B cells and antigen-dependent B cell activation [530–532]. p38 MAPK (p38 mitogen-activated protein kinase) is a stress-activated pathway with functions that include control of cell proliferation, inflammation and arrest of cell cycle [533,534]. Activation of these pathways suggests increased B cell responsiveness to chronic inflammation typical of COPD.
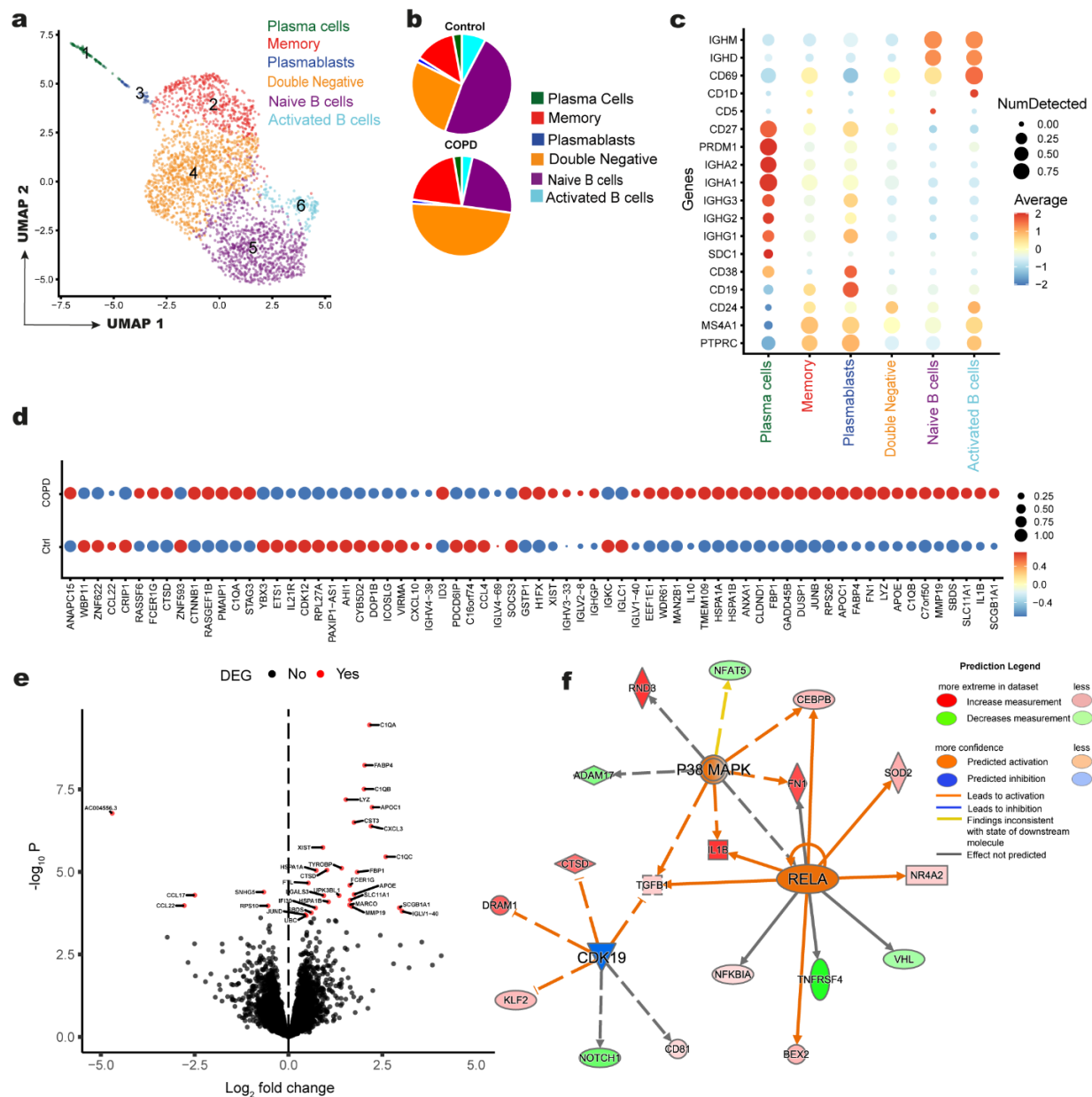
Figure 3. 4: scRNA-seq of B cells from COPD and control lungs identified six major B cell subsets

a) UMAP plot showing B cell subsets identified from scRNA-seq. b) Pie charts showing the percentage of B cell subsets in COPD (n = 3) and control (n= 2). c) Dot plots of selected gene expressed by B cells from the scRNA-seq analysis. d) Dot plots of B cells' top 50 differentially expressed (DE) genes from COPD and control. e) Volcano plot showing significant DE genes from total B cells. f) Ingenuity Pathway Analysis (IPA) of the Regulatory Effects Analysis-based network associated with DE genes from B cells in COPD and control lung.

Additionally, IPA analysis of the DE genes from individual B cell subsets predicted the regulatory effects of several upstream regulators. Analysis of plasma cells revealed predicted activation of the HIF-1α pathway that indirectly influences IL-10 activation in COPD via increased IL-15 activation (**Figure 3.5b**), suggesting hypoxia-related IL-10 activation in COPD lungs, as well as directly as shown in recent studies [535(p1)]. TP53 (a tumour suppressor gene), RELA and SMARCA4 (a component of Brahma-related gene-1; BRG1 that regulates the expression of cell cycle genes in B cells)[536] were all predicted to be activated in the DN B cell population (**Figure 3.5e**). At the same time, IFNG was predicted to be activated in the naïve B cell populations (**Figure S3.7e**). TP53, RELA and SMARCA4 genes are responsible for cellular activation, proliferation, survival and repair [530,536,537]. Hence their activation is suggestive of increased signals for B cell activation, proliferation, maintenance and survival in COPD lungs. However, we did not find any regulatory effects in memory and activated B cells by IPA due to a lack of significant correlation between the DE genes.
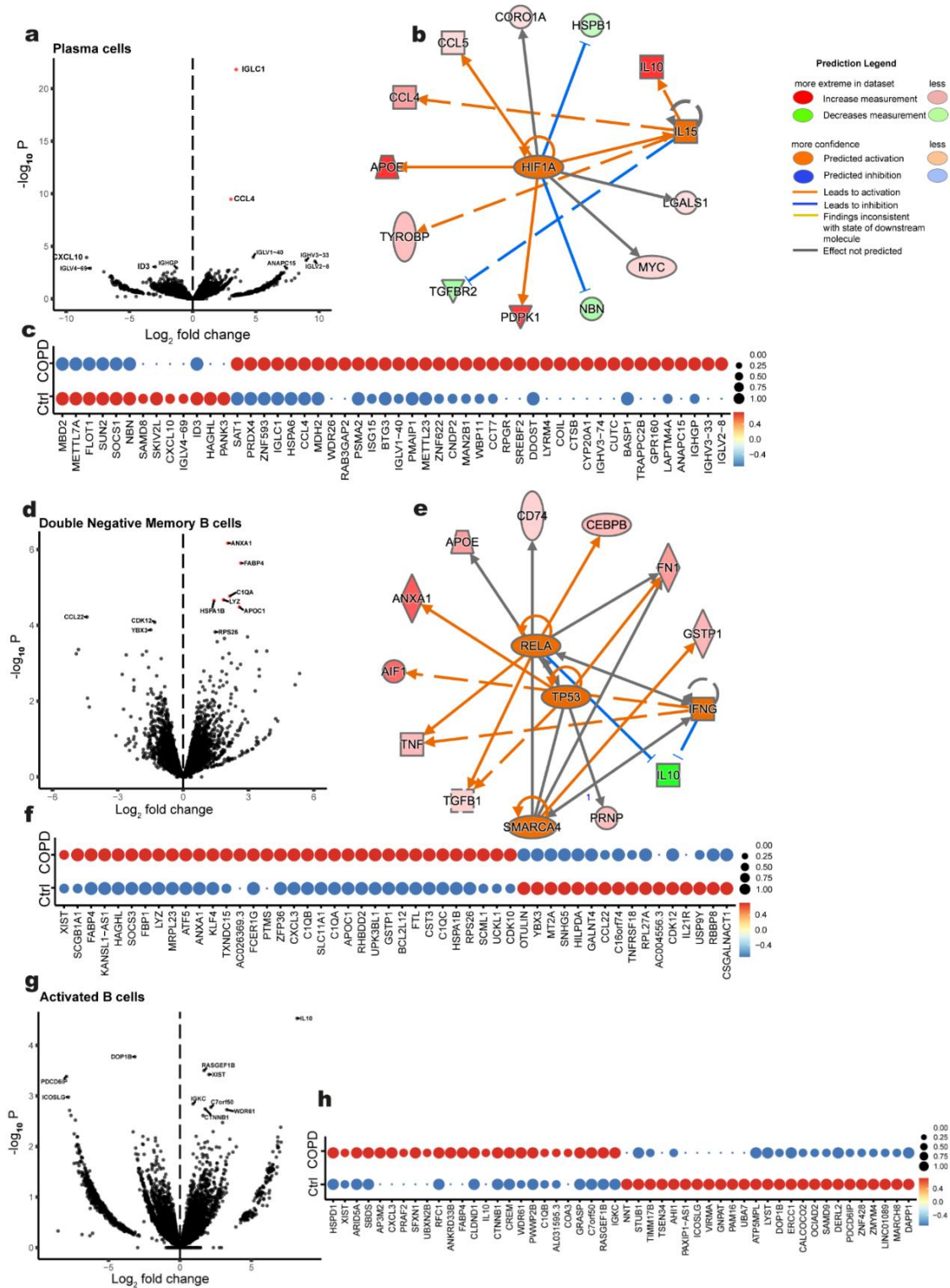
Figure 3. 5: Differential gene expression of B cells from COPD and healthy lungs

a) Volcano plot showing DE genes from plasma cells. b) Ingenuity Pathway Analysis (IPA) of the Regulatory Effects Analysis-based network associated DE genes from plasma cells. c) Dot plot

showing the top 50 DE genes from plasma cells. d) Volcano plot showing DE genes from Double Negative B cells. e) Ingenuity Pathway Analysis (IPA) of the Regulatory Effects Analysis-based network associated DE genes from Double Negative B cells. f) Dot plot showing the top 50 DE genes from Double negative B cells. g) Volcano plot showing DE genes from activated B cells. h) Dot plot showing the top 50 DE genes from activated B cells.

Histology of COPD lung show localized B cell aggregates in close contact with T cells and macrophages

Several studies have reported an increase in B cell aggregates in the lung tissue of COPD patients compared to controls [338]. We also observed increased B cell aggregates in COPD patients versus controls (**Figure 3.6a**). This was done using imaging mass cytometry (IMC) to zoom down on the tissue and characterise lung structure and B cell localisation in COPD lungs. FFPE tissues from COPD and control lungs were stained with a 35-marker panel of metal-conjugated antibodies (**Table S3.3**); this was then ablated on a Hyperion instrument. Lung structure was visualised by cytokeratin-V (basal epithelium), CD31 (blood vessels), collagen-I (connective tissue), histone (DNA) and CD20 (B cells) in COPD and control lung (**Figure 3.6a**). We observed a dramatic expansion of B cell aggregates in the COPD lung compared to the control lung; these aggregates were found near bronchioles and blood vessels (**Figure 3.6a**). Of note, we found more B cell aggregates in the lungs of current smokers compared to non-smokers (**Figure S3.8**). We also observed an increase in CD4/CD8 T cells, the basal epithelium and macrophages in the COPD lung compared to the control lung (**Figure 3.6a, b**, **d** and **S3.8a and b**). Importantly, we observed B cells in COPD patients to be in close proximity with other immune cells, including macrophages (CD68), CD4/CD8 T cells and follicular dendritic cells (FDCs, CD21) in COPD patients but not controls; suggesting the formation of ELTs (**Figure 3.6b** and **S3.9a**). Interestingly, we observed an increase of FoxP3+CD4+ T cells within the B cell aggregates in COPD lungs compared to the control lungs (**Figure 3.6c**), suggesting an increase in the recruitment of regulatory T cells within the ELTs in COPD lungs as previously reported [538,539].

Figure 1
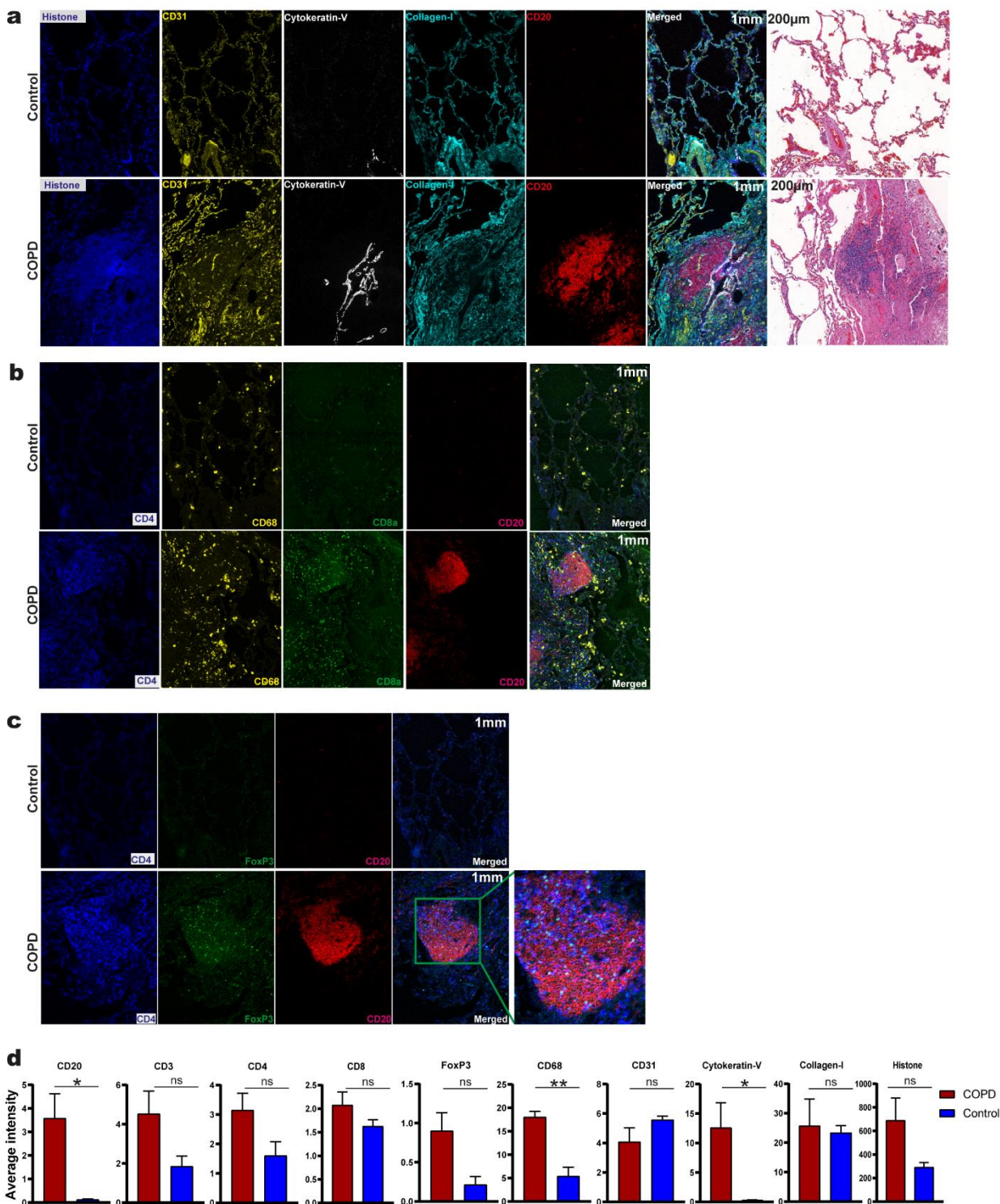
Figure 3. 6: Histological differences in COPD and control lung using imaging mass cytometry

a) Representative IMC-derived images of COPD and control lung showing (left) connective tissue (Collagen-I: Cyan), basal epithelium (Cytokeratin-V: White), vascular endothelial cells (CD31: Yellow), DNA material (Histone: Blue) and B cells (CD20: Red), (right) matched H and E images of COPD and control lung. 200µm. b) IMC-derived images of COPD and control lung showing B cells (CD20: Red), cytotoxic T cells (CD8: Green), helper T cells (CD4: Blue), and macrophages (CD68: Yellow). (right). 200µm. c) IMC-derived images showing B cells (CD20: Red), helper T cells (CD4: Blue), and FoxP3 (Green) in COPD and control lungs. d) Plots showing statistics of cells in COPD (n = 4) and control (n = 4) lungs.

3.4 Discussion

In this study, we sought to perform an in-depth analysis of B cells in the lungs of patients with COPD to improve our understanding of B cells' immunobiology and their potential role in COPD pathogenesis. Imaging mass cytometry (Hyperion) allowed B cells to be analysed at an unprecedented depth. We have demonstrated ELT presence in COPD lungs by observing B cell aggregates with a mixture of T cells, macrophages and FDCs. Smoking is directly associated with forming such lymphoid follicles in the lung. Even though these follicles are positioned near the bronchioles and blood vessels (as previously reported) [540,541], their presence in the lower airways may take up a significant space where airspace should be. We demonstrated that cigarette smoking directly affects deteriorating lung function, where current smokers' lungs, irrespective of disease condition, have increased B cell aggregates with a corresponding increase in B cell numbers and impaired B cells phenotype and function compared to non-smokers.

We showed that B cells in the COPD lung interact with T cells (CD4+ and CD8+) and macrophages. Within the T cells, we saw a specific expansion of CD4+FoxP3+ regulatory T (Tregs) cells within the B cell aggregate in COPD but not control lungs. CD4+FoxP3+ Tregs were previously characterized in lung LFs, BAL fluid, dispersed lung cells and peripheral blood [539,542,543]. Where they reported increased CD4+FoxP3+ Tregs within the inflammatory LFs from COPD patients compared to smokers and non-smokers with normal lung function. Therefore, altered numbers of Treg cells might be associated with changes in immune regulations. CD4+FoxP3+ Tregs' presence within the B cell aggregates might help maintain local immunity.

We also report the differences between lung-resident B cells to the circulating B cells irrespective of the disease condition. We showed that lung-resident B cells are matured and activated with increased proliferation and chemotaxis, with the predominant PC, DN and switched memory subsets in COPD patients. In contrast, the circulating B cells are primarily naïve and less

activated, highlighting the critical role of tissue in studying chronic lung diseases. Additionally, our data highlighted the phenotypic differences in B cells from COPD lung compared to controls.

The accumulation of B cells is well described in COPD lungs [338,504,515]. Our findings build on these data and describe the phenotypic and functional characteristics of B cells in the COPD lung. We observed increased percentages of SM and DN B cell populations in COPD lungs. Similar to our findings, increased DN B cells and their classical markers of identification, CD11c and Tbet, have been reported in other disease settings, including autoimmune diseases like SLE and RA, chronic infections like hepatitis C and malaria infections, older people and several immunodeficiencies [40,172,544–548]. They are thought to be associated with pro-inflammatory cytokine production and essentially pro-inflammatory function [40,172,544–548]. There is accumulating evidence supporting the link between COPD and auto-immunity [338,549]. Thus, seeing an increase in DN and class-switched memory B cells might support the autoimmunity effect of B cells in COPD.

We also showed increased IgG$^+$ with a corresponding decrease in IgA$^+$ B cells in the lungs of COPD current smokers. Increased IgG in COPD, especially in current smokers but not in control current smokers, may suggest that the adaptive immune responses to cigarette smoking differ in COPD compared to control lungs. Furthermore, these IgG could be autoantibodies forming immune complexes that can activate complement components, leading to lung inflammation and subsequent lung injury in COPD. Brandsma et al. reported similar findings, showing increased IgG$^+$ and decreased IgA$^+$ B cells in COPD smokers' lung [550].

Our data also shows for the first time an expansion of Tim1+ and IL-10+ B cells in the COPD lung compared to the control lung. Tim-1 is a critical marker for the expansion and suppressive function of Bregs by inducing IL-10 secretion [381,551,552]. Hence, their presence in COPD lung suggests increased anti-inflammatory effects of B cells in COPD. Furthermore, studies have shown that IL-10+ Bregs are not terminally differentiated B cells [336,553]. They have the potential to further differentiate into APCs or antibody-producing plasmablasts [336,553], hence can switch off the IL-10 production to allow for other functions.

The scRNA-seq analysis of B cells identified novel pathways upregulated or differentially expressed in B cells from COPD lungs. We showed increased IL-10 expression in plasma cells and activated B cells from COPD compared to control lungs, which is consistent with our flow and mass cytometry data. The activation of the HIF-1α pathway observed in B cells from COPD might promote IL-10+ B cell differentiation since HIF-1α is a transcription factor that is a key element in controlling immune cell metabolism and cellular response to low oxygen and has been shown

to be critical in the induction of IL-10-secreting Bregs [488,554]. The increase in the activation of RELA and p38 MAPK pathways in B cells from COPD lung shown in this study might suggest a continuous activation and maturation of B cells within the COPD lung microenvironment.

Interestingly, we also showed upregulation of MMP19, APOE, and SCGB1A1 genes (among others) by B cells in COPD patients. Increased MMP19 was previously shown to play a protective role in IPF and asthma [520,521,555]. In asthma, MMP19 acts on Th2 inflammation homeostasis by preventing the accumulation of tenancin-C (a matricellular protein component of ECM). This subsequently prevents airway eosinophilia and hyperreactivity [521]. While in IPF, upregulation of MMP19 protects the development of fibrosis by regulating the synthesis of ECM components in lung fibroblasts [520,555]. Although MMP19 is typically expressed in lung fibroblasts, myoepithelial cells, basal keratinocytes, and vascular smooth muscle [556–561], its upregulation in B cells from COPD lung might suggest their direct involvement in lung repair in COPD. Additionally, the upregulation of APOE and SCGB1A1 genes in B cells might suggest increased antigen presentation and anti-inflammatory effects of B cells in COPD.

In summary, we visualised and phenotype B cells from lung tissue and blood of COPD patients by spatial analysis and provided an insight into the role of B cells in COPD pathophysiology. Further investigations using patient samples and mouse models of the disease are required to fully understand the role of B cells in COPD pathogenesis and their therapeutic potential.

3.5 Methodology

Tissue samples

Healthy margins of lung tissue (> 6 cm from cancer) were identified by a histopathologist and dissected under the ethical approval of the Manchester Allergy, Respiratory and Thoracic Surgery (ManARTS) Biobank at the University Hospital of South Manchester together with matched peripheral blood samples. National Research Ethics Service Committee granted ethical approval; North West – Haydock (ref; 15/NW/0409). Written consent was obtained from all the patients that participated in the study. Participants with a forced expiratory volume in 1 second/forced vital capacity (FEV1/FVC) of ≥ 0.70 with no other underlying respiratory disease were categorised as 'healthy'. Participants with COPD were defined by physician diagnosis and exhibited an FEV1/FVC < 0.70. Details of patients' demography are outlined in **Table S3.1**. Lung tissue was digested, and mononuclear cells from lung tissue and peripheral blood were isolated as previously described [562,563]. A portion of the tissue is fixed for histology analysis.

Mass Cytometry

All antibodies (Abs) used for mass cytometry analysis are detailed in **Table S3.3** Antibodies conjugated to metal tags from Fluidigm or purchased protein-free elsewhere and conjugated in-house using the Fluidigm MaxPar labelling kits following manufacturer's instructions. Cells were washed with PBS and stained in 200µm Rhodium intercalator (1:500 dilution) for 15 minutes at room temperature for cellular viability. Cells were washed in PBS, then in Cell-staining buffer (CSB) followed by incubation in FcR block (Miltenyi) diluted 1:100 for 15 minutes at room temperature. Cells were stained in primary Abs cocktail in CSB on 30 minutes at room temperature, washed twice in CSB and fixed for 15 minutes in 1X Fix I buffer (Fluidgm). For intracellular staining, cells were permeabilised by a wash in Perm-S-buffer (Fluidigm), followed by staining in intracellular Abs in Perm-S-buffer for a further 30 min on ice, then washed twice in Perm-S-buffer. Cells were then resuspended overnight in cell-ID Iridium intercalator (Fluidigm) diluted 1:2000 in Fix and perm buffer followed by washing in PBS. Data were acquired using CyTOF Helios mass cytometer, and files were exported in flow cytometry files (FCS) format for analysis.

FCS were first normalised using CyTOF Software (Fluidigm); pre-and post- normalisation plots are shown in Supplementary Fig. 1. FCS files were gated in FlowJo as shown in Supplementary Fig 1. For dimensionality reduction, the CD19+ cells were exported and analysed using cytofkit2 R script (available online at https://github.com/JinmiaoChenLab/cytofkit2).

Imaging mass cytometry (Hyperion)

Formalin-fixed paraffin-embedded (FFPE) lung tissues were freshly cut into sections of 5µm thickness and were mounted on superfrost™ adhesion slides (Fisher Scientific: 10149870). Tissue slides were deparaffinised in Xylene and rehydrated in descending ethanol concentrations (100%, 95%, 80%, 70%) and finally washed in Milli-Q water. The tissue slides were then incubated in 1X pre-heated antigen retrieval buffer (Abcam, 100X Tris Buffer, pH = 10.0: ab93682) for 30 min at boiling temperature. Then left in the antigen retrieval solution for another 30 min at room temperature to cool down. The slides were then dried, and a hydrophobic barrier was drawn around the tissue on the slide by a PAP pen. The tissue was then blocked with 3% bovine serum albumin (BSA) in PBS for 45 min at room temperature followed by three washes in PBS and staining with metal-conjugated Abs cocktail (**Table S3.2**) in PBS overnight at 4°C. The slides were then washed in 0.2% Triton™ X-100 (Thermo Scientific: 85111) in PBS at room temperature for 8 min, followed by 3X washing with PBS and staining with cell ID intercalator Iridium (1:400,

Fluidigm) for 30min at room temperature. The slides are finally washed with Milli-Q water and air-dried overnight. Data were acquired on a Hyperion imaging system coupled to a Helios mass cytometer (Fluidigm).

Hyperion Imaging analysis

Separate matched samples were first stained with Haematoxylin and eosin and imaged with a bright field microscope to identify the regions of interest (ROIs) used to reference the IMC signal acquisition. Images created by the Hyperion system were exported as MathCad (MCD) files. They were initially analysed in MCD viewer software (v1.0.560.6) and exported as OME-TIFF 16-bit file format. Cellular segmentation masks were generated using CellProfiler (4.2.1) data analysis pipeline as recommended by Fluidigm. The extracted OME-TIFF ROIs data from MCD and the generated segmented masks were imported into HistoCAT and finally exported as CSV files for statistical analysis in GraphPad Prism.

Cell culture

Frozen mononuclear cells from blood and lung tissue were thawed, washed and resuspended in RPMI containing 10% FBS, L-Glutamine, non-essential amino acids, HEPES, and penicillin plus streptomycin. 5×10^5 cells were stimulated with either; (i) 1 µM CpG-B DNA (Cambridge Bioscience: Hycult HC4039) alone, (ii) 1 µg/ml CD40L (R&D Sysytems: 6245-CL-050) alone, (iii) combination of i and ii for 48 hours followed by 2µL/ml of stimulation cocktail (eBioScience: 00-4970-93) in the presence of 10 µg/ml Brefeldin A (BFA) in the last four hours (B cells). For unstimulated controls, cells were incubated with culture buffer alone for 48 hours followed by incuabtion with the stimulation cocktail and BFA in the last four hours. Following stimulation, cells were washed and stained for flow cytometric analysis.

Flow cytometry analysis and cell sorting

Mononuclear cells from lung and blood (thawed/stimulated) were stained in viability dyes, then with fluorophore-conjugated antibodies (see **Table S3.4**) and acquired on FACS Symphony cell analyser (Becon Dickinson) and analysed using FlowJo (TreeStar: v10.8.1) as previously described[564]. For sc-RNA sequencing and qPCR analysis, cells were stained with DAPI, CD19, CD3, and CD45. CD19^low/+CD45^+CD3^- were sorted as B cells on BD Influx cells sorter (BD Biosciences).

Single-cell isolation and library construction

Gene expression libraries were prepared from B cells single-cell suspension using the Chromium Controller and Single Cell 3' Reagent Kits v3.1 (10x Genomics, Inc. Pleasanton, USA) according to the manufacturer's protocol (CG000315 Rev B). Briefly, nanoliter-scale Gel Beads-in-emulsion (GEMs) were generated by combining barcoded Gel Beads, a master mix containing cells, and partitioning oil onto a Chromium chip. Cells were delivered at a limiting dilution, such that the majority (90-99%) of generated GEMs contain no cell, while the remainder largely contain a single cell. The Gel Beads were then dissolved, primers released, and any co-partitioned cells lysed.

Primers containing an Illumina TruSeq Read 1 sequencing primer, a 16-nucleotide 10x Barcode, a 10-nucleotide unique molecular identifier (UMI) and a 30-nucleotide poly(dT) sequence were then mixed with the cell lysate and a master mix containing reverse transcription (RT) reagents. Incubation of the GEMs then yielded barcoded cDNA from poly-adenylated mRNA.

Following incubation, GEMs were broken and pooled fractions recovered. First-strand cDNA was then purified from the post GEM-RT reaction mixture using silane magnetic beads and amplified via PCR to generate sufficient mass for library construction.

Enzymatic fragmentation and size selection were then used to optimize the cDNA amplicon size. Illumina P5 & P7 sequences, a sample index, and TruSeq Read 2 sequence were added via end repair, A-tailing, adaptor ligation, and PCR to yield final Illumina-compatible sequencing libraries.

Sequencing

The resulting sequencing libraries comprised standard Illumina paired-end constructs flanked with P5 and P7 sequences. The 16 bp 10x Barcode and 10 bp UMI were encoded in Read 1, while Read 2 was used to sequence the cDNA fragment. Sample index sequences were incorporated as the i7 index read. Paired-end sequencing (26:98) was performed on the Illumina NextSeq500 platform using NextSeq 500/550 High Output v2.5 (150 Cycles) reagents. The .bcl sequence data were processed for QC purposes using bcl2fastq software (v. 2.20.0.422) and the resulting .fastq files assessed using FastQC (v. 0.11.3), FastqScreen (v. 0.9.2) and FastqStrand (v. 0.0.5) prior to pre-processing with the CellRanger pipeline.

Raw data processing

Raw sequencing data were processed using the 10x Genomics Cell Ranger pipeline (v6.0.0). The Illumina Binary Base Call (BCL) files were demultiplexed using the command `cellranger mkfastq` to produce FASTQ files. The FASTQ files were then processed using the command `cellranger count` with pre-built Cell Ranger human reference package (GRCh38-2020-A) to generate the gene-cell barcode matrix.

Cell filtering and cell type annotation

Expression matrices were processed in R environment (v4.1) using various R packages. Briefly, the matrix data (HDF5) of each sample was imported as *SingleCellExperiment* object using the `read10xCounts` function in the DropletUtils R package (v1.12.1). The `addPerCellQC` and `addPerFeatureQC` functions from the scuttle R package (v1.2.0) were used to compute and add per-cell and per-gene quality control metrics to the *SingleCellExperiment* object. We used a combination of median absolute deviation (MAD), as implemented by the `isOutlier` function in the scuttle R package and exact thresholds to evaluate the per-cell QC metrics, including UMI count, the UMI count, number of detected genes, proportion of mitochondrial reads and complexity of RNA species, to identify and subsequently remove poor quality cells before further processing.

To computes deconvolution size factors, we first used the `quickCluster` function to group cells into clusters of similar expression, then use the `computeSumFactors` function to normalise for cell-specific biases to compute size factors for each cell. Both functions are available from the scran R package (v1.20.1). The `calculateCPM` function from the scuttle R package was used to calculate counts-per-million (CPM) values from the count data, which make use of the size factors calculated previously. The log2-transformed normalized values were stored in the *logcounts* slot of the *SingleCellExperiment* object.

The SingleR R package (v1.6.1) was used to annotate cells against curated reference expression datasets (namely *DatabaseImmuneCellExpressionData*, *MonacoImmuneData*, and *NovershternHematopoieticData*) from the celldex R package (v1.2.0).

Data integration

The log-normalized expression values of the six samples were re-calculated using the `multiBatchNorm` function from the batchelor R package (v1.8.0) to adjust for the systematic differences in coverage between them. Per-gene variance of the log-expression profiles was

modelled using the `*modelGeneVarByPoisson*` function and top 5000 highly variable genes (HVGs) were identified using the `*getTopHVGs*` function, both from the scran R package. The mutual nearest neighbors (MNN) approach implemented by the `*fastMNN*` function from the batchelor R package was used to integrate the scRNA-seq data. At the same time, multi-sample principal components analysis was performed internally. The proportion of variance lost with each batch at each merge step was examined to detect if the correct process is removing genuine biological heterogeneity.

Data visualization and cell clustering

The first 50 dimensions from the MNN corrected low-dimensional coordinates for each cell were used as input to produce the t-stochastic neighbour embedding (t-SNE) projection and uniform manifold approximation and projection (UMAP) using the `*runTSNE*` and `*runUMAP*` functions from the scater R package (v1.20.0) respectively.

Next, we performed graph-based clustering of cells using the Walktrap algorithm from the igraph R package (v1.2.6) to identify "communities" of cells. Specifically, we used the `*clusterRows*` function from the bluster R package (v1.2.1) to streamline the clustering procedure and obtained 19 clusters.

From the larger dataset, clusters containing B cells (clusters 2 and 5) were subsetted from the main *SingleCellExperiment* object, projected into t-SNE and UMAP and re-clustered into six clusters.

Marker and differential expression analysis

Cluster-specific markers were identified using the `*FindMarkers*` function from the scran R package, which performs pairwise t-tests between clusters. To perform differential expression (DE) analysis, we created "pseudo-bulk" expression profiles from scRNA-seq data by summing raw counts from cells with the same combination of cluster label, sex, and disease state, resulting in 23 profiles in total. Pseudo-bulk profiles with less than 10 cells were removed from the DE analysis. Pseudo-bulk profiles were analysed for differential gene expression using the quasi-likelihood pipeline from edgeR (v3.34.0). Genes with a false discovery rate (FDR) below 10% were considered differentially expressed.

Results returned by edgeR, including Gene ID, log2 fold change, P-value, and FDR, were imported into the Ingenuity Pathway Analysis (IPA) software (QIAGEN Inc.). Pathway and network analysis was conducted with the IPA Winter Release 2021.

Statistics

GraphPad Prism (version 9) was used for all statistical analyses. Normality tests were performed on all datasets. COPD and control groups were compared using an unpaired Mann-Whitney test. One-way ANOVA with Holm-Sidak post hoc testing (normal distribution) or Kruskal-Wallis test with Dunn's post hoc testing (failing normality testing) was for multiple comparisons. Data are presented as the mean ± SED. P-values < 0.05 were considered significant (*P < 0.05, **P < 0.01, ***P < 0.001)

3.7 Supplementary Information

Table S3. 1: Patient demographics

Demography	COPD	Control
Age		
51 - 60	0	4
61 - 70	5	2
71 - 80	3	10
81 - 90	4	3
Smoking history		
Current smokers	6	6
Ex-smokers	5	6
Never-smokers	1	7
FEV1 (% predicted)		
≥ 80	5	13
50 – 79	6	6
30 – 49	1	0
< 30	0	0
Gender		
Male	8	8
Female	4	11
Total	**12**	**19**

Table S3. 2: Specifications of metal conjugated antibodies for CyTOF Helios targets

Antibody Target	Metal Tag	Concentration	Clone	Company
Extracellular Abs				
CD45	89Y	1:100	HI30	Fluidigm
CD19	113In	1:20	HIB19	BioLegend
CD3	115In	1:50	UCHT1	BioLegend
CD10	141Pr	1:33	HI10a	BioLegend
CD5	143Nd	1:100	UCHT2	Fluidigm
CD20	147Sm	1:100	2H7	Fluidigm
CD21	196Pt	1:30	#544408	R&D Systems
CD24	142Nd	1:50	ML5	BioLegend
CD27	195Pt	1:50	323	BioLegend
CD22	159Tb	1:100	HIB22	Fluidigm
CD33	169Tm	1:100	WM53	Fluidigm
CD36	152Sm	1:100	5271	Fluidigm
CD38	194Pt	1:100	HIT2	BioLegend
CD40	151Eu	1:40	5C3	BioLegend
CD43	155Gd	1:33	#290111	R&D Systems
CD44	166Er	1:100	BJ18	Fluidigm
CD62L	153Eu	1:100	DREG56	Fluidigm
CD69	162Dy	1:100	FN50	Fluidigm
CD80 (B7-1)	161Dy	1:100	2D10.4	Fluidigm
CD86	164Dy	1:40	IT2.2	BioLegend
CD138	170Er	1:40	DL-101	BioLegend
CD11c	174Yb	1:50	3.9	BioLegend
CD1c	172Yb	1:20	REA694	Miltenyi Biotec
CD1d	176Yb	1:40	51.1	BioLegend
B220	144Nd	1:50	RA36B2	BioLegend
HLA-DR	198Pt	1:50	L243	BioLegend
IgD	146Nd	1:100	IA62	Fluidigm
IgM	149Sm	1:40	MHM-88	BioLegend

IgG	145Nd	1:30	#97924	R&D Systems
IgA	148Nd	1:100	Polyclonal	Fluidigm
NOTCH-1	165Ho	1:33	#527425	R&D Systems
Tim-1	167Er	1:33	#219211	R&D Systems
TLR-4/CD284	173Yb	1:40	#610015	R&D Systems
CXCR4	156Gd	1:100	12G5	Fluidigm
CXCR5	171Yb	1:100	RF8B2	Fluidigm
CXCR6	160Gd	1:100	K041E5	Fluidigm
CCR4/CD194	175Lu	1:100	L291H4	Fluidigm
BAFF-R (CD268)	158Gd	1:33	#2403C	R&D Systems
CXCR3	154Sm	1:40	#49801	R&D Systems
Intracellular Abs				
IL-10	150Nd	1:50	JES3-9D7	BioLegend
Bcl-2	168Er	1:40	E17	Abcam
Bcl-6	163Dy	1:100	K11291	Fluidigm

Table S3. 3: Specifications of metal conjugated antibodies for CyTOF Hyperion targets

Antibody Target	Metal Tag	Concentration	Clone	Company
aSMA (1A4)	141Pr	1:300	1A4	Fluidigm
Vimentin	143Nd	1:200	D21H3	Fluidigm
E-Cadherin	158Gd	1:200	24E10	Fluidigm
Collagen I	169Tm	1:400	Polyclonal	Fluidigm
Histone H3	171Yb	1:200	D1H2	Fluidigm
Pan-Keratin	148Nd	1:150	C11	Fluidigm
FoxP3	155Gd	1:100	236A/E7	Fluidigm
CD4	156Gd	1:150	EPR6855	Fluidigm
CD68	159Tb	1:100	KP1	Fluidigm
CD20	161Dy	1:100	H1	Fluidigm
CD8a	162Dy	1:100	C8/144B	Fluidigm

			Polyclonal, C-	
CD3	170Er	1:100	Terminal	Fluidigm
CD45RO	173Yb	1:200	UCHL1	Fluidigm
CD14	144Nd	1:100	EPR3653	Fluidigm
CD11b	149Sm	1:100	EPR1344	Fluidigm
CD31	151Eu	1:100	EPR3094	Fluidigm
CD11c	154Sm	1:100	Polyclonal	Fluidigm
CD21	153Eu	1:50	# 544408	R&D Systems
FoxJ1	176Yb	1:50	# 407003	R&D Systems
IgD	150Nd	1:50	IgD26	Miltenyi Biotec
IgA	164Dy	1:50	EPR5367-76	Abcam
IgM	165Ho	1:50	MHM-88	BioLegend
Cytokeratin-5	175Lu	1:100	EP1601Y	Abcam
Cell ID Intercalatorr	Ir	1:400		Fluidigm

Table S3. 4: Specifications of fluorochrome-conjugated antibodies for flow cytometry targets

Antibody Target	Fluorochrome	Concentration	Clone	Company
Extracellular Abs				
Live/Dead	Zombie UV	1:500		BioLegend
CD45	BUV395	1:50	HI30	BD Bioscience
CD3	BV605	1:50	SK7	BioLegend
CD19	BUV737	1:50	HIB19	BD Bioscience
CD24	APC-e-Floor	1:50	eBioSN3	eBioscience
CD38	PerCP-Cy5.5	1:50	HIT2	BioLegend
CD27	BV711	1:50	M-T271	BioLegend
IgD	BV785	1:50	IA6-2	BioLegend
IgM	FITC	1:50	MHM-88	BioLegend

IgA	APC	1:50	REA1014	Miltenyi Biotec
Tim1	PE	1:50	1D12	BioLegend
CXCR3	BV510	1:50	G025H7	BioLegend
Hif-α	PE	1:50	546-16	BioLegend
Pax5	BV421	1:50	1H9	BD Bioscience
CD86	APC	1:50	BU63	BioLegend
CD11c	BB515	1:50	B-ly6	BD Bioscience
Intracellular Abs				
IL-10	APC	1:25	JES3-19F1	BD Bioscience
Bcl-6	APC	1:50	7D1	BioLegend
Tbet	BV421	1:50	4B10	BioLegend
Ki67	PE	1:50	ki-67	BioLegend
Blimp1	AF 488	1:25	646702	R&D Systems
IgG	BV421	1:50	M1310G05	BioLegend
TNF-α	PE-Cy7	1:50	MAb11	BD Bioscience
IL-6	PE	1:100	MQ2-13A5	BioLegend

Table S3. 5: Gene expression metrics for 10x Genomics scRNA-seq of the six lung tissue samples

A detailed description of the metrics can be found on the 10x Genomics website at: https://support.10xgenomics.com/single-cell-gene-expression/software/pipelines/latest/output/gex-metrics

Metric	6209HN	6270CE	6435HE	6435HN	6756CC	6808CC
Disease category	Control	COPD	Control	Control	COPD	COPD
Estimated Number of Cells	4,810	6,069	6,391	3,437	4,043	5,384
Fraction Reads in Cells	78.60%	94.50%	96.00%	83.70%	74.30%	89.50%
Mean Reads per Cell	20,293	32,471	33,691	31,283	25,497	19,608

Median Genes per Cell	1,100	2,238	2,979	1,386	1,236	1,179
Total Genes Detected	22,982	23,293	23,307	22,868	22,034	23,568
Median UMI Counts per Cell	2,836	8,577	12,988	3,708	3,269	3,334
Number of Reads	97,610,684	197,066,854	215,320,178	107,518,846	103,083,854	105,570,365
Number of Short Reads Skipped	0	4,765,998	5,034,128	0	0	0
Valid Barcodes	97.40%	98.00%	98.20%	97.60%	97.40%	97.90%
Valid UMIs	99.90%	99.90%	99.90%	99.90%	99.90%	99.90%
Sequencing Saturation	37.40%	51.00%	42.30%	52.20%	43.40%	36.40%
Q30 Bases in Barcode	97.80%	97.80%	97.80%	97.80%	97.80%	97.80%
Q30 Bases in RNA Read	92.80%	93.20%	92.90%	93.00%	93.00%	92.50%
Q30 Bases in UMI	97.10%	97.20%	97.20%	97.10%	97.10%	97.10%
Reads Mapped to Genome	96.90%	97.50%	97.50%	96.90%	96.90%	95.40%
Reads Mapped Confidently to Genome	93.20%	94.20%	95.50%	93.30%	93.10%	92.20%
Reads Mapped Confidently to Intergenic Regions	5.60%	3.90%	3.10%	5.50%	4.80%	5.50%
Reads Mapped Confidently to Intronic Regions	35.80%	21.10%	18.50%	33.30%	34.20%	28.00%
Reads Mapped Confidently to Exonic Regions	51.80%	69.30%	73.90%	54.50%	54.10%	58.80%

Reads Mapped Confidently to Transcriptome	48.90%	67.30%	72.00%	51.80%	51.30%	56.50%
Reads Mapped Antisense to Gene	1.50%	0.70%	0.60%	1.40%	1.40%	1.00%

Figure S3. 1: Quality control and preliminary gating for mass cytometry data

Beads normalisation, doublet exclusion and preliminary gating for analysis of b cells isolated from tissues. A gate was created around intact cells that ensured that all relvant events in all tissues

were captured. CD3 and CD45 channels and selection of CD20+ cells excluded all but B cells from our analysis.

Blood versus Lung
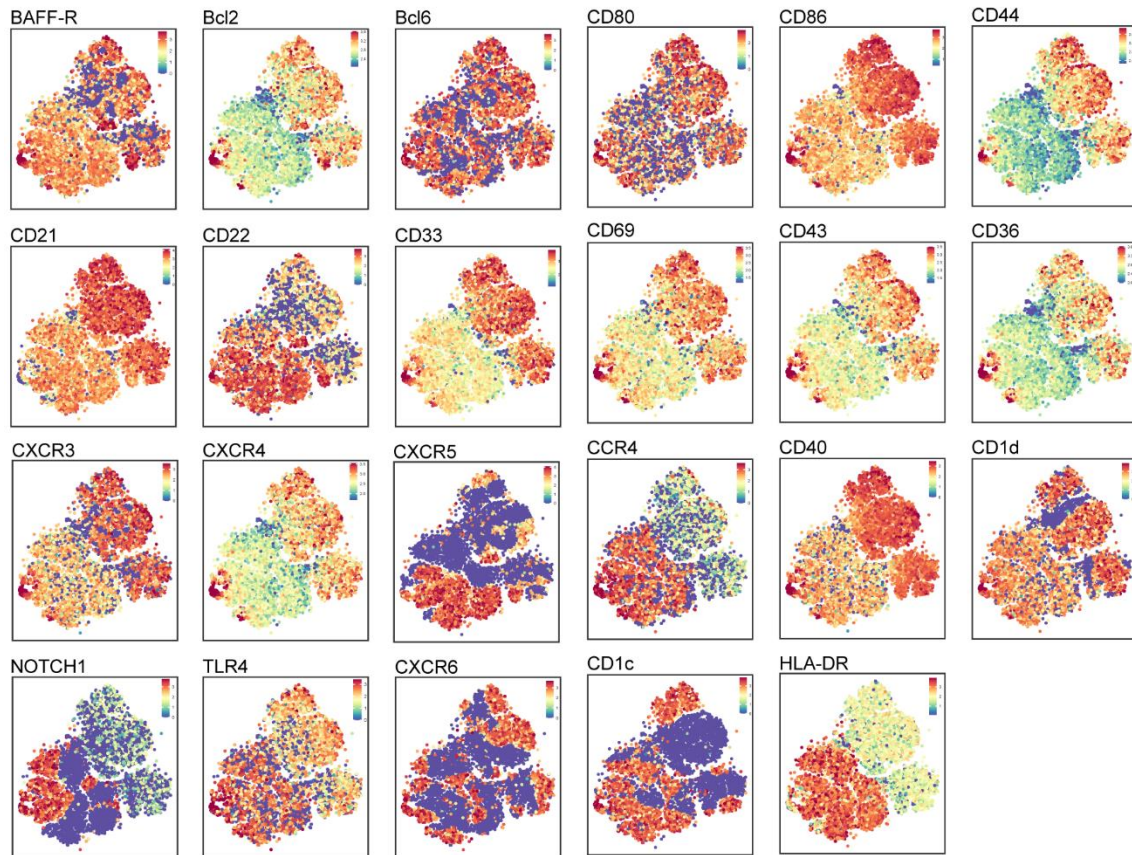
Figure S3. 2: mass cytometry (CyTOF) data showing tSNE plots illustrating the expression of markers used for the clustering in blood versus lung samples.
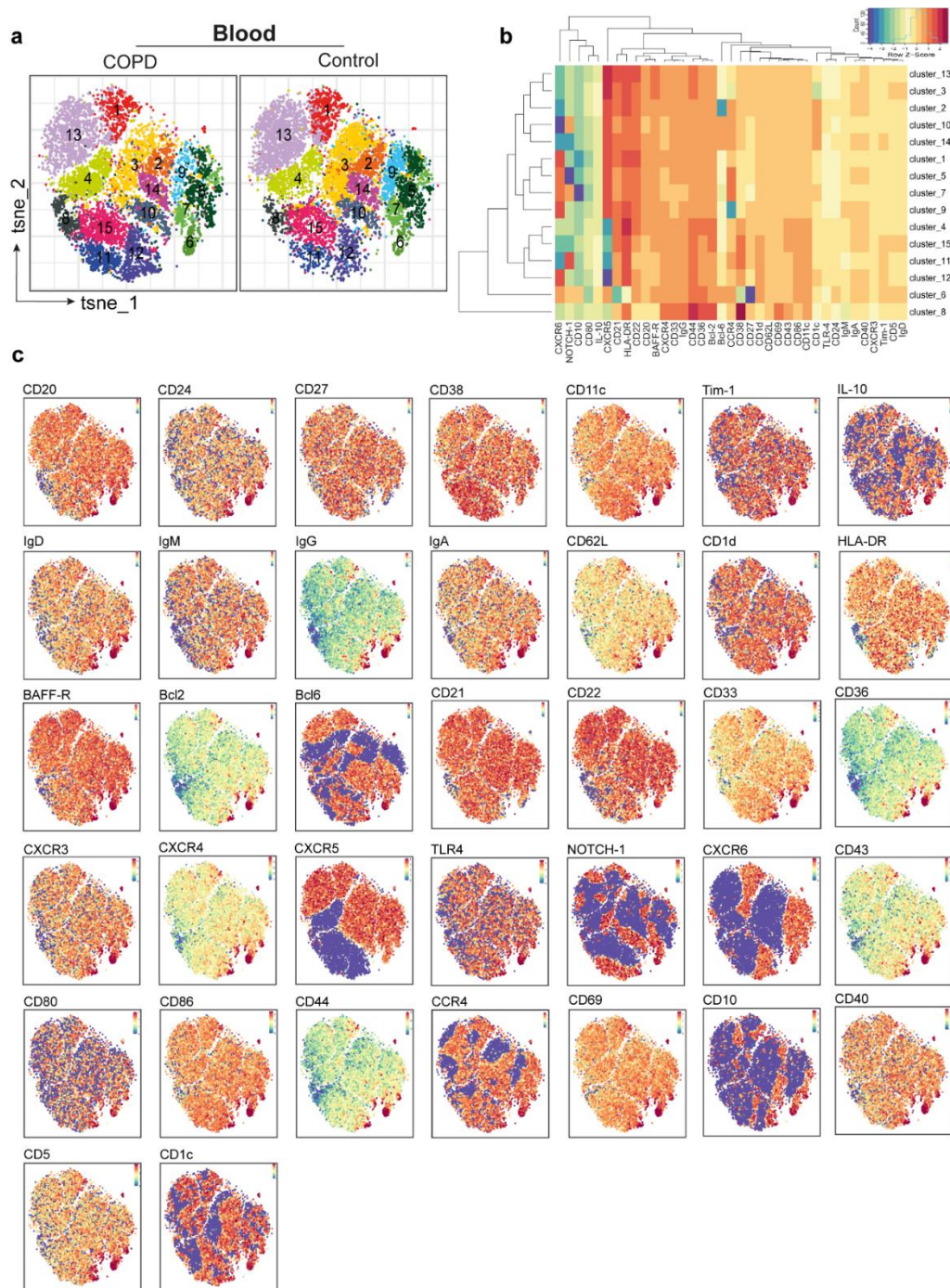
Figure S3. 3: Circulating B cell subsets from COPD and controls have no major differences

a) Mass cytometry data showing tSNE plots of B cells from COPD and control blood, overlaid with Phenograph subcluster and (b) heatmap showing all expressed markers with dendrogram constructed by hierarchical clustering and clusters identified using K-means. c) Expressions of

markers on tSNE of B cell plots from COPD and control blood, overlaid with Phenograph subclusters.

COPD versus Control Lungs
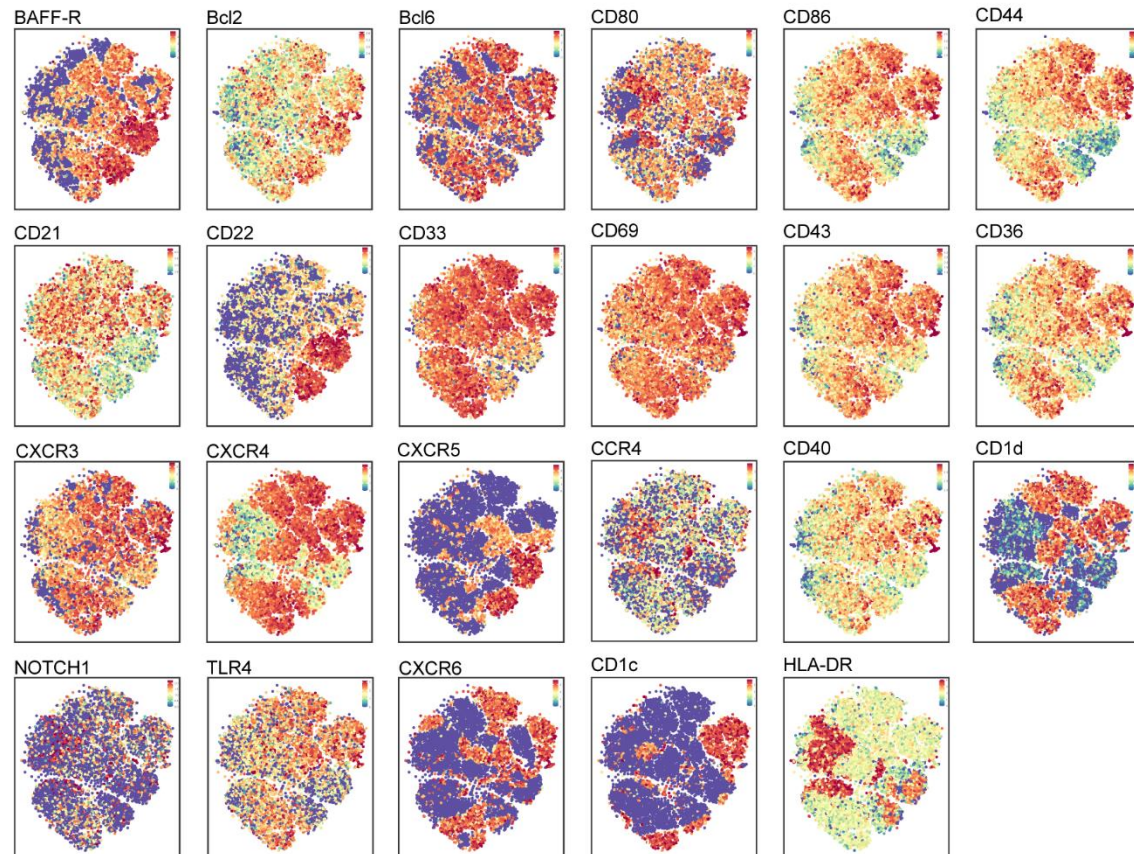
Figure S3. 4: Mass cytometry (CyTOF) data showing tSNE plots illustrating the expression of markers used for the clustering in COPD versus control lung samples
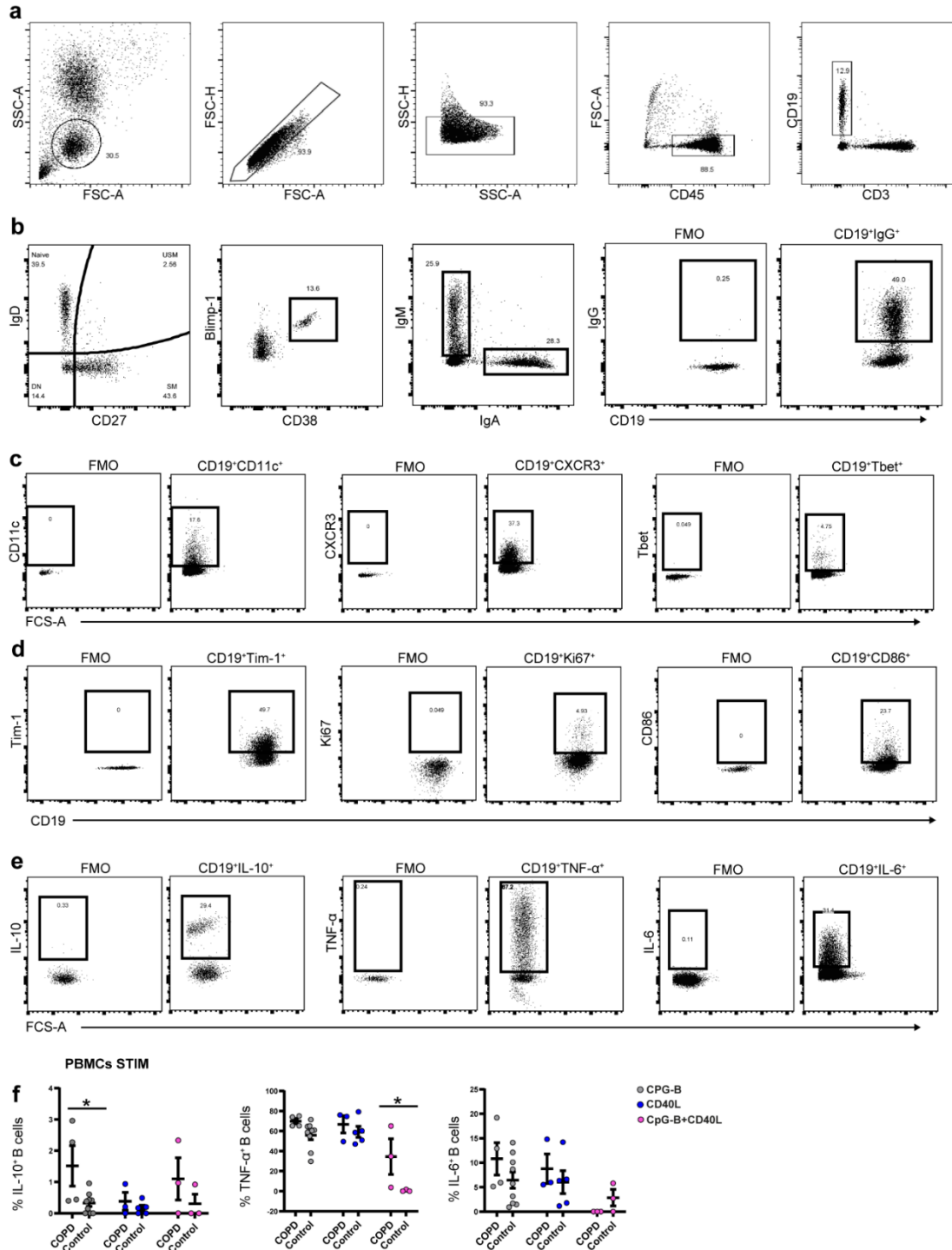
Figure S3. 5: Representative flow cytometry plots and graphs showing frequencies of markers expressed by B cells in COPD versus control lung and blood
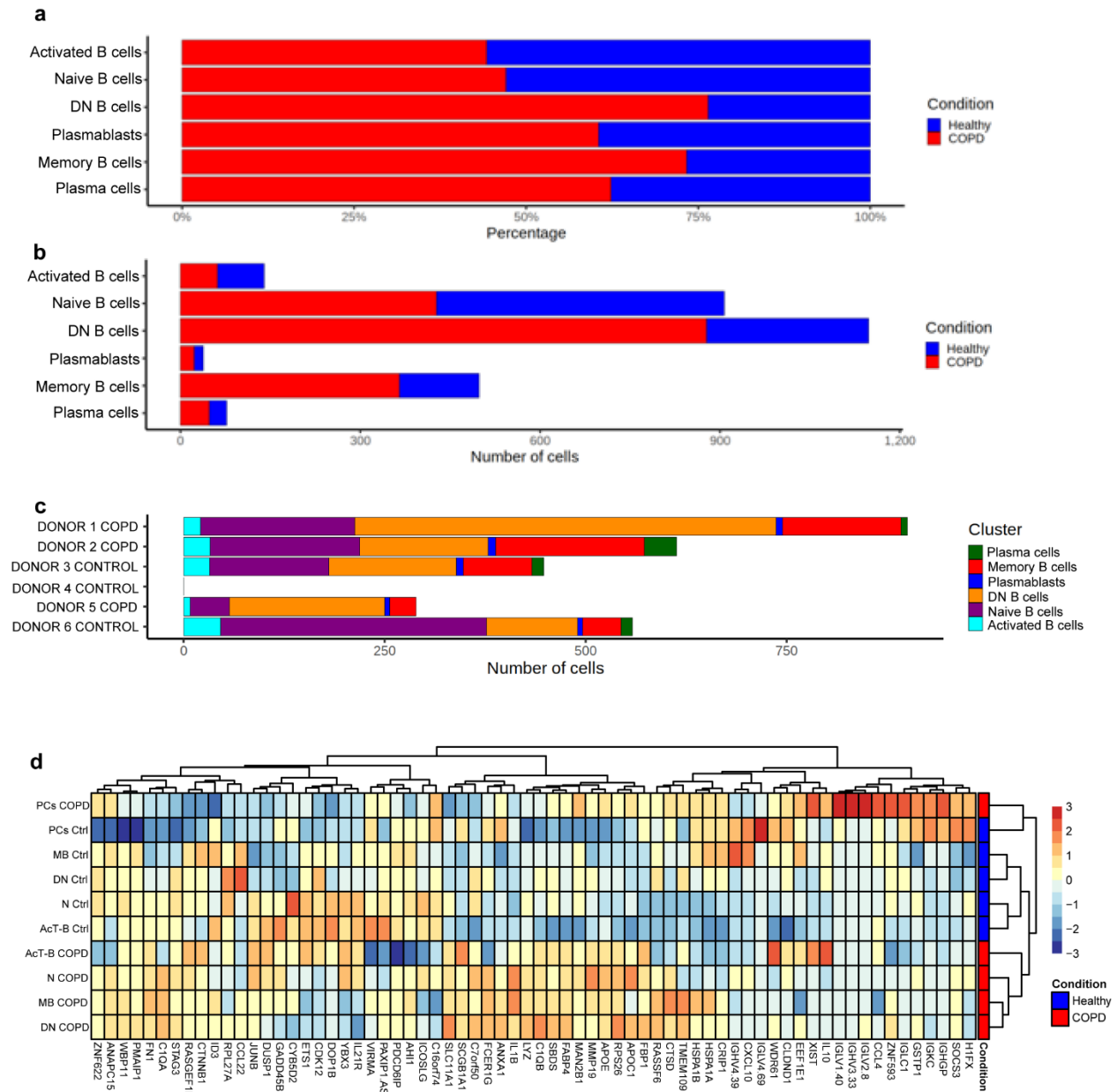
Figure S3. 6: Data from scRNA-sequencing of B cells in COPD and control lung showing

a) percentage of cells in each B cell subsets from COPD and control lungs, b) Total number of cells in each B cell subsets from COPD and control lung and c) Total number of cells per cluster from each donor d) top 50 gene expressed in each B cell subset from COPD and control lung.
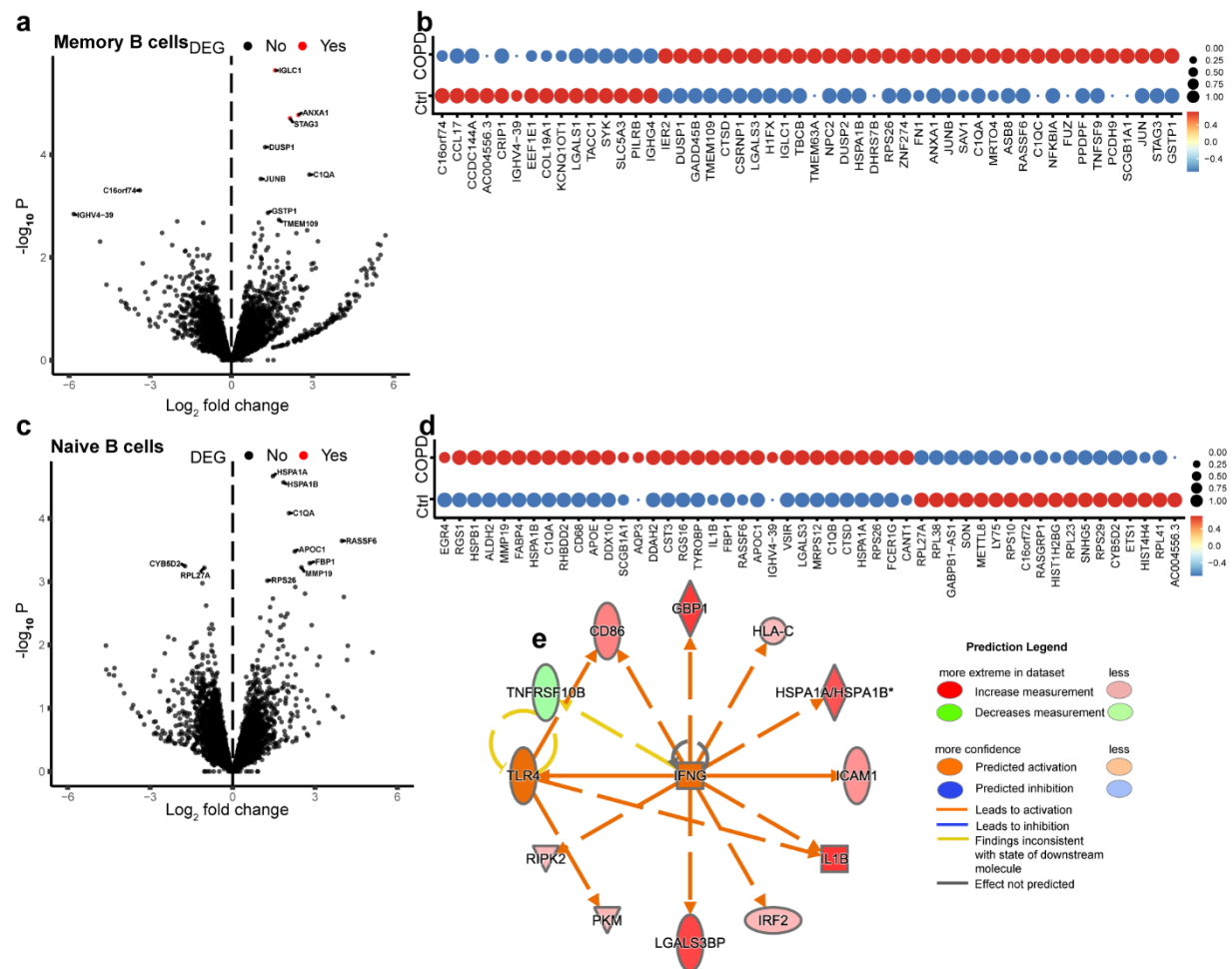
Figure S3. 7: Differentially expressed genes of B cells from COPD and control lungs

Volcano plot showing DE genes from memory B cells. b) Dot plot showing the top 50 DE genes from memory cells. c) Volcano plot showing DE genes from Naïve B cells. d) Dot plot showing the top 50 DE genes from naïve B cells, e) Ingenuity Pathway Analysis (IPA) of the Regulatory Effects Analysis-based network associated DE genes from Naïve B cells.
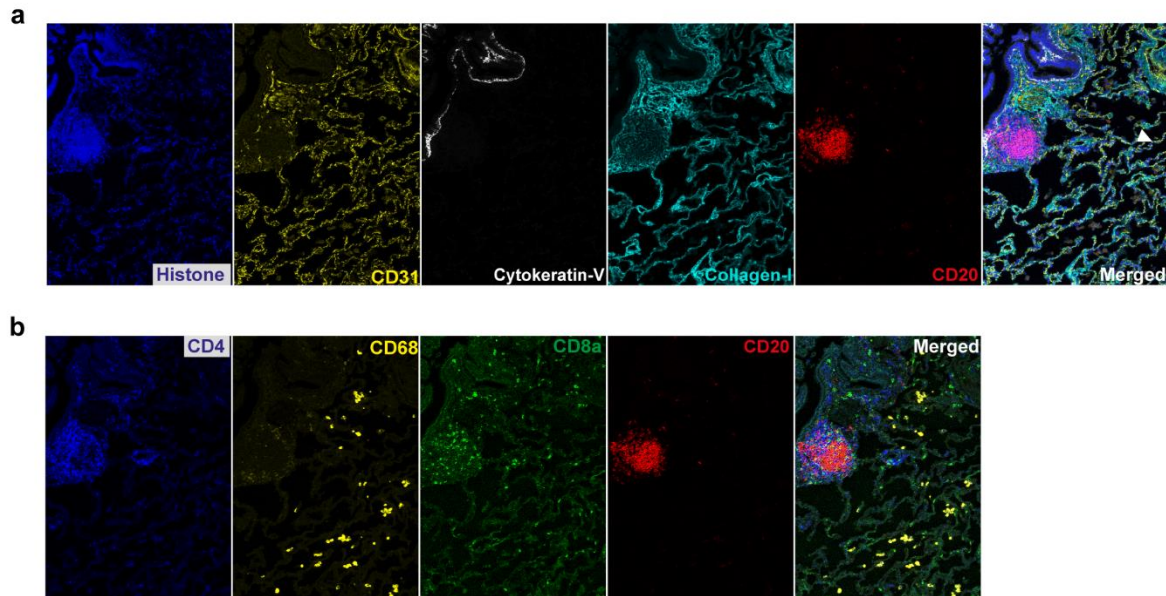
Figure S3. 8: Histology of control current smoker's lung

Showing a) B cell aggregates as CD20 (red), blood vessels as CD31 (yellow), basal epithelium as cytokeratin-V (white) and connective tissues as collagen-I (cyan). b) B cell aggregates as CD20 (red), macrophages as CD68 (yellow), helper T cells as CD4 (blue) and cytotoxic T cells as CD8a (green).
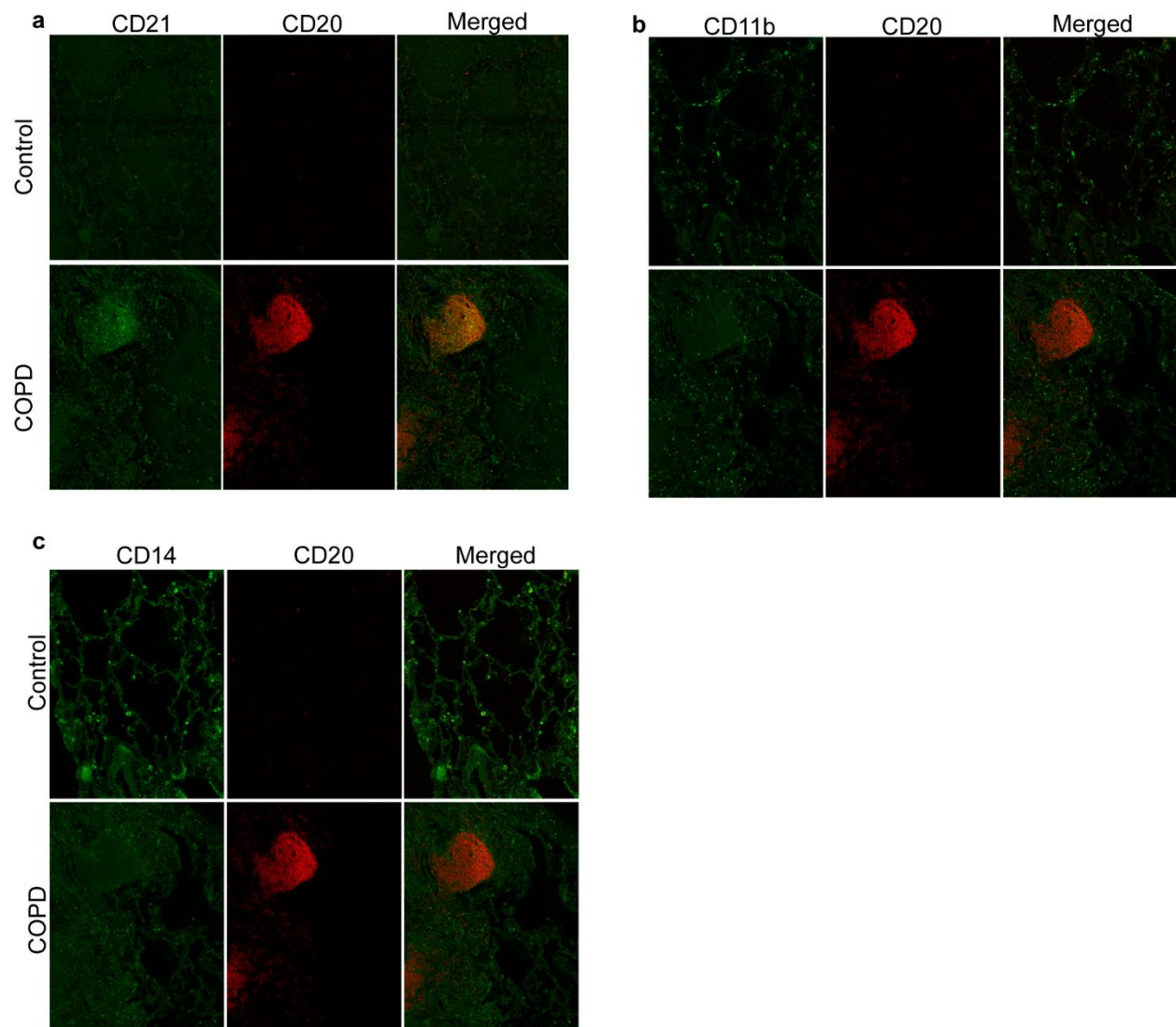
Figure S3. 9: Histology of COPD and control lungs

Showing B cells (CD20; red) and a) Follicular Dendritic Cells (CD21), b) Dendritic cells (CD11b), and Monocytes (CD14) in green.

Chapter 4.

Alterations in T and B cell function persist in convalescent COVID-19 patients

Halima A. Shuwa[#1], Tovah N. Shaw[#1,2], Sean B. Knight[1,3], Kelly Wemyss[1], Flora A. McClure[1], Laurence Pearmain[4,5], Ian Prise[1], Christopher Jagger[1], David. J. Morgan[1], Saba Khan[1], Oliver Brand[1], Elizabeth R. Mann[1,6], Andrew Ustianowski[1,5], Nawar Diar Bakerly[3], Paul Dark[7], Christopher E. Brightling[8], Seema Brij[9], CIRCO[‖], Timothy Felton[5], Angela Simpson[5], John R. Grainger[1]†, Tracy Hussell[1]†, Joanne E. Konkel,[1*]†, Madhvi Menon[1*]†.

\# contributed equally

† joint senior authors

* joint corresponding authors

Affiliations:

[1]Lydia Becker Institute of Immunology and Inflammation, Division of Infection, Immunity & Respiratory Medicine, School of Biological Sciences, Faculty of Biology, Medicine and Health, University of Manchester, Manchester Academic Health Science Centre, Room 2.16, Core Technology Facility, 46 Grafton Street, Manchester, M13 9PL, UK.

[2]Institute of Immunology and Infection Research, School of Biological Sciences, University of Edinburgh, Ashworth Laboratories, Edinburgh, EH9 3FL, UK

[3]Department of Respiratory Medicine, Salford Royal NHS Foundation Trust, Stott Lane, Salford, M6 8HD, UK.

[4]Wellcome Trust Centre for Cell Matrix Research, The University of Manchester, Manchester, M13 9PT, UK.

[5]Division of Infection, Immunity and Respiratory Medicine, Manchester NIHR BRC, Education and Research Centre, Wythenshawe Hospital, UK.

[6]Maternal and Fetal Health Centre, Division of Developmental Biology, School of Medical Sciences, Faculty of Biology, Medicine and Health, The University of Manchester, 5th Floor St. Mary's Hospital, Oxford Road, Manchester M13 9WL, UK.

[7]Regional Infectious Diseases Unit, North Manchester General Hospital, Manchester, UK.

[8]Department of Respiratory Sciences, University of Leicester, Leicester, LE3 9QP, UK.

[9]Department of Respiratory Medicine, Manchester Royal Infirmary, Manchester University NHS Foundation Trust, UK.

Note:

[∥] CIRCO investigators:

R. Ahmed, M. Avery, K. Birchall, E. Charsley, A. Chenery, C. Chew, R. Clark, E .Connolly, K. Connolly, O. Corner, S. Dawson, L. Durrans, H. Durrington, J. Egan, K. Filbey, C. Fox, H. Francis, M. Franklin, S. Glasgow, N. Godfrey, K. J. Gray, S. Grundy, J. Guerin, P. Hackney, C. Hayes, E. Hardy, J. Harris, A. John, B. Jolly, V. Kästele, G. Kelly, G. L., S. Lui, L. Lin, A.G. Mathioudakis, F. A. McClure, J. Mitchell, C. Moizer, K. Moore, S. Moss, S. Murtuza Baker, R. Oliver, G.Padden, C. Parkinson, M. Phuycharoen, A. Saha, B. Salcman, N. A. Scott, S. Sharma, J. Shaw, E. Shepley, L. Smith, S. Stephan, R. Stephens, G. Tavernier, R. Tudge, L. Wareing, R. Warren, T. Williams, L. Willmore and M. Younas.

Lead Contact: J. E. Konkel

Correspondence: joanne.konkel@manchester.ac.uk and madhvi.menon@manchester.ac.uk

Statement

4.0 Abstract

Background: Emerging studies indicate that some COVID-19 patients suffer from persistent symptoms including breathlessness and chronic fatigue; however the long-term immune response in these patients presently remains ill-defined.

Methods: Here we describe the phenotypic and functional characteristics of B and T cells in hospitalised COVID-19 patients during acute disease and at 3-6 months of convalescence.

Findings: We report that the alterations in B cell subsets observed in acute COVID-19 patients were largely recovered in convalescent patients. In contrast, T cells from convalescent patients displayed continued alterations with persistence of a cytotoxic programme evident in CD8$^+$ T cells as well as elevated production of type-1 cytokines and IL-17. Interestingly, B cells from patients with acute COVID-19 displayed an IL-6/IL-10 cytokine imbalance in response to toll-like receptor activation, skewed towards a pro-inflammatory phenotype. Whereas the frequency of IL-6$^+$ B cells was restored in convalescent patients irrespective of clinical outcome, recovery of IL-10$^+$ B cells was associated with resolution of lung pathology.

Conclusions: Our data detail lymphocyte alterations in previously hospitalized COVID-19 patients up to 6 months following hospital discharge and identify 3 subgroups of convalescent patients based on distinct lymphocyte phenotypes, with one subgroup associated with poorer clinical outcome. We propose that alterations in B and T cell function following hospitalisation with COVID-19 could impact longer term immunity and contribute to some persistent symptoms observed in convalescent COVID-19 patients.
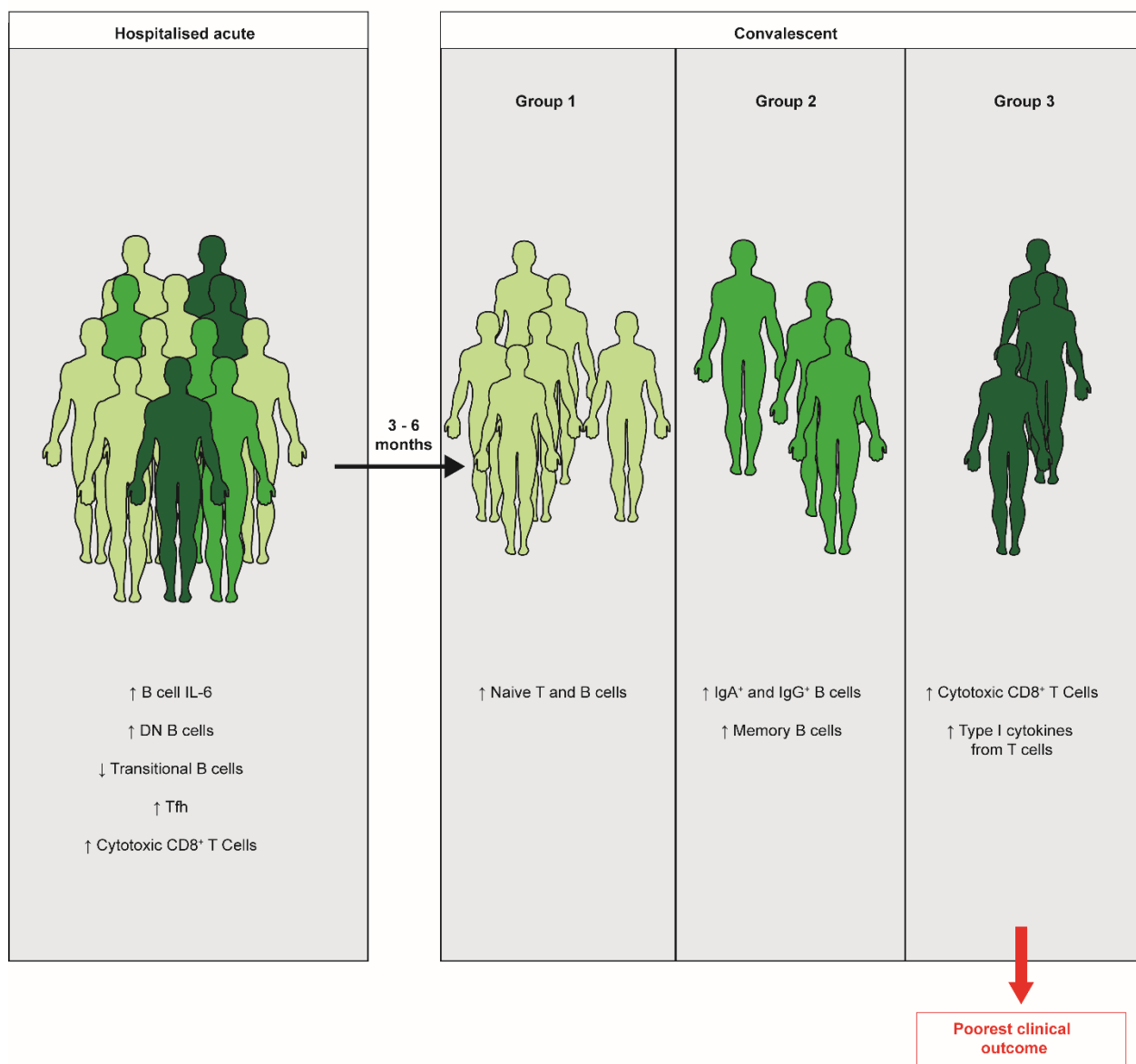
Graphical Abstract:

Shuwa et al. examine lymphocyte characteristics in acute and convalescent COVID-19 patients, detailing persistent alterations in lymphocyte phenotype up to 6 months following hospital discharge. In this report, they identify 3 subgroups of convalescent patients based on distinct lymphocyte signatures, with 1 subgroup associated with poorer clinical outcomes.

4.1 Introduction

The coronavirus disease 2019 (COVID-19) pandemic, caused by the emergence of a novel coronavirus strain, has resulted, at this time, in more than 106 million infections and 2.3 million deaths worldwide. Infection with severe acute respiratory syndrome-coronavirus 2 (SARS-CoV-2) has a plethora of consequences ranging from mild flu-like symptoms to life-threatening and fatal acute respiratory distress syndrome[293,565]. In all cases, the pathology is underpinned by not merely the virus itself but also an aberrant inflammatory host immune response. Research efforts detailing immune parameters in patients with acute COVID-19 have significantly improved our understanding of the disease, highlighting profound alterations in the innate and adaptive immune compartments[564,566–569]. Lymphopenia, as well as altered lymphocyte function, have been reported to correlate with disease severity[293,570], indicating key roles for T and B cells in COVID-19 pathology.

Emerging evidence suggests that COVID-19 patients can develop a spectrum of long-lasting symptoms that include chronic fatigue, myalgia, brain fog, fibrotic lung disease and pulmonary vascular disease[571–573]. Although the immune response in acute COVID-19 patients has been well characterized, long-term consequences of SARS-CoV-2 infection remain poorly understood. Since SARS-CoV-2 specific lymphocytes are likely critical for long-term protection against SARS-CoV-2 following disease resolution, it is pivotal to understand their contribution to acute disease, recovery, as well as long-lasting post-COVID-19 symptoms. Insights into these areas are rapidly required for the development of functional vaccines; indeed ground-breaking studies are demonstrating antigen-specific responses to this virus can persist for several months post-infection[574–577]. However, given the vast numbers of previously infected individuals across the globe, it is also vital to understand the impact of COVID-19 on the phenotype and functional potential of all lymphocytes, not just those reactive to SARS-CoV2. This will allow for better understanding of the long-term impacts of being hospitalised with COVID-19 on effective immunity. Indeed, long-term follow-up of Ebola patients has outlined immune dysfunction persisting for up to 2 years of convalescence[578]. Following much shorter periods of convalescence, individuals hospitalised with influenza infection have been shown to exhibit continued elevation in CD8^{+} T cell activation and proliferation[579]. Given the prolonged and profound immune dysregulation seen during acute SARS-CoV2 infection, there is a compelling need to determine whether these alterations translate into longer-term immune alterations and subsequent dysfunction in convalescent individuals.

Here, we conducted an observational study examining B and T cell populations in COVID-19 patients during hospitalization and in convalescent patients over 6 months following hospital discharge. Specifically, we examined lymphocyte characteristics in PBMCs from blood samples taken from COVID-19 patients within 7 days of hospitalization, at hospital discharge and at up to 6 months post hospital discharge. Samples were collected as part of the Coronavirus Immune Response and Clinical Outcomes (CIRCO) study based at four hospitals in Greater Manchester[564]. Examination of these samples allowed us to ascertain changes to lymphocytes during acute disease and upon convalescence in COVID-19 patients. We identify key alterations in B cell populations in acute COVID-19 patients with severe disease, which indicate imbalances within the B cell compartment could contribute to COVID-19 disease severity. Specifically, we demonstrate that in severe COVID-19 patients there was a loss of transitional B cells and an expansion of double negative memory B cells. Moreover, B cells exhibited altered functionality with increased production of IL-6 during acute disease, which was restored in convalescent patients. Intriguingly, B cell production of IL-10 was higher in convalescent patients with good clinical outcomes compared to patients with poor outcomes. In line with this, we also report changes within the CD4$^+$ T cell compartment of acute COVID-19 patients, specifically increases in T follicular helper cells (Tfh) that were recovered in convalescent patients. In contrast, we outline persistent alterations in the functional potential of CD8$^+$ T cells, with T cells from convalescent patients exhibiting elevated expression of a cytotoxic programme and production of type-I cytokines. These data describe the alterations to lymphocytes, detailing previously undescribed imbalances within the B cell compartment associated with the severity of acute disease and alterations in the potential of both B and T cells that persist for at least 6 months of convalescence. Further, compiling B and T immune parameters from convalescent patients identified 3 patient subgroups, defined by i) increased cytotoxic T cells and T cell type-I cytokine production, ii) high proportions of memory, IgA$^+$ and IgG$^+$ B cells and iii) highest expression of trafficking molecules and increased proportions of naïve B and T cells. It is noteworthy that the convalescent group defined by the highest proportions of cytotoxic CD8$^+$ T cells and type-I cytokine production was enriched in patients with a poorer outcome at follow-up, defined by abnormal chest X-Ray. Our study provides a deeper understanding of lymphocyte responses over the course of COVID-19 and into recovery, highlighting persistent alterations in lymphocyte functionality in convalescent COVID-19 patients up to 6 months following hospital discharge.

4.2 Results and Discussion

Clinical characteristics

Between 29th March and 15th July 2020, we included 80 'acute' patients, recruited during their in-patient stay for COVID-19, who had clinical and lymphocyte data available. For acute disease samples, patients were excluded if they were not recruited within 7 days of admission (16 patients), or there was a significant co-existent pathology (5 patients). 'Convalescent' patients were recruited between 14th July and October 2020 from out-patient clinical follow-up for COVID-19. Convalescent patients are therefore classified as previously hospitalised COVID-19 patients who are clinically stable and have been discharged from any further inpatient care. Convalescent patients were sampled between 53-180 days of convalescence. For convalescent patients sampled twice during their convalescence they were initially sampled between 67-180 days of convalescence and then secondarily sampled between 20-113 days later (with the latest second sample being taken at day 201 following discharge). For convalescent disease samples, one patient was excluded due to a significant co-existent pathology during in-patient admission for COVID-19; all others were included in the analysis. The median age and overall gender proportions were similar between acute and convalescent groups. There was a larger proportion of severe patients within the convalescent group, reflecting that patients with more severe disease were prioritised for limited 'face to face' appointments in participating trusts. The clinical characteristics of all patients recruited to the study are summarised in **Supplemental Tables 4.1-2.**

Altered B cell phenotypes in severe COVID-19 patients are restored upon convalescence

In agreement with previously published studies[564,568], we report significantly reduced circulating B cell frequencies in severe COVID-19 patients, that were normalized in convalescent patients (**Fig. 4.1A**). Further, increased Ki-67 expression (indicative of proliferation) in hospitalized patients was not observed in convalescent patients (**Fig. 4.1B** and **Supplemental Fig. 4.1A**). When characterizing B cell subsets based on expression of CD27 and IgD, we saw an expansion of CD27⁻IgD⁻ double negative (DN) memory B cells in severe COVID-19 patients that was still present in convalescent patients (**Fig. 4.1C, D**). No differences in unswitched memory (USM), switched memory (SM), or naïve B cells were observed between the patient groups and controls. Further classification of B cell subsets into transitional (CD24^{hi}CD38^{hi}) and mature (CD24^{int}CD38^{int}) B cells revealed a significant reduction in transitional B cells in patients with

severe COVID-19 that was restored in convalescent patients (**Fig. 4.1E, F**). A t-distributed stochastic neighbour embedding (tSNE) representation of the data highlights proportions of subsets in acute and convalescent COVID-19 patients compared to healthy controls (**Fig. 4.1G**). Importantly, CD27^{hi}CD38^{hi} plasmablasts were the only B cell subset expanded in all COVID-19 patients irrespective of severity, yet proportions were restored in convalescent patients (**Fig. 4.1H** and **Supplemental Fig. 4.1B**). We found that the frequency of plasmablasts positively correlated with the expression of IgG and IgA, but not with IgM expression by B cells in acute COVID-19 patients (**Fig. 4.1I** and **Supplemental Fig. 4.1C,D**), providing further evidence supporting an expansion of class-switched IgA and IgG antibodies in COVID-19 patients[580–582].

Examining B cell phenotypes in individual COVID-19 patients, tracking them longitudinally from acute hospitalization into convalescence showed similar alterations in B cell populations. Specifically, we observed a reduction in Ki-67$^+$ B cells and plasmablasts at convalescent time-points compared to acute disease, and a trend toward an increase in transitional B cells (**Supplemental Fig. 4.1E**). Interestingly, tracking individual patients from acute disease into convalescence revealed a decrease in DN B cells, despite the global expansion of this subset observed in both severe acute and convalescent patients (**Supplemental Fig. 4.1F**). Combined, these data highlight alterations in B cell subsets during severe acute COVID-19 which are largely restored upon convalescence.
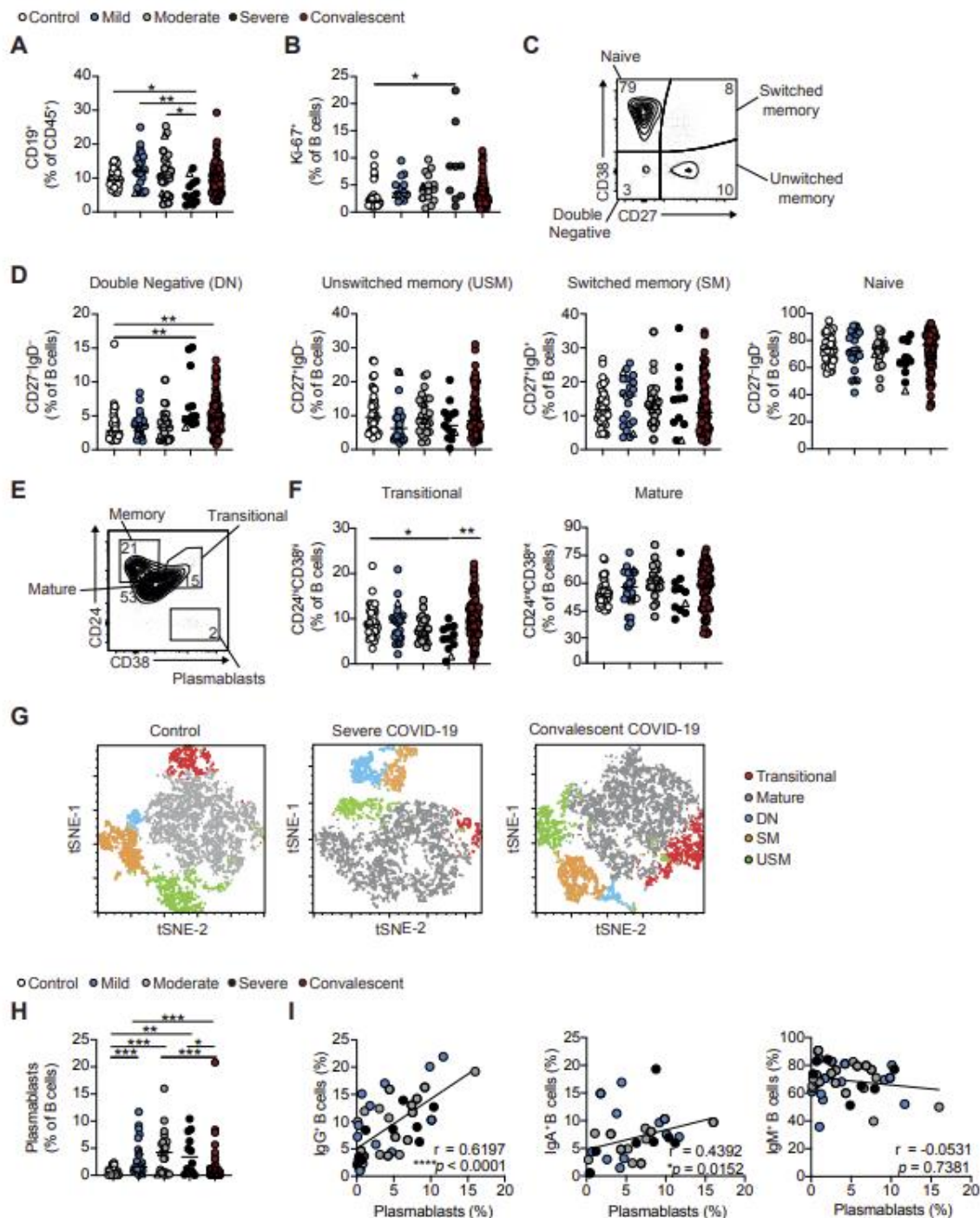
Figure 4. 1: Alterations in B cell subsets during acute COVID-19 are recovered upon convalescence

(A) Cumulative data show ex vivo frequency of CD19+ B cells in healthy individuals (n=38) and COVID-19 patients with mild (n=24), moderate (n=26) and severe (n=12) disease and at

convalescence (n=83). (B) Cumulative data show Ki-67 expression by B cells in healthy individuals (n=28) and COVID-19 patients with mild (n=13), moderate (n=15) and severe (n=9) disease and at convalescence (n=75). (C-D) Representative flow cytometry plots and cumulative data show frequencies of naïve (CD27-IgD+), unswitched memory (CD27+IgD+), switched memory (CD27+IgD-) and double negative (CD27-IgD-) B cells in healthy individuals (n=38-40) and COVID-19 with mild (n=22-24), moderate (n=25-26) and severe (n=12-13) disease and at convalescence (n=78-80). (E-F) Representative flow cytometry plots and cumulative data show ex vivo frequency of CD24hiCD38hi transitional B cells and CD24intCD38int mature B cells in healthy individuals (n=37) and COVID-19 patients with mild (n=24), moderate (n=23) and severe (n=11) disease and at convalescence (n=80). (G) tSNE projection of flow cytometry panel visualizing B cell subsets in PBMCs. Representative images for healthy individuals, severe COVID-19 and convalescent patients. Key indicates cell subsets identified on the image. (H) Cumulative data show frequency of CD27hiCD38hi plasmablasts in healthy controls (n=38) and COVID-19 patients with mild (n=23), moderate (n=23) and severe (n=12) disease and at convalescence (n=81). (I) Graph showing correlation between plasmablasts and IgG+ (left), IgA+ (middle) or IgM+ (right) B cell frequencies in acute COVID-19 patients. Graphs show individual patient data, with the bar representing median values. In all graphs, open triangles represent SARS-CoV-2 PCR-negative patients. *p<0.05, **p<0.01, ***p<0.001, one-way ANOVA with Kruskal-Wallis test with Dunn's post-hoc testing for multiple comparisons or or Spearman ranked coefficient correlation test. See also Supplemental Fig. 1 and 2.

Convalescent COVID-19 patients retain phenotypically altered CD8+ T cells

Previous studies have detailed CD8+ and CD4+ T cell activation in COVID-19 patients[568,583–585]. Here, we show that convalescent patients exhibited elevated proportions of T effector memory cells positive for CD45RA (TEMRA; CD45RA+CCR7-) (**Fig. 4.2A-C**). Despite this, T cells from convalescent patients did not display elevated expression of the proliferation marker Ki-67 (**Fig. 4.2D**; see **Supplemental Fig. 4.1G-K** for examples of representative FACS staining)[568]. CD8+ T cells from acute COVID-19 patients exhibit robust expression of a cytotoxic programme, with increases in perforin, granzyme and CD107a expression in unstimulated cells (**Fig. 4.2E-G**). Induction of this programme was still evident in convalescent patients, whose CD8+ T cells exhibited increased expression of both perforin and granzyme (**Fig. 4.2E, F**). However, the proportions of CD107a+ and Ki-67+GranzymeB+ CD8+ T cells in convalescent patients were

reduced compared to those with acute COVID-19 suggesting cytotoxic CD8$^+$ T cells in convalescent patients were no longer actively proliferating or degranulating (**Fig. 4.2G**). Showing the same pattern, longitudinal tracking of individual patients from their acute time-point into convalescence showed unchanged perforin and granzyme B expression in CD8$^+$ T cells (**Fig. 4.2H**), but reduced Ki-67$^+$, CD107a$^+$ and Ki-67$^+$GranzymeB$^+$ CD8$^+$ T cells at convalescent compared to the acute time-point (**Fig. 4.2I**). We also noted a persistence of this cytotoxic profile in CD8$^+$ T cells in a small subset of convalescent patients examined beyond 6 months after hospital discharge. Obtaining a second convalescent sample from the same patient at a later time-point of convalescence, demonstrated persistence of this cytotoxic programme beyond 6 months (**Supplemental Fig. 4.1L**).

In contrast to these phenotypic changes persisting in the CD8$^+$ T cell compartment up to, and potentially beyond, 6 months of convalescence, alterations noted in acute disease in CD4$^+$ T cells were normalized in convalescent patients. Specifically, although there were no significant changes in regulatory T cells (Tregs) across the disease trajectory (**Fig. 4.2J**), during acute disease, there was an expansion in T follicular helper cells (Tfh), defined as CD4$^+$CXCR5$^+$PD-1$^+$ICOS$^+$ (**Fig. 4.2K**). While an increase in Tfh has been previously reported in acute COVID-19 patients[324,329,568,586], here we show it was reduced in convalescent COVID-19 patients (**Fig. 4.2K**). This decrease in Tfh in convalescent patients occurred following hospital discharge (**Fig. 4.2L**) and could be identified when following the same patient from acute disease into convalescence (**Fig. 4.2M**). Combined these data demonstrate changes in the functional potential of CD8$^+$ T cells up to 6 months following hospital discharge, outlining continued expression of a cytotoxic programme.
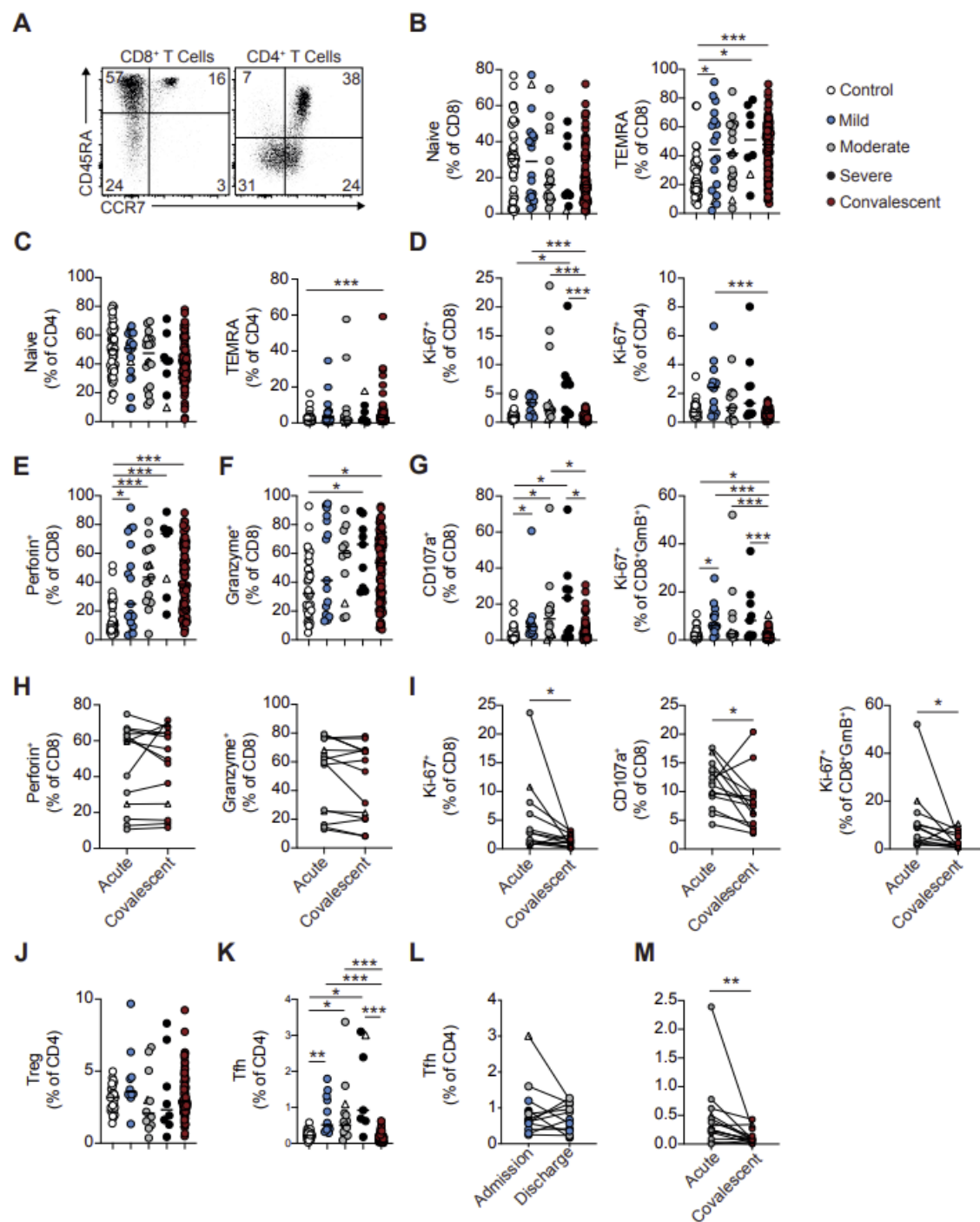
Figure 4. 2: Acute alterations in CD4+ T cells and persistent alterations in CD8+ T cells during COVID-19

(A) Representative FACS plots showing CD45RA and CCR7 staining on CD4$^+$ (gated CD3$^+$CD8$^-$) and CD8$^+$ (gated CD3$^+$CD4$^-$) T cells. **(B,C)** Graphs showing frequencies of **(B)** CD8$^+$ and **(C)** CD4$^+$ T cells which have a naïve (CD45RA$^+$CCR7$^+$) and Temra (CD45RA$^+$CCR7$^-$) phenotype in

healthy individuals (n=44) and COVID-19 patients with mild (n=18-19), moderate (n=18) and severe (n=8) disease and at up to 6 months of convalescence (n=83). **(D)** Graphs showing frequencies of CD8^{+} and CD4^{+} T cells which stain positive for Ki-67 in healthy individuals (n=28-30), and COVID-19 patients with mild (n=14), moderate (n=11-13) and severe (n=9) disease and at convalescence (n=81). **(E-G)** Graphs showing frequencies of **(E)** CD8^{+} Perforin^{+} cells, **(F)** CD8^{+} GranzymeB^{+} cells, and **(G)** CD8^{+} CD107a^{+} cells and CD8^{+} GranzymeB^{+} Ki-67^{+} cells in healthy individuals (n=29-37), and COVID-19 patients with mild (n=12-17), moderate (n=12-15) and severe (n=7-9) disease and at convalescence (n=81-83). **(H, I)** Graphs track frequencies of **(H)** Perforin^{+} and GranzymeB^{+}, and **(I)** Ki-67^{+}, CD107a^{+}, and GranzymeB^{+}Ki-67^{+} CD8^{+} T cells in the same COVID-19 patient at acute (grey circles) and convalescent (maroon circles) time-points (n=14). **(J)** Graph shows frequencies of Tregs within CD4^{+} T cells of healthy individuals (n=20) and COVID-19 patients with mild (n=10), moderate (n=12) and severe (n=8) disease and at convalescence (n=82). **(K)** Graph shows frequencies of Tfh within CD4^{+} T cells of healthy individuals (n=34) and COVID-19 patients with mild (n=12), moderate (n=15) and severe (n=7) disease and at convalescence (n=83). **(L)** Graph shows frequencies of Tfh in acute COVID-19 patients with mild (n=4), moderate (n=5) and severe (n=3) disease at the first and last time points of hospitalization. **(M)** Graph tracks frequency of Tfh CD4^{+} T cells in the same COVID-19 patient at acute (grey circles) and convalescent (maroon circles) time-points (n=14). Graphs show individual patient data, with the bar representing median values. In all graphs, open triangles represent SARS-CoV-2 PCR-negative patients. *p<0.05, **p<0.01, ***p<0.001, one-way ANOVA with Kruskal-Wallis test with Dunn's post-hoc testing for multiple comparisons (for B-G and K) or Wilcoxon matched-pairs signed rank test (I, M). See also Supplemental Fig. 1 and 2.

Lymphocytes from acute COVID-19 patients exhibit altered trafficking molecule expression that is restored upon convalescence

Lymphopenia is a well-established hallmark of COVID-19 patients[293,570]; although the drivers of peripheral blood lymphocyte loss remain unknown altered trafficking could contribute. Given the importance of appropriate co-ordination between immune cells during an effective anti-viral response and the implications of altered trafficking molecule expression, we examined the expression of chemokine receptors on B and T cells during acute and convalescent COVID-19. B cells from acute COVID-19 patients displayed significantly reduced expression of chemokine receptors CXCR3, CXCR5 and the gut homing molecule integrin β7, particularly in patients with

more severe disease (**Supplemental Fig. 4.2A-D**). The expression of CXCR5 and CXCR3 was largely normalised in convalescent patients regardless of disease severity at the time of hospitalization (**Supplemental Fig. 4.2E**).

Similar to B cells, CXCR5 and CXCR3 expression was substantially reduced on both $CD4^+$ and $CD8^+$ T cells in acute COVID-19 patients (**Supplemental Fig. 4.2F-K**), but with β7 exhibiting no alterations in acute disease. This reduction in CXCR3 and CXCR5 occurred irrespective of acute disease severity (**Supplemental Fig. 4.2L, M**). Loss of CXCR3 and CXCR5 expression was recovered on T cells from convalescent patients (**Supplemental Fig. 4.2F, G and I, J**). In agreement with previous reports examining the expression of CXCR5[568], our data outline reduced expression of multiple trafficking molecules on lymphocytes during acute COVID-19, that are mostly restored upon convalescence. Reduced CXCR3 and CXCR5 expression could reflect reduced homing of B and T cells into lymph nodes and follicles, which have been reported to contribute to immune dysfunction in other infections, such as advanced HIV[587–589]. Altogether, here we identify changes in chemokine receptor expression during acute disease that are recovered upon convalescence.

Alterations in lymphocyte cytokine potential in convalescent COVID-19 patients.

To understand the impact of COVID-19 on the potential of lymphocytes to make distinct cytokines, we stimulated PBMCs with phorbol myristrate acetate (PMA) and Ionomycin and examined cytokine production by T cells (see **Supplemental Fig. 4.3A** for example staining). Unlike previously published studies probing antigen specificity of T cells in COVID-19 patients[576,590], we more broadly assessed the potential of all T cells in COVID-19 patients to secrete cytokines. This approach allowed us to assess the impact of COVID-19 hospitalisation on any subsequent immune response, as opposed to the development of SARS-CoV2-specific memory. $IL-10^+CD4^+$ T cells were expanded in acute COVID-19 patients, but this was not observed in convalescent patients (**Fig. 4.3A**). Normalisation of IL-10 production from $CD4^+$ T cells did not occur during hospitalisation, as a decrease in $IL-10^+CD4^+$ T cells was not evident upon discharge (**Supplemental Fig. 4.3B**). As previously reported to occur in response to anti-CD3 and anti-CD28 stimulation[591], PMA and Ionomycin stimulation resulted in a greater proportion of $IL-17^+$ $CD4^+$ T cells in COVID-19 patients (**Fig. 4.3B**). Remarkably, enhanced $IL-17^+CD4^+$ T cells persisted into convalescence. We next queried whether elevated production of IL-17 during convalescence was associated with any specific clinical phenotypes. Increased $IL-17^+CD4^+$ T cells in convalescent patients were seen irrespective of whether patients were stratified by

presentation of normal or abnormal chest X-rays (**Fig. 4.3B**), reporting versus not reporting increased fatigue or based upon initial disease severity (**Supplemental Fig. 4.3C**).

Despite increased IL-10$^+$ and IL-17$^+$ CD4$^+$ T cells, neither CD4$^+$ or CD8$^+$ T cells from acute COVID-19 patients exhibited altered proportions of cells staining positive for the canonical Th1 cytokines IFNγ or TNFα (**Fig. 4.3C, D**). Although a previous study has reported that high proportions of antigen-specific IFNγ T cells are associated with reduced disease severity[329], our observation is in line with other studies demonstrating total peripheral T cell populations exhibit no enhanced production of these cytokines despite on-going disease[568,592], and irrespective of acute disease severity (**Supplemental Fig. 4.3D, E**). In stark contrast, both CD4$^+$ and CD8$^+$ T cells from convalescent COVID-19 patients exhibited enhanced production of type-I cytokines (**Fig. 4.3C, D**). This increase in cytokine production was not evident at hospital discharge (**Supplemental Fig. 4.3F, G**). Increased type-I cytokines occurred when stratifying convalescent patients by presentation of normal or abnormal chest X-rays (**Fig. 4.3C, D**) and those reporting increased fatigue. Of note no significant increase in IFNγ^+CD4$^+$ T cells was seen when stratifying patients for fatigue (**Supplemental Fig. 4.3H**). Increased production of these type-I cytokines in convalescent patients was associated with COVID-19 disease severity, apart from for IFNγ^+CD4$^+$ T cells, as patients who had moderate and severe disease showed significant increases in cytokine positive cells relative to controls (**Fig. 4.3E, F**). As such, the increases seen in total convalescent patients could be due to increased proportions of patients that exhibited severe disease. However, comparing proportions of cytokine-positive cells in severe patients at acute and convalescent time-points still showed an elevation in cytokine producing T cells, apart from for TNFα^+ CD8$^+$ T cells (**Supplemental Fig. 4.3I, J**). More importantly, longitudinal data tracking the same patient across their acute and convalescent disease time-points also showed increased production of these type-I cytokines (except for IFNγ^+TNFα^+ CD4$^+$ T cells) (**Fig. 4.3G,H**). In a small subset of patients we also obtained a second convalescent sample after 6 months from hospital discharge. In this small group we noted unchanged proportions of cytokine positive T cells, suggesting persistence of elevated cytokine production beyond 6 months (**Supplemental Fig. 4.3K,L**). These data fit with previous studies showing IFNγ^+ and TNFα^+ SARS-CoV-2 specific-T cells in convalescent patients[576,590,593] but further outline that altered cytokine potential is a general feature of all T cells during convalescence from COVID-19.

Next, in order to assess cytokine production by B cells, we stimulated PBMCs from COVID-19 patients and healthy individuals with CpGB (a TLR9 agonist) for 48 hours and measured cytokine expression by flow cytometry. We observed a significant expansion of IL-6$^+$ B cells in acute

COVID-19 patients and a trend toward a decrease in IL-10$^+$ B cells; suggesting an imbalance in B cells towards a more pro-inflammatory phenotype (**Fig. 4.3I** and **Supplemental Fig. 4.4A-D**). The frequency of IL-6$^+$ B cells was restored in convalescent patients, and was not impacted by presentation of normal or abnormal chest X-rays (**Fig. 4.3I**) or fatigue (**Supplemental Fig. 4.4D**). Interestingly, B cell production of IL-10 was higher in convalescent patients with a good clinical outcome compared to those with a poor outcome. Increased proportions of IL-10$^+$ B cells in convalescent patients with normal chest X-rays compared to those with abnormal chest X-rays (**Fig. 4.3I**) suggests a positive outcome might be associated with the expansion of regulatory B cells. No significant differences in the frequency of TNFα$^+$ B cell were observed in acute and convalescent COVID-19 patients (**Fig. 4.3I** and **Supplemental Fig. 4.4D**). Frequencies of cytokine positive B cells in both acute and convalescent patients were not affected by disease severity (**Supplemental Fig. 4.4E,F**). Longitudinal analysis of individual patients from acute disease into convalescence showed no change in either IL-6$^+$ or TNFα$^+$ B cells but did demonstrate a recovery of IL-10$^+$ B cells upon convalescence (**Fig. 4.3J**). Of note, only 1 out of 13 patients whose B cells were followed longitudinally exhibited an abnormal chest X-ray at follow-up. Combined, these data demonstrate an expansion of IL-6$^+$ B cells during acute disease and reduced proportions of IL-10$^+$ B cells in convalescent patients with poor clinical outcome.
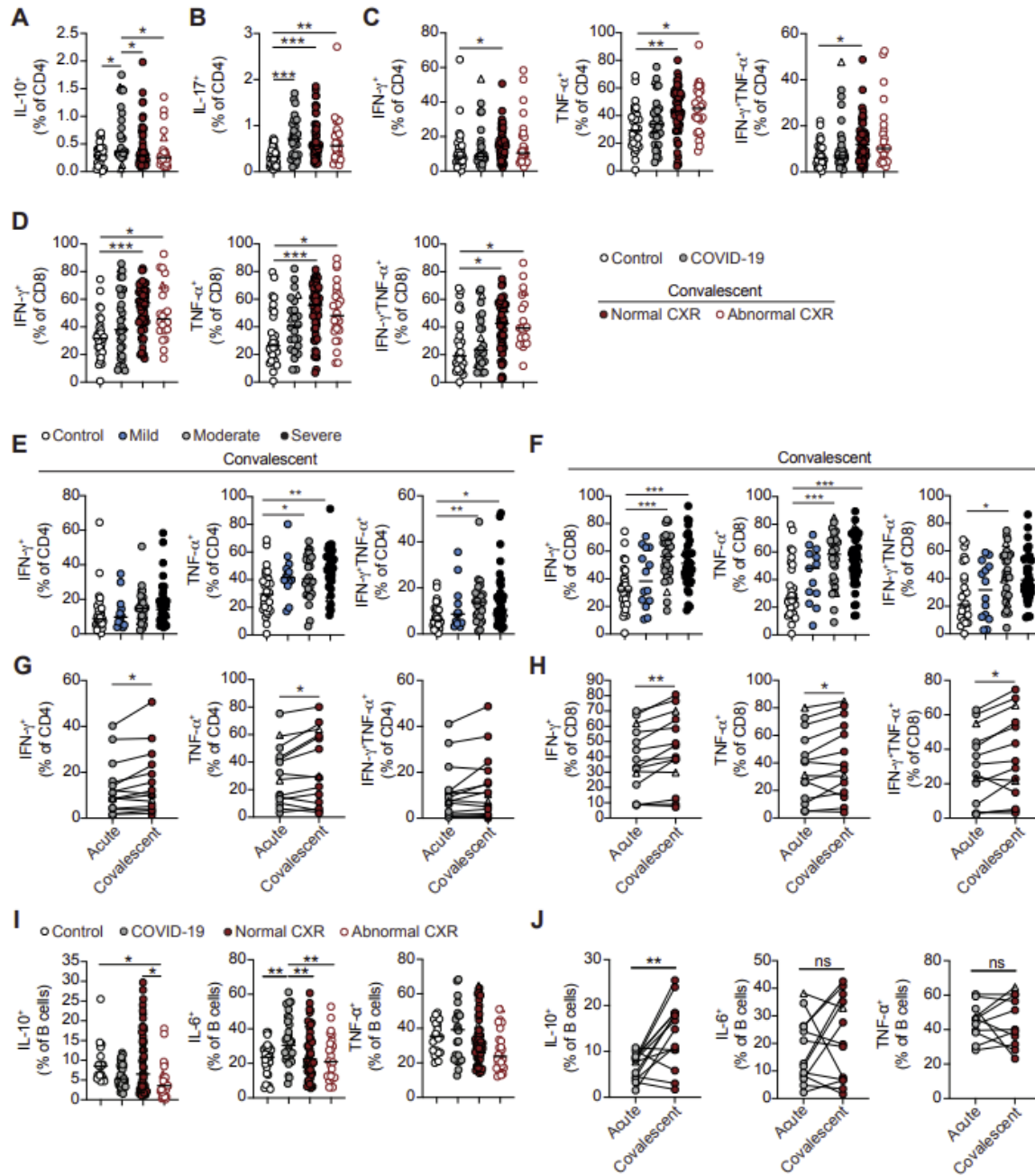
Figure 4. 3: Changes in cytokine production by lymphocytes during acute and convalescent COVID-19

(A-C) Graphs showing frequencies of CD4+ T cells which stain positive for **(A)** IL-10, **(B)** IL-17 and **(C)** IFNγ and TNFα following 3 hour stimulation with PMA and ionomycin in healthy individuals (n=25-30), acute COVID-19 patients (n=29-33) and convalescent COVID-19 patients with normal (n=55-57) or abnormal chest X-ray findings (n=25-26). **(D)** Graphs showing frequencies of CD8+

T cells which stain positive for IFNγ and TNFα following 3 hour stimulation with PMA and ionomycin in healthy individuals (n=28), acute COVID-19 patients (n=24-31) and convalescent COVID-19 patients with normal (n=54-57) or abnormal chest X-ray findings (n=21-24). (**E,F**) Graphs show frequencies of (**E**) CD4$^+$ and (**F**) CD8$^+$ T cells which stain positive for IFNγ and TNFα following 3 hour stimulation with PMA and ionomycin in convalescent COVID-19 patients which initially presented with mild (n=13-14), moderate (n=25-28) and severe (n=34-41) disease. (**G,H**) Graphs track frequencies of (**G**) CD4$^+$ and (**H**) CD8$^+$ T cells which stain positive for IFNγ and TNFα in the same COVID-19 patient at acute (grey circles) and convalescent (maroon circles) time-points (n=14). (**I**) Graphs showing frequencies of CD19$^+$ B cells positive for IL-10, IL-6 and TNFα following 48 hour stimulation with CpGB in healthy individuals (n=22-27), acute COVID-19 patients (n=22-32) and convalescent COVID-19 patients with normal (n=52-54) or abnormal chest X-ray findings (n=24-27). (**J**) Graphs track frequencies of CD19$^+$ B cells which stain positive IL-10, IL-6 and TNFα in the same COVID-19 patient at acute (grey circles) and convalescent (maroon circles) time-points (n=11-14). Graphs show individual patient data, with the bar representing median values. In all graphs, open triangles represent SARS-CoV-2 PCR-negative patients. *$p < 0.05$, **$p < 0.01$, ***$p < 0.001$, one-way ANOVA with Kruskal-Wallis test with Dunn's post-hoc testing for multiple comparisons, (except for graphs showing CD4$^+$TNFα^+ and CD8$^+$IFNγ^+ T cells in E and F where One-way ANOVA with Holm-Sidak post-hoc test was employed), or Wilcoxon matched-pairs signed rank test (G,H and J). See also Supplemental Fig. 3 and 4.

Identification of COVID-19 convalescent immunotypes based on lymphocyte parameters.

Collectively, our data establish alterations in the lymphocyte compartment that persist up to 6 months post hospital discharge in convalescent patients. In order to further probe lymphocyte changes within convalescent COVID-19 patients, we clustered patients based on T and B cell features. Unsupervised clustering revealed three groups of convalescent patients with distinct compositions of T and B cell signatures (**Fig. 4.4A**). Group 1 was associated with high expression of trafficking molecules and increased proportions of naïve B and T cells; Group 2 was characterised by high proportions of IgA$^+$ and IgG$^+$ B cells, and memory B cells (both switched and unswitched); Group 3 displayed increased cytotoxic T cells, CD8$^+$ TEMRA and type-I cytokines by both CD8$^+$ and CD4$^+$ T cells. These data suggest the existence of subgroups of convalescent COVID-19 patients based on B and T cell phenotypes. We next queried whether

these groups could identify convalescent patients based on clinical outcome. Higher proportions of patients in Group 3 presented with an abnormal chest X-Ray and reported breathlessness at their convalescent follow-up compared to patients within Groups 1 and 2 (Group 1; Abnormal Chest X-Ray; 23.7% and Dyspnoea; 43.2%. Group 2; Abnormal Chest X-Ray; 26.3% and Dyspnoea; 44.4%. Group 3; Abnormal Chest X-Ray; 62.5% and Dyspnoea; 62.5%). Examining characteristics of the patients within each group (**Fig. 4.4B-G**), we noted that Group 1 contained most patients who had had mild disease, younger patients and a greater proportion of female patients, indicating these parameters could be impacting this convalescent phenotype. In contrast, we noted very little difference in the demographics or acute disease information between patients in Groups 2 and 3. For example both had a similar proportion of patients who had exhibited severe COVID-19 (Group 2; 66.6%. Group 3; 50%) and a similar proportion of male patients (Group 2; 70.5%. Group 3; 75%). Despite similar patient characteristics, these two patient groups present with distinct lymphocyte profiles and different outcomes, with Group 3 exhibiting the poorest clinical outcome (Abnormal Chest X-Ray; Group 2; 26.3%. Group 3; 62.5%). Our data provide an important foundation for future work supporting the stratification and identification of hospitalised COVID-19 patients at risk of developing long-COVID symptoms. Our study can now be expanded to explore additional clinical implications of COVID-19, ascertaining whether specific clinical outcomes are associated with distinct convalescent patient subgroups. Importantly, these consequences can now be ascertained as platforms such as the post-hospitalisation COVID-19 study (PHOSP-COVID) in the UK now exist to support such future studies. Moreover, these future studies should also explore whether the lymphocyte alterations we have defined are specific to COVID-19 convalescence or occur following hospitalization with any respiratory virus.

A

Row labels
B Cell CD19⁺
B Cell Transitional
★ B Cell IgM⁺
★ B Cell Mature
★ B Cell Naive
★ B Cell β7⁺
★ B Cell CXCR5⁺
★ CD4 Naive
★ CD8 Naive
CD8 CD107a⁺
★ B Cell IgA⁺
B Cell Ki-67⁺
★ B Cell IgG⁺
★ B Cell SM
★ B Cell Memory
★ B Cell USM
B Cell DN
B Cell Pb
B Cell TNF-α⁺
CD4 IL-6⁺
CD4 IL-17⁺
★ B Cell IL-6⁺
★ CD4 TEMRA
★ CD4 TEM
★ CD4 IFN-γ⁺
★ CD4 IFN-γ⁺TNF-α⁺
★ CD4 TNF-α⁺
★ CD8 IFN-γ⁺
★ CD8 IFN-γ⁺TNF-α⁺
★ CD8 TNF-α⁺
CD8 Perforin⁺
★ CD8 GrmB⁺
★ CD8 TEMRA
CD4 Treg
B Cell IL-10⁺
CD4 β7⁺
CD4 IL-10⁺
CD8 TEM
★ B Cell CXCR3⁺
CD4 CXCR3⁺
CD4 CXCR5⁺
CD4 Tfh
CD4 Ki-67⁺Treg
CD4 Ki-67⁺
CD8 Ki-67⁺
CD8 GrmB⁺Ki-67⁺
CD4 TCM
CD8 β7⁺
CD8 CXCR5⁺
CD8 CXCR3⁺
CD8 TCM
X-ray

■ Abnormal □ Normal

row max — row min

Convalescent COVID-19 patients

1	2	3
High β7, CXCR5 on B cells. High naive B and T cells.	High IgA⁺ and IgG⁺ B cells. High memory B cells.	High IFN-γ and TNF-α from T cells. High cytotoxic T cells.

B Age (years) — *

C BMI

D Sex (F / M)

E Disease severity

F Length of hospital stay (days)

G Time to follow up (days)

Figure 4. 4: Distinct immune profiles emerge in previously hospitalised convalescent COVID-19 patients

(A) Heatmap of indicated immune parameters by row; each column represents an individual convalescent COVID-19 patient. The patients were clustered using one minus Pearson correlation hierarchical clustering. Significance was determined by Two-way ANOVA followed by a Tukey's multiple comparison test, *next to lymphocyte characteristic indicates significant difference between patient groups. Dominant immune characteristics of each group are indicated at the bottom of the heat map. Black and White squares indicate patients displaying a normal (white) or abnormal (black) chest X-Ray at follow-up. **(B-G)** Graphs show patient characteristics and clinical details of convalescent COVID-19 patients in each of the three immune groups identified, specifically; **(B)** age, **(C)** BMI, **(D)** sex, **(E)** Severity of acute COVID-19, **(F)** Length, in days, of hospitalization for acute COVID-19, **(G)** Time, in days, from hospital discharge to follow-up of convalescent patients. Graphs show individual patient data, with the bar representing median values. *p<0.05, one-way ANOVA with Kruskal-Wallis test with Dunn's post-hoc testing for multiple comparisons

In sum, here we report changes to T and B cell populations across the COVID-19 disease trajectory into convalescence. Our data demonstrate a high degree of activation of a cytotoxic programme within CD8$^+$ T cells during acute disease as previously reported[330,564,566]. We extend these data by showing persistence of this programme within circulating CD8$^+$ T cells up to at least 6 months of convalescence. Whereas previous studies have shown persistence of low frequencies of SARS-CoV2-specific CD8$^+$ T cells with a cytotoxic profile[593], importantly here we show elevation of cytotoxic markers within total circulating CD8$^+$ T cells. Although the specificity of T cells in our study remains to be determined, increases in CD8$^+$ T cells with a cytotoxic potential would result in an altered T cell landscape that could impact tissue integrity depending on their trafficking capabilities and cytokine responsiveness. Moreover, our data raise questions about the impact this increase in cytotoxic cells would have on subsequent infection, be that bacterial, viral or fungal. The importance of this question is further underscored by the elevated potential of total CD8$^+$ and CD4$^+$ T cells to produce both IFNγ and TNFα in convalescent patients, outlining persistent alteration in cytokine potential which could be either beneficial or detrimental to subsequent immune responses.

In contrast, altered B cell subsets in acute disease are recovered upon convalescence. Several recent studies have reported detection of virus-specific antibodies for several months post recovery from SARS-CoV2 infection[594–596]. Here we show that circulating plasmablast frequencies correlate positively with IgA/IgG and negatively with IgM, further supporting an expansion of class-switched antibodies in COVID-19 patients. In addition to secreting antibodies, B cells produce cytokines and are classified into effector (Beff; IL-6$^+$ and TNFα$^+$) and regulatory B cell (Breg; IL-10$^+$) subsets based on the cytokines they produce[597]. Significant decreases in transitional B cells, the precursors of human Bregs[364], along with IL-10$^+$ B cells, suggests a loss of immunosuppressive Bregs and an expansion of Beff cells in severe COVID-19 patients, as also observed in chronic inflammatory disorders such as systemic lupus erythematosus (SLE) and rheumatoid arthritis (RA)[364,497,598]. Interestingly, resolution of lung pathology in COVID-19 patients was found to be associated with higher proportions of IL-10$^+$ B cells, suggesting that these cells could be important in suppressing excess inflammation and are associated with positive long-term outcomes.

In summary, we report phenotypic and functional alterations to B and T cells across the trajectory of SARS-CoV2 responses from acute disease requiring hospitalisation into convalescence, identifying immune alterations that persist in convalescent COVID-19 patients for up to 6 months. Our study therefore identifies lymphocyte changes in convalescent COVID-19 patients which could have longer term impacts on subsequent anti-pathogen or auto-inflammatory responses.

4.3 Acknowledgements

and Tracy Hussell are supported by the NIHR Manchester Biomedical Research Centre. In addition, we would like to thank the following groups for technical and scientific discussions; the Lydia Becker Institute of Immunology and Inflammation, The NIHR Respiratory TRC, UK Coronavirus Immunology Consortium, and PHOSP-COVID.

Author contributions

Conceptualization, JEK and MM; Methodology, JEK, MM, JRG, and TH; Investigation, HAS, TNS, KW, FAM, SBK, IP, CJ, DJM, SK, OB, ERM, CIRCO; Formal Analysis, IP and SBK; Resources, SBK, LP, AU, NDB, PD, CEB, SB, TF, AS; Data Curation, SBK; Writing – Original Draft, JEK and MM; Writing – Review and Editing, HAS, TNS, JEK, MM, JRG, and TH; Visualization, KW; Supervision, JEK and MM; Funding Acquisition, JEK, MM, JRG, and TH.

Declaration of Interests

None to declare.

4.5 Star Methods

Resource Availability

Lead Contact: Further information and requests for resources and information should be directed to the Lead Contact, Joanne E. Konkel (Joanne.konkel@manchester.ac.uk).

Materials Availability: This study did not generate new unique reagents.

Data and Code Availability: All relevant data outputs are within the paper and supplemental information.

Experimental Models and Subject details

Study design and Participants

Two cohorts of patients were recruited from Manchester University Foundation Trust (MFT), Salford Royal NHS Foundation Trust (SRFT) and Pennine Acute NHS Trust (PAT) under the framework of the Manchester Allergy, Respiratory and Thoracic Surgery (ManARTS) Biobank (study no M2020-88) for MFT or the Northern Care Alliance Research Collection (NCARC) tissue biobank (study no NCA-009) for SRFT and PAT. Ethical approval obtained from the National Research Ethics Service (REC reference 15/NW/0409 for ManARTS and 18/WA/0368 for

NCARC). Informed consent was obtained from each patient, clinical information was extracted from written/electronic medical records including demographic data, presenting symptoms, comorbidities, radiographic findings, vital signs, and laboratory data. Patients were included if they tested positive for SARS-CoV-2 by reverse-transcriptase–polymerase-chain-reaction (RT-PCR) on nasopharyngeal/oropharyngeal swabs or sputum during their in-patient admission for COVID-19. Patients with negative nasopharyngeal RTPCR results were also included if there was a high clinical suspicion of COVID-19, the radiological findings supported the diagnosis, and there was no other explanation for symptoms. Patients were excluded if an alternative diagnosis was reached, where indeterminate imaging findings were combined with negative SARS-CoV-2 nasopharyngeal (NP) test, or there was another confounding acute illness not directly related to COVID-19. The severity of disease was scored each day, based on criteria for escalation of care (**Supplemental Table 3**). Where severity of disease changed during admission, the highest disease severity score was selected for classification. Peripheral blood samples were collected within 7 days of hospital admission, at discharge and then at 3-9 months post hospital discharge when patients returned to out-patient clinics.

Demographics and clinical information for acute and convalescent patients can be found in **Supplemental Tables 1-2.**

Healthy controls

Recruiting healthy individuals from the community for blood sampling during the SARS-CoV-2 outbreak was not possible, and therefore we sampled frontline workers from NHS Trusts and University of Manchester staff with an age range that was similar to our COVID-19 patients (age range 35-71; median age=50.9; 52% males). All healthy controls tested negative for anti-Spike1 receptor binding domain antibodies.

4.6 Methods Detail

PBMC isolation

Fresh blood samples from COVID-19 patients and healthy individuals were collected in EDTA tubes. Blood was diluted 1:1 with PBS and layered gently on Ficoll-Paque followed by density gradient centrifugation. Cells were thoroughly washed and were either freshly stained for flow cytometry or are stored in 10% dimethyl sulfoxide (DMSO) in fetal bovine serum (FBS) at -150°C.

Cell culture

Frozen PBMC were thawed, washed and resuspended in RPMI containing 10% FBS, L-Glutamine, non-essential amino acids, HEPES, and penicillin plus streptomycin. 2.5×10^5 cells were stimulated with; (i) 2µL/ml of stimulation cocktail (eBioScience) in the presence of 10 µg/ml Brefeldin A for three hours (T cells), (ii) 1 µM CpG for 48 hours followed by 2µL/ml of stimulation cocktail (eBioScience) in the presence of 10 µg/ml Brefeldin A in the last four hours (B cells). Following stimulation cells were washed and stained for flow cytometric analysis.

Flow cytometry

PBMCs (fresh/thawed/stimulated) were stained with fluorophore conjugated antibodies (see Key Resource Table) and viability dyes. Samples were acquired on an LSRFortessa cell analyser (Becon Dickinson) and analysed using FlowJo (TressStar).

Quantification and statistical Analysis

Clustering of T and B cell phenotypes

T cell and B cell data were scaled using unit variance scaling, clustered and graphed using correlation distance and average linkage on the heatmap tool on ClustVis[599].

Statistics

Results are presented as individual data points with medians. Normality tests were performed on all datasets. Groups were compared using an unpaired Mann-Whitney test for healthy individuals versus COVID-19 patients, one-way ANOVA with Holm-Sidak post-hoc testing (normal distribution) or Kruskal-Wallis test with Dunn's post-hoc testing (failing normality testing) for multiple comparisons, or Spearman's rank correlation coefficient test for correlation of separate parameters within the COVID-19 patient group, using Prism 8 software (GraphPad). In all cases, a p value of ≤ 0.05 was considered significant. Where no statistical difference is shown there was no significant difference. Details of statistical tests and definitions of n can be found in each figure legend.

Supplemental Information

Supplemental Methods

PBMC isolation: Fresh blood samples from COVID-19 patients and healthy individuals were collected in EDTA tubes. Blood was diluted 1:1 with PBS and layered gently on Ficoll-Paque followed by density gradient centrifugation. Cells were thoroughly washed and were either freshly stained for flow cytometry or are stored in 10% dimethyl sulfoxide (DMSO) in fetal bovine serum (FBS) at -150°C.

Cell culture and flow cytometry: Frozen PBMC were thawed, washed and resuspended in RPMI containing 10% FBS, L-Glutamine, non-essential amino acids, HEPES, and penicillin plus streptomycin. 2.5×10^5 cells were stimulated with; 2µL/ml of stimulation cocktail (eBioScience) in the presence of 10 µg/ml Brefeldin A for three hours (T cells), 1 µM CpG for 48 hours followed by 2µL/ml of stimulation cocktail (eBioScience) in the presence of 10 µg/ml Brefeldin A in the last four hours (B cells). PBMCs (fresh/thawed/stimulated) were stained with flow staining antibodies (see table I) and viabilities dyes (Zombie dyes; Biolegend) and samples were acquired on an LSRFortessa cell analyser (Becon Dickinson) and analysed using FlowJo (TressStar).

Table 4. 1: Details of antibody clones and suppliers

Marker	Clone	Company
CD19	HIB19	BioLegend
CD27	M-T271	BioLegend
CD38	HIT2	BioLegend
IgD	IA6-2	BioLegend
IgG	M1310G05	BioLegend
IgM	MHM-88	BioLegend
CD21	Bu32	BioLegend
CD11c	3.9	BioLegend
CD3	SK7	BioLegend
CD4	SK3	BioLegend
CD8	SK1	BioLegend

CD86	BU63	BioLegend
CD56	5.1H11	BioLegend
CD45RA	HI100	BioLegend
IL-6	MQ2-13A5	BioLegend
IL-10	JES3-19F1	BioLegend
Ki67	Ki-67	BioLegend
HLA-DR	L243	BioLegend
IFN-γ	4S.B3	BioLegend
PD-1	EH12.2H7	BioLegend
CD69	FN50	BioLegend
CD62L	SK11	BioLegend
CXCR3	G025H7	BioLegend
CXCR5	J252D4	BioLegend
CCR7	G043H7	BioLegend
ICOS	C398.4A	BioLegend
Granzyme-B	QA18A28	BioLegend
CD127	A019D5	BioLegend
CD25	BC96	BioLegend
CD107a	H4A3	BioLegend
Perforin	dG9	BioLegend
TCRγδ	B1	BioLegend
IL-17	BL168	BioLegend
TNF-α	MAb11	BD Bioscience
IgA	REA1014	Miltenyi Biotec
CD24	eBioSN3	eBioscience
Foxp3	236A/E7	eBioscience

Clustering of T and B cell phenotypes: T cell and B cell data were scaled using unit variance scaling, clustered and graphed using correlation distance and average linkage on the heatmap tool on ClustVis[1].

Statistics: Results are presented as individual data points with medians. Normality tests were performed on all datasets. Groups were compared using an unpaired Mann-Whitney test for healthy individuals versus COVID-19 patients, one-way ANOVA with Holm-Sidak post-hoc testing

(normal distribution) or Kruskal-Wallis test with Dunn's post-hoc testing (failing normality testing) for multiple comparisons, or Spearman's rank correlation coefficient test for correlation of separate parameters within the COVID-19 patient group, using Prism 8 software (GraphPad). In all cases, a p value of ≤ 0.05 was considered significant. Where no statistical difference is shown there was no significant difference.

4.7 Supplemental Figures and Table

Supplemental Table 4. 1: Clinical characteristics of acute COVID-19 patients

Data are median (IQR)[m] , where[m] is the number of missing data points, n (%) or n/N (%), where N is the total number with available data. PE, pulmonary embolism, AKI, Acute kidney injury. [a] Admission observations.

Acute Patients

	Overall (58)	Mild (22)	Moderate (23)	Severe (13)
Age	58.5 (49.5-71)	58 (45-71)	58 (50-66.5)	67 (55-74)
Gender				
Male	36/58 (62.1%)	13/22 (59.1%)	13/23 (56.5%)	10/13 (77%)
Female	22/58 (37.9%)	9/22 (40.9%)	10/23 (43.5%)	3/13 (23%)
BMI	28.5 (25.2-30.6)[14]	27.8 (23.2-33.1)[8]	29 (26.8-30.3)[3]	27.6 (25.4-30.2)[3]
Day of admission recruited	2 (2-3)	3 (2-4.75)	2 (2-3)	2 (2-3)
Medical History				
Diabetes	13/58 (22.41%)	6/22 (27.27%)	2/23 (8.7%)	5/13 (38.46%)
Ischaemic Heart Disease	8/58 (13.79%)	3/22 (13.64%)	2/23 (8.7%)	3/13 (23.08%)
Hypertension	20/58 (34.48%)	6/22 (27.27%)	9/23 (39.13%)	5/13 (38.46%)
COPD	11/58 (18.97%)	5/22 (22.73%)	4/23 (17.39%)	2/13 (15.38%)

Asthma	9/58 (15.52%)	4/22 (18.18%)	4/23 (17.39%)	1/13 (7.69%)
Malignancy	5/58 (8.6%)	0/22 (0%)	2/23 (8.7%)	3/13 (23%)
Differential counts on admission (x 10^9/L)				
Total white cell count	7.1 (6-10)[9]	6.85 (5.55-8.42)[4]	7.3 (6.3-10)[2]	7.25 (6.55-10.02)[3]
Lymphocytes	1 (0.82-1.5)[9]	1.2 (0.92-1.77)[4]	0.9 (0.8-1.5)[2]	0.9 (0.82-0.98)[3]
Neutrophils	5.3 (4.4-8)[9]	5.15 (3.8-7.05)[4]	5.5 (4.7-7.7)[2]	6.25 (4.82-8.62)[3]
Monocytes	0.4 (0.2-0.6)[9]	0.25 (0.2-0.73)[4]	0.5 (0.4-0.7)[2]	0.35 (0.3-0.57)[3]
Other inpatient investigations				
Positive SARS CoV2 PCR	49/58 (84%)	18/22 (81%)	20/23 (87%)	11/13 (85%)
Highest CRP (mg/L)	144 (83.9-226)	99 (35-176)	131 (86.5-195.6)	256 (198-283)
Chest Imaging				
Bilateral opacification	49/56 (87.5%)	14/20 (70%)	22/23 (95.7%)	13/13 (100%)
Unilateral opacification	3/56 (5.4%)	2/20 (10%)	1/23 (4.3%)	0/13 (0%)
Clear	4/56 (7.1%)	4/20 (20%)	0/23 (0%)	0/13 (0%)
Outcome				
Length of stay (days)	6 (4-11.3)[2]	5.5 (3.3-9.2)	6 (4-10)[2]	10 (6-13)
Mortality	9/58 (15.5%)	1/22 (4.5%)	0/23 (0%)	8/13 (61.5%)

Supplemental Table 4.2: Clinical characteristics of convalescent COVID-19 patients

Data are median (IQR)[m] , where[m] is the number of missing data points, n (%) or n/N (%), where N is the total number with available data. PE, pulmonary embolism, AKI, Acute kidney injury. [a] Admission observations.

Convalescent Patients

	Overall (81)	Mild (14)	Moderate (26)	Severe (41)
Age (years)	60 (51 - 67)	51.5 (45.5 - 60.3)	59.5 (51.25 - 71.5)	60 (56 - 66)
Gender				
Male	49/81	9/14 (64.3%)	13/26 (50%)	27/41 (65.9%)
Female	32/81	5/14 (35.7%)	13/26 (50%)	14/41 (34.1%)
BMI	31 (28.7 - 34.7)[29]	34.8 (31.9 - 38.4)[4]	30.9 (28.8 - 34.6)[12]	29.6 (28.5 - 33.1)[13]
Medical History				
Diabetes	20/81 (24.69%)	4/14 (28.57%)	8/26 (30.77%)	8/41 (19.51%)
Ischaemic heart disease	16/81 (19.75%)	2/14 (14.29%)	11/26 (42.31%)	3/41 (7.32%)
Hypertension	31/81 (38.27%)	3/14 (21.43%)	12/26 (46.15%)	16/41 (39.02%)
COPD	13/81 (16.05%)	3/14 (21.43%)	8/26 (30.77%)	2/41 (4.88%)
Asthma	28/81 (34.57%)	6/14 (42.86%)	8/26 (30.77%)	14/41 (34.15%)
Malignancy	5/81	0/14	3/26	2/41
ACUTE ADMISSION				
Differential blood counts on acute admission (x10^9/L)				
Total white cell count	7.3 (5.75 - 10.1)[10]	5.95 (4.7 - 7.2)[2]	6.65 (5.63 - 9.55)[6]	8.7 (6.8 - 11.35)[2]
Lymphocytes	0.88 (0.69 - 1.19)[10]	1.08 (0.86 - 1.54)[2]	0.98 (0.73 - 1.42)[6]	0.8 (0.62 - 0.95)[2]
Neutrophils	6.1 (4.12 - 8.8)[10]	4.02 (3.59 - 5.8)[2]	4.81 (4.04 - 7.68)[6]	7.03 (5.34 - 10.2)[2]
Monocytes	0.4 (0.26 - 0.55)[10]	0.26 (0.22 - 0.44)[2]	0.48 (0.3 - 0.6)[6]	0.4 (0.3 - 0.52)[2]
Other inpatient investigations				
Positive SARS CoV2 test	76/81 (93.8%)	14/14 (100%)	24/26 (92.3%)	38/41 (92.7%)
Highest CRP (mg/L)	135 (70 - 252.5)[3]	51 (31.3 - 94.8)	113 (68 - 147)[1]	256 (131 - 330)[2]
Chest imaging				

Bilateral opacification	58/63 (92.1%)	6/8 (75%)	21/23 (91.3%)	31/32 (96.9%)
Unilateral opacification	4/63 (6.3%)	1/8 (12.5%)	2/23 (8.7%)	1/32 (3.1%)
Clear	1/63 (1.6%)	1/8 (12.5%)	0/23 (0%)	0/32 (0%)
Outcome				
Length of stay (days)	11 (6 - 21)	2.5 (1.25 - 5.75)	6.5 (4.25 - 12.5)	20 (13 - 39)
CONVALESCENCE				
Symptoms and investigations at follow up				
Dyspnoea	37/80 (46.25%)	5/14 (35.71%)	16/26 (61.54%)	16/40 (40%)
Resolved CXR	53/81 (65.4%)	11/14 (78.6%)	18/26 (69.2%)	24/41 (58.5%)
Persistent CXR features	28/81 (34.6%)	3/14 (21.4%)	8/26 (30.8%)	17/41 (41.5%)

Supplemental Table 4. 3: Patient categorisation Information

Criteria for patient stratification. NIV, non-invasive ventilation; CPAP, continuous positive airway pressure; ICU, intensive care.

<u>Severity Score</u>	<u>Criteria</u>
Mild	- <3l or 28% supplemental oxygen required to maintain oxygen saturations. - Managed in a ward based environment.
Moderate	- Breathless - <10l or <60% supplemental oxygen required to maintain oxygen saturations. - Managed in a ward based environment. - Chronic NIV or CPAP (home use) or acute NIV for COPD.
Severe	Any of: - >10l or 60% supplemental oxygen required to maintain oxygen saturations.

- Use of acute NIV (not for COPD)
- Managed in ICU/invasive ventilation.
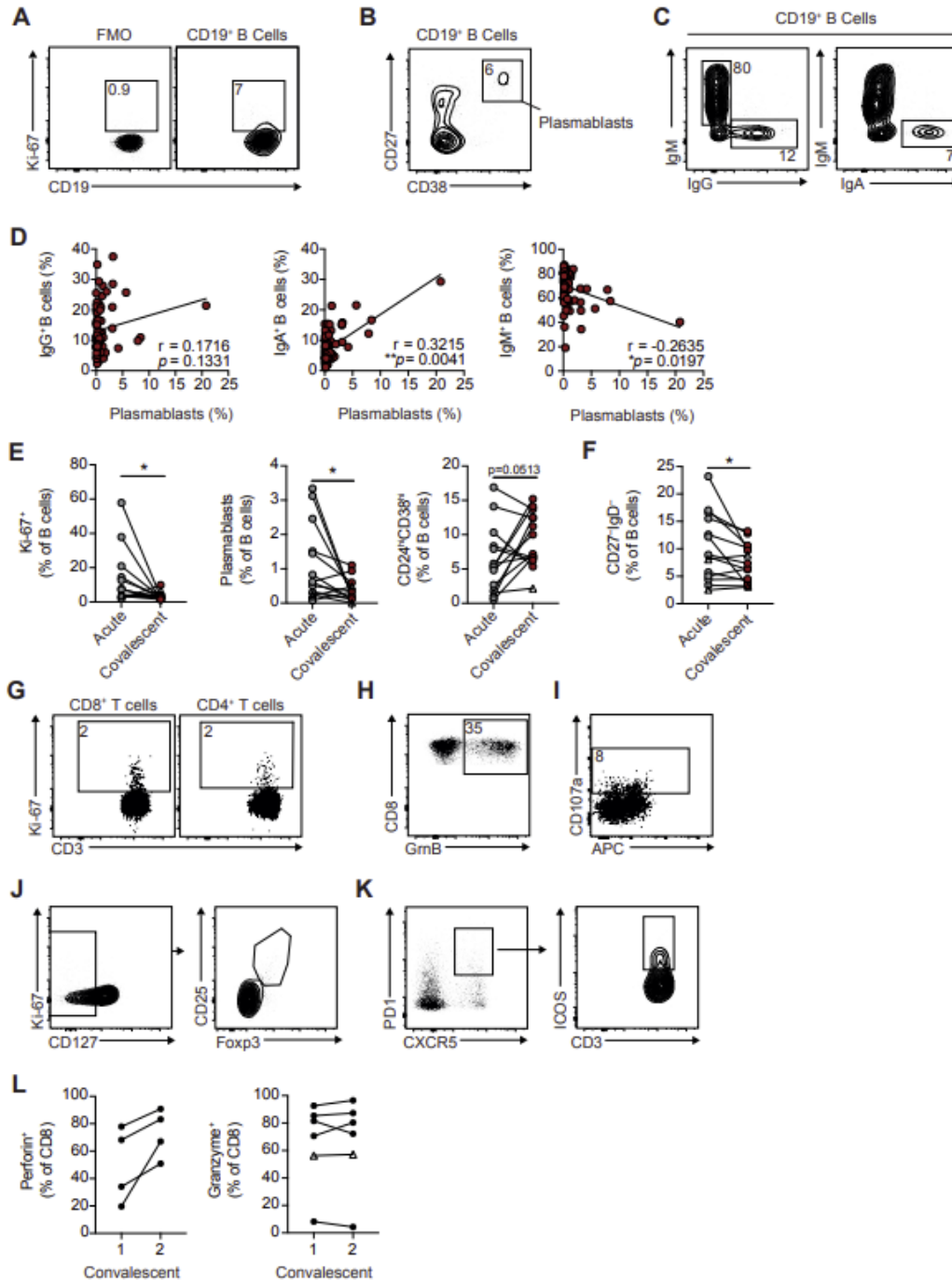
Supplemental Figure 4. 1: T and B cell subsets in hospitalized COVID-19 patients

(A) Representative FACS plots showing Ki-67 staining on $CD19^+$ B cells. **(B)** Representative FACS plots showing the gating strategy for $CD27^{hi}CD38^{hi}$ plasmablasts. **(C)** Representative FACS plots gated on $CD19^+$ B cells staining positive for IgG, IgM or IgA. **(D)** Graphs showing correlation between plasmablasts and IgG^+ (left), IgA^+ (middle) or IgM^+ (right) B cell frequencies in convalescent COVID-19 patients (n=78) . **(E,F)** Graphs track frequencies of **(E)** $Ki67^+$ B cells, plasmablasts, transitional ($CD24^{hi}CD38^{hi}$) B cells, and **(F)** $CD27^-IgD^-$ B cells in the same COVID-19 patient at acute (grey circles) and convalescent (maroon circles) time-points (n=14). (**G**) Representative FACS plots showing Ki-67 staining on $CD4^+$ and $CD8^+$ T cells. **(H,I)** Representative FACS plots showing $CD8^+$ T cells staining positive for **(H)** GranzymeB and **(I)** CD107a. **(J)** Representative FACS plots gated on $CD3^+CD4^+CD127^{lo/neg}$ T cells staining positive for CD25 and foxp3. **(K)** Representative FACS plots showing gating to identify Tfh cells ($CD3^+CD4^+PD- 1^+CXCR5^+ ICOS^+$). **(L)** Graphs track frequencies of $CD8^+$ T cells which are $perforin^+$ and $granzymeB^+$ in the same COVID-19 patient at convalescent time-points pre (1) and post (2) 6 months since hospital discharge (n=4-6).
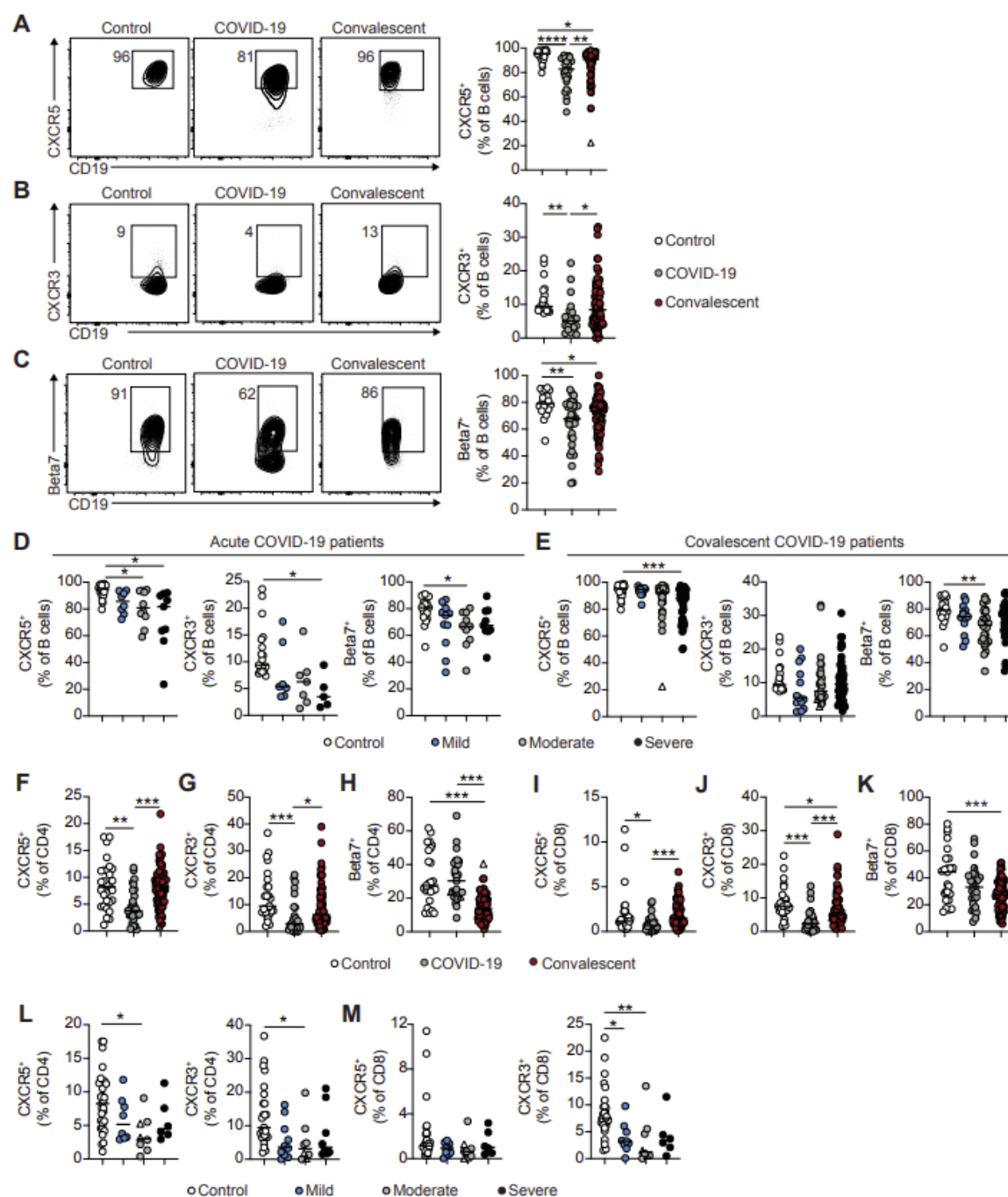
Supplemental Figure 4. 2: Altered expression of migratory markers in acute but not convalescent COVID-19 patients

(A-C) Representative flow cytometry plots and graphs showing frequencies of B cells expressing (A) CXCR5, (B) CXCR3 and (C) β7 in healthy individuals (n=19-21), acute (n=21-34) and

convalescent (n=81) COVID-19 patients. **(D)** Graphs showing frequencies of B cells expressing CXCR3, CXCR5 and β7 in healthy individuals (n=19) and acute COVID-19 patients with mild (n=7-11), moderate (n=7-10) and severe (n=5-9) disease. **(E)** Graphs showing frequencies of B cells staining positive for CXCR3, CXCR5 and β7 in healthy individuals (n=19-21) and convalescent COVID-19 patients which initially presented with mild (n=13), moderate (n=26) and severe (n=41) disease. **(F-H)** Graphs showing frequencies of CD4+ cells positive for **(F)** CXCR5, **(G)** CXCR3 and **(H)** β7 in healthy individuals (n=25-29), acute (n=26-27) and convalescent (n=80-83) COVID-19 patients. **(I-K)** Graphs showing frequencies of CD8+ cells positive for **(I)** CXCR5, **(J)** CXCR3 and **(K)** β7 in healthy individuals (n=25-29), acute (n=27-28) and convalescent (n=80-81) COVID-19 patients. **(L,M)** Graphs showing frequencies of **(L)** CD4+ and **(M)** CD8+ T cells staining positive for CXCR3 and CXCR5 in healthy individuals (n=25-29) and acute COVID-19 patients with mild (n=8-10), moderate (n=8) and severe (n=6-8) disease. Graphs show individual patient data, with the bar representing median values. In all graphs, open triangles represent SARS-CoV-2 PCR-negative patients. *p<0.05, **p<0.01, ***p<0.001, ****p<0.0001, one-way ANOVA with Holm-Sidak post-hoc testing (A-E, K and L (CXCR5)) or Kruskal-Wallis test with Dunn's post-hoc testing (F-J, L(CXCR3), M) for multiple comparisons.

162
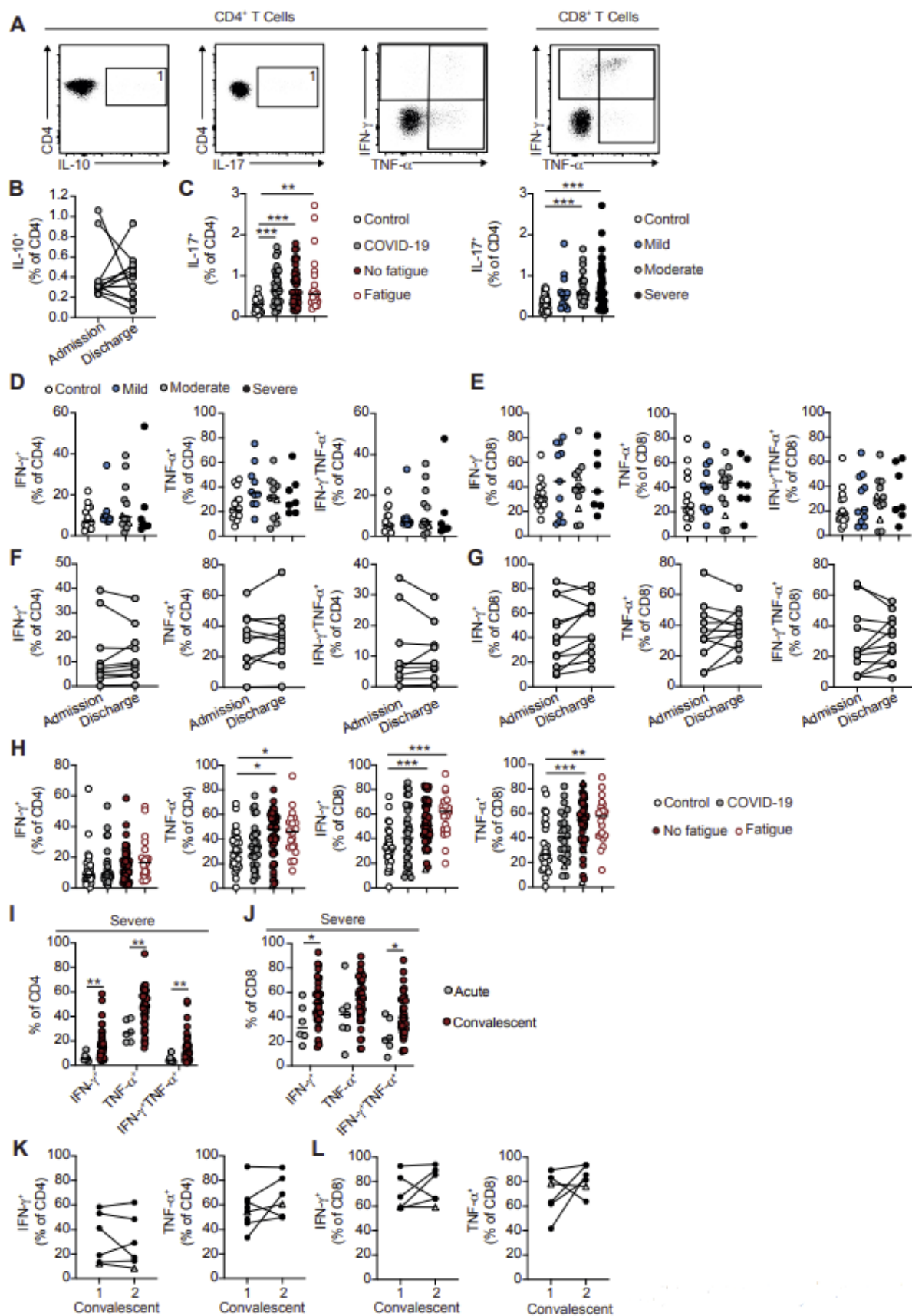
Supplemental Figure 4. 3: Long-lasting changes in type-I cytokine production T cells in convalescent COVID-19 patients

(A) Representative FACS plots showing example staining for cytokine$^+$ CD4$^+$ and CD8$^+$ T cells. **(B)** Graph shows frequency of IL-10$^+$CD4$^+$ T cells following 3 hour stimulation with PMA and ionomycin in acute COVID-19 patients at the first and last time points of hospitalization. **(C)** Graph show frequencies of IL-17$^+$CD4$^+$ T cells following 3 hour stimulation with PMA and ionomycin in healthy individuals (n=22-30), acute COVID-19 patients (n=31) and convalescent COVID-19 patients stratified by fatigue reporting (not reporting (n=50) and reporting (n=20) enhanced fatigue) and mild (n=14), moderate (n=27) and severe (n=36) acute disease severity. **(D, E)** Graphs show frequencies of (**D**) CD4$^+$ and (**E**) CD8$^+$ T cells which stain positive for IFNγ and TNFα following 3 hour stimulation with PMA and ionomycin in healthy individuals (n=14) and acute COVID-19 patients with mild (n=10-11), moderate (n=12) and severe (n=7) disease. (**F, G**) Graphs show frequencies of **(F)** CD4$^+$ and **(G)** CD8$^+$ T cells that stain positive for IFNγ and TNFα following 3 hour stimulation with PMA and ionomycin in acute COVID-19 patients at the first and last time points of hospitalization. **(H)** Graphs show frequencies of CD4$^+$ and CD8$^+$ T cells which stain positive for IFNγ and TNFα following 3 hour stimulation with PMA and ionomycin in healthy individuals (n=28-30), acute COVID-19 patients (n=24-33) and convalescent COVID-19 patients not reporting (n=44-49) and reporting (n=20-21) enhanced fatigue. **(I, J)** Graphs show frequencies of CD4$^+$ and CD8$^+$ T cells which stain positive for IFNγ and TNFα in all severe COVID-19 patients at acute (grey) and convalescent (maroon) time-points. **(K, L)** Graphs track frequencies of CD4$^+$ and CD8$^+$ T cells which stain positive for IFNγ and TNFα following 3 hour stimulation with PMA and ionomycin in the same COVID-19 patient at convalescent time-points pre (1) and post (2) 6 months since hospital discharge (n=4-6). Graphs show individual patient data, with the bar representing median values. In all graphs, open triangles represent SARS-CoV-2 PCR-negative patients. *$p<0.05$, **$p<0.01$, ***$p<0.001$, one-way ANOVA with Kruskal-Wallis test with Dunn's post-hoc testing for multiple comparisons (except for graphs showing CD4$^+$TNFα^+ and CD8$^+$TNFα^+ T cells in D and E where One-way ANOVA with Holm-Sidak post-hoc test was employed).
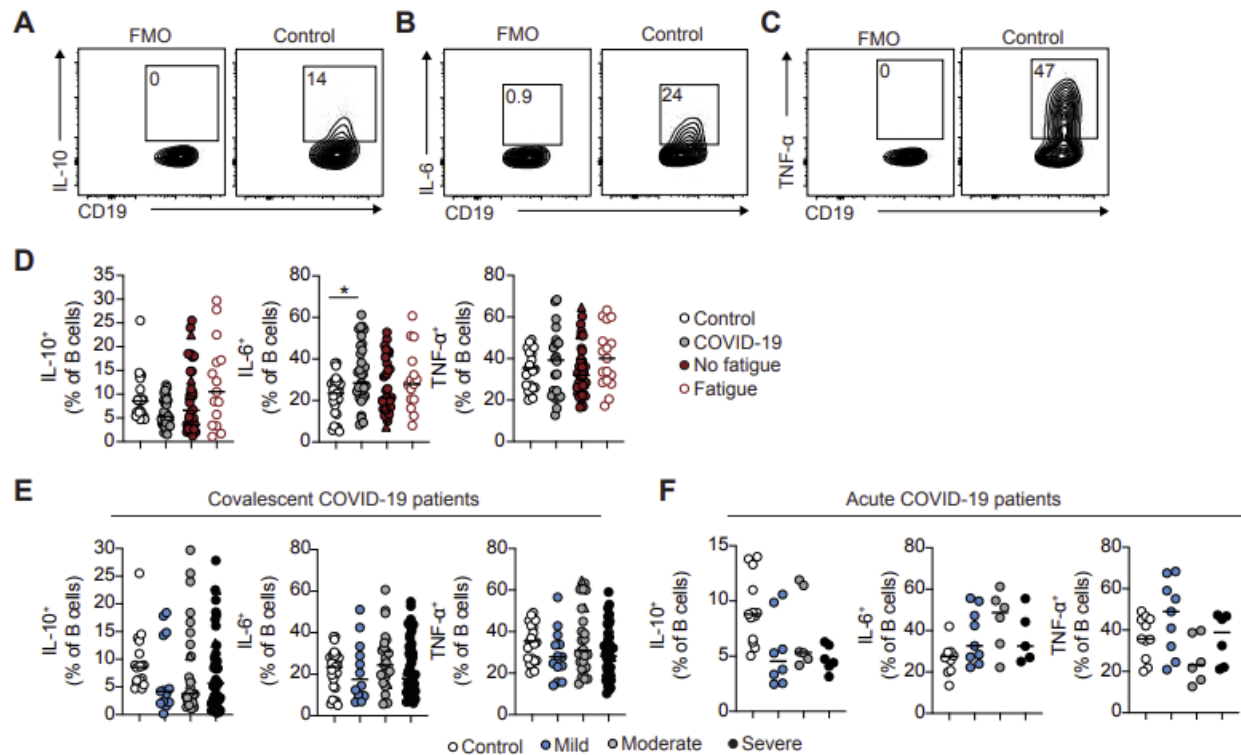
Supplemental Figure 4.4: Cytokine production by B cells from acute and convalescent COVID-19 patients

(A-C) Representative flow cytometry plots showing gating strategy of CD19^{+} B cells positive for IL-10, IL-6 and TNFα following 48 hour stimulation with CpGB. **(D)** Graphs show frequencies of CD19^{+} B cells staining positive IL-10, IL-6 and TNFα following 48 hour stimulation with CpGC in healthy individuals (n=22-27), acute COVID-19 patients (n=22-37) and convalescent COVID-19 patients not reporting (n=36-38) and reporting (n=15-17) enhanced fatigue. **(E)** Graphs show frequencies CD19^{+} B cells staining positive for IL-10, IL-6 and TNFα in healthy individuals (n=22-23), and convalescent COVID-19 patients which initially presented with mild (n=12-13), moderate (n=25-26) and severe (n=41) disease. **(F)** Graphs show frequencies CD19^{+} B cells staining positive for IL-10, IL-6 and TNFα in healthy individuals (n=11-13), and acute COVID-19 patients with mild (n=8-9), moderate (n=6) and severe (n=6) disease. Graphs show individual patient data, with the bar representing median values. In all graphs, open triangles represent SARS-CoV-2 PCR-negative patients. *p<0.05, one-way ANOVA with Kruskal-Wallis test with Dunn's post-hoc testing for multiple comparisons.

Chapter 5:

Final Discussion

Unlike T cells and members of the innate immune system, the role of B cells in inflammation is relatively less appreciated. Once thought of as antibody factories, they also produce cytokines such as IL-6 and TNF-α [600], contributing significantly to the pathogenesis of many disease conditions. B cells are influenced by their microenvironment, just like T cells and macrophages, and so display aberrant phenotypes that are amenable to therapeutic modulation. In this thesis, the B cell responses in acute and chronic inflammatory conditions of the lung were studied, where very different B cell profiles between the two conditions were observed. This is likely due to the slowly progressive nature of chronic inflammation in COPD versus the acute inflammatory events of infection.

Furthermore, COPD is a more silent disease concerning immunity. In contrast, infection provides a precise target plus the inflammatory mediators released upon cell damage. COPD and infection share some immune commonalities. For example, IFN-γ is found in both disease conditions [601,602]. However, the kinetics in viral infection is faster and with greater amplitude than in COPD. Thus, though the cytokine environment affects local immune cells, so does its kinetics, amplitude and duration, which can mean the difference between immune activation versus exhaustion.

Overall the thesis has contributed new discoveries specific to COPD or infection or common to both as follows:

A) B cell profiles in the blood and lung are distinct

Most studies of B cells in COPD have focused on circulating B cells, with few examining in situ lung histologies. The access to fresh lung tissue and matched blood samples from patients has provided an opportunity to compare the phenotypic characteristics of B cells in tissue and circulation. We found increased numbers of B cells in the lung (especially in COPD) compared to the circulation. Most of the tissue-resident B cells are mature and activated PCs, DN and SM B cells with mostly switched Igs that are predominantly IgG in nature. This might be from prolonged inflammation due to the constant exposure to antigens from 1) auto-antigens consisting of smoke-induced neo-antigens consequential to the degradation products of extracellular matrix, 2) cigarette smoke components, and 3) microbial [603,604]. The circulating B cells, on the other hand,

consist primarily of naïve B cells with increased tissue trafficking that will allow for the recruitment of more B cells into the lung tissue to handle the ongoing inflammation.

B) Alterations in B cells in COPD

In this thesis, we performed a detailed characterisation of B cells in COPD lungs. We found expansion of more mature B cells and B cell-rich follicles in the COPD compared to control lungs. Accumulating B cells in the COPD lung can promote adaptive immunity, especially during acute exacerbation of COPD caused by chronic infections typically observed in COPD patients [605], hence could have protective features.

Increased percentage of B cells and B cell-rich follicles in COPD have been previously reported [418,421,606]. The increase in B cell frequency might be in response to the chronic inflammation within the COPD lung following excessive exposure to cigarette smoke. The presence of B cells might be important in regulating the ongoing immune responses within the COPD lung microenvironment. Interestingly, the B cells in COPD are mostly switched-memory and IgG+ B cells. This indicates that most of these cells are antigen-experienced and somatically hypermutated, probably due to their constant exposure to microbial, cigarette smoke and neo-antigens at the site of inflammation in COPD lungs [603,604].

B cells in COPD also have increased Ki67 and CXCR3 expression, signifying active proliferation and chemotaxis that probably help maintain the B cell follicles by recruiting other immune cells (like T cells, DCs, macrophages and neutrophils) to the site inflammation [607]. Furthermore, we show that B cells from COPD lung have increased double-negative memory B cells with increased expression of CD11c and Tbet; two of the most used markers in identifying or describing double-negative memory or atypical B cells. Since atypical B cells are almost always associated with autoimmune conditions, chronic infection and ageing, it is tempting to speculate that their presence in COPD lungs might contribute to the presence of auto-antibodies usually seen in COPD patients, especially those that frequently exacerbate upon infection. However, further studies are required to understand their role in COPD fully. Hence targeting these particular B cell subsets might be of therapeutic potential. Of note, previous studies have reported higher frequencies of DN B cell subsets in various immunodeficiencies and autoimmune conditions like systemic lupus erythematosus, rheumatoid arthritis, and chronic infections such as malaria and hepatitis C, and in older people [40,172,544–548].

Our findings also show a significant expansion of Tim-1^{+} and IL-10^{+} B cells in COPD compared to control lungs. Tim-1 contributes to Breg induction, expansion, and suppressor function by inducing IL-10^{+} Bregs [552]. Therefore, the presence of Tim-1^{+} and IL-10^{+} B cells in COPD indicates their potential regulatory effect within the lung microenvironment by suppressing the immune responses to chronic inflammation.

C) Alterations in B cells in COVID-19

The quality of the B cell response following an acute infection like SARS-CoV-2 determines the duration and breadth of protective immunity. Interestingly, we saw reduced frequencies of B cells, with a corresponding increase in Ki67^{+} B cells in the circulation of severe acute COVID-19 patients that normalised in convalescent patients. A reduction of B cells in the blood may reflect recruitment into the lung, which is reduced in inflammatory resolution, hence their return to higher levels. Alternatively, or in addition, B cell reduction in severe COVID-19 may be due to viral-induced immunosuppression or direct cytopathic effects of the virus.

Like COPD, we also saw increased double-negative memory B cells in severe COVID-19 patients' blood that persisted in convalescence. Several studies have reported a similar expansion of double-negative B cells in COVID-19 [608–612]. However, our knowledge regarding the role of these cells in COVID-19 disease is still minimal. A similar B cell phenotype is evident following influenza vaccination, HIV infection and malaria infection [173,613,614], and it could be suggested that these cells are part of the protective immune response. The same B cell phenotype is reported to be expanded in several autoimmune diseases like SLE and rheumatoid arthritis. Thus, double-negative memory B cells might be responsible for an elevated autoimmune response in COVID-19 patients. We also report a decreased frequency of transitional B cells in severe COVID-19 patients that are partly restored upon convalescence. Transitional B cells are precursors of Bregs and IL-10^{+} B cells. Their reduction in severe COVID-19 patients may therefore cause a loss of immunosuppressive Bregs and an expansion of effector B cells, similar to previous observations in chronic inflammatory diseases like SLE and rheumatoid arthritis [364,497,598]. In COPD, however, we saw an expansion of IL-10^{+} B cells, especially in severe COPD, suggesting increased immunosuppression by B cells in COPD lungs.

Severe acute COVID-19 disease is associated with expanded switched memory, IgG[+] and IgA^{+} B cells that are restored upon convalescence. Enhanced switch memory B cells correlate with decreased unswitched memory and naïve B cells. The increase in switched memory B cells may

167

reflect the generation of robust extrafollicular B cell responses that correlate with increased proinflammatory cytokines and antibodies observed in severely ill individuals. Also, the expansion of IgG[+] and IgA^{+} B cells in severe COVID-19 patients positively correlates to frequencies of plasmablast, suggesting the expansion of class-switched IgG and IgA antibodies in COVID-19 patients.

B and T cells have essential roles in the clearance of viral infection. The effector function of T cell subsets is determined by chemokines and cytokines secreted from antigen-presenting cells. In this thesis, we observed increased proliferation and degranulation (CD107a^{+} and Ki67^{+}GranzymeB^{+}) of cytotoxic CD8^{+} T cells in acute COVID-19 with a corresponding reduction in convalescent patients. CD8^{+} T cells are vital in controlling infection by directly killing virally infected cells and by cytokine production. We also show increased expansion of T follicular helper cells (Tfh) in acute COVID-19 patients that are reduced in convalescent patients. Tfh cells are critical in promoting the germinal reaction that drives cognate B cell differentiation for antibody production.

D) B cells location and structure of follicles in inflammation

In this thesis, we have identified B cell follicles positioned next to bronchioles embedded in an additional extracellular matrix by Hyperion imaging mass cytometry. The multiplex nature of this technique also allowed us to identify communication between B cells and macrophages. It is known that B cells accumulate early in COPD disease pathogenesis, either as individual cells or as organised follicles and self-maintain by the production of growth factors that drive macrophage activation (amongst other cells) [283]. B cell follicles take up a significant area of what should be airspaces. Though associated with the small airways, their positioning may be dictated by the type of blood vessels in that vicinity. Small airways are dominated by fine capillaries whose basement membrane is fused to that of the epithelial barrier to allow efficient gaseous exchange [615]. It is likely that B cells (and other immune cells) transmigration is not facilitated in the more delicate capillaries where relatively flat endothelium exists, compared to the larger bronchioles. Examining this would require examining the integrins and chemokine receptors on the alveoli and bronchiole vasculature.

Such a comparison has not been performed to date. However, it would be advantageous for lung function to exclude follicle development in the delicate structures of the terminal airways. What is also unknown is the influence of B cell follicles on lung function and its physical properties [334].

Lung compliance, peak expiratory flow, and elasticity will likely change if organised lymphoid tissue is present. This is difficult to test in patients unless they are on B cell-depleting therapies for other indications, such as arthritis or B cell lymphoma. However, no investigations have been published examining this, though studies may be forthcoming in the future with the current interest in multi-morbidity. B cell knock-out mice would be an option though models of COPD are poor in this species. In any system where B cells are absent, consideration should be given to indirect influences, for example, by T cells. Clearly, B cell phenotype is important, but positioning is too and may be amenable to manipulation.

E) Effect of smoking on B cell phenotype and function

In addition to more B cell follicles in COPD versus healthy lungs, we also saw alterations to this immune compartment in patients who smoked versus those that did not, irrespective of their disease condition. This included an expansion of plasma cells, IgG[+], double-negative, Tim-1^{+} and IL-10^{+} B cells within the COPD current smokers' lung. Very little information is available on the influence of smoking on lung B cells [616]. Two studies imply that cigarette smoking increases the prevalence of class-switched memory B cells in peripheral blood and memory IgG^{+} B cells in the lung [550,617]. Double-negative B cells are also raised in NSCLC and correlate with improved survival [618]. Lung transcriptomes of COPD patients with emphysema show an mRNA signature associated with B cell homing and activation and the presence of lymphoid follicles with activated B cells and class-switched B cells (IgG[+]) [419]. Generally, studies are in agreement, though comparison with non-smokers' lungs is rare. To our knowledge, an upregulation of Tim1 and IL-10 by B cells in smokers' lungs has not been described.

F) Reduction of IL-10-producing B cells in convalescent COVID

Longitudinal analysis showed that in one group of patients with persistent disease indicative of long COVID, IL-10-expressing B cells (Bregs) failed to recover. Conversely, B cell production of IL-10 was higher in convalescent patients with good clinical outcomes. The lack of Bregs in the persistent disease group is not likely to reflect different disease stages as patients were aligned based on their reported onset of symptoms. However, it is not certain that recollection of disease onset was accurate in every case. Significant decreases in transitional B cells, the precursors of human Bregs [364], were also observed, reflecting their rapid differentiation into APCs. However, further studies would be required to address this. It should also be remembered that we only had access to peripheral blood. It is possible that a deficit in the blood could reflect increased

recruitment to the lung. Also, if IL-10-producing B cells were present in the lung, then they may contribute to a deleterious fibrotic response, as has been observed in some postmortem specimens [619]. Our current hypothesis, however, is that a reduction in IL-10-producing B cells is associated with an inflammatory B cell phenotype that feeds the disease process. More studies on lung samples themselves are required, though the only source to date seems to be from autopsy [620]. Transbronchial cryobiopsy has been performed on an isolated patient, though concern over the generation of aerosols has restricted its application [621,622].

G) B cell plasticity and not just inhibitors of inflammation

B cells are likely to play pleitropic roles in the lung, including immune suppression, secretion of pro-inflammatory cytokines like IL-6 and TNF-α, production of antibodies and auto-antibodies and antigen presentation.

Unlike T cells, B cell subsets are less well-defined, and no transcription factors are currently associated with different functions. Depending on the microenvironmental stimuli, B cells can differentiate into diverse subsets and secrete inflammatory or anti-inflammatory mediators to modulate various disease settings. Previous studies have shown that IL-10-producing Bregs are not in a terminally differentiated state and that they can further differentiate into antibody-producing plasmablasts [336,497]. This indicates plasticity to some extent, though its extent is currently unclear.

H) Key pathways from scRNA sequencing

Differentially expressed genes of Plasma cells from COPD lung show activation of the HIF-1α pathway influencing IL-10 gene signalling, probably due to hypoxia. HIF-1α is a transcription factor that targets genes under hypoxic conditions [623]. Oxidative stress and inflammation are essential in COPD pathogenesis [624]. Studies have reported that HIF-1α significantly promotes inflammation, emphysema and airway goblet cell hyperplasia in COPD [535(p1),625,626]. The increased activation of the RELA pathway in COPD ensures proper formation and maintenance of GCs since RELA is a critical component of NF-κB pathway [627]. At the same time, activation of the p38 MAPK pathway in COPD maintains B cell activation, proliferation and survival in COPD lung. Combined, increased activities from these pathways signify active B cell involvement in the pathophysiology of COPD.

Furthermore, RNA sequencing data suggest that B cell function may be altered in COPD. Though requiring further study, down-regulated genes imply reduced T cell help. For example, ICOS ligand gene (ICOSLG) is reduced in COPD B cells. ICOS ligand is required to prevent antigen-activated T cells undergoing activation-induced apoptosis [527,628]. And its downregulation might suggest impaired B-T cell interaction in COPD that might lead to increased susceptibility to infection typically observed in COPD patients. To our knowledge, there is no data showing downregulation of ICOS ligands in B cells from COPD lung. However, gene expression analysis of PBMCs from COPD patients shows decreased gene expression in ICOS-ICOS ligand signalling in T helper cell pathway, suggesting impaired T cell response in COPD [629].

Recruitment of cells responding to CCL4 and 22 is also reduced. These chemokines recruit regulatory T cells and follicular helper T cells [528,529], implying that though B cell follicles are increased in COPD, they may lack specific activities due to reduced recruitment of other cells.

A number of interesting genes were up-regulated in COPD B cells that warrant further study. For example, upregulation of MMP19 by B cells in COPD was intriguing. MMP19 (also known as gelatinase-B) is up-regulated in activated B cells from MS patients [630], where it disrupts the blood-brain barrier and degrades myelin basic protein, worsening MS [631,632]. To our knowledge, upregulation of MM19 in B cells in the lung has not been previously reported. Thus, MMP19 expression in B cells in COPD lungs might indicate their involvement in lung repair, or they might contribute to the worsening of COPD by contributing to autoimmunity. Additional studies are needed to better understand B cells' contribution to COPD pathology.

I) Challenges and future perspectives

A complete understanding of disease pathogenesis requires analysis of the affected tissue. However, most studies on humans rely on peripheral blood. Some have suggested that examining what is missing from the blood is more appropriate for studying lung disease than what is elevated. A reduction in a particular blood population may, for example, reflect their migration into the damaged lung. We cannot rule out this influence, but in the case of COVID, lymphopenia was observed in both blood and lung. Some observed aspects may tally, whereas others may not. We were, therefore, lucky to have a reliable method of obtaining lung margins from cancer resections. However, this raises another potential confounder – are the healthy margins of the lung in cancer really healthy? We did not address this issue in this thesis. However, we could argue that all samples were from cancer resection material. Yet, we still observed B cell changes in COPD and smoking.

171

Furthermore, another PhD student in the lab has compared cancer regions with uninvolved healthy margins and does observe significant differences. A more appropriate source of lung tissue would be from transplant material – specifically, healthy lungs not suitable for transplant. This tissue is extremely rare though we have begun to receive fibrotic lungs removed from patients with idiopathic pulmonary fibrosis.

In this thesis, we have examined B cells in isolation. However, B cells are often in contact with other cells, so any changes in B cells may be due to the interacting cells. It is important to note that when analysing cells by flow cytometry, doublets are excluded to prevent erroneous assumptions of protein co-expression when in fact, the signal is due to two cells joined together. The exclusion of doublets may miss a critical pathogenic event. This came to light during the immune analysis of blood from COVID-19 patients, where monocytes interacting with neutrophils dominated. Cellular interaction in the bloodstream is likely undesirable as they would occlude blood vessels and produce inflammatory molecules that could act systemically. It would be of interest to revisit archived data from this thesis to see if B cells are also present in the doublet gate by flow cytometry. RNA scope could also be used to probe the transcriptomics of interacting cells. Though our emphasis is on B cells, it is worth remembering that receptor-ligand pairs cause signaling to both cells. Therefore, it would be of interest in the future to examine the impact of B cell cognate interactions on the non-B cell partner.

In COVID-19 disease, we were fortunate to do a longitudinal study that clearly shows how disease trajectory is associated with changes in immune cell profile. This should be performed for COPD, though defining onset is trickier for a chronic disease compared to a viral infection. The longevity of this disease has precluded this analysis to date. Mouse models would enable onset to be determined, but those for COPD are highly criticized as the duration of exposure to tobacco smoke is short, and delivery of smoke-induced enzymes, e.g. elastase, is very harsh. Furthermore, mouse models of COVID-19 disease require category III facilities currently unavailable at Manchester. Overall new discoveries have been made, but future studies should define contribution to pathology by examining O_2/CO_2 exchange and plethysmography to define lung function in mice lacking specific subsets of B cells as global B cell deletion may perturb many systems in health and disease.

References

1. Ichii M, Oritani K, Kanakura Y. Early B lymphocyte development: Similarities and differences in human and mouse. *World J Stem Cells*. 2014;6(4):421-431. doi:10.4252/wjsc.v6.i4.421

2. Ryan DH, Nuccie BL, Abboud CN, Winslow JM. Vascular cell adhesion molecule-1 and the integrin VLA-4 mediate adhesion of human B cell precursors to cultured bone marrow adherent cells. *J Clin Invest*. 1991;88(3):995-1004. doi:10.1172/JCI115403

3. Clark MR, Mandal M, Ochiai K, Singh H. Orchestrating B cell lymphopoiesis through interplay of IL-7 receptor and pre-B cell receptor signalling. *Nat Rev Immunol*. 2014;14(2):69-80. doi:10.1038/nri3570

4. Nodland SE, Berkowska MA, Bajer AA, et al. IL-7R expression and IL-7 signaling confer a distinct phenotype on developing human B-lineage cells. *Blood*. 2011;118(8):2116-2127. doi:10.1182/blood-2010-08-302513

5. Baizan-Edge A, Stubbs BA, Stubbington MJT, et al. IL-7R signaling activates widespread VH and DH gene usage to drive antibody diversity in bone marrow B cells. *Cell Reports*. 2021;36(2):109349. doi:10.1016/j.celrep.2021.109349

6. Döbbeling U. The influence of IL-7 V(D)J recombination. *Immunology*. 1996;89(4):569-572. doi:10.1046/j.1365-2567.1996.d01-770.x

7. Henderson A, Calame K. TRANSCRIPTIONAL REGULATION DURING B CELL DEVELOPMENT. *Annu Rev Immunol*. 1998;16(1):163-200. doi:10.1146/annurev.immunol.16.1.163

8. Meng W, Yunk L, Wang LS, et al. Selection of individual VH genes occurs at the pro-B to pre-B cell transition. *J Immunol*. 2011;187(4):1835-1844. doi:10.4049/jimmunol.1100207

9. LeBien TW, Tedder TF. B lymphocytes: how they develop and function. *Blood*. 2008;112(5):1570-1580. doi:10.1182/blood-2008-02-078071

10. Willard-Mack CL. Normal Structure, Function, and Histology of Lymph Nodes. *Toxicol Pathol*. 2006;34(5):409-424. doi:10.1080/01926230600867727

11. Liao W, Hua Z, Liu C, Lin L, Chen R, Hou B. Characterization of T-Dependent and T-Independent B Cell Responses to a Virus-like Particle. *JI*. 2017;198(10):3846-3856. doi:10.4049/jimmunol.1601852

12. Defrance T TM. Genestier L. T cell-independent B cell memory. *Current Opinion in Immunology*. 2011;23:330-336.

13. DeFranco AL, Rookhuizen DC, Hou B. Contribution of Toll-like receptor signaling to germinal center antibody responses. *Immunol Rev*. 2012;247(1):64-72. doi:10.1111/j.1600-065X.2012.01115.x

14. Rawlings DJ, Schwartz MA, Jackson SW, Meyer-Bahlburg A. Integration of B cell responses through Toll-like receptors and antigen receptors. *Nat Rev Immunol*. 2012;12(4):282-294. doi:10.1038/nri3190

15. Zhang J, Liu YJ, MacLennan IC, Gray D, Lane PJ. B cell memory to thymus-independent antigens type 1 and type 2: the role of lipopolysaccharide in B memory induction. *Eur J Immunol*. 1988;18(9):1417-1424. doi:10.1002/eji.1830180918

16. Miles K, Heaney J, Sibinska Z, Salter D, Savill J, Gray D. A tolerogenic role for toll-like receptor 9 is revealed by B-cell interaction with DNA complexes expressed on apoptotic cells. *Proc Natl Acad Sci USA*. 2012;109(3):887-892.

17. Crotty S. T follicular helper cell differentiation, function, and roles in disease. *Immunity*. 2014;41(4):529-542. doi:10.1016/j.immuni.2014.10.004

18. Parker DC. T cell-dependent B cell activation. *Annu Rev Immunol*. 1993;11:331-360. doi:10.1146/annurev.iy.11.040193.001555

19. Foy TM, Laman JD, Ledbetter JA, Aruffo A, Claassen E, Noelle RJ. gp39-CD40 interactions are essential for germinal center formation and the development of B cell memory. *J Exp Med*. 1994;180(1):157-163. doi:10.1084/jem.180.1.157

20. Kawabe T, Naka T, Yoshida K, et al. The immune responses in CD40-deficient mice: impaired immunoglobulin class switching and germinal center formation. *Immunity*. 1994;1(3):167-178. doi:10.1016/1074-7613(94)90095-7

21. Crotty S. A brief history of T cell help to B cells. *Nat Rev Immunol*. 2015;15(3):185-189. doi:10.1038/nri3803

22. Cyster JG, Allen CDC. B Cell Responses: Cell Interaction Dynamics and Decisions. *Cell*. 2019;177(3):524-540. doi:10.1016/j.cell.2019.03.016

23. Junttila IS. Tuning the Cytokine Responses: An Update on Interleukin (IL)-4 and IL-13 Receptor Complexes. *Front Immunol*. 2018;9:888. doi:10.3389/fimmu.2018.00888

24. Duperray C, Boiron JM, Boucheix C, et al. The CD24 antigen discriminates between pre-B and B cells in human bone marrow. *J Immunol*. 1990;145(11):3678-3683.

25. Palanichamy A, Bauer JW, Yalavarthi S, et al. Neutrophil-mediated IFN activation in the bone marrow alters B cell development in human and murine systemic lupus erythematosus. *J Immunol*. 2014;192(3):906-918. doi:10.4049/jimmunol.1302112

26. LeBien TW. Fates of human B-cell precursors. *Blood*. 2000;96(1):9-23.

27. Tangye SG, Liu YJ, Aversa G, Phillips JH, de Vries JE. Identification of functional human splenic memory B cells by expression of CD148 and CD27. *J Exp Med*. 1998;188(9):1691-1703. doi:10.1084/jem.188.9.1691

28. Avery DT, Ellyard JI, Mackay F, Corcoran LM, Hodgkin PD, Tangye SG. Increased expression of CD27 on activated human memory B cells correlates with their commitment to the plasma cell lineage. *J Immunol*. 2005;174(7):4034-4042. doi:10.4049/jimmunol.174.7.4034

29. Ehrhardt GRA, Hsu JT, Gartland L, et al. Expression of the immunoregulatory molecule FcRH4 defines a distinctive tissue-based population of memory B cells. *J Exp Med*. 2005;202(6):783-791. doi:10.1084/jem.20050879

30. Kaminski DA, Wei C, Qian Y, Rosenberg AF, Sanz I. Advances in human B cell phenotypic profiling. *Front Immunol*. 2012;3:302. doi:10.3389/fimmu.2012.00302

31. Cappione A, Anolik JH, Pugh-Bernard A, et al. Germinal center exclusion of autoreactive B cells is defective in human systemic lupus erythematosus. *J Clin Invest*. 2005;115(11):3205-3216. doi:10.1172/JCI24179

32. Wei C, Anolik J, Cappione A, et al. A new population of cells lacking expression of CD27 represents a notable component of the B cell memory compartment in systemic lupus erythematosus. *J Immunol*. 2007;178(10):6624-6633. doi:10.4049/jimmunol.178.10.6624

33. Palanichamy A, Barnard J, Zheng B, et al. Novel human transitional B cell populations revealed by B cell depletion therapy. *J Immunol*. 2009;182(10):5982-5993. doi:10.4049/jimmunol.0801859

34. Descatoire M, Weller S, Irtan S, et al. Identification of a human splenic marginal zone B cell precursor with NOTCH2-dependent differentiation properties. *J Exp Med*. 2014;211(5):987-1000. doi:10.1084/jem.20132203

35. Küppers R, Klein U, Hansmann ML, Rajewsky K. Cellular origin of human B-cell lymphomas. *N Engl J Med*. 1999;341(20):1520-1529. doi:10.1056/NEJM199911113412007

36. Di Sabatino A, Rosado MM, Ciccocioppo R, et al. Depletion of immunoglobulin M memory B cells is associated with splenic hypofunction in inflammatory bowel disease. *Am J Gastroenterol*. 2005;100(8):1788-1795. doi:10.1111/j.1572-0241.2005.41939.x

37. Berkowska MA, Driessen GJA, Bikos V, et al. Human memory B cells originate from three distinct germinal center-dependent and -independent maturation pathways. *Blood*. 2011;118(8):2150-2158. doi:10.1182/blood-2011-04-345579

38. Seifert M, Küppers R. Molecular footprints of a germinal center derivation of human IgM+(IgD+)CD27+ B cells and the dynamics of memory B cell generation. *J Exp Med*. 2009;206(12):2659-2669. doi:10.1084/jem.20091087

39. Weill JC, Weller S, Reynaud CA. Human marginal zone B cells. *Annu Rev Immunol*. 2009;27:267-285. doi:10.1146/annurev.immunol.021908.132607

40. Rakhmanov M, Keller B, Gutenberger S, et al. Circulating CD21low B cells in common variable immunodeficiency resemble tissue homing, innate-like B cells. *Proc Natl Acad Sci U S A*. 2009;106(32):13451-13456. doi:10.1073/pnas.0901984106

41. Falini B, Tiacci E, Pucciarini A, et al. Expression of the IRTA1 receptor identifies intraepithelial and subepithelial marginal zone B cells of the mucosa-associated lymphoid tissue (MALT). *Blood*. 2003;102(10):3684-3692. doi:10.1182/blood-2003-03-0750

42. Bohnhorst JØ, Bjørgan MB, Thoen JE, Natvig JB, Thompson KM. Bm1-Bm5 classification of peripheral blood B cells reveals circulating germinal center founder cells in healthy individuals and disturbance in the B cell subpopulations in patients with primary Sjögren's syndrome. *J Immunol*. 2001;167(7):3610-3618. doi:10.4049/jimmunol.167.7.3610

43. Sims GP, Ettinger R, Shirota Y, Yarboro CH, Illei GG, Lipsky PE. Identification and characterization of circulating human transitional B cells. *Blood*. 2005;105(11):4390-4398. doi:10.1182/blood-2004-11-4284

44. Pascual V, Liu YJ, Magalski A, de Bouteiller O, Banchereau J, Capra JD. Analysis of somatic mutation in five B cell subsets of human tonsil. *J Exp Med*. 1994;180(1):329-339. doi:10.1084/jem.180.1.329

45. I.E. Godin, J.A. Garcia-Porrero, A. Coutinho, F. Dieterlen-Lievre, M.A. Marcos. Para-aortic splanchnopleura from early mouse embryos contains B1a cell progenitors. *Nature*. 1993;22:67-70.

46. K. Hayakawa, R.R. Hardy, M. Honda, L.A. Herzenberg, A.D. Steinberg, Herzenberg LA. Ly-1, B Cells: functionally distinct lymphocytes that secrete IgM autoantibodies. *Proceedings of the National Academy of Sciences of the USA*. 1984;81:2494-2498.

47. R. Berland, H.H. Wortis. Origins and functions of B-1 cells with notes on the role of CD5,. *Annual Review of Immunology*. 2002;20:253-300.

48. Y.S. Choi, N. Baumgarth. Dual role for B-1a cells in immunity to influenza virus infection. *Journal of Eperimental Medicine*. 2008;205:3053-3064.

49. M. Yoshimoto, E. Montecino-Rodriguez, M.J. Ferkowicz PP, W.C. Shelley, S.J. Conway et al. Embryonic day 9 yolk sac and intra-embryonic hemogenic endothelium independently generate a B-1 and marginal zone progenitor lacking B-2 potential. *Proceedings of the National Academy of Sciences of the USA*. 2011;108:1468-1473.

50. S. Casola, K.L. Otipoby, M. Alimzhanov, S. Humme, N. Uyttersprot JLK, et al. B cell receptor signal strength determines B cell fate,. *Nature Immunology*. 2004;5:317-327.

51. F. Martin, A.M. Oliver JFK. Marginal zone and B1 B cells unite in the early response against T-independent blood-borne particulate antigens. *Immunity*. 14:617-629.

52. H. Song, J. Cerny. Functional heterogeneity of marginal zone B cells revealed by their ability to generate both early antibody-forming cells and germinal centers with

hypermutation and memory in response to a T-dependent antigen. *Journal of Eperimental Medicine*. 2003;198:1923-1935.

53. A. Cerutti, M. Cols, I. Puga. Marginal zone B cells: virtues of innate-like antibodyproducing lymphocytes. *Nature Reviews Immunology*. 2013;13:118-132.

54. N. Baumgarth. The double life of a B-1 cell: self-reactivity selects for protective effector functions,. *Nature Reviews Immunology*. 2011;11:34-46.

55. E. Montecino-Rodriguez KDorshkind. New perspectives in B-1 B cell development and function. *Trends in Immunology*. 2006;27:428-433.

56. Y.Y. Wu, I. Georg, A. Diaz-Barreiro, N. Varela, B. Lauwerys, R. Kumar, et al. Concordance of increased B1 cell subset and lupus phenotypes in mice and humans is dependent on BLK expression levels. *Journal of Immunology*. 2015;194:5692-5702.

57. Y. Yang, J.W. Tung, E.E. Ghosn, L.A. Herzenberg, L.A. Herzenberg. Division and differentiation of natural antibody-producing cells in mouse spleen,. *Proceedings of the National Academy of Sciences of the USA*. 2007;104:4542-4546.

58. F.G. Kroese, E.C. Butcher, A.M. Stall, P.A. Lalor, S. Adams, L.A. Herzenberg. Many of the IgA producing plasma cells in murine gut are derived from self-replenishing precursors in the peritoneal cavity. *International Journal of Immunology*. 1989;1:75-84.

59. D.A. Kaminski, J. Stavnezer. Enhanced IgA class switching in marginal zone and B1 B cells relative to follicular/B2 B cells,. *Journal of Immunology*. 2006;177:6025-6029.

60. D.M. Tarlinton, M. McLean, G.J. Nossal. B1 and B2 cells differ in their potential to switch immunoglobulin isotype. *European Journal of Immunology*. 1995;25:3388-3398.

61. Montecino-Rodriguez E, Dorshkind K. B-1 B cell development in the fetus and adult. *Immunity*. 2012;36(1):13-21. doi:10.1016/j.immuni.2011.11.017

62. K. Hayakawa, C.E. Carmack, R. Hyman, R.R. Hardy. Natural autoantibodies to thymocytes: origin, VH genes, fine specificities, and the role of Thy-1 glycoprotein,. *Journal of Eperimental Medicine*. 1990;172:869-878.

63. K. Hayakawa, R.R. Hardy, D.R. Parks LAH. The, Ly-1 B cell subpopulation in normal immunodefective, and autoimmune mice. *Journal of Eperimental Medicine*. 1983;157:202-218.

64. R.R. Hardy, C.E. Carmack, S.A. Shinton, R.J. Riblet, K. Hayakawa. A single VH gene is utilized predominantly in anti-BrMRBC hybridomas derived from purified Ly-1 B cells. Definition of the VH11 family,. *Journal of Immunology*. 1989;142:3643-3651.

65. A.M. Stall, S. Adams, L.A. Herzenberg, A.B. Kantor. Characteristics and development of the murine B-1b (Ly-1 B sister) cell population. *Annals of the New York Academy of Science*. 1992;651:33-43.

66. J.W. Tung, D.R. Parks, W.A. Moore, L.A. Herzenberg, L.A. Herzenberg. Identification of B-cell subsets: an exposition of 11-color (Hi-D) FACS methods. *Methods of Molecular Biology*. 2004;271:37-58.

67. L.A. Herzenberg, A.M. Stall, J. Braun, D. Weaver, D. Baltimore LAH, et al. Depletion of the predominant B-cell population in immunoglobulin mu heavy-chain transgenic mice,. *Nature*. 1987;329:71-73.

68. K. Yanaba, J.D. Bouaziz, T. Matsushita, T. Tsubata, T.F. Tedder. The development and function of regulatory B cells expressing IL-10 (B10 cells) requires antigen receptor diversity and TLR signals. *Journal of Immunology*. 2009;182:7459-7472.

69. P. Casali, S.E. Burastero, M. Nakamura, G. Inghirami, A.L. Notkins. Human lymphocytes making rheumatoid factor and antibody to ssDNA belong to Leu-1+ Bcell subset. *Science*. 1987;236:77-81.

70. A. Gagro, N. McCloskey, A. Challa, M. Holder, G. Grafton, J.D. Pound, et al. CD5- positive and CD5-negative human B cells converge to an indistinguishable population on signaling through B-cell receptors and CD40. *Immunology*. 2000;101:201-209.

71. R. Carsetti, M.M. Rosado, H. Wardmann. Peripheral development of B cells in mouse and man. *Immunology Reviews*. 2004;197:179-191.

72. A. Dalloul. CD5: a safeguard against autoimmunity and a shield for cancer cells,. *Autoimmunity Review*. 2009;8:349-353.

73. J. Lee, S. Kuchen, R. Fischer, S. Chang, P.E. Lipsky. Identification and characterization of a human CD5+ pre-naive B cell population. *Journal of Immunology*. 2009;182:4116-4126.

74. H. Gary-Gouy, J. Harriague, G. Bismuth, C. Platzer, C. Schmitt, A.H. Dalloul. Human CD5 promotes B-cell survival through stimulation of autocrine IL-10 production. *Blood*. 2002;100:4537-4543.

75. R.R. Hardy, K. Hayakawa, M. Shimizu, K. Yamasaki, T. Kishimoto. Rheumatoid factor secretion from human Leu-1+ B cells. *Science*. 1987;81-83.

76. P. Casali, A.L. Notkins. CD5+ B lymphocytes, polyreactive antibodies and the human B-cell repertoire. *Immunology Today*. 1989;10:364-368.

77. P. Youinou, C. Jamin, P.M. Lydyard. CD5 expression in human B-cell populations,. *Immunology Today*. 1999;20:312-316.

78. T.L. Rothstein, D.O. Griffin, N.E. Holodick, T.D. Quach, H. Kaku. Human B-1 cells take the stage,. *Annals of the New York Academy of Science*. 2013;1285:97-114.

79. Bronte V, Pittet MJ. The spleen in local and systemic regulation of immunity. *Immunity*. 2013;39(5):806-818. doi:10.1016/j.immuni.2013.10.010

80. Kraal G. Cells in the marginal zone of the spleen. *International Review of Cytology*. 1992;132:31-74.

81. Cyster JG. B cell follicles and antigen encounters of the third kind. *Nature Immunology*. 2010;11:989-996.

82. Koike R, Nishimura T, Yasumizu R, Tanaka H, Hataba Y H, Y et al. The splenic marginal zone is absent in alymphoplastic aly mutant mice. *European Journal of Immunology*. 1996;26:669-675.

83. Carsetti R, Kohler G LMC. Transitional B cells are the target of negative selection in the B cell compartment. *Journal of Eperimental Medicine*. 1995;181:2129-2140.

84. Allman DM, Ferguson SE, Lentz VM CMP. Peripheral B cell maturation. II. Heat-stable antigen(hi) splenic B cells are an immature developmental intermediate in the production of long-lived marrow-derived B cells. *Journal of Immunology*. 1993;151:4431-4444.

85. Loder F, Mutschler B, Ray RJ, Paige CJ, Sideras P, Torres R et al. B cell development in the spleen takes place in discrete steps and is determined by the quality of B cell receptor-derived signals. *Journal of Eperimental Medicine*. 1999;190:75-89.

86. Allman D, Lindsley RC, DeMuth W, Rudd K, Shinton SA H, RR. Resolution of three nonproliferative immature splenic B cell subsets reveals multiple selection points during peripheral B cell maturation. *Journal of Immunology*. 2001;167:6834-6840.

87. Su TT RDJ. Transitional B lymphocyte subsets operate as distinct checkpoints in murine splenic B cell development. *Journal of Immunology*. 2002;168:2101-2110.

88. Gaudin E, Rosado M, Agenes F, McLean A FAA. B-cell homeostasis, competition, resources, and positive selection by selfantigens. *Immunology Reviews*. 2004;197:102-115.

89. Hardy RR HK. Positive and negative selection of natural autoreactive B cells. *Advances in Experimental Medical Biology*. 2012;750:227-238.

90. Shlomchik MJ WF. Germinal center selection and the development of memory B and plasma cells. *Immunology Reviews*. 2012;247:52-63.

91. Okamoto M, Murakami M, Shimizu A, Ozaki S TT, Kumagai S et al. A transgenic model of autoimmune hemolytic anemia. *Journal of Eperimental Medicine*. 1992;175:71-79.

92. Shapiro-Shelef M CK. Regulation of plasma-cell development. *Nature Reviews Immunology*. Published online 2005:230-242.

93. King C. New insights into the differentiation and function of T follicular helper cells. *Nature Reviews Immunology*. 2009;9:757-766.

94. Ma CS, Deenick EK, Batten M TSG. The origins, function, and regulation of T follicular helper cells. *Journal of Eperimental Medicine*. 2012;209:1241-1253.

95. Cariappa A, Tang M, Parng C, Nebelitskiy E CM, Georgopoulos K et al. The follicular versus marginal zone B lymphocyte cell fate decision is regulated by Aiolos, Btk, and CD21. *Immunity*. 2001;14:603-615.

96. Pillai S, Cariappa A M ST. Marginal zone B cells. *Annual Review of Immunology*. 2005;23:161-196.

97. Lopes-Carvalho T KJF. Development and selection of marginal zone B cells. *Immunology Reviews*. 2004;197:192-205.

98. Puga I et al. B cell-helper neutrophils stimulate the diversification and production of immunoglobulin in the marginal zone of the spleen. *Nature Immunology*. 2012;13:170-180.

99. Spencer, J., Finn, T., Pulford, K. A., Mason DY&, Isaacson PG. The human gut contains a novel population of B lymphocytes which resemble marginal zone cells. *Clinical and Experimental Immunology*. 1985;62:607-612.

100. Tierens, A., Delabie, J., Michiels, L., Vandenberghe P, & De Wolf-Peeters C. Marginal-zone B cells in the human lymph node and spleen show somatic hypermutations and display clonal expansion. *Blood*. 1999;93:226-234.

101. Dono M et al. Heterogeneity of tonsillar subepithelial B lymphocytes, the splenic marginal zone equivalents. *Journal of Immunology*. 2000;164:5596-5604.

102. Steiniger, B., Timphus, E. & Barth P. The splenic marginal zone in humans and rodents: an enigmatic compartment and its inhabitants. *Histochemistry and Cell Biologyy*. 2006;126:641-648.

103. Weller S et al. Human blood IgM "memory" B cells are circulating splenic marginal zone B cells harboring a prediversified immunoglobulin repertoire. *Blood*. 2004;104:3647-3654.

104. Timens, W., Boes, A. & Poppema S. Human marginal zone B cells are not an activated B cell subset: strong expression of CD21 as a putative mediator for rapid B cell activation. *European Journal of Immunology*. 1989;19:2163-2166.

105. Tangye, S. G., Liu, Y. J., Aversa, G., Phillips JH&, de Vries JE. Identification of functional human splenic memory B cells by expression of CD148 and CD27. *Journal of Eperimental Medicine*. 1998;188:1691-1703.

106. Castadot P, Geets X, Lee JA, Christian N, Grégoire V. Assessment by a deformable registration method of the volumetric and positional changes of target volumes and organs at risk in pharyngo-laryngeal tumors treated with concomitant chemo-radiation. *Radiotherapy and Oncology*. 2010;95(2):209-217. doi:10.1016/j.cimid.2017.08.002

107. Gunn MD, Ngo VN, Ansel KM, Ekland EH, Cyster JG W, LT. A B-cell-homing chemokine made in lymphoid follicles activates Burkitt's lymphoma receptor-1. *Nature*. 1998;391:799-803.

108. Cyster JG. Chemokines and cell migration in secondary lymphoid organs. *Science*. 1999;286:2098-2102.

109. Lo CG, Lu TT CJG. Integrin-dependence of lymphocyte entry into the splenic white pulp. *Journal of Eperimental Medicine*. 2003;197:353-361.

110. Vale AM, Kearney JF, Nobrega A, Schroeder HW. *Development and Function of B Cell Subsets*. Second Edi. Elsevier Ltd; 2014. doi:10.1016/B978-0-12-397933-9.00007-2

111. Mackay F BJL. BAFF: a fundamental survival factor for B cells. *Nature Reviews Immunology*. 2002;2:465-475.

112. Mackay F SP. Cracking the BAFF code. *Nature Reviews Immunology*. 2009;9:491-502.

113. Rajewsky K. Clonal selection and learning in the antibody system. *Nature*. 1996;381:751-758.

114. Jacob J KG. In situ studies of the primary immune response to (4-hydroxy- 3-nitrophenyl)acetyl. II. A common clonal origin for periarteriolar lymphoid sheath-associated foci and germinal centers. *Journal of Eperimental Medicine*. 1992;176:679-687.

115. Klein U DFR. Germinal centres: role in B-cell physiology and malignancy. *Nature Reviews Immunology*. 2008;8:22-33.

116. Sanz I, Wei C, Jenks SA, et al. Challenges and Opportunities for Consistent Classification of Human B Cell and Plasma Cell Populations. *Front Immunol*. 2019;10:2458. doi:10.3389/fimmu.2019.02458

117. Srivastava B, Quinn WJ, Hazard K, Erikson J, Allman D. Characterization of marginal zone B cell precursors. *J Exp Med*. 2005;202(9):1225-1234. doi:10.1084/jem.20051038

118. Oleinika K, Mauri C, Salama AD. Effector and regulatory B cells in immune-mediated kidney disease. *Nature Reviews Nephrology*. 2019;15(1):11-26. doi:10.1038/s41581-018-0074-7

119. Simon Q, Pers JO, Cornec D, Le Pottier L, Mageed RA, Hillion S. In-depth characterization of CD24(high)CD38(high) transitional human B cells reveals different regulatory profiles. *J Allergy Clin Immunol*. 2016;137(5):1577-1584.e10. doi:10.1016/j.jaci.2015.09.014

120. Suryani S, Fulcher DA, Santner-Nanan B, et al. Differential expression of CD21 identifies developmentally and functionally distinct subsets of human transitional B cells. *Blood*. 2010;115(3):519-529. doi:10.1182/blood-2009-07-234799

121. Maarof G, Bouchet-Delbos L, Gary-Gouy H, Durand-Gasselin I KR, A. D. Interleukin-24 inhibits the plasma cell differentiation program in human germinal center B cells. *Blood*. 2010;115:1718-1726.

122. Kaji T, Ishige A, Hikida M, Taka J, Hijikata A KM et al. Distinct cellular pathways select germline-encoded and somatically mutated antibodies into immunological memory. *Journal of Eperimental Medicine*. 2012;209:2079-2097.

123. Taylor JJ, Pape KA JMKA. germinal center-independent pathway generates unswitched memory B cells early in the primary response. *Journal of Eperimental Medicine*. 2012;209:597-606.

124. Liu YJ, Zhang J, Lane PJ, Chan EY, MacLennan IC. Sites of specific B cell activation in primary and secondary responses to T cell-dependent and T cell-independent antigens. *Eur J Immunol*. 1991;21(12):2951-2962. doi:10.1002/eji.1830211209

125. Liu YJ, Oldfield S, MacLennan IC. Memory B cells in T cell-dependent antibody responses colonize the splenic marginal zones. *Eur J Immunol*. 1988;18(3):355-362. doi:10.1002/eji.1830180306

126. Tangye SG, Avery DT, Hodgkin PD. A division-linked mechanism for the rapid generation of Ig-secreting cells from human memory B cells. *J Immunol*. 2003;170(1):261-269. doi:10.4049/jimmunol.170.1.261

127. Klein U, Rajewsky K KR. Human immunoglobulin (Ig)M+IgD+ peripheral blood B cells expressing the CD27 cell surface antigen carry somatically mutated variable region genes: CD27 as a general marker for somatically mutated (memory) B cells. *Journal of Eperimental Medicine*. 1998;188:1679-1689.

128. Klein U, Küppers R RK. Evidence for a large compartment of IgMexpressing memory B cells in humans. *Blood*. 1997;89:1288-1298.

129. Bernasconi NL, Traggiai E LA. Maintenance of serological memory by polyclonal activation of human memory B cells. *Science*. 2002;298:2199-2202.

130. Good KL, Avery DT TSG. Resting human memory B cells are intrinsically programmed for enhanced survival and responsiveness to diverse stimuli compared to naive B cells. *Journal of Immunology*. 2009;182:890-901.

131. Dogan I, Bertocci B, Vilmont V, Delbos F, Megret J SS et al. Multiple layers of B cell memory with different effector functions. *Nature Immunology*. 2009;10:1292-1299.

132. Avery DT, Deenick EK, Ma CS, Suryani S, Simpson N CG et al. B cell-intrinsic signaling through IL-21 receptor and STAT3 is required for establishing longlived antibody responses in humans. *Journal of Eperimental Medicine*. 2010;207:155-171.

133. Bernasconi NL, Onai N LA. A role for Toll-like receptors in acquired immunity: up-regulation of TLR9 by BCR triggering in naive B cells and constitutive expression in memory B cells. *Blood*. 2007;101:4500-4504.

134. Good KL TSG. Decreased expression of Kruppel-like factors in memory B cells induces the rapid response typical of secondary antibody responses. *Proceedings of the National Academy of Sciences of the USA*. 2007;104:13420-13425.

135. Seifert M, Küppers R. Human memory B cells. *Leukemia*. 2016;30(12):2283-2292. doi:10.1038/leu.2016.226

136. Dogan I, Bertocci B, Vilmont V, et al. Multiple layers of B cell memory with different effector functions. *Nat Immunol*. 2009;10(12):1292-1299. doi:10.1038/ni.1814

137. Klein U, Küppers R, Rajewsky K. Evidence for a large compartment of IgM-expressing memory B cells in humans. *Blood*. 1997;89(4):1288-1298.

138. Klein U, Rajewsky K, Küppers R. Human immunoglobulin (Ig)M+IgD+ peripheral blood B cells expressing the CD27 cell surface antigen carry somatically mutated variable region genes: CD27 as a general marker for somatically mutated (memory) B cells. *J Exp Med*. 1998;188(9):1679-1689. doi:10.1084/jem.188.9.1679

139. Agematsu K, Nagumo H, Yang FC, et al. B cell subpopulations separated by CD27 and crucial collaboration of CD27+ B cells and helper T cells in immunoglobulin production. *Eur J Immunol*. 1997;27(8):2073-2079. doi:10.1002/eji.1830270835

140. Shi Y, Agematsu K, Ochs HD, Sugane K. Functional analysis of human memory B-cell subpopulations: IgD+CD27+ B cells are crucial in secondary immune response by producing high affinity IgM. *Clin Immunol*. 2003;108(2):128-137. doi:10.1016/s1521-6616(03)00092-5

141. Bagnara D, Squillario M, Kipling D, et al. A Reassessment of IgM Memory Subsets in Humans. *J Immunol*. 2015;195(8):3716-3724. doi:10.4049/jimmunol.1500753

142. Sutton HJ, Aye R, Idris AH, et al. Atypical B cells are part of an alternative lineage of B cells that participates in responses to vaccination and infection in humans. *Cell Rep*. 2021;34(6):108684. doi:10.1016/j.celrep.2020.108684

143. Forsgren A GAO. Many bacterial species bind human IgD. J. *Immunology*. 1979;122:1468-1472.

144. Liu YJ, de Bouteiller O, Arpin C, Briere F, Galibert L HS et al. Normal human IgD +IgM-germinal center B cells can express up to 80 mutations in the variable region of their IgD transcripts. *Immunity*. 1996;4:603-613.

145. Seifert M, Steimle-Grauer SA, Goossens T, Hansmann ML BA, R. K. A model for the development of human IgD-only B cells: genotypic analyses suggest their generation in superantigen driven immune responses. *Molecular Immunology*. 2009;46:630-639.

146. Giesecke C, Frölich D, Reiter K, Mei HE, Wirries I KR et al. Tissue distribution and dependence of responsiveness of human antigen-specific memory B cells. *Journal of Immunology*. 2014;192:3091-3100.

147. Weill JC, Weller S RCA. Human marginal zone B cells. *Annual Review of Immunology*. 2009;27:267-285.

148. Bagnara D, Squillario M, Kipling D, Mora T, Walczak AM DSL et al. A reassessment of IgM memory subsets in humans. *Journal of Immunology*. 2015;195:3716-3724.

149. Sathe A, Cusick JK. Biochemistry, Immunoglobulin M. In: *StatPearls*. StatPearls Publishing; 2022. Accessed July 25, 2022. http://www.ncbi.nlm.nih.gov/books/NBK555995/

150. Brandtzaeg P. Secretory IgA: Designed for Anti-Microbial Defense. *Front Immunol*. 2013;4. doi:10.3389/fimmu.2013.00222

151. Keyt BA, Baliga R, Sinclair AM, Carroll SF, Peterson MS. Structure, Function, and Therapeutic Use of IgM Antibodies. *Antibodies (Basel)*. 2020;9(4):E53. doi:10.3390/antib9040053

152. Law ECY, Leung DTM, Tam FCH, Cheung KKT, Cheng NHY, Lim PL. IgM Antibodies Can Access Cryptic Antigens Denied to IgG: Hypothesis on Novel Binding Mechanism. *Front Immunol*. 2019;10:1820. doi:10.3389/fimmu.2019.01820

153. Fecteau JF, Cote G NS. A new memory CD27-IgG+ B cell population in peripheral blood expressing VH genes with low frequency of somatic mutation. *Journal of Immunology*. 2006;177:3728-3736.

154. Colonna-Romano G, Bulati M, Aquino A, Pellicano M, Vitello S LD et al. A double-negative (IgD-CD27-) B cell population is increased in the peripheral blood of elderly people. *Mechanism of Ageing and Development*. 2009;130:681-690.

155. Budeus B, Schweigle de Reynoso S, Przekopowitz M, Hoffmann D SM, R. K. Complexity of the human memory B-cell compartment is determined by the versatility of clonal diversification in germinal centers. *Proceedings of the National Academy of Sciences of the USA*. 2015;112:E5281-E5289.

156. Wu YC, Kipling D DWDK. The relationship between CD27 negative and positive B cell populations in human peripheral blood. *Frontiers in Immunology*. 2011;2:81.

157. Shlomchik MJ. Do Memory B Cells Form Secondary Germinal Centers? Yes and No. *Cold Spring Harb Perspect Biol*. 2018;10(1):a029405. doi:10.1101/cshperspect.a029405

158. Lee CM, Oh JE. Resident Memory B Cells in Barrier Tissues. *Front Immunol*. 2022;13:953088. doi:10.3389/fimmu.2022.953088

159. Matsuda Y, Imamura R, Takahara S. Evaluation of Antigen-Specific IgM and IgG Production during an In Vitro Peripheral Blood Mononuclear Cell Culture Assay. *Front Immunol*. 2017;8:794. doi:10.3389/fimmu.2017.00794

160. Soe PT, Hanthamrongwit J, Saelee C, et al. Circulating IgA/IgG memory B cells against Mycobacterium tuberculosis dormancy-associated antigens Rv2659c and Rv3128c in active and latent tuberculosis. *International Journal of Infectious Diseases*. 2021;110:75-82. doi:10.1016/j.ijid.2021.07.033

161. Ndungu FM, Cadman ET, Coulcher J, et al. Functional Memory B Cells and Long-Lived Plasma Cells Are Generated after a Single Plasmodium chabaudi Infection in Mice. Kim K, ed. *PLoS Pathog*. 2009;5(12):e1000690. doi:10.1371/journal.ppat.1000690

162. Neutra MR, Pringault E, Kraehenbuhl JP. Antigen sampling across epithelial barriers and induction of mucosal immune responses. *Annu Rev Immunol*. 1996;14:275-300. doi:10.1146/annurev.immunol.14.1.275

163. Neutra MR, Pringault E KJP. Antigen sampling across epithelial barriers and induction of mucosal immune responses. *Annual Review of Immunology*. 1996;14:275-300.

164. Berkowska MA, Schickel JN, Grosserichter-Wagener C, de Ridder D NY, Al. van DJ et. Circulating human CD27-IgA+ memory b cells recognize bacteria with polyreactive Igs. *Journal of Immunology*. 2015;195:1417-1426.

165. Kumar Bharathkar S, Parker BW, Malyutin AG, et al. The structures of secretory and dimeric immunoglobulin A. *eLife*. 2020;9:e56098. doi:10.7554/eLife.56098

166. Lycke NY, Bemark M. The regulation of gut mucosal IgA B-cell responses: recent developments. *Mucosal Immunol*. 2017;10(6):1361-1374. doi:10.1038/mi.2017.62

167. Erazo A, Kutchukhidze N, Leung M, Christ AP, Urban Jr JF C de LM, Al. E. Unique maturation program of the IgE response in vivo. *Immunity*. 2007;26:191-203.

168. Stone KD, Prussin C, Metcalfe DD. IgE, mast cells, basophils, and eosinophils. *J Allergy Clin Immunol*. 2010;125(2 Suppl 2):S73-80. doi:10.1016/j.jaci.2009.11.017

169. Mukai K, Tsai M, Starkl P, Marichal T, Galli SJ. IgE and mast cells in host defense against parasites and venoms. *Semin Immunopathol*. 2016;38(5):581-603. doi:10.1007/s00281-016-0565-1

170. Moir S, Ho J, Malaspina A, et al. Evidence for HIV-associated B cell exhaustion in a dysfunctional memory B cell compartment in HIV-infected viremic individuals. *J Exp Med*. 2008;205(8):1797-1805. doi:10.1084/jem.20072683

171. Charles ED, Brunetti C, Marukian S, et al. Clonal B cells in patients with hepatitis C virus-associated mixed cryoglobulinemia contain an expanded anergic CD21low B-cell subset. *Blood*. 2011;117(20):5425-5437. doi:10.1182/blood-2010-10-312942

172. Weiss GE, Crompton PD, Li S, et al. Atypical memory B cells are greatly expanded in individuals living in a malaria-endemic area. *J Immunol*. 2009;183(3):2176-2182. doi:10.4049/jimmunol.0901297

173. Andrews SF, Chambers MJ, Schramm CA, et al. Activation Dynamics and Immunoglobulin Evolution of Pre-existing and Newly Generated Human Memory B cell Responses to Influenza Hemagglutinin. *Immunity*. 2019;51(2):398-410.e5. doi:10.1016/j.immuni.2019.06.024

174. Lau D, Lan LYL, Andrews SF, et al. Low CD21 expression defines a population of recent germinal center graduates primed for plasma cell differentiation. *Sci Immunol*. 2017;2(7):eaai8153. doi:10.1126/sciimmunol.aai8153

175. Kim CC, Baccarella AM, Bayat A, Pepper M, Fontana MF. FCRL5+ Memory B Cells Exhibit Robust Recall Responses. *Cell Rep*. 2019;27(5):1446-1460.e4. doi:10.1016/j.celrep.2019.04.019

176. Isnardi I, Ng YS, Menard L, et al. Complement receptor 2/CD21- human naive B cells contain mostly autoreactive unresponsive clones. *Blood*. 2010;115(24):5026-5036. doi:10.1182/blood-2009-09-243071

177. Ehrhardt GR, Hsu JT, Gartland L, Leu CM, Zhang S DR et al. Expression of the immunoregulatory molecule FcRH4 defines a distinctive tissue-based population of memory B cells. *Journal of Eperimental Medicine*. 2005;202:783-791.

178. Portugal S, Tipton CM, Sohn H, Kone Y, Wang J LS et al. Malaria-associated atypical memory B cells exhibit markedly reduced B cell receptor signaling and effector function. *Elife*. 2015;4:e07218.

179. Sullivan RT, Kim CC, Fontana MF, Feeney ME, Jagannathan P BM et al. FCRL5 delineates functionally impaired memory B cells associated with Plasmodium falciparum exposure. *PLoS Pathology*. 2015;11:e1004894.

180. Jenks SA, Cashman KS, Zumaquero E, et al. Distinct Effector B Cells Induced by Unregulated Toll-like Receptor 7 Contribute to Pathogenic Responses in Systemic Lupus Erythematosus. *Immunity*. 2018;49(4):725-739.e6. doi:10.1016/j.immuni.2018.08.015

181. Rivera-Correa J, Mackroth MS, Jacobs T, Schulze Zur Wiesch J, Rolling T, Rodriguez A. Atypical memory B-cells are associated with Plasmodium falciparum anemia through anti-phosphatidylserine antibodies. *Elife*. 2019;8:e48309. doi:10.7554/eLife.48309

182. Wrammert J, Smith K, Miller J, et al. Rapid cloning of high-affinity human monoclonal antibodies against influenza virus. *Nature*. 2008;453(7195):667-671. doi:10.1038/nature06890

183. Adachi Y, Onodera T, Yamada Y, et al. Distinct germinal center selection at local sites shapes memory B cell response to viral escape. *Journal of Experimental Medicine*. 2015;212(10):1709-1723. doi:10.1084/jem.20142284

184. Qian Y, Wei C, Eun-Hyung Lee F, et al. Elucidation of seventeen human peripheral blood B-cell subsets and quantification of the tetanus response using a density-based method for

the automated identification of cell populations in multidimensional flow cytometry data. *Cytometry*. 2010;78B(S1):S69-S82. doi:10.1002/cyto.b.20554

185. Medina F, Segundo C, Campos-Caro A, González-García I, Brieva JA. The heterogeneity shown by human plasma cells from tonsil, blood, and bone marrow reveals graded stages of increasing maturity, but local profiles of adhesion molecule expression. *Blood*. 2002;99(6):2154-2161. doi:10.1182/blood.V99.6.2154

186. González-García I, Ocaña E, Jiménez-Gómez G, Campos-Caro A, Brieva JA. Immunization-Induced Perturbation of Human Blood Plasma Cell Pool: Progressive Maturation, IL-6 Responsiveness, and High PRDI-BF1/BLIMP1 Expression Are Critical Distinctions between Antigen-Specific and Nonspecific Plasma Cells. *J Immunol*. 2006;176(7):4042-4050. doi:10.4049/jimmunol.176.7.4042

187. Arce S, Luger E, Muehlinghaus G, et al. CD38 low IgG-secreting cells are precursors of various CD38 high-expressing plasma cell populations. *Journal of Leukocyte Biology*. 2004;75(6):1022-1028. doi:10.1189/jlb.0603279

188. Chu VT, Berek C. The establishment of the plasma cell survival niche in the bone marrow. *Immunol Rev*. 2013;251(1):177-188. doi:10.1111/imr.12011

189. Mei HE, Yoshida T, Sime W, et al. Blood-borne human plasma cells in steady state are derived from mucosal immune responses. *Blood*. 2009;113(11):2461-2469. doi:10.1182/blood-2008-04-153544

190. Wols HAM, College B, Forest L. Plasma Cells. Published online 2005:1-8. doi:10.1038/npg.els.0004030

191. McHeyzer-WilliamsMG. Immune response decisions at the single cell level. *Seminars in Immunology*. 1997;9:219-227.

192. Bataille R, Jégo G, Robillard N, et al. The phenotype of normal, reactive and malignant plasma cells. Identification of "many and multiple myelomas" and of new targets for myeloma therapy. *Haematologica*. 2006;91(9):1234-1240.

193. Shapiro-Shelef M, Lin KI, McHeyzer-Williams LJ, Liao J, McHeyzer-Williams MG, Calame K. Blimp-1 is required for the formation of immunoglobulin secreting plasma cells and pre-plasma memory B cells. *Immunity*. 2003;19(4):607-620. doi:10.1016/s1074-7613(03)00267-x

194. Klein U, Casola S, Cattoretti G, et al. Transcription factor IRF4 controls plasma cell differentiation and class-switch recombination. *Nat Immunol*. 2006;7(7):773-782. doi:10.1038/ni1357

195. Shaffer AL, Shapiro-Shelef M, Iwakoshi NN, et al. XBP1, downstream of Blimp-1, expands the secretory apparatus and other organelles, and increases protein synthesis in plasma cell differentiation. *Immunity*. 2004;21(1):81-93. doi:10.1016/j.immuni.2004.06.010

196. Iwakoshi NN, Lee AH, Vallabhajosyula P, Otipoby KL, Rajewsky K, Glimcher LH. Plasma cell differentiation and the unfolded protein response intersect at the transcription factor XBP-1. *Nat Immunol*. 2003;4(4):321-329. doi:10.1038/ni907

197. Reimold AM, Iwakoshi NN, Manis J, et al. Plasma cell differentiation requires the transcription factor XBP-1. *Nature*. 2001;412(6844):300-307. doi:10.1038/35085509

198. Shaffer AL, Lin KI, Kuo TC, et al. Blimp-1 orchestrates plasma cell differentiation by extinguishing the mature B cell gene expression program. *Immunity*. 2002;17(1):51-62. doi:10.1016/s1074-7613(02)00335-7

199. Wang X, Hao GL, Wang BY, et al. Function and dysfunction of plasma cells in intestine. *Cell Biosci*. 2019;9:26. doi:10.1186/s13578-019-0288-9

200. Pelletier N, McHeyzer-Williams LJ, Wong KA, Urich E, Fazilleau N, McHeyzer-Williams MG. Plasma cells negatively regulate the follicular helper T cell program. *Nat Immunol*. 2010;11(12):1110-1118. doi:10.1038/ni.1954

201. M. Horikawa, E.T. Weimer, D.J. DiLillo, G.M. Venturi, R. Spolski, W.J. Leonard et al. Regulatory B cell (B10 Cell) expansion during Listeria infection governs innate and cellular immune responses in mice. *Journal of Immunology*. 2013;190(3):1158-1168.

202. R. Bankoti, K. Gupta, A. Levchenko, S. Stager. Marginal zone B cells regulate antigen-specific T cell responses during infection. *Journal of Immunology*. 2012;188(8):3961-3971.

203. P. Neves, V. Lampropoulou, E. Calderon-Gomez, T. Roch, U. Stervbo, P. Shen et al. Signaling via theMyD88 adaptor protein in B cells suppresses protective immunity during Salmonella typhimurium infection. *Immunity*. 2010;33(5):777-790.

204. Q. Ding, M. Yeung, G. Camirand, Q. Zeng, H. Akiba, H. Yagita, et al. Regulatory B cells are identified by expression of Tim-1 and can be induced through Tim-1 ligation to promote tolerance in mice,. *Journal of Clinical Investigation*. 2011;121(9):3645-3656.

205. G. Lal, Y. Nakayama, A. Sethi, A.K. Singh, B.E. Burrell, N. Kulkarni, et al. Interleukin- 10 from marginal zone precursor B-cell subset is required for costimulatory blockade- induced transplantation tolerance. *Transplantation*. 2015;99(9):1817-1828.

206. R. Alhabbab, P. Blair, R. Elgueta, E. Stolarczyk, E. Marks, P.D. Becker, et al. Diversity of gut microflora is required for the generation of B cell with regulatory properties in a skin graft model. *Scientific Reports*. 2015;5:11554.

207. N.A. Carter, E.C. Rosser C. Mauri, Interleukin-10 produced by B cells is crucial for the suppression of Th17/Th1 responses, induction of T regulatory type 1 cells and reduction of collagen-induced arthritis. *Arthritis Research and Therapy*. 2012;14(1):R32.

208. J.G. Evans, K.A. Chavez-Rueda, A. Eddaoudi, A. Meyer-Bahlburg, D.J. Rawlings MR, Ehrenstein et al. Novel suppressive function of transitional 2 B cells in experimental arthritis. *Journal of Immunology*. 2007;178(12):7868-7878.

209. R.Watanabe, N. Ishiura, H. Nakashima, Y. Kuwano, H. Okochi, K. Tamaki, et al. Regulatory B cells (B10 cells) have a suppressive role in murine lupus: CD19 and B10 cell deficiency exacerbates systemic autoimmunity. *Journal of Immunology*. 2010;184(9):4801-4809.

210. T. Matsushita, M. Horikawa, Y. Iwata, T.F. Tedder. Regulatory B cells (B10 cells) and regulatory T cells have independent roles in controlling experimental autoimmune encephalomyelitis initiation and late-phase immunopathogenesis. *Journal of Immunology*. 2010;185(4):2240-2252.

211. M. Matsumoto, A. Baba, T. Yokota, H. Nishikawa, Y. Ohkawa, H. Kayama, et al. Interleukin- 10-producing plasmablasts exert regulatory function in autoimmune inflammation,. *Immunity*. 2014;41(6):1040-1051.

212. Haddad M, Sharma S. Physiology, Lung. In: *StatPearls*. StatPearls Publishing; 2022. Accessed July 25, 2022. http://www.ncbi.nlm.nih.gov/books/NBK545177/

213. Patwa A, Shah A. Anatomy and physiology of respiratory system relevant to anaesthesia. *Indian J Anaesth*. 2015;59(9):533. doi:10.4103/0019-5049.165849

214. Sobiesk JL, Munakomi S. Anatomy, Head and Neck, Nasal Cavity. In: *StatPearls*. StatPearls Publishing; 2022. Accessed July 25, 2022. http://www.ncbi.nlm.nih.gov/books/NBK544232/

215. Downey RP, Samra NS. Anatomy, Thorax, Tracheobronchial Tree. In: *StatPearls*. StatPearls Publishing; 2022. Accessed July 25, 2022. http://www.ncbi.nlm.nih.gov/books/NBK556044/

216. Khan YS, Lynch DT. Histology, Lung. In: *StatPearls*. StatPearls Publishing; 2022. Accessed July 25, 2022. http://www.ncbi.nlm.nih.gov/books/NBK534789/

217. Kia'i N, Bajaj T. Histology, Respiratory Epithelium. In: *StatPearls*. StatPearls Publishing; 2022. Accessed July 25, 2022. http://www.ncbi.nlm.nih.gov/books/NBK541061/

218. Rokicki W, Rokicki M, Wojtacha J, Dżeljijli A. The role and importance of club cells (Clara cells) in the pathogenesis of some respiratory diseases. *Kardiochir Torakochirurgia Pol*. 2016;13(1):26-30. doi:10.5114/kitp.2016.58961

219. Ochs M, Nyengaard JR, Jung A, et al. The number of alveoli in the human lung. *Am J Respir Crit Care Med*. 2004;169(1):120-124. doi:10.1164/rccm.200308-1107OC

220. McKleroy W, Lyn-Kew K. 500 Million Alveoli from 30,000 Feet: A Brief Primer on Lung Anatomy. *Methods Mol Biol*. 2018;1809:3-15. doi:10.1007/978-1-4939-8570-8_1

221. Brandt JP, Mandiga P. Histology, Alveolar Cells. In: *StatPearls*. StatPearls Publishing; 2022. Accessed July 25, 2022. http://www.ncbi.nlm.nih.gov/books/NBK557542/

222. Naeem A, Rai SN, Pierre L. Histology, Alveolar Macrophages. In: *StatPearls*. StatPearls Publishing; 2022. Accessed July 25, 2022. http://www.ncbi.nlm.nih.gov/books/NBK513313/

223. Han S, Mallampalli RK. The Role of Surfactant in Lung Disease and Host Defense against Pulmonary Infections. *Ann Am Thorac Soc*. 2015;12(5):765-774. doi:10.1513/AnnalsATS.201411-507FR

224. Castranova V, Rabovsky J, Tucker JH, Miles PR. The alveolar type II epithelial cell: a multifunctional pneumocyte. *Toxicol Appl Pharmacol*. 1988;93(3):472-483. doi:10.1016/0041-008x(88)90051-8

225. Kasper M, Barth K. Potential contribution of alveolar epithelial type I cells to pulmonary fibrosis. *Biosci Rep*. 2017;37(6):BSR20171301. doi:10.1042/BSR20171301

226. Frank JA. Claudins and alveolar epithelial barrier function in the lung. *Ann N Y Acad Sci*. 2012;1257:175-183. doi:10.1111/j.1749-6632.2012.06533.x

227. Patel VI, Metcalf JP. Airway Macrophage and Dendritic Cell Subsets in the Resting Human Lung. *Crit Rev Immunol*. 2018;38(4):303-331. doi:10.1615/CritRevImmunol.2018026459

228. Parker D, Prince A. Innate immunity in the respiratory epithelium. *Am J Respir Cell Mol Biol*. 2011;45(2):189-201. doi:10.1165/rcmb.2011-0011RT

229. Johnston SL, Goldblatt DL, Evans SE, Tuvim MJ, Dickey BF. Airway Epithelial Innate Immunity. *Front Physiol*. 2021;12:749077. doi:10.3389/fphys.2021.749077

230. Roan F, Obata-Ninomiya K, Ziegler SF. Epithelial cell-derived cytokines: more than just signaling the alarm. *J Clin Invest*. 2019;129(4):1441-1451. doi:10.1172/JCI124606

231. Hammad H, Lambrecht BN. Barrier Epithelial Cells and the Control of Type 2 Immunity. *Immunity*. 2015;43(1):29-40. doi:10.1016/j.immuni.2015.07.007

232. Hampton HR, Chtanova T. Lymphatic Migration of Immune Cells. *Front Immunol*. 2019;10:1168. doi:10.3389/fimmu.2019.01168

233. Hewitt RJ, Lloyd CM. Regulation of immune responses by the airway epithelial cell landscape. *Nat Rev Immunol*. 2021;21(6):347-362. doi:10.1038/s41577-020-00477-9

234. Han ST, Mosher DF. IL-5 Induces Suspended Eosinophils to Undergo Unique Global Reorganization Associated with Priming. *Am J Respir Cell Mol Biol*. 2014;50(3):654-664. doi:10.1165/rcmb.2013-0181OC

235. McBrien CN, Menzies-Gow A. The Biology of Eosinophils and Their Role in Asthma. *Front Med*. 2017;4:93. doi:10.3389/fmed.2017.00093

236. Carragher DM, Rangel-Moreno J RTD. Ectopic lymphoid tissues and local immunity. *Seminars in Immunology*. 2008;20:26-42.

237. Aloisi F PBR. Lymphoid neogenesis in chronic inflammatory diseases. *Nat Rev Immunol*. 2006;6:205-217.

238. Brandtzaeg P. Mucosal immunity: induction, dissemination, and effector functions. *Scandinavian Journal of Immunology*. 2009;70:505-515.

239. Corthesy B. Role of secretory immunoglobulin A and secretory component in the protection of mucosal surfaces. *Future Microbiology*. 2010;5:817-829.

240. Kaetzel CS, Robinson JK, Chintalacharuvu KR, Vaerman JP LME. The polymeric immunoglobulin receptor (secretory component) mediates transport of immune complexes across epithelial cells: a local defense function for IgA. *Proceedings of the National Academy of Sciences of the USA*. 1991;88:8796-8800.

241. Tomasi TB Jr, Tan EM, Solomon A PRA. Characteristics of an immune system common to certain external secretions. *Journal of Eperimental Medicine*. 1965;121:101-124.

242. Kiyono H FS. NALT- versus Peyer's-patch-mediated mucosal immunity. *Nature Reviews Immunology*. 2004;4:699-710.

243. Global strategy for the diagnosis, management, and prevention of chronic obstructive pulmonary disease. www.goldcopd.org. In: *Global Initiative for Chronic Obstructive Lung Disease*. ; 2016.

244. Lozano R, Naghavi M, Foreman K, Lim S, Shibuya K, Aboyans V et al. Global and regional mortality from 235 causes of death for 20 age groups in 1990 and 2010: a systematic analysis for the Global Burden of Disease Study 2010. *lancet*. 2012;380:2095-2128.

245. Gnatiuc L CG. COPD in nonsmokers: the biomass hypothesis—to be or not to be? *European Respiratory Journal*. 2014;44:8-10.

246. Kato A, Hanaoka M. Pathogenesis of COPD (Persistence of Airway Inflammation): Why Does Airway Inflammation Persist After Cessation of Smoking? In: Nakamura H, Aoshiba K, eds. *Chronic Obstructive Pulmonary Disease*. Respiratory Disease Series: Diagnostic Tools and Disease Managements. Springer Singapore; 2017:57-72. doi:10.1007/978-981-10-0839-9_4

247. Rovina N, Koutsoukou A, Koulouris NG. Inflammation and Immune Response in COPD: Where Do We Stand? *Mediators of Inflammation*. 2013;2013:1-9. doi:10.1155/2013/413735

248. Pahal P, Avula A, Sharma S. Emphysema. In: *StatPearls*. StatPearls Publishing; 2022. Accessed July 25, 2022. http://www.ncbi.nlm.nih.gov/books/NBK482217/

249. Dunlap DG, Semaan R, Riley CM, Sciurba FC. Bronchoscopic device intervention in chronic obstructive pulmonary disease. *Curr Opin Pulm Med*. 2019;25(2):201-210. doi:10.1097/MCP.0000000000000561

250. Fernandez-Bussy S, Labarca G, Herth FJF. Bronchoscopic Lung Volume Reduction in Patients with Severe Emphysema. *Semin Respir Crit Care Med*. 2018;39(6):685-692. doi:10.1055/s-0038-1676774

251. Rustagi N, Singh S, Dutt N, et al. Efficacy and Safety of Stent, Valves, Vapour ablation, Coils and Sealant Therapies in Advanced Emphysema: A Meta-Analysis. *Turk Thorac J*. 2019;20(1):43-60. doi:10.5152/TurkThoracJ.2018.18062

252. Moldoveanu B, Otmishi P, Jani P, et al. Inflammatory mechanisms in the lung. *J Inflamm Res*. 2009;2:1-11.

253. Chakraborty K, Bhattacharyya A. Role of Proteases in Inflammatory Lung Diseases. In: Chakraborti S, Dhalla NS, eds. *Proteases in Health and Disease*. Springer New York; 2013:361-385. doi:10.1007/978-1-4614-9233-7_21

254. Barnes PJ CB. Systemic manifestations and comorbidities of COPD. *European Respiratory Journal*. 2009;33:1165-1185.

255. Chung KF, Adcock IM. Multifaceted mechanisms in COPD: inflammation, immunity, and tissue repair and destruction. *European Respiratory Journal*. 2008;31(6):1334-1356. doi:10.1183/09031936.00018908

256. Pandey KC, De S, Mishra PK. Role of Proteases in Chronic Obstructive Pulmonary Disease. *Front Pharmacol*. 2017;8:512. doi:10.3389/fphar.2017.00512

257. Choudhury G, MacNee W. Role of Inflammation and Oxidative Stress in the Pathology of Ageing in COPD: Potential Therapeutic Interventions. *COPD: Journal of Chronic Obstructive Pulmonary Disease*. 2017;14(1):122-135. doi:10.1080/15412555.2016.1214948

258. MacNee W. Pathology, pathogenesis, and pathophysiology. *BMJ*. 2006;332(7551):1202-1204. doi:10.1136/bmj.332.7551.1202

259. Vollmer WM, Gislason T, Burney P et al. Spirometry, Comparison of criteria for the diagnosis of COPD: results from the BOLD study. *European Respiratory Journal*. 2009;34:588-597.

260. Wedzicha JA, Donaldson GC. Exacerbations of chronic obstructive pulmonary disease. *Respir Care*. 2003;48(12):1204-1213; discussion 1213-1215.

261. Sapey E, Stockley RA. COPD exacerbations . 2: aetiology. *Thorax*. 2006;61(3):250-258. doi:10.1136/thx.2005.041822

262. Miravitlles M. Exacerbations of chronic obstructive pulmonary disease: when are bacteria important? *European Respiratory Journal*. 2002;20(Supplement 36):9S - 19s. doi:10.1183/09031936.02.00400302

263. Doll H MM. Health-related QOL in acute exacerbations of chronic bronchitis and chronic obstructive pulmonary disease: a review of the literature. *Pharmacoeconomics*. 2005;23:345-363.

264. Hurst JR, Vestbo J, Anzueto A et al. Susceptibility to exacerbation in chronic obstructive pulmonary disease. *New England Journal of Medicine*. 2010;363:1128-1138.

265. Barnes PJ. Cellular and molecular mechanisms of chronic obstructive pulmonary disease. *clinics in chest medicine*. 2014;35:71-86.

266. Postma DS, Reddel HK, ten Hacken NH van den B. Asthma and chronic obstructive pulmonary disease: similarities and differences. *clinics in chest medicine*. 2014;35:143-156.

267. Caramori G, Casolari P, Giuffrè S, Barczyk A, Adcock I PA. COPD pathology in the small airways. *Panminerva Medica*. 2011;53:51-70.

268. Hogg JC T. The pathology of chronic obstructive pulmonary disease. *Annual Reviews in Pathology*. 2009;4:435-459.

269. Hogg JC. Pathophysiology of airflow limitation in chronic obstructive pulmonary disease. *lancet*. 2004;364:709-721.

270. Barnes PJ. Small airways in COPD. 2004;(350):2635-2637.

271. Barnes PJ. Chronic obstructive pulmonary disease. *New England Journal of Medicine*. 2000;343:269-280.

272. Hogg JC, Chu F, Utokaparch S, Woods R, Elliott WM, Buzatu L et al. The nature of small-airway obstruction in chronic obstructive pulmonary disease. *New England Journal of Medicine*. 2004;350:45-53.

273. Saetta M, Turato G, Maestrelli P, Mapp CE, Fabbri LM. Cellular and structural bases of chronic obstructive pulmonary disease. *Am J Respir Crit Care Med*. 2001;163(6):1304-1309. doi:10.1164/ajrccm.163.6.2009116

274. Brusselle GG, Joos GF, Bracke KR. New insights into the immunology of chronic obstructive pulmonary disease. *Lancet*. 2011;378(9795):1015-1026. doi:10.1016/S0140-6736(11)60988-4

275. Chen Y, Thai P, Zhao YH, Ho YS, DeSouza MM, Wu R. Stimulation of airway mucin gene expression by interleukin (IL)-17 through IL-6 paracrine/autocrine loop. *J Biol Chem*. 2003;278(19):17036-17043. doi:10.1074/jbc.M210429200

276. Nyunoya T, Mebratu Y, Contreras A, Delgado M, Chand HS, Tesfaigzi Y. Molecular processes that drive cigarette smoke-induced epithelial cell fate of the lung. *Am J Respir Cell Mol Biol*. 2014;50(3):471-482. doi:10.1165/rcmb.2013-0348TR

277. Brusselle GG, Demoor T, Bracke KR, Brandsma CA TW. Lymphoid follicles in (very) severe COPD: beneficial or harmful? *Eur Respir J*. 2009;34:219-230.

278. van der Strate BW, Postma DS, Brandsma CA, Melgert BN L, MA, Geerlings M, Hylkema MN, van den Berg A, Timens W K, HA. Cigarette smoke-induced emphysema: a role for the B cell? *American Journal of Respiratory and Critical Care Medicine*. 2006;173:751-758.

279. Faner R, Cruz T, Casserras T, López-Giraldo A, Noell G CI, Tal-Singer R, Miller B, Rodriguez-Roisin R, Spira A KS, A A. Network analysis of lung transcriptomics reveals a distinct B cell signature in emphysema. *American Journal of Respiratory and Critical Care Medicine*. 2016;193(11):1190-1192.

280. Baraldo S, Turato G, Lunardi F, Bazzan E, Schiavon M FI, Molena B, Cazzuffi R, Damin M, Balestro E, Luisetti M RF, Calabrese F, Cosio MG SM. Immune activation in alpha1-antitrypsin-deficiency emphysema. Beyond the protease-antiprotease paradigm. *Am J Respir Crit Care Med*. 2015;191:402-409.

281. Faner R, Cruz T, Casserras T, Lopez-Giraldo A, Noell G CI, Tal-Singer R, Miller B, Rodriguez-Roisin R, Spira A KS, A. A. Network analysis of lung transcriptomics reveals a distinct B-cell signature in emphysema. *American Journal of Respiratory and Critical Care Medicine*. 2016;193:1242-1253.

282. Demoor T, Bracke KR, Maes T, Vandooren B, Elewaut D PC, Joos GF BGG. Role of lymphotoxin-alpha in cigarette smokeinduced inflammation and lymphoid neogenesis. *European Respiratory Journal*. 2009;34:405-416.

283. Polverino F, Seys LJM, Bracke KR, Owen CA. B cells in chronic obstructive pulmonary disease: moving to center stage. *American Journal of Physiology - Lung Cellular and Molecular Physiology*. 2016;311(4):L687-L695. doi:10.1152/ajplung.00304.2016

284. Gregersen PK OL. Recent advances in the genetics of autoimmune disease. *Annual Review of Immunology*. 2009;27:363-391.

285. Costenbader KH KEW. Cigarette smoking and autoimmune disease: what can we learn from epidemiology? *lupus*. 2006;15:737-745.

286. Agusti A, Macnee W, Donaldson K CM. Hypothesis: does COPD have an autoimmune component? *Thorax*. 2003;58:832-834.

287. Kheradmand F, Shan M, Xu C CDB. Autoimmunity in chronic obstructive pulmonary disease: clinical and experimental evidence. *Expert Review of Clinical Immunology*. 2012;8:285-292.

288. Kirkham PA, Caramori G, Casolari P, Papi AA, Edwards M S, B, Triantaphyllopoulos K, Hussain F, Pinart M, Khan Y H, L, Stevens L, Yeadon M, Barnes PJ, Chung KF AIM. Oxidative stress-induced antibodies to carbonyl-modified protein correlate with severity of

chronic obstructive pulmonary disease. *American Journal of Respiratory and Critical Care Medicine*. 2011;184:796-802.

289. Abdul RM, Fernstrand AM, Redegeld FA, Blalock JE GA, G. F. The matrikine PGP as a potential biomarker in COPD. *Am J Physiol Lung Cell Mol Physiol*. 2015;308:L1095-L1101.

290. Sellami M, Meghraoui-Kheddar A, Terryn C, Fichel C BN, Diebold MD, Guenounou M, Hery-Huynh S LNR. Induction and regulation of murine emphysema by elastin peptides. *American Journal of Physiology - Lung Cellular and Molecular Physiology*. 2016;310:L8-L23.

291. Agusti A, Calverley PM, Celli B, Coxson HO, Edwards LD L, DA, Macnee W, Miller BE, Rennard S, Silverman EK TSR, Wouters E, Yates JC VJ. Characterisation of COPD heterogeneity in the ECLIPSE cohort. *Respir Res*. 2010;11:122.

292. Zhu N, Zhang D, Wang W, et al. A Novel Coronavirus from Patients with Pneumonia in China, 2019. *New England Journal of Medicine*. 2020;382(8):727-733. doi:10.1056/NEJMoa2001017

293. Huang C, Wang Y, Li X, et al. Clinical features of patients infected with 2019 novel coronavirus in Wuhan, China. *The Lancet*. 2020;395(10223):497-506. doi:10.1016/S0140-6736(20)30183-5

294. Yan R, Zhang Y, Li Y, Xia L, Guo Y, Zhou Q. Structural basis for the recognition of SARS-CoV-2 by full-length human ACE2. *Science*. 2020;367(6485):1444-1448. doi:10.1126/science.abb2762

295. Huang AT, Garcia-Carreras B, Hitchings MDT, et al. A systematic review of antibody mediated immunity to coronaviruses: antibody kinetics, correlates of protection, and association of antibody responses with severity of disease. *medRxiv*. Published online April 17, 2020:2020.04.14.20065771. doi:10.1101/2020.04.14.20065771

296. Wertheim JO. A Glimpse Into the Origins of Genetic Diversity in the Severe Acute Respiratory Syndrome Coronavirus 2. *Clin Infect Dis*. 2020;71(15):721-722. doi:10.1093/cid/ciaa213

297. B L, Hr S, Y Z, et al. Discovery of Bat Coronaviruses through Surveillance and Probe Capture-Based Next-Generation Sequencing. *mSphere*. 2020;5(1). doi:10.1128/msphere.00807-19

298. Li X, Zai J, Zhao Q, et al. Evolutionary history, potential intermediate animal host, and cross-species analyses of SARS-CoV-2. *J Med Virol*. Published online March 11, 2020. doi:10.1002/jmv.25731

299. Raoult D, Zumla A, Locatelli F, Ippolito G, Kroemer G. Coronavirus infections: Epidemiological, clinical and immunological features and hypotheses. *Cell Stress*. 4(4):66-75. doi:10.15698/cst2020.04.216

300. García LF. Immune Response, Inflammation, and the Clinical Spectrum of COVID-19. *Front Immunol*. 2020;11. doi:10.3389/fimmu.2020.01441

301. Fung TS, Liu DX. Human Coronavirus: Host-Pathogen Interaction. *Annual Review of Microbiology*. 2019;73(1):529-557. doi:10.1146/annurev-micro-020518-115759

302. Walls AC, Park YJ, Tortorici MA, Wall A, McGuire AT, Veesler D. Structure, Function, and Antigenicity of the SARS-CoV-2 Spike Glycoprotein. *Cell*. 2020;181(2):281-292.e6. doi:10.1016/j.cell.2020.02.058

303. Fauci AS, Lane HC, Redfield RR. Covid-19 — Navigating the Uncharted. *New England Journal of Medicine*. 2020;382(13):1268-1269. doi:10.1056/NEJMe2002387

304. Chen T, Wu D, Chen H, et al. Clinical characteristics of 113 deceased patients with coronavirus disease 2019: retrospective study. *BMJ*. 2020;368. doi:10.1136/bmj.m1091

305. Wu C, Chen X, Cai Y, et al. Risk Factors Associated With Acute Respiratory Distress Syndrome and Death in Patients With Coronavirus Disease 2019 Pneumonia in Wuhan, China. *JAMA Intern Med*. 2020;180(7):934-943. doi:10.1001/jamainternmed.2020.0994

306. Yang J, Zheng Y, Gou X, et al. Prevalence of comorbidities and its effects in patients infected with SARS-CoV-2: a systematic review and meta-analysis. *International Journal of Infectious Diseases*. 2020;94:91-95. doi:10.1016/j.ijid.2020.03.017

307. Zhang H, Zhou P, Wei Y, et al. Histopathologic Changes and SARS-CoV-2 Immunostaining in the Lung of a Patient With COVID-19. *Annals of Internal Medicine*. 2020;172(9):629-632. doi:10.7326/M20-0533

308. Zhou Y, Zhang Z, Tian J, Xiong S. Risk factors associated with disease progression in a cohort of patients infected with the 2019 novel coronavirus. *Annals of Palliative Medicine*. 2020;9(2):428-436-436. doi:10.21037/apm.2020.03.26

309. Vabret N, Britton GJ, Gruber C, et al. Immunology of COVID-19: Current State of the Science. *Immunity*. 2020;52(6):910-941. doi:10.1016/j.immuni.2020.05.002

310. Moore JB, June CH. Cytokine release syndrome in severe COVID-19. *Science*. 2020;368(6490):473-474. doi:10.1126/science.abb8925

311. Shi Y, Wang Y, Shao C, et al. COVID-19 infection: the perspectives on immune responses. *Cell Death & Differentiation*. 2020;27(5):1451-1454. doi:10.1038/s41418-020-0530-3

312. Dandekar AA, Perlman S. Immunopathogenesis of coronavirus infections: implications for SARS. *Nature Reviews Immunology*. 2005;5(12):917-927. doi:10.1038/nri1732

313. Fung TS, Liu DX. The ER stress sensor IRE1 and MAP kinase ERK modulate autophagy induction in cells infected with coronavirus infectious bronchitis virus. *Virology*. 2019;533:34-44. doi:10.1016/j.virol.2019.05.002

314. Shi CS, Qi HY, Boularan C, et al. SARS-CoV ORF-9b suppresses innate immunity by targeting mitochondria and the MAVS/TRAF3/TRAF6 signalosome. *J Immunol*. 2014;193(6):3080-3089. doi:10.4049/jimmunol.1303196

315. Kuba K, Imai Y, Rao S, et al. A crucial role of angiotensin converting enzyme 2 (ACE2) in SARS coronavirus–induced lung injury. *Nature Medicine*. 2005;11(8):875-879. doi:10.1038/nm1267

316. Imai Y, Kuba K, Rao S, et al. Angiotensin-converting enzyme 2 protects from severe acute lung failure. *Nature*. 2005;436(7047):112-116. doi:10.1038/nature03712

317. Tan YJ, Goh PY, Fielding BC, et al. Profiles of Antibody Responses against Severe Acute Respiratory Syndrome Coronavirus Recombinant Proteins and Their Potential Use as Diagnostic Markers. *Clin Diagn Lab Immunol*. 2004;11(2):362-371. doi:10.1128/CDLI.11.2.362-371.2004

318. Wu HS, Hsieh YC, Su IJ, et al. Early Detection of Antibodies against Various Structural Proteins of the SARS-Associated Coronavirus in SARS Patients. *JBS*. 2004;11(1):117-126. doi:10.1159/000075294

319. Meyer B, Drosten C, Müller MA. Serological assays for emerging coronaviruses: Challenges and pitfalls. *Virus Research*. 2014;194:175-183. doi:10.1016/j.virusres.2014.03.018

320. Li G, Chen X, Xu A. Profile of Specific Antibodies to the SARS-Associated Coronavirus. *New England Journal of Medicine*. 2003;349(5):508-509. doi:10.1056/NEJM200307313490520

321. Li CK fai, Wu H, Yan H, et al. T Cell Responses to Whole SARS Coronavirus in Humans. *J Immunol*. 2008;181(8):5490-5500.

322. Prompetchara E, Ketloy C, Palaga T. Immune responses in COVID-19 and potential vaccines: Lessons learned from SARS and MERS epidemic. *Asian Pac J Allergy Immunol*. 2020;38(1):1-9. doi:10.12932/AP-200220-0772

323. Hou H, Wang T, Zhang B, et al. Detection of IgM and IgG antibodies in patients with coronavirus disease 2019. *Clin Transl Immunology*. 2020;9(5):e01136. doi:10.1002/cti2.1136

324. Thevarajan I, Nguyen THO, Koutsakos M, et al. Breadth of concomitant immune responses prior to patient recovery: a case report of non-severe COVID-19. *Nat Med*. 2020;26(4):453-455. doi:10.1038/s41591-020-0819-2

325. Plotkin SA. Correlates of protection induced by vaccination. *Clin Vaccine Immunol*. 2010;17(7):1055-1065. doi:10.1128/CVI.00131-10

326. Newell KL, Clemmer DC, Cox JB, et al. Switched and unswitched memory B cells detected during SARS-CoV-2 convalescence correlate with limited symptom duration. *PLoS One*. 2021;16(1):e0244855. doi:10.1371/journal.pone.0244855

327. Mateus J, Grifoni A, Tarke A, et al. Selective and cross-reactive SARS-CoV-2 T cell epitopes in unexposed humans. *Science*. 2020;370(6512):89-94. doi:10.1126/science.abd3871

328. Remy KE, Mazer M, Striker DA, et al. Severe immunosuppression and not a cytokine storm characterizes COVID-19 infections. *JCI Insight*. 2020;5(17):140329. doi:10.1172/jci.insight.140329

329. Moderbacher CR, Ramirez SI, Dan JM, et al. Antigen-specific adaptive immunity to SARS-CoV-2 in acute COVID-19 and associations with age and disease severity. *Cell*. Published online 2020. doi:https://doi.org/10.1016/j.cell.2020.09.038

330. Zheng HY, Zhang M, Yang CX, et al. Elevated exhaustion levels and reduced functional diversity of T cells in peripheral blood may predict severe progression in COVID-19 patients. *Cell Mol Immunol*. 2020;17(5):541-543. doi:10.1038/s41423-020-0401-3

331. Kaneko N, Kuo HH, Boucau J, et al. Loss of Bcl-6-Expressing T Follicular Helper Cells and Germinal Centers in COVID-19. *Cell*. 2020;183(1):143-157.e13. doi:10.1016/j.cell.2020.08.025

332. Van Cleemput J, van Snippenberg W, Lambrechts L, et al. Organ-specific genome diversity of replication-competent SARS-CoV-2. *Nat Commun*. 2021;12(1):6612. doi:10.1038/s41467-021-26884-7

333. Cox RJ, Brokstad KA. Not just antibodies: B cells and T cells mediate immunity to COVID-19. *Nat Rev Immunol*. 2020;20(10):581-582. doi:10.1038/s41577-020-00436-4

334. Kato A, Hulse KE, BK T, S.R.P. B-lymphocyte lineage cells and the respiratory system. *J Allergy Clin Immunol*. 2013;131:933-957.

335. Mauri C, Bosma A. Immune Regulatory Function of B Cells. *Annu Rev Immunol*. 2012;30(1):221-241. doi:10.1146/annurev-immunol-020711-074934

336. Mauri C, Menon M. The expanding family of regulatory B cells. *Int Immunol*. 2015;27(10):479-486. doi:10.1093/intimm/dxv038

337. Mauri C, Menon M. Human regulatory B cells in health and disease: therapeutic potential. *J Clin Invest*. 2017;127(3):772-779. doi:10.1172/JCI85113

338. Polverino F, Seys LJM, Bracke KR, Owen CA. B cells in chronic obstructive pulmonary disease: moving to center stage. *American Journal of Physiology-Lung Cellular and Molecular Physiology*. 2016;311(4):L687-L695. doi:10.1152/ajplung.00304.2016

339. Zhou J, Min Z, Zhang D, Wang W, Marincola F, Wang X. Enhanced frequency and potential mechanism of B regulatory cells in patients with lung cancer. *Journal of translational medicine*. 2014;12:304. doi:10.1186/s12967-014-0304-0

340. Zhang M, Zheng X, Zhang J, et al. CD19(+)CD1d(+)CD5(+) B cell frequencies are increased in patients with tuberculosis and suppress Th17 responses. *Cellular immunology*. 2012;274(1-2):89-97. doi:10.1016/j.cellimm.2012.01.007

341. Vlugt LE, E.Mlejnek AOF, TRD MJB, Labuda LA. CD24(hi)CD27(+) B cells from patients with allergic asthma have impaired regulatory activity in response to lipopolysaccharide. *Clin Exp Allergy*. 2014;44(4):517-528.

342. Mavropoulos A, Simopoulou T, Varna A, et al. Breg Cells Are Numerically Decreased and Functionally Impaired in Patients With Systemic Sclerosis. *Arthritis & Rheumatology (Hoboken, NJ)*. 2016;68(2):494-504. doi:10.1002/art.39437

343. Rosser EC, Oleinika K, Tonon S, et al. Regulatory B cells are induced by gut microbiota–driven interleukin-1β and interleukin-6 production. *Nature Medicine*. 2014;20(11):1334-1339. doi:10.1038/nm.3680

344. Menon M, Blair PA, Isenberg DA, Mauri C. A Regulatory Feedback between Plasmacytoid Dendritic Cells and Regulatory B Cells Is Aberrant in Systemic Lupus Erythematosus. *Immunity*. 2016;44(3):683-697. doi:10.1016/j.immuni.2016.02.012

345. Schubert RD, Hu Y, Kumar G, et al. IFN-β treatment requires B cells for efficacy in neuroautoimmunity. *J Immunol*. 2015;194(5):2110-2116. doi:10.4049/jimmunol.1402029

346. Yoshizaki A, Miyagaki T, DiLillo DJ, Matsushita T, EIK MH. Regulatory B cells control T-cell autoimmunity through IL-21-dependent cognate interactions. *Nature*. 2012;491(7423):264-268.

347. Yang M, Sun L, Wang S, et al. Novel function of B cell-activating factor in the induction of IL-10-producing regulatory B cells. *J Immunol*. 2010;184(7):3321-3325. doi:10.4049/jimmunol.0902551

348. Wang RX, Yu CR, Dambuza IM, et al. Interleukin-35 Induces Regulatory B Cells that Suppress CNS Autoimmune Disease. *Nat Med*. 2014;20(6):633-641. doi:10.1038/nm.3554

349. Li X, Mai J, Virtue A, et al. IL-35 is a novel responsive anti-inflammatory cytokine--a new system of categorizing anti-inflammatory cytokines. *PLoS ONE*. 2012;7(3):e33628. doi:10.1371/journal.pone.0033628

350. Liu BS, Cao Y, Huizinga TW, Hafler DA, Toes REM. TLR-mediated STAT3 and ERK activation controls IL-10 secretion by human B cells. *Eur J Immunol*. 2014;44(7):2121-2129. doi:10.1002/eji.201344341

351. Piper CJM, Rosser EC, Oleinika K, et al. Aryl Hydrocarbon Receptor Contributes to the Transcriptional Program of IL-10-Producing Regulatory B Cells. *Cell Reports*. 2019;29(7):1878-1892.e7. doi:10.1016/j.celrep.2019.10.018

352. Xiao S, Bod L, Pochet N, et al. Checkpoint Receptor TIGIT Expressed on Tim-1+ B Cells Regulates Tissue Inflammation. *Cell Rep*. 2020;32(2):107892. doi:10.1016/j.celrep.2020.107892

353. Wang YH, Tsai DY, Ko YA, et al. Blimp-1 Contributes to the Development and Function of Regulatory B Cells. *Front Immunol*. 2019;10:1909. doi:10.3389/fimmu.2019.01909

354. Matsumoto M, Baba A, Yokota T, et al. Interleukin-10-Producing Plasmablasts Exert Regulatory Function in Autoimmune Inflammation. *Immunity*. 2014;41(6):1040-1051. doi:10.1016/j.immuni.2014.10.016

355. Shen P, Roch T, Lampropoulou V, et al. IL-35-producing B cells are critical regulators of immunity during autoimmune and infectious diseases. *Nature*. 2014;507(7492):366-370. doi:10.1038/nature12979

356. Pioli PD. Plasma Cells, the Next Generation: Beyond Antibody Secretion. *Front Immunol*. 2019;10:2768. doi:10.3389/fimmu.2019.02768

357. Fehres CM, van Uden NO, Yeremenko NG, et al. APRIL Induces a Novel Subset of IgA+ Regulatory B Cells That Suppress Inflammation via Expression of IL-10 and PD-L1. *Front Immunol*. 2019;10:1368. doi:10.3389/fimmu.2019.01368

358. Fillatreau S. Natural regulatory plasma cells. *Curr Opin Immunol*. 2018;55:62-66. doi:10.1016/j.coi.2018.09.012

359. Amu S, Saunders SP, Kronenberg M, Mangan NE, Atzberger A, Fallon PG. Regulatory B cells prevent and reverse allergic airway inflammation via FoxP3-positive T regulatory cells in a murine model. *J Allergy Clin Immunol*. 2010;125(5):1114-1124.e8. doi:10.1016/j.jaci.2010.01.018

360. Lal G, Nakayama Y, Sethi A, Singh AK, Burrell BE, Kulkarni N. Interleukin- 10 from marginal zone precursor B-cell subset is required for costimulatory blockade- induced transplantation tolerance. *Transplantation*. 2015;99(9):1817-1828.

361. Alhabbab R, Blair P, Elgueta R, Stolarczyk E, Marks E, Becker PD. Diversity of gut microflora is required for the generation of B cell with regulatory properties in a skin graft model. *Sci Rep*. 2015;5(11554).

362. Evans JG, Chavez-Rueda KA, Eddaoudi A, et al. Novel Suppressive Function of Transitional 2 B Cells in Experimental Arthritis. *The Journal of Immunology*. 2007;178(12):7868-7878. doi:10.4049/jimmunol.178.12.7868

363. Watanabe R, Ishiura N, Nakashima H, et al. Regulatory B Cells (B10 Cells) Have a Suppressive Role in Murine Lupus: CD19 and B10 Cell Deficiency Exacerbates Systemic

Autoimmunity. *The Journal of Immunology*. 2010;184(9):4801-4809. doi:10.4049/jimmunol.0902385

364.   Blair PA, Norena LY, Flores-Borja F, Rawlings DJ, MRE DAI. CD19(+)CD24(hi)CD38(hi) B cells exhibit regulatory capacity in healthy individuals but are functionally impaired in systemic lupus erythematosus patients. *Immunity*. 2010;32(1):129-140.

365.   Sheng JR, Soliven SQB. IL-10 derived from CD1dhiCD5(+) B cells regulates experimental autoimmune myasthenia gravis. *J Neuroimmunol*. 2015;289:130-138.

366.   Bankoti R, Gupta K, Levchenko A, Stager S. Marginal zone B cells regulate antigen-specific T cell responses during infection. *J Immunol*. 2012;188(8):3961-3971.

367.   Blair PA, Chavez-Rueda KA, Evans JG, Shlomchik MJ, DAI AE. Selective targeting of B cells with agonistic anti-CD40 is an efficacious strategy for the generation of induced regulatory T2-like B cells and for the suppression of lupus in MRL/lpr mice. *J Immunol*. 2009;182(6):3492-3502.

368.   Ding Q, Yeung M, Camirand G, et al. Regulatory B cells are identified by expression of TIM-1 and can be induced through TIM-1 ligation to promote tolerance in mice. *J Clin Invest*. 2011;121(9):3645-3656. doi:10.1172/JCI46274

369.   Xiao S, Brooks CR, Sobel RA, Kuchroo VK. Tim-1 Is Essential for Induction and Maintenance of IL-10 in Regulatory B Cells and Their Regulation of Tissue Inflammation. *The Journal of Immunology*. 2015;194(4):1602-1608. doi:10.4049/jimmunol.1402632

370.   Khan AR, Hams E, Floudas A, Sparwasser T, Weaver CT, Fallon PG. PD-L1 hi B cells are critical regulators of humoral immunity. *Nature Communications*. 2015;6(1):5997. doi:10.1038/ncomms6997

371.   Iwata Y, Matsushita T, Horikawa M, et al. Characterization of a rare IL-10–competent B-cell subset in humans that parallels mouse regulatory B10 cells. *Blood*. 2011;117(2):530-541. doi:10.1182/blood-2010-07-294249

372.   Veen W, Stanic B, Yaman G, Wawrzyniak M, Sollner S, Akdis DG. IgG4 production is confined to human IL-10-producing regulatory B cells that suppress antigen-specific immune responses. *J Allergy Clin Immunol*. 2013;131(4):1204-1212.

373.   Lindner S, Dahlke K, Sontheimer K, et al. Interleukin 21-induced granzyme B-expressing B cells infiltrate tumors and regulate T cells. *Cancer Res*. 2013;73(8):2468-2479. doi:10.1158/0008-5472.CAN-12-3450

374.   Kaku H, Cheng KF, Al-Abed Y, Rothstein TL. A Novel Mechanism of B Cell–Mediated Immune Suppression through CD73 Expression and Adenosine Production. *The Journal of Immunology*. 2014;193(12):5904-5913. doi:10.4049/jimmunol.1400336

375. Saze Z, Schuler PJ, Hong CS, Cheng D, Jackson EK, Whiteside TL. Adenosine production by human B cells and B cell-mediated suppression of activated T cells. *Blood*. 2013;122(1):9-18. doi:10.1182/blood-2013-02-482406

376. Aravena O, Ferrier A, Menon M, et al. TIM-1 defines a human regulatory B cell population that is altered in frequency and function in systemic sclerosis patients. *Arthritis Res Ther*. 2017;19(1):8. doi:10.1186/s13075-016-1213-9

377. Baba Y, Saito Y, Kotetsu Y. Heterogeneous subsets of B-lineage regulatory cells (Breg cells). *Int Immunol*. 2020;32(3):155-162. doi:10.1093/intimm/dxz068

378. Sheng JR, Soliven SQB. CD1d(hi)CD5+ B cells expanded by GM-CSF in vivo suppress experimental autoimmune myasthenia gravis. *J Immunol*. 2014;193(6):2669-2677.

379. Chien CH, Chiang BL. Regulatory T cells induced by B cells: a novel subpopulation of regulatory T cells. *J Biomed Sci*. 2017;24(1):86. doi:10.1186/s12929-017-0391-3

380. Flores-Borja F, Bosma A, Ng D, Reddy V, Ehrenstein MR, Isenberg DA. CD19+CD24hiCD38hi B cells maintain regulatory T cells while limiting TH1 and TH17 differentiation. *Sci Transl Med*. 2013;5(173).

381. Bankoti R, Gupta K, Levchenko A, Stäger S. Marginal Zone B Cells Regulate Antigen-Specific T Cell Responses during Infection. *The Journal of Immunology*. 2012;188(8):3961-3971. doi:10.4049/jimmunol.1102880

382. Watanabe R, Fujimoto M, Ishiura N, et al. CD19 Expression in B Cells Is Important for Suppression of Contact Hypersensitivity. *The American Journal of Pathology*. 2007;171(2):560-570. doi:10.2353/ajpath.2007.061279

383. Loxton AG. Bcells and their regulatory functions during Tuberculosis: Latency and active disease. *Molecular Immunology*. 2019;111:145-151. doi:10.1016/j.molimm.2019.04.012

384. Grainger JR, Smith KA, Hewitson JP, et al. Helminth secretions induce de novo T cell Foxp3 expression and regulatory function through the TGF-β pathway. *J Exp Med*. 2010;207(11):2331-2341. doi:10.1084/jem.20101074

385. Oleinika K, Rosser EC, Matei DE, et al. CD1d-dependent immune suppression mediated by regulatory B cells through modulations of iNKT cells. *Nature Communications*. 2018;9(1):684. doi:10.1038/s41467-018-02911-y

386. Nouël A, Pochard P, Simon Q, et al. B-Cells induce regulatory T cells through TGF-β/IDO production in A CTLA-4 dependent manner. *Journal of Autoimmunity*. 2015;59:53-60. doi:10.1016/j.jaut.2015.02.004

387. Bosma A, Abdel-Gadir A, Isenberg DA, Jury EC, CMauri. Lipid-antigen presentation by CD1d(+) B cells is essential for the maintenance of invariant natural killer T cells. *Immunity*. 2012;36(3):477-490.

388. Parekh VV, Prasad DV, Banerjee PP, Joshi BN, Kumar A, Mishra GC. B cells activated by lipopolysaccharide, but not by anti-Ig and anti-CD40 antibody, induce anergy in CD8+ T cells: role of TGF-beta 1. *J Immunol*. 2003;170(12):5897-5911.

389. Tian J, Zekzer D, Hanssen L, Lu Y, Olcott A, Kaufman DL. Lipopolysaccharide-activated B cells down-regulate Th1 immunity and prevent autoimmune diabetes in nonobese diabetic mice. *J Immunol*. 2001;167(2):1081-1089. doi:10.4049/jimmunol.167.2.1081

390. Salvi S, Holgate ST. Could the airway epithelium play an important role in mucosal immunoglobulin A production? *Clin Exp Allergy*. 1999;29(12):1597-1605. doi:10.1046/j.1365-2222.1999.00644.x

391. Carragher DM, Rangel-Moreno J, Randall TD. Ectopic lymphoid tissues and local immunity. *Semin Immunol*. 2008;20(1):26-42. doi:10.1016/j.smim.2007.12.004

392. Barone F, Gardner DH, Nayar S, Steinthal N, Buckley CD, Luther SA. Stromal Fibroblasts in Tertiary Lymphoid Structures: A Novel Target in Chronic Inflammation. *Front Immunol*. 2016;7:477. doi:10.3389/fimmu.2016.00477

393. Carlsen HS, Baekkevold ES, Johansen FE, Haraldsen G, Brandtzaeg P. B cell attracting chemokine 1 (CXCL13) and its receptor CXCR5 are expressed in normal and aberrant gut associated lymphoid tissue. *Gut*. 2002;51(3):364-371.

394. Nerviani A, Pitzalis C. Role of chemokines in ectopic lymphoid structures formation in autoimmunity and cancer. *J Leukoc Biol*. 2018;104(2):333-341. doi:10.1002/JLB.3MR0218-062R

395. Alsughayyir J, Pettigrew GJ, Motallebzadeh R. Spoiling for a Fight: B Lymphocytes As Initiator and Effector Populations within Tertiary Lymphoid Organs in Autoimmunity and Transplantation. *Front Immunol*. 2017;8:1639. doi:10.3389/fimmu.2017.01639

396. Tang H, Zhu M, Qiao J, Fu YX. Lymphotoxin signalling in tertiary lymphoid structures and immunotherapy. *Cell Mol Immunol*. 2017;14(10):809-818. doi:10.1038/cmi.2017.13

397. Rasheed AU, Rahn HP, Sallusto F, Lipp M, Müller G. Follicular B helper T cell activity is confined to CXCR5(hi)ICOS(hi) CD4 T cells and is independent of CD57 expression. *Eur J Immunol*. 2006;36(7):1892-1903. doi:10.1002/eji.200636136

398. Rao DA. T Cells That Help B Cells in Chronically Inflamed Tissues. *Front Immunol*. 2018;9:1924. doi:10.3389/fimmu.2018.01924

399. Stebegg M, Kumar SD, Silva-Cayetano A, Fonseca VR, Linterman MA, Graca L. Regulation of the Germinal Center Response. *Front Immunol*. 2018;9:2469. doi:10.3389/fimmu.2018.02469

400. Jones GW, Jones SA. Ectopic lymphoid follicles: inducible centres for generating antigen-specific immune responses within tissues. *Immunology*. 2016;147(2):141-151. doi:10.1111/imm.12554

401. Allie SR, Bradley JE, Mudunuru U, et al. The establishment of resident memory B cells in the lung requires local antigen encounter. *Nature Immunology*. 2019;20(1):97-108. doi:10.1038/s41590-018-0260-6

402. Barker KA, Shenoy AT, Stauffer-Smith N, et al. Lung resident memory B cells are a common and functionally significant component of lung adaptive immunity. *The Journal of Immunology*. 2020;204(1 Supplement):85.8-85.8.

403. Brandtzaeg P. Mucosal immunity: induction, dissemination, and effector functions. *Scand J Immunol*. 2009;70(6):505-515. doi:10.1111/j.1365-3083.2009.02319.x

404. Corthésy B. Role of secretory immunoglobulin A and secretory component in the protection of mucosal surfaces. *Future Microbiol*. 2010;5(5):817-829. doi:10.2217/fmb.10.39

405. Kaetzel CS, Robinson JK, Chintalacharuvu KR, Vaerman JP, Lamm ME. The polymeric immunoglobulin receptor (secretory component) mediates transport of immune complexes across epithelial cells: a local defense function for IgA. *PNAS*. 1991;88(19):8796-8800. doi:10.1073/pnas.88.19.8796

406. Kiyono H, Fukuyama S. NALT- versus Peyer's-patch-mediated mucosal immunity. *Nat Rev Immunol*. 2004;4(9):699-710. doi:10.1038/nri1439

407. Brandtzaeg P, Johansen FE. Mucosal B cells: phenotypic characteristics, transcriptional regulation, and homing properties. *Immunological Reviews*. 2005;206(1):32-63. doi:10.1111/j.0105-2896.2005.00283.x

408. Morteau O, Gerard C, Lu B, et al. An Indispensable Role for the Chemokine Receptor CCR10 in IgA Antibody Secreting Cell Accumulation. *J Immunol*. 2008;181(9):6309-6315.

409. Kunkel EJ, Butcher EC. Plasma-cell homing. *Nature Reviews Immunology*. 2003;3(10):822-829. doi:10.1038/nri1203

410. Cook-Mills JM. VCAM-1 signals during lymphocyte migration: role of reactive oxygen species. *Mol Immunol*. 2002;39(9):499-508.

411. Xu B, Wagner N, Pham LN, et al. Lymphocyte Homing to Bronchus-associated Lymphoid Tissue (BALT) Is Mediated by L-selectin/PNAd, α4β1 Integrin/VCAM-1, and LFA-1 Adhesion Pathways. *J Exp Med*. 2003;197(10):1255-1267. doi:10.1084/jem.20010685

412. Onodera T, Takahashi Y, Yokoi Y, et al. Memory B cells in the lung participate in protective humoral immune responses to pulmonary influenza virus reinfection. *Proc Natl Acad Sci USA*. 2012;109(7):2485-2490. doi:10.1073/pnas.1115369109

413. Hamelmann E, Vella AT, Oshiba A, Kappler JW, Marrack P, Gelfand EW. Allergic airway sensitization induces T cell activation but not airway hyperresponsiveness in B cell-deficient mice. *Proc Natl Acad Sci USA*. 1997;94(4):1350. doi:10.1073/pnas.94.4.1350

414. Samitas K, Malmhäll C, Rådinger M, et al. Precursor B Cells Increase in the Lung during Airway Allergic Inflammation: A Role for B Cell-Activating Factor. *PLoS One*. 2016;11(8):e0161161. doi:10.1371/journal.pone.0161161

415. Turner DL, Verter J, Turner R, Cao M. Tissue resident memory B cells established in lungs in allergic asthma. *J Immunol*. 2017;198(1 Supplement):71.3.

416. Habener A, Behrendt AK, Skuljec J, Jirmo AC, Meyer-Bahlburg A, Hansen G. B cell subsets are modulated during allergic airway inflammation but are not required for the development of respiratory tolerance in a murine model. *Eur J Immunol*. 2017;47(3):552-562. doi:10.1002/eji.201646518

417. Kirkham PA, Caramori G, Casolari P, et al. Oxidative stress-induced antibodies to carbonyl-modified protein correlate with severity of chronic obstructive pulmonary disease. *Am J Respir Crit Care Med*. 2011;184(7):796-802. doi:10.1164/rccm.201010-1605OC

418. Hogg JC, Chu F, Utokaparch S, et al. The nature of small-airway obstruction in chronic obstructive pulmonary disease. *N Engl J Med*. 2004;350(26):2645-2653. doi:10.1056/NEJMoa032158

419. Faner R, Cruz T, Casserras T, et al. Network Analysis of Lung Transcriptomics Reveals a Distinct B-Cell Signature in Emphysema. *Am J Respir Crit Care Med*. 2016;193(11):1242-1253. doi:10.1164/rccm.201507-1311OC

420. Baraldo S, Turato G, Lunardi F, et al. Immune activation in α1-antitrypsin-deficiency emphysema. Beyond the protease-antiprotease paradigm. *Am J Respir Crit Care Med*. 2015;191(4):402-409. doi:10.1164/rccm.201403-0529OC

421. van der Strate BWA, Postma DS, Brandsma CA, et al. Cigarette smoke-induced emphysema: A role for the B cell? *Am J Respir Crit Care Med*. 2006;173(7):751-758. doi:10.1164/rccm.200504-594OC

422. Todd NW, Scheraga RG, Galvin JR, et al. Lymphocyte aggregates persist and accumulate in the lungs of patients with idiopathic pulmonary fibrosis. *J Inflamm Res*. 2013;6:63-70. doi:10.2147/JIR.S40673

423. Xue J, Kass DJ, Bon J, et al. Plasma B lymphocyte stimulator and B cell differentiation in idiopathic pulmonary fibrosis patients. *J Immunol*. 2013;191(5):2089-2095. doi:10.4049/jimmunol.1203476

424. Feng Y, Yang M, Wu H, Lu Q. The pathological role of B cells in systemic lupus erythematosus: From basic research to clinical. *null*. 2020;53(2):56-64. doi:10.1080/08916934.2019.1700232

425. Bugatti S, Vitolo B, Caporali R, Montecucco C, Manzo A. B cells in rheumatoid arthritis: from pathogenic players to disease biomarkers. *Biomed Res Int*. 2014;2014:681678. doi:10.1155/2014/681678

426. Yoshizaki A. Pathogenic roles of B lymphocytes in systemic sclerosis. *Immunol Lett*. 2018;195:76-82. doi:10.1016/j.imlet.2018.01.002

427. Nocturne G, Mariette X. B cells in the pathogenesis of primary Sjögren syndrome. *Nat Rev Rheumatol*. 2018;14(3):133-145. doi:10.1038/nrrheum.2018.1

428. Rangel-Moreno J, Hartson L, Navarro C, Gaxiola M, Selman M, Randall TD. Inducible bronchus-associated lymphoid tissue (iBALT) in patients with pulmonary complications of rheumatoid arthritis. *J Clin Invest*. 2006;116(12):3183-3194. doi:10.1172/JCI28756

429. Lafyatis R, O'Hara C, Feghali-Bostwick CA, Matteson E. B cell infiltration in systemic sclerosis–associated interstitial lung disease. *Arthritis & Rheumatism*. 2007;56(9):3167-3168. doi:10.1002/art.22847

430. Salomonsson S, Jonsson MV, Skarstein K, et al. Cellular basis of ectopic germinal center formation and autoantibody production in the target organ of patients with Sjögren's syndrome. *Arthritis Rheum*. 2003;48(11):3187-3201. doi:10.1002/art.11311

431. Sakkas LI, Bogdanos DP. Systemic sclerosis: New evidence re-enforces the role of B cells. *Autoimmun Rev*. 2016;15(2):155-161. doi:10.1016/j.autrev.2015.10.005

432. Levine DJ, Glanville AR, Aboyoun C, et al. Antibody-mediated rejection of the lung: A consensus report of the International Society for Heart and Lung Transplantation. *J Heart Lung Transplant*. 2016;35(4):397-406. doi:10.1016/j.healun.2016.01.1223

433. Roux A, Bendib Le Lan I, Holifanjaniaina S, et al. Antibody-Mediated Rejection in Lung Transplantation: Clinical Outcomes and Donor-Specific Antibody Characteristics. *Am J Transplant*. 2016;16(4):1216-1228. doi:10.1111/ajt.13589

434. Hunninghake GW, Crystal RG. Mechanisms of hypergammaglobulinemia in pulmonary sarcoidosis. Site of increased antibody production and role of T lymphocytes. *J Clin Invest*. 1981;67(1):86-92. doi:10.1172/JCI110036

435. Kamphuis LS, van Zelm MC, Lam KH, et al. Perigranuloma Localization and Abnormal Maturation of B Cells. *Am J Respir Crit Care Med*. 2013;187(4):406-416. doi:10.1164/rccm.201206-1024OC

436. Matsushita T, Hamaguchi Y, Hasegawa M, Takehara K, Fujimoto M. Decreased levels of regulatory B cells in patients with systemic sclerosis: association with autoantibody production and disease activity. *Rheumatology*. 2016;55(2):263-267. doi:10.1093/rheumatology/kev331

437. Su DL, Lu ZM, Shen MN, Li X, Sun LY. Roles of pro- and anti-inflammatory cytokines in the pathogenesis of SLE. *J Biomed Biotechnol*. 2012;2012:347141. doi:10.1155/2012/347141

438. Vazquez MI, Catalan-Dibene J, Zlotnik A. B cells responses and cytokine production are regulated by their immune microenvironment. *Cytokine*. 2015;74(2):318-326. doi:10.1016/j.cyto.2015.02.007

439. Mohd Jaya FN, Garcia SG, Borràs FE, Chan GCF, Franquesa M. Paradoxical role of Breg-inducing cytokines in autoimmune diseases. *Journal of Translational Autoimmunity*. 2019;2:100011. doi:10.1016/j.jtauto.2019.100011

440. Landskron G, De la Fuente M, Thuwajit P, Thuwajit C, Hermoso MA. Chronic inflammation and cytokines in the tumor microenvironment. *J Immunol Res*. 2014;2014:149185. doi:10.1155/2014/149185

441. Patel AJ, Richter A, Drayson MT, Middleton GW. The role of B lymphocytes in the immuno-biology of non-small-cell lung cancer. *Cancer Immunol Immunother*. 2020;69(3):325-342. doi:10.1007/s00262-019-02461-2

442. Miller YE. Pathogenesis of lung cancer: 100 year report. *Am J Respir Cell Mol Biol*. 2005;33(3):216-223. doi:10.1165/rcmb.2005-0158OE

443. Xiao X, Lao XM, Chen MM, et al. PD-1hi Identifies a Novel Regulatory B-cell Population in Human Hepatoma That Promotes Disease Progression. *Cancer Discov*. 2016;6(5):546-559. doi:10.1158/2159-8290.CD-15-1408

444. Varn FS, Wang Y, Cheng C. A B cell-derived gene expression signature associates with an immunologically active tumor microenvironment and response to immune checkpoint blockade therapy. *Oncoimmunology*. 2019;8(1):e1513440. doi:10.1080/2162402X.2018.1513440

445. Zhang Y, Morgan R, Chen C, et al. Mammary-tumor-educated B cells acquire LAP/TGF-β and PD-L1 expression and suppress anti-tumor immune responses. *International immunology*. 2016;28(9):423-433. doi:10.1093/intimm/dxw007

446. Sarvaria A, Madrigal JA, Saudemont A. B cell regulation in cancer and anti-tumor immunity. *Cellular & Molecular Immunology*. 2017;14(8):662-674. doi:10.1038/cmi.2017.35

447. Wang WW, Yuan XL, Chen H, et al. CD19+CD24hiCD38hiBregs involved in downregulate helper T cells and upregulate regulatory T cells in gastric cancer. *Oncotarget*. 2015;6(32):33486-33499. doi:10.18632/oncotarget.5588

448. Bodogai M, Moritoh K, Lee-Chang C, et al. Immunosuppressive and Prometastatic Functions of Myeloid-Derived Suppressive Cells Rely upon Education from Tumor-Associated B Cells. *Cancer research*. 2015;75(17):3456-3465. doi:10.1158/0008-5472.CAN-14-3077

449. Olkhanud PB, Damdinsuren B, Bodogai M, et al. Tumor-evoked regulatory B cells promote breast cancer metastasis by converting resting CD4^{+} T cells to T-regulatory cells. *Cancer research*. 2011;71(10):3505-3515. doi:10.1158/0008-5472.CAN-10-4316

450. Yang C, Lee H, Pal S, et al. B Cells Promote Tumor Progression via STAT3 Regulated-Angiogenesis. *PLOS ONE*. 2013;8(5):e64159. doi:10.1371/journal.pone.0064159

451. Dai YC, Zhong J, Xu JF. Regulatory B cells in infectious disease (Review). *Molecular Medicine Reports*. 2017;16(1):3-10. doi:10.3892/mmr.2017.6605

452. Tang X, Du RH, Wang R, et al. Comparison of Hospitalized Patients With ARDS Caused by COVID-19 and H1N1. *Chest*. 2020;158(1):195-205. doi:10.1016/j.chest.2020.03.032

453. Torres Acosta MA, Singer BD. Pathogenesis of COVID-19-induced ARDS: implications for an ageing population. *Eur Respir J*. 2020;56(3). doi:10.1183/13993003.02049-2020

454. Woodruff M, Ramonell R, Cashman K, et al. Dominant extrafollicular B cell responses in severe COVID-19 disease correlate with robust viral-specific antibody production but poor clinical outcomes. *medRxiv*. Published online June 22, 2020:2020.04.29.20083717. doi:10.1101/2020.04.29.20083717

455. Shuwa HA, Shaw TN, Knight SB, et al. *Long-Lasting Alterations in T and B Cell Function in Convalescent COVID-19 Patients*. Social Science Research Network; 2020. doi:10.2139/ssrn.3720301

456. Acharya D, Liu G, Gack MU. Dysregulation of type I interferon responses in COVID-19. *Nature Reviews Immunology*. 2020;20(7):397-398. doi:10.1038/s41577-020-0346-x

457. Zhivaki D, Lemoine S, Lim A, et al. Respiratory Syncytial Virus Infects Regulatory B Cells in Human Neonates via Chemokine Receptor CX3CR1 and Promotes Lung Disease Severity. *Immunity*. 2017;46(2):301-314. doi:10.1016/j.immuni.2017.01.010

458. Duggal NA, Upton J, Phillips AC, Sapey E, Lord JM. An age-related numerical and functional deficit in CD19(+) CD24(hi) CD38(hi) B cells is associated with an increase in systemic autoimmunity. *Aging Cell*. 2013;12(5):873-881. doi:10.1111/acel.12114

459. Cheepsattayakorn A, Cheepsattayakorn R. Parasitic pneumonia and lung involvement. *Biomed Res Int*. 2014;2014:874021. doi:10.1155/2014/874021

460. McSorley HJ, Chayé MAM, Smits HH. Worms: Pernicious parasites or allies against allergies? *Parasite Immunology*. 2019;41(6):e12574. doi:10.1111/pim.12574

461. Wilson MS, Taylor MD, O'Gorman MT, et al. Helminth-induced CD19+CD23hi B cells modulate experimental allergic and autoimmune inflammation. *European Journal of Immunology*. 2010;40(6):1682-1696. doi:10.1002/eji.200939721

462. van der Vlugt LEPM, Labuda LA, Ozir-Fazalalikhan A, et al. Schistosomes induce regulatory features in human and mouse CD1d(hi) B cells: inhibition of allergic inflammation by IL-10 and regulatory T cells. *PLoS ONE*. 2012;7(2):e30883. doi:10.1371/journal.pone.0030883

463. Stark AK, Chandra A, Chakraborty K, et al. PI3Kδ hyper-activation promotes development of B cells that exacerbate Streptococcus pneumoniae infection in an antibody-independent manner. *Nature Communications*. 2018;9(1):3174. doi:10.1038/s41467-018-05674-8

464. Rong HM, Li T, Zhang C, et al. IL-10-producing B cells regulate Th1/Th17-cell immune responses in Pneumocystis pneumonia. *American Journal of Physiology-Lung Cellular and Molecular Physiology*. 2018;316(1):L291-L301. doi:10.1152/ajplung.00210.2018

465. Murdoch JR, Lloyd CM. Chronic inflammation and asthma. *Mutat Res*. 2010;690(1-2):24-39. doi:10.1016/j.mrfmmm.2009.09.005

466. Habener A, Happle C, Skuljec J, et al. B cells are crucial in the regulation of airway hyperreactivity in an experimental model of asthma. *Eur Respir J*. 2019;54(suppl 63):PA4362. doi:10.1183/13993003.congress-2019.PA4362

467. Brosseau C, Durand M, Colas L, et al. CD9+ Regulatory B Cells Induce T Cell Apoptosis via IL-10 and Are Reduced in Severe Asthmatic Patients. *Front Immunol*. 2018;9:3034. doi:10.3389/fimmu.2018.03034

468. Tedder TF, Matsushita T. Regulatory B Cells That Produce IL-10: a Breath of Fresh Air in Allergic Airway Disease. *J Allergy Clin Immunol*. 2010;125(5):1125-1127. doi:10.1016/j.jaci.2010.03.024

469. Fallon PG, Mangan NE. Suppression of TH2-type allergic reactions by helminth infection. *Nat Rev Immunol*. 2007;7(3):220-230. doi:10.1038/nri2039

470. MacNee W. Pathogenesis of Chronic Obstructive Pulmonary Disease. *Proc Am Thorac Soc*. 2005;2(4):258-266. doi:10.1513/pats.200504-045SR

471. Sgalla G, Iovene B, Calvello M, Ori M, Varone F, Richeldi L. Idiopathic pulmonary fibrosis: pathogenesis and management. *Respir Res*. 2018;19(1):32. doi:10.1186/s12931-018-0730-2

472. Asai Y, Chiba H, Nishikiori H, et al. Aberrant populations of circulating T follicular helper cells and regulatory B cells underlying idiopathic pulmonary fibrosis. *Respir Res*. 2019;20(1):244. doi:10.1186/s12931-019-1216-6

473. COJOCARU M, COJOCARU IM, SILOSI I, VRABIE CD. Pulmonary Manifestations of Systemic Autoimmune Diseases. *Maedica (Buchar)*. 2011;6(3):224-229.

474. Lin W, Jin L, Chen H, et al. B cell subsets and dysfunction of regulatory B cells in IgG4-related diseases and primary Sjögren's syndrome: the similarities and differences. *Arthritis Research & Therapy*. 2014;16(3):R118. doi:10.1186/ar4571

475. Singh RR, Prasad P, Fishbein M, Valera I. II-07 Pathogenesis of pulmonary lupus and vasculitis: trafficking of innate B1 B cells to the lungs as a novel mechanism. *Lupus Sci & Med*. 2018;5(Suppl 2):A63. doi:10.1136/lupus-2018-lsm.106

476. Atkins SR, Turesson C, Myers JL, et al. Morphologic and quantitative assessment of CD20+ B cell infiltrates in rheumatoid arthritis–associated nonspecific interstitial pneumonia and usual interstitial pneumonia. *Arthritis & Rheumatism*. 2006;54(2):635-641. doi:10.1002/art.21758

477. Ma L, Liu B, Jiang Z, Jiang Y. Reduced numbers of regulatory B cells are negatively correlated with disease activity in patients with new-onset rheumatoid arthritis. *Clin Rheumatol*. 2014;33(2):187-195. doi:10.1007/s10067-013-2359-3

478. Narshi CB, Haider S, Ford CM, Isenberg DA, Giles IP. Rituximab as early therapy for pulmonary haemorrhage in systemic lupus erythematosus. *Rheumatology (Oxford)*. 2010;49(2):392-394. doi:10.1093/rheumatology/kep356

479. Pinto LF, Candia L, Garcia P, et al. Effective Treatment of Refractory Pulmonary Hemorrhage with Monoclonal Anti-CD20 Antibody (Rituximab). *RES*. 2009;78(1):106-109. doi:10.1159/000156965

480. Mohammed AGA, Alshihre A, Al-Homood IA. Rituximab treatment in patients with systemic sclerosis and interstitial lung disease. *Ann Thorac Med*. 2017;12(4):294-297. doi:10.4103/atm.ATM_30_17

481. Fui A, Bergantini L, Selvi E, et al. Rituximab therapy in interstitial lung disease associated with rheumatoid arthritis. *Intern Med J*. 2020;50(3):330-336. doi:10.1111/imj.14306

482. Anolik JH, Barnard J, Owen T, et al. Delayed memory B cell recovery in peripheral blood and lymphoid tissue in systemic lupus erythematosus after B cell depletion therapy. *Arthritis Rheum*. 2007;56(9):3044-3056. doi:10.1002/art.22810

483. Crickx E, Weill JC, Reynaud CA, Mahévas M. Anti-CD20–mediated B-cell depletion in autoimmune diseases: successes, failures and future perspectives. *Kidney International*. 2020;97(5):885-893. doi:10.1016/j.kint.2019.12.025

484. Didierlaurent A, Goulding J, Hussell T. The impact of successive infections on the lung microenvironment. *Immunology*. 2007;122(4):457-465. doi:10.1111/j.1365-2567.2007.02729.x

485. Sarkar M, Niranjan N, Banyal P. Mechanisms of hypoxemia. *Lung India*. 2017;34(1):47-60. doi:10.4103/0970-2113.197116

486. Daijo H, Hoshino Y, Kai S, et al. Cigarette smoke reversibly activates hypoxia-inducible factor 1 in a reactive oxygen species-dependent manner. *Sci Rep*. 2016;6:34424. doi:10.1038/srep34424

487. Harris AJ, Thompson AR, Whyte MK, Walmsley SR. HIF-mediated innate immune responses: cell signaling and therapeutic implications. *Hypoxia (Auckl)*. 2014;2:47-58. doi:10.2147/HP.S50269

488. Meng X, Grötsch B, Luo Y, et al. Hypoxia-inducible factor-1α is a critical transcription factor for IL-10-producing B cells in autoimmune disease. *Nat Commun*. 2018;9(1):251. doi:10.1038/s41467-017-02683-x

489. Beamer CA, Shepherd DM. Role of the aryl hydrocarbon receptor (AhR) in lung inflammation. *Semin Immunopathol*. 2013;35(6):693-704. doi:10.1007/s00281-013-0391-7

490. Chang YD, Li CH, Tsai CH, Cheng YW, Kang JJ, Lee CC. Aryl hydrocarbon receptor deficiency enhanced airway inflammation and remodeling in a murine chronic asthma model. *FASEB J*. Published online September 22, 2020. doi:10.1096/fj.202001529R

491. Chiba T, Chihara J, Furue M. Role of the Arylhydrocarbon Receptor (AhR) in the Pathology of Asthma and COPD. *J Allergy (Cairo)*. 2012;2012:372384. doi:10.1155/2012/372384

492. Maseda D, Smith SH, DiLillo DJ, et al. Regulatory B10 Cells Differentiate Into Antibody-Secreting Cells After Transient IL-10 Production In Vivo. *J Immunol*. 2012;188(3):1036-1048. doi:10.4049/jimmunol.1102500

493. Picard C. [The lungs and immunosuppressants: practical problems]. *Rev Pneumol Clin*. 2011;67(4):226-232. doi:10.1016/j.pneumo.2011.04.004

494. Massarelli E, Papadimitrakopoulou V, Welsh J, Tang C, Tsao AS. Immunotherapy in lung cancer. *Transl Lung Cancer Res*. 2014;3(1):53-63. doi:10.3978/j.issn.2218-6751.2014.01.01

495. Sun X, Zhang T, Li M, Yin L, Xue J. Immunosuppressive B cells expressing PD-1/PD-L1 in solid tumors: A mini review. *QJM*. Published online June 26, 2019. doi:10.1093/qjmed/hcz162

496. Schulze AB, Schmidt LH. PD-1 targeted Immunotherapy as first-line therapy for advanced non-small-cell lung cancer patients. *J Thorac Dis*. 2017;9(4):E384-E386. doi:10.21037/jtd.2017.03.118

497. Mauri C, Menon M. Human regulatory B cells in health and disease: therapeutic potential. *J Clin Invest*. 2017;127(3):772-779. doi:10.1172/JCI85113

498. Menon M, Hussell T, Ali Shuwa H. Regulatory B cells in respiratory health and diseases. *Immunol Rev*. 2021;299(1):61-73. doi:10.1111/imr.12941

499. Silva-Sanchez A, Randall TD. Role of iBALT in Respiratory Immunity. *Curr Top Microbiol Immunol*. 2020;426:21-43. doi:10.1007/82_2019_191

500. Tschernig T, Pabst R. Bronchus-associated lymphoid tissue (BALT) is not present in the normal adult lung but in different diseases. *Pathobiology*. 2000;68(1):1-8. doi:10.1159/000028109

501. Xiong J, Zhou L, Tian J, et al. Cigarette Smoke-Induced Lymphoid Neogenesis in COPD Involves IL-17/RANKL Pathway. *Front Immunol*. 2020;11:588522. doi:10.3389/fimmu.2020.588522

502. Rangel-Moreno J, Carragher DM, de la Luz Garcia-Hernandez M, et al. The development of inducible bronchus-associated lymphoid tissue depends on IL-17. *Nat Immunol*. 2011;12(7):639-646. doi:10.1038/ni.2053

503. Roos AB, Sandén C, Mori M, Bjermer L, Stampfli MR, Erjefält JS. IL-17A Is Elevated in End-Stage Chronic Obstructive Pulmonary Disease and Contributes to Cigarette Smoke-induced Lymphoid Neogenesis. *Am J Respir Crit Care Med*. 2015;191(11):1232-1241. doi:10.1164/rccm.201410-1861OC

504. Polverino F, Cosio BG, Pons J, et al. B Cell-Activating Factor. An Orchestrator of Lymphoid Follicles in Severe Chronic Obstructive Pulmonary Disease. *Am J Respir Crit Care Med*. 2015;192(6):695-705. doi:10.1164/rccm.201501-0107OC

505. Jia J, Conlon TM, Sarker RS, et al. Cholesterol metabolism promotes B-cell positioning during immune pathogenesis of chronic obstructive pulmonary disease. *EMBO Mol Med*. 2018;10(5):e8349. doi:10.15252/emmm.201708349

506. Nunez B, Sauleda J, Anto JM, et al. Anti-tissue antibodies are related to lung function in chronic obstructive pulmonary disease. *Am J Respir Crit Care Med*. 2011;183:1025-1031.

507. Lee SH, Goswami S, Grudo A, et al. Antielastin autoimmunity in tobacco smoking-induced emphysema. *Nat Med*. 2007;13:567-569.

508. Southworth T, Higham A, Kolsum U, et al. The relationship between airway immunoglobulin activity and eosinophils in COPD. *J Cell Mol Med*. 2021;25(4):2203-2212. doi:10.1111/jcmm.16206

509. Tezuka H, Abe Y, Iwata M, et al. Regulation of IgA production by naturally occurring TNF/iNOS-producing dendritic cells. *Nature*. 2007;448(7156):929-933. doi:10.1038/nature06033

510. Pilette C, Godding V, Kiss R, et al. Reduced epithelial expression of secretory component in small airways correlates with airflow obstruction in chronic obstructive pulmonary disease. *Am J Respir Crit Care Med*. 2001;163(1):185-194. doi:10.1164/ajrccm.163.1.9912137

511. Polosukhin VV, Cates JM, Lawson WE, et al. Bronchial secretory immunoglobulin a deficiency correlates with airway inflammation and progression of chronic obstructive pulmonary disease. *Am J Respir Crit Care Med*. 2011;184(3):317-327. doi:10.1164/rccm.201010-1629OC

512. Gohy ST, Detry BR, Lecocq M, et al. Polymeric immunoglobulin receptor down-regulation in chronic obstructive pulmonary disease. Persistence in the cultured epithelium and role of

transforming growth factor-β. *Am J Respir Crit Care Med*. 2014;190(5):509-521. doi:10.1164/rccm.201311-1971OC

513. Barker KA, Etesami NS, Shenoy AT, et al. Lung-resident memory B cells protect against bacterial pneumonia. *Journal of Clinical Investigation*. 2021;131(11):e141810. doi:10.1172/JCI141810

514. Parris BA, O'Farrell HE, Fong KM, Yang IA. Chronic obstructive pulmonary disease (COPD) and lung cancer: common pathways for pathogenesis. *J Thorac Dis*. 2019;11(Suppl 17):S2155-S2172. doi:10.21037/jtd.2019.10.54

515. Sullivan JL, Bagevalu B, Glass C, et al. B Cell-Adaptive Immune Profile in Emphysema-Predominant Chronic Obstructive Pulmonary Disease. *Am J Respir Crit Care Med*. 2019;200(11):1434-1439. doi:10.1164/rccm.201903-0632LE

516. Sun X, Kaufman PD. Ki-67: more than a proliferation marker. *Chromosoma*. 2018;127(2):175-186. doi:10.1007/s00412-018-0659-8

517. Muehlinghaus G, Cigliano L, Huehn S, et al. Regulation of CXCR3 and CXCR4 expression during terminal differentiation of memory B cells into plasma cells. *Blood*. 2005;105(10):3965-3971. doi:10.1182/blood-2004-08-2992

518. Azuma M, Ito D, Yagita H, et al. B70 antigen is a second ligand for CTLA-4 and CD28. *Nature*. 1993;366(6450):76-79. doi:10.1038/366076a0

519. Klinman DM. Immunotherapeutic uses of CpG oligodeoxynucleotides. *Nat Rev Immunol*. 2004;4(4):249-258. doi:10.1038/nri1329

520. Yu G, Kovkarova-Naumovski E, Jara P, et al. Matrix metalloproteinase-19 is a key regulator of lung fibrosis in mice and humans. *Am J Respir Crit Care Med*. 2012;186(8):752-762. doi:10.1164/rccm.201202-0302OC

521. Gueders MM, Hirst SJ, Quesada-Calvo F, et al. Matrix metalloproteinase-19 deficiency promotes tenascin-C accumulation and allergen-induced airway inflammation. *Am J Respir Cell Mol Biol*. 2010;43(3):286-295. doi:10.1165/rcmb.2008-0426OC

522. Tenger C, Zhou X. Apolipoprotein E modulates immune activation by acting on the antigen-presenting cell. *Immunology*. 2003;109(3):392-397. doi:10.1046/j.1365-2567.2003.01665.x

523. Yao X, Gordon EM, Figueroa DM, Barochia AV, Levine SJ. Emerging Roles of Apolipoprotein E and Apolipoprotein A-I in the Pathogenesis and Treatment of Lung Disease. *Am J Respir Cell Mol Biol*. 2016;55(2):159-169. doi:10.1165/rcmb.2016-0060TR

524. Christensen DJ, Ohkubo N, Oddo J, et al. Apolipoprotein E and peptide mimetics modulate inflammation by binding the SET protein and activating protein phosphatase 2A. *J Immunol*. 2011;186(4):2535-2542. doi:10.4049/jimmunol.1002847

525. Miyata M, Smith JD. Apolipoprotein E allele-specific antioxidant activity and effects on cytotoxicity by oxidative insults and beta-amyloid peptides. *Nat Genet*. 1996;14(1):55-61. doi:10.1038/ng0996-55

526. Mootz M, Jakwerth CA, Schmidt-Weber CB, Zissler UM. Secretoglobins in the big picture of immunoregulation in airway diseases. *Allergy*. 2022;77(3):767-777. doi:10.1111/all.15033

527. Wikenheiser DJ, Stumhofer JS. ICOS Co-Stimulation: Friend or Foe? *Front Immunol*. 2016;7. doi:10.3389/fimmu.2016.00304

528. Bystry RS, Aluvihare V, Welch KA, Kallikourdis M, Betz AG. B cells and professional APCs recruit regulatory T cells via CCL4. *Nat Immunol*. 2001;2(12):1126-1132. doi:10.1038/ni735

529. Liu B, Lin Y, Yan J, et al. Affinity-coupled CCL22 promotes positive selection in germinal centres. *Nature*. 2021;592(7852):133-137. doi:10.1038/s41586-021-03239-2

530. Sasaki Y, Iwai K. Roles of the NF-κB Pathway in B-Lymphocyte Biology. *Curr Top Microbiol Immunol*. 2016;393:177-209. doi:10.1007/82_2015_479

531. Kaileh M, Sen R. NF-κB function in B lymphocytes. *Immunol Rev*. 2012;246(1):254-271. doi:10.1111/j.1600-065X.2012.01106.x

532. Gerondakis S, Siebenlist U. Roles of the NF-kappaB pathway in lymphocyte development and function. *Cold Spring Harb Perspect Biol*. 2010;2(5):a000182. doi:10.1101/cshperspect.a000182

533. Vega GG, Avilés-Salas A, Chalapud JR, et al. P38 MAPK expression and activation predicts failure of response to CHOP in patients with Diffuse Large B-Cell Lymphoma. *BMC Cancer*. 2015;15:722. doi:10.1186/s12885-015-1778-8

534. Khiem D, Cyster JG, Schwarz JJ, Black BL. A p38 MAPK-MEF2C pathway regulates B-cell proliferation. *Proc Natl Acad Sci U S A*. 2008;105(44):17067-17072. doi:10.1073/pnas.0804868105

535. Zhang HX, Yang JJ, Zhang SA, et al. HIF-1α promotes inflammatory response of chronic obstructive pulmonary disease by activating EGFR/PI3K/AKT pathway. *Eur Rev Med Pharmacol Sci*. 2018;22(18):6077-6084. doi:10.26355/eurrev_201809_15946

536. Schmiedel D, Hezroni H, Hamburg A, Shulman Z. Brg1 Supports B Cell Proliferation and Germinal Center Formation Through Enhancer Activation. *Front Immunol*. 2021;12:705848. doi:10.3389/fimmu.2021.705848

537. Voropaeva EN, Pospelova TI, Voevoda MI, Maksimov VN, Orlov YL, Seregina OB. Clinical aspects of TP53 gene inactivation in diffuse large B-cell lymphoma. *BMC Med Genomics*. 2019;12(Suppl 2):35. doi:10.1186/s12920-019-0484-9

538. Dancer R, Sansom DM. Regulatory T cells and COPD. *Thorax*. 2013;68(12):1176-1178. doi:10.1136/thoraxjnl-2013-203878

539. Plumb J, Smyth LJC, Adams HR, Vestbo J, Bentley A, Singh SD. Increased T-regulatory cells within lymphocyte follicles in moderate COPD. *European Respiratory Journal*. 2009;34(1):89-94. doi:10.1183/09031936.00100708

540. Brusselle GG, Demoor T, Bracke KR, Brandsma CA, Timens W. Lymphoid follicles in (very) severe COPD: beneficial or harmful? *European Respiratory Journal*. 2009;34(1):219-230. doi:10.1183/09031936.00150208

541. Yadava K, Marsland BJ. Lymphoid follicles in chronic lung diseases. *Thorax*. 2013;68(6):597-598. doi:10.1136/thoraxjnl-2012-203008

542. Barceló B, Pons J, Ferrer JM, Sauleda J, Fuster A, Agustí AGN. Phenotypic characterisation of T-lymphocytes in COPD: abnormal CD4+CD25+ regulatory T-lymphocyte response to tobacco smoking. *Eur Respir J*. 2008;31(3):555-562. doi:10.1183/09031936.00010407

543. Smyth LJC, Starkey C, Vestbo J, Singh D. CD4-regulatory cells in COPD patients. *Chest*. 2007;132(1):156-163. doi:10.1378/chest.07-0083

544. Portugal S, Tipton CM, Sohn H, et al. Malaria-associated atypical memory B cells exhibit markedly reduced B cell receptor signaling and effector function. *Elife*. 2015;4. doi:10.7554/eLife.07218

545. Sullivan RT, Kim CC, Fontana MF, et al. FCRL5 Delineates Functionally Impaired Memory B Cells Associated with Plasmodium falciparum Exposure. *PLoS Pathog*. 2015;11(5):e1004894. doi:10.1371/journal.ppat.1004894

546. Wehr C, Eibel H, Masilamani M, et al. A new CD21low B cell population in the peripheral blood of patients with SLE. *Clin Immunol*. 2004;113(2):161-171. doi:10.1016/j.clim.2004.05.010

547. Clancy LJ, Critchley JA, Leitch AG, Kirby BJ, Ungar A, Flenley DC. Arterial catecholamines in hypoxic exercise in man. *Clin Sci Mol Med*. 1975;49(5):503-506. doi:10.1042/cs0490503

548. Ciocca M, Zaffina S, Fernandez Salinas A, et al. Evolution of Human Memory B Cells From Childhood to Old Age. *Front Immunol*. 2021;12:690534. doi:10.3389/fimmu.2021.690534

549. Agusti A. Hypothesis: Does COPD have an autoimmune component? *Thorax*. 2003;58(10):832-834. doi:10.1136/thorax.58.10.832

550. Brandsma CA, Kerstjens HAM, van Geffen WH, et al. Differential switching to IgG and IgA in active smoking COPD patients and healthy controls. *Eur Respir J*. 2012;40(2):313-321. doi:10.1183/09031936.00011211

551. Wong SH, Barlow JL, Nabarro S, Fallon PG, McKenzie ANJ. Tim-1 is induced on germinal centre B cells through B-cell receptor signalling but is not essential for the germinal centre response. *Immunology*. 2010;131(1):77-88. doi:10.1111/j.1365-2567.2010.03276.x

552. Cherukuri A, Mohib K, Rothstein DM. Regulatory B cells: TIM-1, transplant tolerance, and rejection. *Immunol Rev*. 2021;299(1):31-44. doi:10.1111/imr.12933

553. Michée-Cospolite M, Boudigou M, Grasseau A, et al. Molecular Mechanisms Driving IL-10- Producing B Cells Functions: STAT3 and c-MAF as Underestimated Central Key Regulators? *Front Immunol*. 2022;13:818814. doi:10.3389/fimmu.2022.818814

554. McGettrick AF, O'Neill LAJ. The Role of HIF in Immunity and Inflammation. *Cell Metab*. 2020;32(4):524-536. doi:10.1016/j.cmet.2020.08.002

555. Jara P, Calyeca J, Romero Y, et al. Matrix metalloproteinase (MMP)-19-deficient fibroblasts display a profibrotic phenotype. *American Journal of Physiology-Lung Cellular and Molecular Physiology*. 2015;308(6):L511-L522. doi:10.1152/ajplung.00043.2014

556. Mauch S, Kolb C, Kolb B, Sadowski T, Sedlacek R. Matrix metalloproteinase-19 is expressed in myeloid cells in an adhesion-dependent manner and associates with the cell surface. *J Immunol*. 2002;168(3):1244-1251. doi:10.4049/jimmunol.168.3.1244

557. Sadowski T, Dietrich S, Koschinsky F, Sedlacek R. Matrix metalloproteinase 19 regulates insulin-like growth factor-mediated proliferation, migration, and adhesion in human keratinocytes through proteolysis of insulin-like growth factor binding protein-3. *Mol Biol Cell*. 2003;14(11):4569-4580. doi:10.1091/mbc.e03-01-0009

558. Sadowski T, Dietrich S, Müller M, et al. Matrix metalloproteinase-19 expression in normal and diseased skin: dysregulation by epidermal proliferation. *J Invest Dermatol*. 2003;121(5):989-996. doi:10.1046/j.1523-1747.2003.12526.x

559. Djonov V, Högger K, Sedlacek R, Laissue J, Draeger A. MMP-19: cellular localization of a novel metalloproteinase within normal breast tissue and mammary gland tumours. *J Pathol*. 2001;195(2):147-155. doi:10.1002/path.927

560. Kolb C, Mauch S, Krawinkel U, Sedlacek R. Matrix metalloproteinase-19 in capillary endothelial cells: expression in acutely, but not in chronically, inflamed synovium. *Exp Cell Res*. 1999;250(1):122-130. doi:10.1006/excr.1999.4493

561. Kolb C, Mauch S, Peter HH, Krawinkel U, Sedlacek R. The matrix metalloproteinase RASI-1 is expressed in synovial blood vessels of a rheumatoid arthritis patient. *Immunol Lett*. 1997;57(1-3):83-88. doi:10.1016/s0165-2478(97)00057-6

562. Connolly E, Morgan DJ, Franklin M, et al. Neurturin regulates the lung-resident macrophage inflammatory response to viral infection. *Life Sci Alliance*. 2020;3(12):e202000780. doi:10.26508/lsa.202000780

563. Shuwa HA, Shaw TN, Knight SB, et al. Alterations in T and B cell function persist in convalescent COVID-19 patients. *Med (N Y)*. 2021;2(6):720-735.e4. doi:10.1016/j.medj.2021.03.013

564. Mann ER, Menon M, Knight SB, et al. Longitudinal immune profiling reveals key myeloid signatures associated with COVID-19. *Science Immunology*. 2020;5(51). doi:10.1126/sciimmunol.abd6197

565. Guan WJ, Ni ZY, Hu Y, et al. Clinical Characteristics of Coronavirus Disease 2019 in China. *N Engl J Med*. 2020;382(18):1708-1720. doi:10.1056/NEJMoa2002032

566. Kuri-Cervantes L, Pampena MB, Meng W, et al. Comprehensive mapping of immune perturbations associated with severe COVID-19. *Sci Immunol*. 2020;5(49). doi:10.1126/sciimmunol.abd7114

567. Lucas C, Wong P, Klein J, et al. Longitudinal analyses reveal immunological misfiring in severe COVID-19. *Nature*. 2020;584(7821):463-469. doi:10.1038/s41586-020-2588-y

568. Mathew D, Giles JR, Baxter AE, et al. Deep immune profiling of COVID-19 patients reveals distinct immunotypes with therapeutic implications. *Science*. 2020;369(6508). doi:10.1126/science.abc8511

569. Wilk AJ, Rustagi A, Zhao NQ, et al. A single-cell atlas of the peripheral immune response in patients with severe COVID-19. *Nat Med*. 2020;26(7):1070-1076. doi:10.1038/s41591-020-0944-y

570. Chen G, Wu D, Guo W, et al. Clinical and immunological features of severe and moderate coronavirus disease 2019. *J Clin Invest*. 2020;130(5):2620-2629. doi:10.1172/JCI137244

571. Fraser E. Long term respiratory complications of covid-19. *BMJ*. 2020;370. doi:10.1136/bmj.m3001

572. Williams FMK, Muirhead N, Pariante C. Covid-19 and chronic fatigue. *BMJ*. 2020;370. doi:10.1136/bmj.m2922

573. Greenhalgh T, Knight M, A'Court C, Buxton M, Husain L. Management of post-acute covid-19 in primary care. *BMJ*. 2020;370. doi:10.1136/bmj.m3026

574. Rodda LB, Netland J, Shehata L, et al. Functional SARS-CoV-2-Specific Immune Memory Persists after Mild COVID-19. *Cell*. 2021;184(1):169-183.e17. doi:10.1016/j.cell.2020.11.029

575. Dan JM, Mateus J, Kato Y, et al. Immunological memory to SARS-CoV-2 assessed for up to 8 months after infection. *Science*. 2021;371(6529). doi:10.1126/science.abf4063

576. Peng Y, Mentzer AJ, Liu G, et al. Broad and strong memory CD4+ and CD8+ T cells induced by SARS-CoV-2 in UK convalescent individuals following COVID-19. *Nat Immunol*. 2020;21(11):1336-1345. doi:10.1038/s41590-020-0782-6

577. Pradenas E, Trinité B, Urrea V, et al. Stable neutralizing antibody levels six months after mild and severe COVID-19 episode. *Med (N Y)*. Published online January 31, 2021. doi:10.1016/j.medj.2021.01.005

578. Wiedemann A, Foucat E, Hocini H, et al. Long-lasting severe immune dysfunction in Ebola virus disease survivors. *Nat Commun*. 2020;11(1):3730. doi:10.1038/s41467-020-17489-7

579. Wong SS, Oshansky CM, Guo XZJ, et al. Severe Influenza Is Characterized by Prolonged Immune Activation: Results From the SHIVERS Cohort Study. *J Infect Dis*. 2018;217(2):245-256. doi:10.1093/infdis/jix571

580. Ma H, Zeng W, He H, et al. Serum IgA, IgM, and IgG responses in COVID-19. *Cellular & Molecular Immunology*. 2020;17(7):773-775. doi:10.1038/s41423-020-0474-z

581. Long QX, Liu BZ, Deng HJ, et al. Antibody responses to SARS-CoV-2 in patients with COVID-19. *Nature Medicine*. 2020;26(6):845-848. doi:10.1038/s41591-020-0897-1

582. Yu H qiong, Sun B qing, Fang Z fu, et al. Distinct features of SARS-CoV-2-specific IgA response in COVID-19 patients. *European Respiratory Journal*. 2020;56(2). doi:10.1183/13993003.01526-2020

583. Laing AG, Lorenc A, Del Molino Del Barrio I, et al. A dynamic COVID-19 immune signature includes associations with poor prognosis. *Nat Med*. Published online August 17, 2020. doi:10.1038/s41591-020-1038-6

584. Hadjadj J, Yatim N, Barnabei L, et al. Impaired type I interferon activity and inflammatory responses in severe COVID-19 patients. *Science*. 2020;369(6504):718-724. doi:10.1126/science.abc6027

585. Chen Z, John Wherry E. T cell responses in patients with COVID-19. *Nat Rev Immunol*. 2020;20(9):529-536. doi:10.1038/s41577-020-0402-6

586. Yang X, Dai T, Zhou X. Analysis of adaptive immune cell populations and phenotypes in the patients infected by SARS-CoV-2. medRxiv. *Published online April*. 3:2020 03 23 20040675. doi:10.1101/2020.03.23.20040675

587. Brainard DM, Tager AM, Misdraji J, et al. Decreased CXCR3+ CD8 T Cells in Advanced Human Immunodeficiency Virus Infection Suggest that a Homing Defect Contributes to Cytotoxic T-Lymphocyte Dysfunction. *Journal of Virology*. 2007;81(16):8439-8450. doi:10.1128/JVI.00199-07

588. Henneken M, Dörner T, Burmester GR, Berek C. Differential expression of chemokine receptors on peripheral blood B cells from patients with rheumatoid arthritis and systemic lupus erythematosus. *Arthritis Research & Therapy*. 2005;7(5):R1001. doi:10.1186/ar1776

589. Moser B. CXCR5, the Defining Marker for Follicular B Helper T (TFH) Cells. *Front Immunol*. 2015;6. doi:10.3389/fimmu.2015.00296

590. Sekine T, Perez-Potti A, Rivera-Ballesteros O, et al. Robust T cell immunity in convalescent individuals with asymptomatic or mild COVID-19. *Cell*. Published online August 2020:S0092867420310084. doi:10.1016/j.cell.2020.08.017

591. De Biasi S, Meschiari M, Gibellini L, et al. Marked T cell activation, senescence, exhaustion and skewing towards TH17 in patients with COVID-19 pneumonia. *Nat Commun*. 2020;11(1):3434. doi:10.1038/s41467-020-17292-4

592. Qin C, Zhou L, Hu Z, et al. Dysregulation of Immune Response in Patients With Coronavirus 2019 (COVID-19) in Wuhan, China. *Clin Infect Dis*. 2020;71(15):762-768. doi:10.1093/cid/ciaa248

593. Neidleman J, Luo X, Frouard J, et al. SARS-CoV-2-Specific T Cells Exhibit Phenotypic Features of Helper Function, Lack of Terminal Differentiation, and High Proliferation Potential. *CR Med*. 2020;1(6). doi:10.1016/j.xcrm.2020.100081

594. Compeer EB, Uhl LFK. Antibody response to SARS-CoV-2 — sustained after all? *Nature Reviews Immunology*. Published online August 11, 2020:1-1. doi:10.1038/s41577-020-00423-9

595. Ni L, Ye F, Cheng ML, et al. Detection of SARS-CoV-2-Specific Humoral and Cellular Immunity in COVID-19 Convalescent Individuals. *Immunity*. 2020;52(6):971-977.e3. doi:10.1016/j.immuni.2020.04.023

596. Tonn T, Corman VM, Johnsen M, et al. Stability and neutralising capacity of SARS-CoV-2-specific antibodies in convalescent plasma. *The Lancet Microbe*. 2020;1(2):e63. doi:10.1016/S2666-5247(20)30037-9

597. Matsushita T. Regulatory and effector B cells: Friends or foes? *Journal of Dermatological Science*. 2019;93(1):2-7. doi:10.1016/j.jdermsci.2018.11.008

598. Flores-Borja F, Bosma A, Ng D, et al. CD19+CD24hiCD38hi B cells maintain regulatory T cells while limiting TH1 and TH17 differentiation. *Sci Transl Med*. 2013;5(173):173ra23. doi:10.1126/scitranslmed.3005407

599. Metsalu T, Vilo J. ClustVis: a web tool for visualizing clustering of multivariate data using Principal Component Analysis and heatmap. *Nucleic Acids Research*. 2015;43(W1):W566-570. doi:10.1093/nar/gkv468

600. Duddy ME, Alter A, Bar-Or A. Distinct profiles of human B cell effector cytokines: a role in immune regulation? *J Immunol*. 2004;172(6):3422-3427. doi:10.4049/jimmunol.172.6.3422

601. Briend E, Ferguson GJ, Mori M, et al. IL-18 associated with lung lymphoid aggregates drives IFNγ production in severe COPD. *Respir Res*. 2017;18(1):159. doi:10.1186/s12931-017-0641-7

602. Akamatsu MA, de Castro JT, Takano CY, Ho PL. Off balance: Interferons in COVID-19 lung infections. *EBioMedicine*. 2021;73:103642. doi:10.1016/j.ebiom.2021.103642

603. Lee SH, Goswami S, Grudo A, et al. Antielastin autoimmunity in tobacco smoking-induced emphysema. *Nat Med*. 2007;13(5):567-569. doi:10.1038/nm1583

604. Feghali-Bostwick CA, Gadgil AS, Otterbein LE, et al. Autoantibodies in patients with chronic obstructive pulmonary disease. *Am J Respir Crit Care Med*. 2008;177(2):156-163. doi:10.1164/rccm.200701-014OC

605. MacIntyre N, Huang YC. Acute exacerbations and respiratory failure in chronic obstructive pulmonary disease. *Proc Am Thorac Soc*. 2008;5(4):530-535. doi:10.1513/pats.200707-088ET

606. Gosman MME, Willemse BWM, Jansen DF, et al. Increased number of B-cells in bronchial biopsies in COPD. *Eur Respir J*. 2006;27(1):60-64. doi:10.1183/09031936.06.00007005

607. Ni L, Dong C. Roles of Myeloid and Lymphoid Cells in the Pathogenesis of Chronic Obstructive Pulmonary Disease. *Front Immunol*. 2018;9. doi:10.3389/fimmu.2018.01431

608. Oliviero B, Varchetta S, Mele D, et al. Expansion of atypical memory B cells is a prominent feature of COVID-19. *Cell Mol Immunol*. 2020;17(10):1101-1103. doi:10.1038/s41423-020-00542-2

609. Woodruff MC, Ramonell RP, Nguyen DC, et al. Extrafollicular B cell responses correlate with neutralizing antibodies and morbidity in COVID-19. *Nat Immunol*. 2020;21(12):1506-1516. doi:10.1038/s41590-020-00814-z

610. Farris AD, Guthridge JM. Overlapping B cell pathways in severe COVID-19 and lupus. *Nat Immunol*. 2020;21(12):1478-1480. doi:10.1038/s41590-020-00822-z

611. Sosa-Hernández VA, Torres-Ruíz J, Cervantes-Díaz R, et al. B Cell Subsets as Severity-Associated Signatures in COVID-19 Patients. *Front Immunol*. 2020;11:611004. doi:10.3389/fimmu.2020.611004

612. Cervantes-Díaz R, Sosa-Hernández VA, Torres-Ruíz J, et al. Severity of SARS-CoV-2 infection is linked to double-negative (CD27- IgD-) B cell subset numbers. *Inflamm Res*. 2022;71(1):131-140. doi:10.1007/s00011-021-01525-3

613. Knox JJ, Buggert M, Kardava L, et al. T-bet+ B cells are induced by human viral infections and dominate the HIV gp140 response. *JCI Insight*. 2017;2(8):92943. doi:10.1172/jci.insight.92943

614. Muellenbeck MF, Ueberheide B, Amulic B, et al. Atypical and classical memory B cells produce Plasmodium falciparum neutralizing antibodies. *J Exp Med*. 2013;210(2):389-399. doi:10.1084/jem.20121970

615. Hsia CCW, Hyde DM, Weibel ER. Lung Structure and the Intrinsic Challenges of Gas Exchange. *Compr Physiol*. 2016;6(2):827-895. doi:10.1002/cphy.c150028

616. Qiu F, Liang CL, Liu H, et al. Impacts of cigarette smoking on immune responsiveness: Up and down or upside down? *Oncotarget*. 2017;8(1):268-284. doi:10.18632/oncotarget.13613

617. Brandsma CA, Hylkema MN, Geerlings M, et al. Increased levels of (class switched) memory B cells in peripheral blood of current smokers. *Respir Res*. 2009;10:108. doi:10.1186/1465-9921-10-108

618. Centuori SM, Gomes CJ, Kim SS, et al. Double-negative (CD27-IgD-) B cells are expanded in NSCLC and inversely correlate with affinity-matured B cell populations. *J Transl Med*. 2018;16(1):30. doi:10.1186/s12967-018-1404-z

619. Frisoni P, Neri M, D'Errico S, et al. Cytokine storm and histopathological findings in 60 cases of COVID-19-related death: from viral load research to immunohistochemical quantification of major players IL-1β, IL-6, IL-15 and TNF-α. *Forensic Sci Med Pathol*. 2022;18(1):4-19. doi:10.1007/s12024-021-00414-9

620. Rendeiro AF, Ravichandran H, Bram Y, et al. The spatial landscape of lung pathology during COVID-19 progression. *Nature*. 2021;593(7860):564-569. doi:10.1038/s41586-021-03475-6

621. Ehab A, Reissfelder F, Laufer J, Kempa AT. Transbronchial lung cryobiopsy performed in acute COVID-19 pneumonia: first report. *Adv Respir Med*. 2021;89(1):72-74. doi:10.5603/ARM.a2021.0032

622. Sampsonas F, Kakoullis L, Karampitsakos T, et al. Bronchoscopy during the COVID-19 pandemic: effect on current practices and strategies to reduce procedure-associated transmission. *Expert Rev Respir Med*. 2021;15(6):773-779. doi:10.1080/17476348.2021.1913058

623. Distler JHW, Wenger RH, Gassmann M, et al. Physiologic responses to hypoxia and implications for hypoxia-inducible factors in the pathogenesis of rheumatoid arthritis. *Arthritis Rheum*. 2004;50(1):10-23. doi:10.1002/art.11425

624. Vogelmeier CF, Criner GJ, Martinez FJ, et al. Global Strategy for the Diagnosis, Management, and Prevention of Chronic Obstructive Lung Disease 2017 Report. GOLD Executive Summary. *Am J Respir Crit Care Med*. 2017;195(5):557-582. doi:10.1164/rccm.201701-0218PP

625. Besiktepe N, Kayalar O, Ersen E, Oztay F. The copper dependent-lysyl oxidases contribute to the pathogenesis of pulmonary emphysema in chronic obstructive pulmonary disease patients. *J Trace Elem Med Biol*. 2017;44:247-255. doi:10.1016/j.jtemb.2017.08.011

626. Guan R, Wang J, Li Z, et al. Sodium Tanshinone IIA Sulfonate Decreases Cigarette Smoke-Induced Inflammation and Oxidative Stress via Blocking the Activation of MAPK/HIF-1α Signaling Pathway. *Front Pharmacol*. 2018;9:263. doi:10.3389/fphar.2018.00263

627. Milanovic M, Heise N, De Silva NS, et al. Differential requirements for the canonical NF-κB transcription factors c-REL and RELA during the generation and activation of mature B cells. *Immunol Cell Biol*. 2017;95(3):261-271. doi:10.1038/icb.2016.95

628. Mahajan S, Cervera A, MacLeod M, et al. The role of ICOS in the development of CD4 T cell help and the reactivation of memory T cells. *Eur J Immunol*. 2007;37(7):1796-1808. doi:10.1002/eji.200636661

629. Wang L, Zhao H, Raman I, Yan M, Chen Q, Li QZ. Peripheral Blood Mononuclear Cell Gene Expression in Chronic Obstructive Pulmonary Disease: miRNA and mRNA Regulation. *J Inflamm Res*. 2022;15:2167-2180. doi:10.2147/JIR.S337894

630. Trocmé C, Gaudin P, Berthier S, Barro C, Zaoui P, Morel F. Human B lymphocytes synthesize the 92-kDa gelatinase, matrix metalloproteinase-9. *J Biol Chem*. 1998;273(32):20677-20684. doi:10.1074/jbc.273.32.20677

631. Chandler S, Coates R, Gearing A, Lury J, Wells G, Bone E. Matrix metalloproteinases degrade myelin basic protein. *Neurosci Lett*. 1995;201(3):223-226. doi:10.1016/0304-3940(95)12173-0

632. Asahi M, Wang X, Mori T, et al. Effects of matrix metalloproteinase-9 gene knock-out on the proteolysis of blood-brain barrier and white matter components after cerebral ischemia. *J Neurosci*. 2001;21(19):7724-7732.